THE INFLUENCE OF NON-UV LIGHT ON SOIL SURFACE MICROBIAL COMMUNITY DEVELOPMENT AND THE FATE OF CROP PROTECTION PRODUCTS

MARK CALLUM JOHN DAY

A thesis submitted for the degree of Doctor of Philosophy

School of Life Sciences, University of Warwick

May 2015

Contents

Contents ..... **I**

List of Figures ..... **VI**

List of Tables ..... **XII**

Acknowledgements ..... **XVI**

Declaration ..... **XVII**

List of Abbreviations ..... **XVIII**

Summary ..... **XX**

CHAPTER 1: GENERAL INTRODUCTION **1**

1.1 CROP PROTECTION PRODUCTS IN AGRICULTURE **1**

1.1.1 Worldwide use of crop protection products 1

1.1.2 UK crop protection product use 2

1.2 MODERN REGULATION OF CPP ENVIRONMENTAL FATE IN THE EUROPEAN UNION **3**

1.2.1 Silent Spring 3

1.2.2 Crop protection product registration within the European Union 4

1.2.3 Organisation for Economic Co-operation and Development (OECD) guidelines 5

1.3 THE FATE OF CROP PROTECTION PRODUCTS IN SOIL **6**

1.3.1 Abiotic degradation of crop protection products 6

1.3.1.1 Photolysis 6

1.3.1.2 Hydrolytic degradation 9

1.3.2 Biotic degradation 9

1.3.3 Non-extractable residues (NERs) 11

1.3.4 Factors determining the fate of CPPs within the soil 13

1.3.4.1 The effect of pH on crop protection product degradation 13

1.3.4.2 The effect of soil organic matter on the degradation of crop protection products 15

1.3.4.3 The effect of clay on the degradation of crop protection products 16

1.3.4.4 The effect of moisture on the degradation of crop protection products 16

1.3.4.5 The effect of temperature on the degradation of crop protection products 17

1.4 CROP PROTECTION PRODUCT FATE ASSESSMENT **18**

1.4.1 OECD regulatory laboratory study 18

1.4.2 Regulatory field trials 20

1.4.3 Bridging the gap between the laboratory and the field 21

1.4.3.1 Inclusion of non-UV light in test systems 23

1.5 THE BIOLOGICAL SOIL CRUST **25**

1.5.1 Successional development of biological soil crusts 26

1.5.2 Microbial community structure 27

1.5.2.1 Photosynthetic communities 27

1.5.2.2 Heterotrophic communities 28
1.5.3 Soil structure and water infiltration rates 30
1.5.4 The biological soil crust of temperate environments 32
1.5.5 Why study the agricultural importance of the BSC and phototrophs? 33
1.6 AIMS AND OBJECTIVES 36
CHAPTER 2: THE IMPACT OF NON-UV LIGHT ON CPP FATE IN AN OECD 307 REGULATORY-LIKE SYSTEM 39
2.1 INTRODUCTION 39
2.1.1 Question to be addressed 41
2.2 MATERIALS AND METHODS 42
2.2.1 Soil 42
2.2.2 Test chemical/CPPs 43
2.2.3 The transformation of [^{14}C]-labelled CPPs in an aerobic environment 47
2.2.3.1 Test system 47
2.2.3.2 Light spectra 48
2.2.3.3 Moisture and temperature 49
2.2.4 Application of CPPs 50
2.2.5 Sampling and extraction of CPPs 51
2.2.6 Analysis of crop protection product fate 52
2.2.7 Degradation kinetics 55
2.2.8 Statistical Analysis 57
2.3 RESULTS 59
2.3.1 Pesticide A 59
2.3.2 Benzovindiflupyr 63
2.3.3 Cinosulfuron 67
2.3.4 Paclobutrazol 71
2.3.5 Fludioxonil 75
2.4 DISCUSSION 80
CHAPTER 3: THE SPECTRAL QUALITY OF LIGHT INFLUENCES THE BEHAVIOUR OF TWO CPPS WITHIN SOIL CORES IN A FIELD SYSTEM 87
3.1 INTRODUCTION 87
3.1.1 Questions to be addressed 89
3.2 MATERIALS AND METHODS 90
3.2.1 Soil 90
3.2.2 Semi-field plot 90
3.2.3 Plot preparation 91
3.2.4 Light filters 91
3.2.5 Light Spectra 92
3.2.6 Cores 94
3.2.7 Moisture and Temperature 94
3.2.8 Compounds 95
3.2.9 Application 95
3.2.10 Sampling 97
3.2.11 Soil processing 97

3.2.12 Parent compound quantitation 99
3.2.13 Non-extractable residues (NERs) 100
3.2.14 Degradation kinetics 100
3.2.15 Data analysis 101
3.2.16 Combination of CLEAR and UV treatments 102
3.3 RESULTS 103
3.3.1 Soil temperature and moisture 103
3.3.2 Paclobutrazol 104
3.3.2.1 Parent transformation 104
3.3.2.2 Mass balance, solvent extract, NERs 105
3.3.2.3 Paclobutrazol movement 107
3.3.3 Benzovindiflupyr 111
3.3.3.1 Parent transformation 111
3.3.3.2 Mass balance, solvent extract, and NERs 112
3.3.3.3 Benzovindiflupyr movement 114
3.4 DISCUSSION 118

CHAPTER 4: THE SPECTRAL QUALITY OF LIGHT INFLUENCES MICROBIAL COMMUNITY STRUCTURE AT THE SOIL SURFACE IN SOIL CORES INCUBATED IN THE FIELD 127
4.1 INTRODUCTION 127
4.1.1 Questions/Aims to be addressed 129
4.2 MATERIALS AND METHODS 130
4.2.1 Experimental outline 130
4.2.2 pH 130
4.2.3 Chlorophyll *a* 130
4.2.4 DNA isolation 131
4.2.5 DNA quantitation 132
4.2.6 Illumina MiSeq amplicon library preparation 133
4.2.6.2 Amplicon PCR 134
4.2.6.3 PCR clean up I 135
4.2.6.4 Index PCR 137
4.2.6.5 PCR clean up II 138
4.2.6.6 Library quantitation 138
4.2.6.7 Normalisation to 10 nM 139
4.2.6.8 Pooling 139
4.2.6.9 Sequencing details 140
4.2.7 Bioinformatic Analyses 140
4.2.8 Statistical analyses 142
4.3 RESULTS 144
4.3.1 Soil surface pH 144
4.3.2 Chlorophyll *a* 145
4.3.3 Sequence processing 146
4.3.4 Chemical comparison 148
4.3.5 Bacterial community composition 152
4.3.5.1 Bacterial community structure 152

4.3.5.2 Bacterial community composition 154
4.3.6 Phototrophic community composition and structure 161
4.3.6.1 Phototrophic community structure 161
4.3.6.2 Phototrophic community composition 163
4.4 DISCUSSION 168

CHAPTER 5: CROP CANOPY COVER INFLUENCES THE TEMPORAL AND SPATIAL DEVELOPMENT OF MICROBIAL COMMUNITIES AT THE SOIL SURFACE 175
5.1 INTRODUCTION 175
5.1.1 Questions to be addressed 177
5.2 MATERIALS AND METHODS 178
5.2.1 Soil 178
5.2.2 Plot preparation 178
5.2.3 Planting patterns 179
5.2.4 Plot maintenance 180
5.2.5 Environmental monitoring 180
5.2.6 Sampling and processing 181
5.2.7 Chlorophyll *a* 182
5.2.8 DNA isolation and quantitation 182
5.2.9 Library preparation, sequencing, and bioinformatic analyses 182
5.2.10 Statistical Analyses 182
5.3 RESULTS 183
5.3.1 Temperature and moisture 183
5.3.2 Chlorophyll *a* 185
5.3.3 Surface vs. bulk 186
5.3.3.1 Phyla driving bacterial community dissimilarity between surface and bulk soil 190
5.3.3.2 Taxa driving phototrophic community dissimilarity between surface and bulk soil 194
5.3.4 Bulk soil 199
5.3.4.1 Bacterial composition summary – Bulk soil 203
5.3.4.2 Phototrophic composition summary – Bulk soil 204
5.3.5 Surface soil 210
5.3.5.1 Bacterial community composition – soil surface 214
5.3.5.2 Phototrophic community composition – soil surface 215
5.4 DISCUSSION 222

CHAPTER 6: GENERAL DISCUSSION 228
6.1 Chemical fate 228
6.2 Soil surface microbiology 232
6.3 Soil surface community comparisons 233
6.4 Implications for industry 237
6.5 Future work 238

7. REFERENCES 243

APPENDIX I: OECD 307 REGULATORY LIKE STUDY – FURTHER METHODS 262
I.1 Application rate calculations 262
I.2 Application checks 263
I.3 Mass balance 263
I.4 Concentration calculations – procedural recoveries 264
I.5 Example HPLC chromatograms 265

APPENDIX II: FIELD DEGRADATION – FURTHER METHODS 268
II.1 Plot layout 268
II.2 Application rates 270
II.4 Mass balance 271
II.5 Combination of parent values 271
II.6 Samples removed from analysis 272
II.6.1 Benzovindiflupyr 272
II.6.2 Paclobutrazol 272
II.7 Example HPLC chromatograms 273

APPENDIX III: FIELD DEGRADATION – MICROBIOLOGY FURTHER METHODS 275
III.1 Tree construction for unassigned OTUs – 23S rRNA 275
III.2 Samples lost during bioinformatic analysis 277
III.2.1 16S rRNA samples 277
III.2.2 23S rRNA samples 277
III.3 SIMPER analysis results 278

APPENDIX IV: CROP CANOPY COVER – FURTHER METHODS 280
IV.1 Experimental plot layout 280
IV.2 Samples lost during bioinformatic analyses 281
IV.2.1 16S rRNA samples 281
IV.2.2 23S rRNA samples 282
IV.3 SIMPER analysis results 283

APPENDIX V: FIELD STUDY COMMUNITY COMPARISON 287
V.1 Analysis of similarities 287
V.2 SIMPER analysis results 288

List of Figures

Figure 1.1: Total area treated (bars), and total mass of crop protection product applied (—•—) in commercial agriculture in the UK, during the period 1990-2013 (taken from FERA 2013).

Figure 1.2: A conceptual diagram of crop protection product degradation and bacterial population size under (a) growth-linked catabolism, and (b) co-metabolic degradation. (Taken from Alexander 1981).

Figure 2.1: Structures of CPPs used in lab degradation studies: (a) Fludioxonil (b) Cinosulfuron, (c) Paclobutrazol, (d) Benzovindiflupyr. Radiolabel position is denoted by an asterisk. The structure of pesticide A is not shown.

Figure 2.2: A schematic of the OECD 307 regulatory-like system used.

Figure 2.3: Spectral profile comparison between spring, summer, and Sanyo cabinet light.

Figure 2.4: Extractable parent compound for pesticide A under light (□) and dark (■) conditions. The fitted hockey-stick models are shown as (—) for light predicted, and (- - -) for dark predicted kinetics.

Figure 2.5: Mass balance for pesticide A under light (open symbols) and dark (closed symbols) conditions. Overall mass balance (—●—), and solvent extractable radioactivity (···■···) are shown on y-axis one. NERs (–··▲··–), and mineralization (– –◆– –) are shown on y-axis 2.

Figure 2.6: Extractable parent compound for the fungicide benzovindiflupyr under light (□) and dark (■) conditions. The fitted hockey-stick models are shown as (—) for light predicted, and (- - -) for dark predicted kinetics.

Figure 2.7: Mass balance for the fungicide benzovindiflupyr under light (open symbols) and dark (closed symbols) conditions. The partitioned radioactivity is shown for overall mass balance (—●—), and solvent extract (···■···) on y-axis one. NERs (–··▲··–), and mineralization (– –◆– –) are shown on y-axis 2.

Figure 2.8: Extractable parent compound for the herbicide cinosulfuron under light (□) and dark (■) conditions. The fitted hockey-stick models are shown as (—) for light predicted, and (- - -) for dark predicted kinetics.

Figure 2.9: Mass balance for the herbicide cinosulfuron under light (open symbols) and dark (closed symbols) conditions. The partitioned radioactivity is shown for overall mass balance (—●—), and solvent extract (···■···) on y-axis one. NERs (–··▲··–), and mineralization (– –◆– –) are shown on y-axis 2.

Figure 2.10: Extractable parent compound for the plant growth regulator paclobutrazol under light (□) and dark (■) conditions. The fitted single first order models are shown as (—) for light predicted, and (- - -) for dark predicted kinetics.

Figure 2.11: Mass balance for the plant growth regulator paclobutrazol under light (open symbols) and dark (closed symbols) conditions. The partitioned radioactivity is shown for overall mass balance (—●— , and solvent extract (·····■·····) on y-axis one. NERs (–··▲··–), and mineralization (– –◆– –) are shown on y-axis 2.

Figure 2.12: Extractable parent compound for the fungicide fludioxonil under light (□) and dark (■) conditions. The fitted single first order models are shown as (—) for light predicted, and (- - -) for dark predicted kinetics.

Figure 2.13: Mass balance for the fungicide fludioxonil under light (open symbols) and dark (closed symbols) conditions. The partitioned radioactivity is shown for overall mass balance (—●—), and primary solvent extract (·····■·····) on y-axis one. NERs (–··▲··–), and mineralization (– –◆– –) are shown on y-axis 2.

Figure 3.1: Spectral profile of light transmitted through CLEAR (black), UV-limiting (blue), and PAR-limiting (red) filters.

Figure 3.2: A comparison of soil temperature (a) and moisture (b) recorded across a 120 DAT time course under LIGHT (black), and PAR limiting (red) conditions.

Figure 3.3: Extractable parent compound for paclobutrazol under LIGHT (□) and PAR-limited (■) conditions. The fitted hockey-stick models are shown as (—) for LIGHT predicted, and (- - -) for PAR-limited predicted. Error bars represent ±1 S.E.

Figure 3.4: Mass balance for paclobutrazol under LIGHT conditions (open symbols) and PAR-limited conditions (closed symbols). The partitioned radioactivity is shown for overall mass balance (—●—), and solvent extract (·····■·····), and NERs (–··▲··–.) Error bars represent ±1 S.E.

Figure 3.5: Graphs displaying the position of extractable paclobutrazol under (a) LIGHT and (b) PAR-L conditions. Amount of parent compound, as a percentage of applied, is shown in the surface (green), top bulk (red), and lower bulk (blue). Error bars represent ±1 S.E.

Figure 3.6: Extractable parent compound for benzovindiflupyr under LIGHT (□) and PAR-limiting (■) conditions. The fitted hockey-stick models are shown as (—) for LIGHT predicted, and (- - -) for PAR-limited predicted. Error bars represent ±1 S.E.

Figure 3.7: Mass balance for benzovindiflupyr under LIGHT (open symbols) and PAR-limiting conditions (closed symbols). The partitioned radioactivity is

shown for overall mass balance (—●—), and solvent extract (·····■·····) on y-axis one. NERs (–··▲··–) are shown on y-axis 2. Error bars represent ±1 S.E.

Figure 3.8: Graphs displaying the position of extractable benzovindiflupyr under (a) LIGHT and (b) PAR-L conditions. Amount of parent compound, as a percentage of applied, is shown in the surface (green), top bulk (red), and lower bulk (blue). Error bars represent ±1 S.E.

Figure 4.1: Time course of soil surface pH under LIGHT (open symbols) and PAR-L conditions (closed symbols). Error bars represent ±1 S.E.

Figure 4.2: Time course of chlorophyll *a* development at the soil surface under LIGHT (open symbols) and PAR-L conditions (closed symbols). Error bars are ±1 S.E.

Figure 4.3: Non-metric multidimensional scaling analysis of Bray-Curtis similarities of community structure for (a) bacterial, and (b) phototrophic communities at the soil surface under CLEAR (green), UV-Limiting (blue), and PAR-Limiting (red) filters. Clustering is based on similarity of community structure. The green lines in (a) represent bacterial communities sharing 89% similarity. The green lines in (b) represent phototrophic communities sharing 40% similarity.

Figure 4.4: (a) Bacterial α diversity estimates of *Observed Species* for LIGHT (open circle) and PAR-L (closed circle) and; (b) Ordination plot from non-metric multidimensional scaling analysis of Bray-Curtis similarities of community structure for bacterial communities at the soil surface under LIGHT (blue) and PAR-L (red) conditions. Clustering is based on similarity of bacterial community structure: at 70% (green line), and 88% (blue lines).

Figure 4.5: Comparison of the average relative abundance of bacterial phyla under LIGHT (blue) and PAR-L (red) conditions. Error bars represent ±1 S.E. Asterisks denote phyla identified by SIMPER analysis as main drivers of dissimilarity.

Figure 4.6: Graphs displaying the temporal development of the relative abundance of bacterial phyla identified by SIMPER analysis as driving dissimilarity by treatment and time. LIGHT samples are represented by open symbols, and PAR-L by closed symbols. Error bars represent ±1S.E.

Figure 4.7: (a) Phototrophic α diversity estimates of *Observed Species* for LIGHT (open circles) and PAR-L (closed circles) and; (b) Ordination plot from non-metric multidimensional scaling analysis of Bray-Curtis similarities of community structure for phototrophic communities at the soil surface. Clustering is based on similarity of phototrophic community structure: green lines (40% similarity).

Figure 4.8: Comparison of the average relative abundance of cyanobacterial and eukaryotic phototrophic taxa, between LIGHT (blue) and PAR-L (red) conditions and a breakdown summary of the major taxa composing the eukaryotic phototrophs. Error bars represent ±1 S.E.

Figure 4.9: Graphs displaying the temporal development of the relative abundance of phototrophic taxa identified by SIMPER analysis as driving dissimilarity by treatment and time. LIGHT samples are represented by open symbols, and PAR-L by closed symbols. Error bars are ±1 S.E.

Figure 5.1: Planting patterns of: (a) onion, (b) wheat and (c) potato. All plots were 1 m^2.

Figure 5.2: A comparison of average daily soil temperature recorded across a 150-day time course under Bare (green), Onion (blue), Wheat (cyan), and Potato (red) treatments.

Figure 5.3: A comparison of average daily soil moisture content (VWC) across a 150-day time course under Bare (green), Onion (blue), Wheat (cyan), and Potato (red) treatments.

Figure 5.4: Time course of chlorophyll concentration at the soil surface under crops with differing canopy characteristics. Bare (–○–), Onion (–□–), Wheat (–◆–), and Potato (–▼–). Error bars represent ±1 S.E.

Figure 5.5: Observed Species α diversity estimates of (a) bacterial, and (b) phototrophic communities present in surface (open circles) and bulk (closed circles) samples. Error bars represent ±1 S.E.

Figure 5.6: Ordination plots from non-metric multidimensional scaling analysis of Bray Curtis similarities of (a) bacterial, and (b) phototrophic community structure between bulk and surface soil samples. Green lines represent a similarity threshold of (a) 85%, and (b) 70%.

Figure 5.7: The temporal development of the relative read abundance of bacterial phyla identified by SIMPER analysis as driving dissimilarity by layer and time. Surface samples are represented by open symbols, and bulk by closed symbols. Error bars represent ±1 S.E.

Figure 5.8: The temporal development of the relative read abundance of phototrophic taxa identified by SIMPER analysis as driving dissimilarity by layer and time. Surface samples are represented by open symbols, and bulk by closed symbols. Error bars represent ±1 S.E.

Figure 5.9: Observed Species α diversity estimates of (a) bacterial, and (b) phototrophic communities present in bulk soil under Bare (–○–), Onion (–□–), Wheat (–◆–), and Potato (–▼–) canopies. Error bars represent ±1 S.E.

Figure 5.10: Ordination plots from non-metric multidimensional scaling analysis of Bray Curtis similarities of (a) bacterial, and (b) phototrophic community structure in bulk soil taken from under crops exhibiting differing canopy characteristics. Green lines represent a similarity threshold of (a) 90%, and (b) 70%.

Figure 5.11: Comparison of the average relative abundance of bacterial phyla in bulk soil samples between crop canopy treatments. Errors bars represent ±1 S.E.

Figure 5.12: Comparison of the average relative abundance of phototrophic taxa between different crop canopy treatments in bulk soil samples. Error bars represent ±1 S.E.

Figure 5.13: The temporal development of the relative read abundance of phototrophic taxa identified by SIMPER analysis as driving dissimilarity by treatment and time in bulk soil. Treatments are: Bare (–○–), Onion (–□–), Wheat (–◆–), and Potato (–▼–). Error bars represent ±1 S.E.

Figure 5.14: Observed Species α diversity estimates of (a) bacterial, and (b) phototrophic communities present in surface soil under Bare (–○–), Onion (–□–), Wheat (–◆–), and Potato (–▼–) canopies. Error bars represent ±1 S.E.

Figure 5.15: Ordination plots from non-metric multidimensional scaling analysis of Bray Curtis similarities of (a) bacterial, and (b) phototrophic community structure in surface soil taken from under crops exhibiting differing canopy characteristics. Green lines represent a similarity threshold of (a) 90%, and (b) 64%.

Figure 5.16: Comparison of the average relative abundance of bacterial phyla at the soil surface between crop canopy treatments. Errors bars represent ±1 S.E.

Figure 5.17: Comparison of the average relative abundance of phototrophic taxa between different crop canopy treatments. Error bars represent ±1 S.E.

Figure 5.18: Graphs displaying the relative read abundance of phototrophic taxa in surface soil samples. Treatments are: Bare (–○–), Onion (–□–), Wheat (–◆–), and Potato (–▼–). Error bars represent ±1 S.E.

Figure 6.1:Ordination plot from non-metric multidimensional scaling analysis of Bray-Curtis similarities of community structure for (a) bacterial, and (b) phototrophic soil surface communities from the semi-field degradation experiment (red symbols) and those found under crop canopy cover (green symbols). Clustering is based on similarity of phototrophic community structure: green lines represent (a) 89% similarity, and (b) 40% similarity.

Figure I.1: HPLC chromatograms from analysis of [^{14}C]-pesticide A at (a) 0 DAT, and (b) 120 DAT in an OECD 307 regulatory like study.

Figure I.2: HPLC chromatograms from analysis of [^{14}C]-benzovindiflupyr at (a) 0 DAT, and (b) 118 DAT in an OECD 307 regulatory like study.

Figure I.3: HPLC chromatograms from analysis of [^{14}C]-cinosulfuron at (a) 0 DAT, and (b) 60 DAT in an OECD 307 regulatory like study.

Figure I.4: HPLC chromatograms from analysis of [^{14}C]-paclobutrazol at (a) 0 DAT, and (b) 118 DAT in an OECD 307 regulatory like study.

Figure I.5: HPLC chromatograms from analysis of [^{14}C]-fludioxonil at (a) 0 DAT, and (b) 120 DAT in an OECD 307 regulatory like study.

Figure II.1: The plot layout used in the field degradation experiment detailed in Chapters 3 & 5.

Figure II.2: (a) A photograph of the plot used in Chapters 3 & 4. (b) An example of the cores installed in the ground under a LIGHT filter at 0 DAT. (c) Cores removed from the ground pre-processing, 57 DAT.

Figure II.3: Example HPLC chromatograms from analysis of [^{14}C]-benzovindiflupyr at: (a) 0 DAT (b) 120 DAT Surface.

Figure II.4: Example HPLC chromatograms from analysis of [^{14}C]-paclobutrazol at: (a) 0 DAT, and 106 DAT (b) Surface (c) Top Bulk (d) Lower Bulk, under a CLEAR filter

Figure III.1: Phylogenetic tree of unassigned 23S rRNA sequences (green) with selected sequences from the ARB SILVA 119 LSU Ref database.

Figure IV.1: The plot layout used in the crop canopy cover study detailed in Chapter 5. Treatments were Bare (B), Onion (O), Wheat (W), and Potato (P). An asterisk denotes a plot with temperature and moisture probes.

Figure IV.2: The semi-field plot from the Chapter 5 study 14 days after planting.

List of Tables

Table 2.1: A comparison of physical soil characteristics between Gartenacker and Boughton Loam soils.

Table 2.2: Selected information of the CPPs investigated. Information was taken from EFSA conclusions for fludioxonil, paclobutrazol, and benzovindiflupyr (EFSA Journal 2007, 2010 & 2015), and from Tomlin (2006) for cinosulfuron.

Table 2.3: Target and actual application rates of CPPs in OECD 307-like lab degradation study.

Table 2.4: A breakdown of the average radioactivity present in the fractions summed to give the overall mass balance of pesticide A under light and dark conditions. Parent compound remaining is also shown. Errors, in brackets, represent ±1 S.E.

Table 2.5: A breakdown of the average radioactivity present in the fractions summed to give the overall mass balance of benzovindiflupyr under light and dark conditions. Parent compound remaining is also shown. Errors, in brackets, represent ±1 S.E

Table 2.6: A breakdown of the average radioactivity present in the fractions summed to give the overall mass balance of Cinosulfuron under light and dark conditions. Parent compound remaining is also shown. Errors, in brackets, represent ±1 S.E.

Table 2.7: A breakdown of the average radioactivity present in the fractions summed to give the overall mass balance of paclobutrazol under light and dark conditions. Parent compound remaining is also shown. Errors, in brackets, represent ±1 S.E.

Table 2.8: A breakdown of the average radioactivity present in the fractions summed to give the overall mass balance of fludioxonil under light and dark conditions. Parent compound remaining is also shown. Errors, in brackets, represent ±1 S.E.

Table 2.9: Kinetic models used for analysis of parent degradation in an OECD 307 regulatory-like system. Key parameters included are goodness of fit (χ^2), correlation of between observed and expected (r^2), probability that degradation rate > 0 (Prob > t), and $DegT_{50}$ values. The break point of the Hockey stick kinetics was set at 14 DAT for all analyses.

Table 3.1: Target and actual application rates of Paclobutrazol and benzovindiflupyr in field degradation study.

Table 3.2: The percentage of applied paclobutrazol remaining in the surface, top bulk, lower bulk, and combined bulk (top + lower bulk) of treated cores under LIGHT and PAR-L conditions. Errors, in brackets, are ±1 S.E.

Table 3.3: The percentage of applied benzovindiflupyr remaining in the surface, top bulk, lower bulk, and combined bulk (top + lower bulk) of treated cores under LIGHT and PAR-L conditions. Errors, in brackets, are ±1 S.E.

Table 3.4: Kinetic model parameter used for analysis of parent degradation in cores incubated in the field. Parameters included are goodness of fit (χ^2), correlation between observed and expected (r^2), rate constants for degradation (k), probability that degradation rate > 0 (Prob > t), and DT_{50} values.

Table 4.1: Primers and adapters used for MiSeq library construction.

Table 4.2: Reaction components of amplicon PCR.

Table 4.3: Bacterial OTU table summary before and after sequence-based OTU abundance filtering.

Table 4.4: Phototrophic OTU table summary, showing filtering of non-target sequences and sequence based abundance filtering of target sequences.

Table 4.5: Bacterial and phototrophic OTU table summary (non-rarefied and rarefied).

Table 4.6: Analysis of similarities (ANOSIM) evaluating the variation of soil surface bacterial and phototrophic community structure by CPP and filter treatment.

Table 4.7: Analysis of similarities (ANOSIM) evaluating the variation of soil surface bacterial community structure by treatment and time.

Table 4.8: Analysis of similarities (ANOSIM) evaluating the variation of soil surface phototrophic community structure by treatment and time.

Table 5.1: Bacterial and phototrophic OTU table summaries (non-rarefied and rarefied) for comparison of Surface and Bulk samples.

Table 5.2: Results of analyses of similarity (ANOSIM) evaluating variation in the structure of Surface and Bulk soil samples by treatment and by time.

Table 5.3: Results of pairwise comparisons of the *Observed* Species rarefaction measure of phototrophic communities in bulk soil samples between treatments.

Table 5.4: Results of analyses of similarity (ANOSIM) evaluating variation in the structure of bacterial and phototrophic communities in bulk soil samples by treatment, and by time.

Table 5.5: Results of analyses of similarity (ANOSIM) evaluating variation in the structure of Surface soil samples by treatment, and by time.

Table I.1: An example of a mass balance table. Values shown are for 30 DAT paclobutrazol light samples.

Table I.2: An example of a concentration step required prior to HPLC analysis. Example from 59 DAT paclobutrazol light sample.

Table II.1: An example of a mass balance table from the study in Chapter 3. Values shown are for a 0 DAT paclobutrazol core from under a CLEAR filter.

Table II.2: Samples removed from benzovindiflupyr analysis in the Chapter 3 study.

Table II.3: Samples removed from paclobutrazol analysis in the Chapter 3 study.

Table III.1: Details of 16S rRNA samples lost during analysis in the Chapter 4 study.

Table III.2: Details of 23S rRNA samples lost during analysis in the Chapter 4 study.

Table III.3: SIMPER analysis results of bacterial communities present at the soil surface in the Chapter 4 study.

Table III.4: SIMPER analysis results of phototrophic communities present at the soil surface in the Chapter 4 study.

Table IV.1: Details of 16S rRNA samples lost during analysis in the Chapter 5 study.

Table IV.2: Details of 23S rRNA samples lost during processing and analysis in the Chapter 5 study.

Table IV.3: SIMPER analysis results of bacterial communities present in Bulk and Surface soil.

Table IV.4: SIMPER analysis results of phototrophic communities present in Bulk and Surface soil.

Table IV.5: SIMPER analysis results of comparisons by treatment and terminal time points of phototrophic communities present in Bulk soil.

Table IV.6: SIMPER analysis results of comparisons by treatment and terminal time points of phototrophic communities present in Surface soil.

Table V.1: Analysis of similarities (ANOSIM) results evaluating the variation of bacterial and phototrophic soil surface communities between the Chapter 4 and 5 studies.

Table V.2: SIMPER analysis of bacterial communities between the Chapter 4 and Chapter 5 studies.

Table V.3: SIMPER analysis of phototrophic communities between the Chapter 4 and Chapter 5 studies.

Acknowledgements

I would like to thank my supervisors Gary Bending, Hendrik Schäfer, Samantha Marshall and Laurence Hand for their help, guidance, and advice. I would also like to acknowledge the National Environmental Research Council and Syngenta for providing funding for this project.

During my project I was fortunate to spend 18 months working at Syngenta's Jealott's Hill International Research Centre. I would specifically like to acknowledge Carol Nichols for her stewardship, pragmatic approaches, and friendship during my time in industry. From Syngenta's Product Safety team thanks also go to Kevin Thomas, Christine Dougan, Paul Seymour, Karine Bourcier, Rob Stass, and Irene Bramke.

Special thanks also go to the Wells family, particularly Sarah and Helena, for making me welcome in their home during my stints in industry.

From the Warwick School of Life Sciences I would like to thank members, past and present, of the Bending, Schäfer, Chen, Wellington lab groups, and office members of C146. Specific thanks go to Lawrence Davies for all his guidance, Serena Thomson and Jenny Pratscher for discussions about, and help with, next generation sequence analysis, Julie Jones for statistical help, and Sally Hilton for her help with MiSeq library preparation and guidance with all things molecular.

Finally I would like to thank my friends, and my family for always supporting me. I dedicate this work to my mother, because she'd like it if I did

Declaration

I declare that the work presented in this thesis was conducted by me under the direct supervision of Professor Gary D. Bending, Doctor Hendrik Schäfer, Doctor Samantha Marshall, Carol Nichols, and Laurence Hand, with the exception of those instances where the contribution of others has been specifically acknowledged. The work contained in this thesis has not been submitted previously for any other degree.

Mark Callum John Day

List of Abbreviations

2,4-D - 2,4-dichlorophenooxyacetic acid

^{14}C – The radioactive isotope carbon 14

AI – Active ingredient

ANOSIM – Analysis of similarities

ANOVA – Analysis of variance

AR – Applied radioactivity

BL – Boughton Loam soil

BLAST – Basic local alignment search tool

BP – Break point of the hockey stick kinetic model

BSC – Biological soil crust

CAKE – Computer aided kinetic evaluation software package

CL – Clay-loam soil

CPP – Crop protection product

DOM – Dissolved organic matter

DOC – Dissolved organic carbon

DAT – Days after treatment

DAP – Days after planting

$DegT_{50}$ – Degradation time to 50% of applied mass/concentration

DT_{50} – Time taken for 50% of applied mass/concentration to dissipate

dwe – Dry weight equivalent

EFSA – European Food Safety Authority

E.P.A – Environmental Protection Agency

EU – European Union

FAO – Food and Agriculture Organisation of the United Nations

FERA – The Food and Environment Research Agency

FOCUS – Forum for the co-ordination of pesticide fate models and their use

HPLC – High Performance Liquid Chromatography

HS – Hockey stick degradation kinetics model

K_{OC} – Soil organic carbon-water partitioning coefficient

LSC – Liquid scintillation counting

NER – Non-extractable residue

NMDS – Non-metric multidimensional scaling

OECD – Organisation for economic co-operation and development

OM – Organic matter

OTU – Operational taxonomic unit

PAR – Photosynthetically active radiation

PAR-L – Photosynthetically active radiation limiting filter

PCR – Polymerase chain reaction

PLFA – Phospholipid-derived fatty acids

QIIME – Quantitative Insights Into Microbial Ecology

rRNA – Ribosomal RNA

S.E. – Standard error

SFO – Simple first order degradation kinetics model

SIMPER – Similarity percentages analysis

SL – Silt-loam soil

SOM – Soil organic matter

UPW – UltraPure Water

UV – Ultraviolet light, of wavelength ≤400 nm

Summary

Crop protection products (CPPs) are an essential component of modern agriculture, necessary to improve crop yield to feed the ever-increasing world population. Regulation and safety testing of CPPs entering the environment is mandatory to ensure that their use is not at the detriment of environmental or human health. Regulatory laboratory studies typically over-estimate the persistence of CPPs within the environment as they are not representative of environmental conditions.. This study investigated the role of non-UV light on CPP degradation and the development of soil surface communities.

The inclusion of non-UV light in laboratory studies impacted the degradation of fludioxonil and cinosulfuron, increasing and decreasing the rate of transformation relative to dark conditions, respectively. Further, the inclusion of light increased non-extractable residues (NER) formation in fludioxonil, paclobutrazol and benzovindiflupyr. In a field based degradation experiment, the availability of photosynthetically active radiation (PAR) increased the transformation of benzovindiflupyr relative to when PAR was restricted. Further, the formation of paclobutrazol and benzovindiflupyr NERs was increased when PAR was not restricted, and the proportion of CPP remaining at the soil surface (0-5 mm) was higher when PAR was restricted.

Targeted amplicon sequencing (Illumina MiSeq) revealed that bacterial and phototrophic communities at the soil surface changed with time, and that communities formed when PAR was available were structurally distinct relative to communities when PAR was restricted. In a further experiment, analysis of bacterial and phototrophic communities under crops with differing canopy characteristics showed that distinct communities formed at the soil surface relative to bulk soil, and that phototrophic communities of bare soil and under low-density canopies were structurally distinct to those that formed under high-density canopies. This work has potential implications for regulatory CPP degradation studies, and furthers the understanding of soil surface community development in temperate environments.

CHAPTER 1: GENERAL INTRODUCTION

1.1 CROP PROTECTION PRODUCTS IN AGRICULTURE

1.1.1 Worldwide use of crop protection products

The Agricultural Revolution of Western Asia occurred ~11 000 years ago (Kislev *et al.* 2004). However, it was not until ~4 500 years ago that rudimentary crop protection products (CPPs) were first used in agriculture, when Sumerians applied sulphur compounds to their crops to control insects and mites (IUPC 2010). Ever since, the use of CPPs has been intimately linked to crop productivity.

CPPs have been defined by the United Nation as (FAO 2002):

"Any substance or mixture of substances intended for preventing, destroying, or controlling any pest, including vectors of human or animal disease, unwanted species of plant or animals causing harm during or otherwise interfering with the production, processing, storage, transport or marketing of food."

There is a wide range of CPPs and a classification system is used, which first groups compounds based on the organisms that they target such as fungicides or insecticides targeting fungi and insects, respectively, and then by their chemical structure, such as an organochlorine or carbamate.

Crop protection is a multi-billion dollar industry. In 2007, worldwide expenditure on CPPs was estimated at US$ 39 443 million, and usage at 2 634 million kg (Grube *et al.* 2011). Herbicide usage was estimated to account

for 40% of worldwide CPP use in 2007, with insecticides, fungicides and 'other' (e.g. nemanticides, fumigants) CPPs accounting for 28%, 23% and 33% of CPP use, respectively (Grube *et al*. 2011).

1.1.2 UK crop protection product use

In the UK, the total area of land treated with CPPs (active substance area) has been generally increasing, rising from 45 million hectares (ha) in 1990 to 78 million ha by 2013 (Figure 1.1). However, improved use practices, increased efficacy, and better targeted CPPs have meant the total mass of pesticide applied has been following a general pattern of decline, approximately halving from 34.4 million kg in 1990 to 17 million kg in 2013 (FERA 2013).

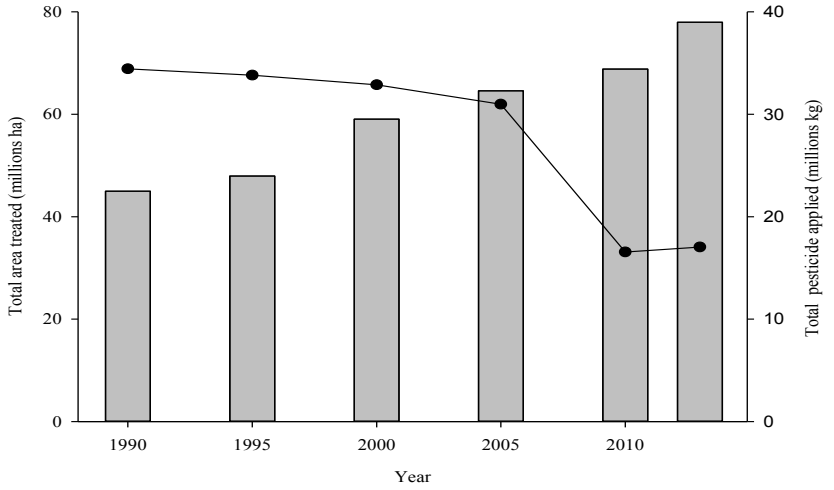

Figure 1.1: Total area treated (bars), and total mass of crop protection product applied (—•—) in commercial agriculture in the UK during the period 1990-2013 (taken from FERA 2013).

In 2013, fungicide application accounted for ~50% of the overall land area in the UK treated with CPPs, and 35% by total mass. In contrast, herbicide application accounted for ~31% of total area treated, but the greatest percentage of mass applied, ~45% of total.

1.2 MODERN REGULATION OF CPP ENVIRONMENTAL FATE IN THE EUROPEAN UNION

1.2.1 Silent Spring

In 1962, *The New Yorker* published of a series of essays by Rachel Carson, later published as *Silent Spring*. Using the insecticide dichlorodiphenyltrichloroethane (DDT) and its impact on wildlife (e.g. eggshell thinning in raptors) and human health (e.g. genotoxicity) as a case study, the potential adverse effects of CPPs to human health and the environment were brought sharply into the public eye. Previous regulation by the U.S. government had been targeted at creating a stable and competitive marketplace promoting the commercial needs of chemical companies and farmers (Bosso 1988). However, *Silent Spring,* and a growing body of evidence that CPPs could negatively affect human health, helped to spur the creation of the modern environmental movement (Thayer and Houlihan 2004), eventually leading to stricter regulatory controls. The potential for CPPs to contaminate groundwater or freshwater bodies (Stoate *et al.* 2001; Arias-Estévez *et al.* 2008; Younes *et al.* 2000), to bioaccumulate (Coat *et al.* 2011), and to impact non-target higher vertebrates (Bernanke and Köhler 2009), invertebrates (Canty *et al.* 2007), and

microorganisms (Xin-Yu *et al.* 2010; DeLorenzo *et al.* 2001) has since been discussed. As a consequence, the regulatory framework for the registration and licensing of CPPs has become far more stringent than in 1962 and, provided Good Agricultural Practice is followed, associated adverse effects of CPP application are far less common nowadays.

1.2.2 Crop protection product registration within the European Union

Before registering a new active ingredient (AI) within a European Union (EU) member state, the AI must first meet EU registration criteria. For a CPP to be approved for use within the EU, it must first be scientifically proven to be effective against its target without having adverse effects on human health, or unacceptable effects on animal health and the environment. An extensive submission that fully addresses the requirements set out in Commission Regulation (EU) No 283/2013 (for active substances) and Commission Regulation (EU) No 284/2013 (for the plant protection product) must be produced by entities wishing to register a new AI. This submission represents a detailed risk assessment of the AI, which includes environmental data and safety testing. If requirements are met, the Directive 2009/128/EC sets out rules for use of the CPP, according to Good Agricultural Practice. In addition to these submissions, the Organisation for Economic Co-operation and Development (OECD) provides guidance on a number of tests to evaluate a new AI. Active substances are approved for a maximum of ten years within the EU requiring a renewal of approval after this time period.

1.2.3 Organisation for Economic Co-operation and Development (OECD) guidelines

The ‘OECD Guidelines for the Testing of Chemicals’ are a collection of internationally agreed test methods used by government, industry, and independent laboratories to determine the safety of chemicals and chemical preparations. The guidelines are divided into five sections, each composed of a number of tests to identify specific chemical characteristics of the AI, or the impact of an AI on a particular organism or system. Section 1 is aimed at identifying the physical properties of the chemical, such as the boiling and melting point, and adsorption–desorption using a batch equilibrium method. Section 2 addresses the effects of the chemical on a wide range of biotic systems, ranging from freshwater algae and cyanobacteria growth inhibition tests to fish sexual development tests. Section 3 is on the degradation and accumulation characteristics of the AI, such as the aerobic and anaerobic transformation in soil. Section 4 documents effects on human health, including toxicokinetics and carcinogenicity tests. Section 5 addresses ‘Other Test Guidelines’, such as the crop field trials and the nature of pesticide residues in crops, livestock and stored and processed commodities.

1.3 THE FATE OF CROP PROTECTION PRODUCTS IN SOIL

In modern agriculture, CPPs are typically applied by spraying directly onto the soil surface or crops, but can also be applied to seeds prior to planting. Once CPPs have been released to the environment, they can enter water bodies through leaching and erosive run-off, the atmosphere through volatilisation (U.S. EPA 1994), crops though plant uptake (Fantke *et al.* 2013), or remain within the soil environment. The fate of a CPP within the soil is dependent on three main processes; (i) abiotic and biotic transformation of the parent compound to metabolites; (ii) mineralisation to harmless by-products, such as carbon dioxide, water, and nitrate; (iii) the formation of non-extractable residues.

The rate of CPP degradation has been shown to be influenced by several abiotic factors (Burrows *et al.* 2002; Wallace *et al.* 2010), as well as edaphic and climatic variables that influence biotic degradation, including pH (Singh *et al.* 2003 & 2006), soil organic matter content (Kästner *et al.* 2014), soil clay content and type (Chen *et al.* 2009), water content and temperature (Dungan *et al.* 2001).

1.3.1 Abiotic degradation of crop protection products

1.3.1.1 Photolysis

Photodegradation is one of the major abiotic degradation processes for some compounds and has been defined as *"the photochemical transformation of a molecule into lower molecular weight fragments, usually in an oxidation process"*

(Bravlavsky 2007). It is comprised of two major pathways, direct and indirect photolysis.

1.3.1.1.1 Direct photolysis

Direct photolysis refers to degradation of a CPP resulting from the direct absorption of UV radiation (290-400 nm). Susceptibility of CPPs to direct photolysis depends on their structure, though it is noted by Burrows *et al.* (2002) that as only a very small amount of short wavelength UV radiation (<290 nm) reaches the earth's surface, direct photolysis is likely to be of limited importance for most compounds.

The herbicide atrazine has been shown to be rapidly photodegraded in aqueous solution, with >99% transformed within 15 mins of treatment (Beltran *et al.* 1993), and it has also been shown that direct photolysis within soil systems is slower compared to aqueous systems. Curran *et al*. (1992) showed that 100% of imidazolinone herbicides imazapyr, imazethapyr and imazaquin, and 87% and 8% of imazamethabenz and atrazine were photodegraded in aqueous solution after 48 hours, respectively. However, in sand or a silt-clay loam soil, degradation of the same CPPs was <10% in the same time period. Reduced degradation rates within soil are likely due to the attenuation of light intensity below the top few millimetres of the soil surface (Benvenuti 1995) and the presence of humic substances and natural chromophores (an atom or group responsible for the colour of a compound) that absorb UV light

(Beltran *et al.* 1993). In Beltran *et al*. (1993), the addition of humic substances to an aqueous solution reduced the rate of atrazine transformation.

1.3.1.1.2 Indirect photolysis

Indirect photolysis refers to the degradation of CPPs resulting from interactions with reactive intermediates produced by the photochemical reactions of photosensitisers within the environment (Wallace *et al.* 2010). Nitrate, nitrite and dissolved organic matter (DOM) are important photosensitisers due to the production of the hydroxyl radical (HO*), carbonate radical, and triplet state DOM when in direct interaction with light (Brekken and Brezonik 1998; Miller and Chin 2002, 2005; Sharpless 2012). Wallace *et al.* (2010) highlighted the role of indirect photolysis in the photodegradation of chlorotoluron, chlorothalonil, propiconazole and prometryn, with faster photodegradation rates in surface waters relative to pH 7 buffer. They also linked the photodegradation of chlorotoluron, pinoxaden, propiconazole and prometryn to the concentration of nitrate, suggesting a significant role of the HO* radical as a reactive intermediate, whilst increased concentrations of dissolved organic carbon (DOC) and bicarbonate relative to nitrate were found to decrease the rate of degradation. Conversely, chlorothalonil appeared be rapidly degraded by the carbonate radical ($*CO_3^-$), highlighting the compound-specific nature of photosensitisers.

Whilst atrazine was shown to be directly degraded by UV light (Beltran *et al.* 1993), nitrate-mediated hydroxyl radical degradation of atrazine has

been shown to increase the rate of photolytic degradation relative to direct photolysis (Torrents *et al.* 1997).

1.3.1.2 Hydrolytic degradation

Hydrolysis of a CPP occurs as a reaction with a water molecule involving specific catalysis by a proton, hydroxide, or, sometimes, an inorganic ion such as phosphate, that play a role in general acid/base catalysis (Katagi *et al.* 2002). Hydrolytic profiles of CPPs depend on the chemical structure and functional groups of the CPP, and pH and temperature dependencies vary for different classes. In the soil, hydrolysis is influenced by edaphic and environmental factors that also affect the behaviour of CPPs in the environment, such as dissolved organic matter, clay content, pH and temperature (Katagi *et al*. 2006).

1.3.2 Biotic degradation

The biotic degradation of CPPs by microorganisms can be characterised as either growth-linked, or co-metabolic. In growth-linked catabolism, the CPP is directly broken down and used as a carbon and/or nitrogen source. This is characterised by an initial lag phase in degradation, where appropriate enzymes are synthesised and the population of the degrading community increases, followed by an increase in the rate of degradation. The degrading communities continue to proliferate over the period that the CPP is present in the environment as a substrate (Figure 1.2a) (Alexander 1981).

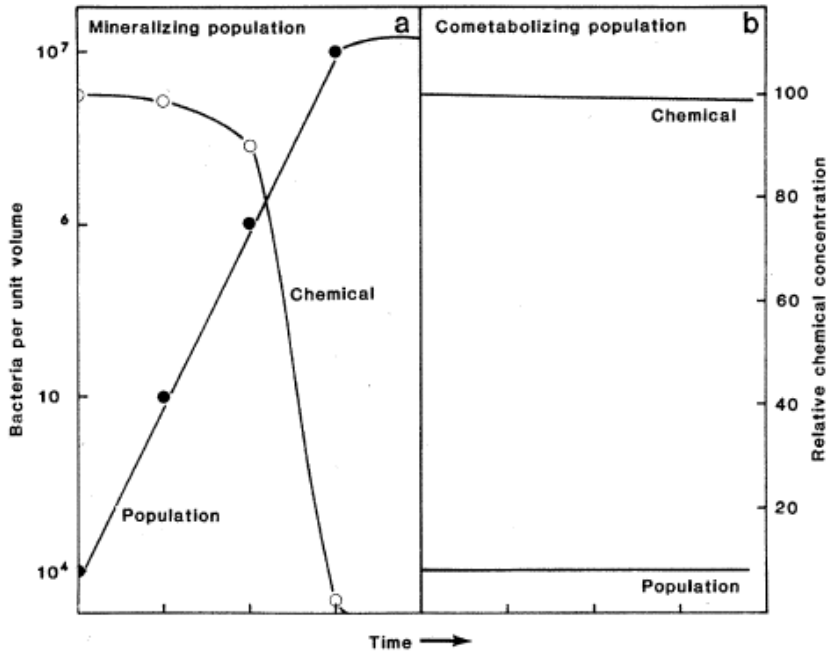

Figure 1.2: A conceptual diagram of crop protection product degradation and bacterial population size under (a) growth-linked catabolism, and (b) co-metabolic degradation. (Taken from Alexander 1981).

Co-metabolism occurs when a CPP is either modified or broken down by non-specific enzymes. The CPP is not used as an energy source by the degrading population, and so the degradation kinetics are characterised by a continuous, steady rate of degradation (Figure 1.2b) (Alexander 1981).The degradation of CPPs can be incomplete, resulting in the formation of secondary metabolites within the environment, or complete, where CPP degradation results in the production of carbon dioxide and water (mineralisation) (Muller *et al.* 2007). Complete mineralisation of compounds is preferable, as in some cases secondary metabolites can be toxic (Madigan *et al*. 2003).

1.3.3 Non-extractable residues (NERs)

Within the soil matrix, CPPs can either be present in the aqueous phase of the soil, or be bound to the soil. Residues can be bound reversibly or irreversibly to the soil, and residues remaining after an extraction procedure has been employed are often referred to as NERs (Semple *et al.* 2004). However, defining exactly what constitutes a NER is difficult, as the extractability characteristics of a CPP are controlled by the type of extraction procedure used (Gevao *et al.* 2000), and the intensity, and timing of said extraction. (Alexander 1995). For the purposes of this thesis, a NER will simply refer to the proportion of an applied CPP and its metabolites that are not recovered by solvent extraction methods defined in the methods sections.

A CPP can bind to the soil matrix in several ways to form NERs, with Kästner *et al.* (2014) suggesting a three-class classification system. The first, sequestered NER (Type I), covers the common physical binding modes of adsorption and entrapment. *Adsorption* describes the non-covalent binding of residues to the surface of solid soil particles, and is considered the most reversible form of association. Adsorption can occur by van der Waals' forces, ionic interactions, hydrogen bonding, charge-transfer, ligand exchange, and hydrophobic bonding (Gevao *et al.* 2000; Kästner *et al.* 2014). *Entrapment* describes the mechanical sequestration of residues by other organic molecules (Schaumann and Bertmer 2008). The second, covalently bound NER (Type II), covers what is generally accepted to be an irreversible association (Kästner *et al.* 2014) which results in the formation of persistent CPP NER in the soil. The third, biogenic non-extractable residue ($_{BIO}$NER, Type III), occurs during

growth-linked catabolism. If an organism assimilates CPP residue into its biomass, the subsequent death of the organism returns the residue to organic matter within the soil (Kästner *et al.* 2014; Nowak *et al.* 2011 & 2013).

There are several biological consequences of NER formation, such as reduced CPP toxicity (Kelsey *et al.* 1997; Kästner *et al. 2014*), and a reduction in bioaccessibility/bioavailability to microbial communities (Semple *et al.* 2004). A review by Semple *et al.* (2004) identified that it is difficult to produce a single, appropriate definition for these terms from the literature, and offered the following definitions:

Bioaccessible compound – *"That which is available to cross an organism's cellular membrane from the environment, if the organism has access to the chemical. However the chemical may be physically removed from the organism or only be bioavailable after a period of time"*

Bioavailable compound - *"That which is freely available to cross an organism's cellular membrane from the medium the organism inhabits at a given time. Once transfer across the membrane has occurred, storage transformation, assimilation, or degradation can take place within the organism"*

The bioavailability and bioaccessibility of CPP residues is intimately linked with the biodegradation rate of CPPs within the environment, and sorption of CPPs has been shown to reduce CPP degradation rates due to reduction in

bioavailability and bioaccessibility (Karpouzas and Walker 2000; Gaultier *et al.* 2008).

1.3.4 Factors determining the fate of CPPs within the soil

The route of degradation in the environment depends on the chemical nature of the compound, though can be influenced by edaphic and climatic variables. Similarly, the rate of CPP biodegradation within the environment has been shown to be influenced by edaphic and climatic variables, including pH, soil organic matter content, clay type, moisture content and temperature.

1.3.4.1 The effect of pH on crop protection product degradation

Soil pH has been shown to influence the rates of degradation of several CPPs. For example, Singh *et al.* (2003) demonstrated that an increase in soil pH accelerated the rate of degradation of organophosphate insecticide chloropyrifos, from a half-life of 256 days at pH 4.7 to a half-life of 35 days at pH 6.7. This effect was further demonstrated by Singh *et al.* (2006) with the organophosphate insecticide fenamiphos, with an increase in the rate of degradation in soil at pH >5.7 relative to pH 4.7. Awasthi *et al.* (2000) showed that degradation of organochlorine insecticide endosulfan was not detectable at acidic pH, and increased gradually to an optimal degrading pH of 8.7. However, continued increase in pH can reduce degradation rates. In Benimeli *et al.* (2007), the degradation rate of organochlorine insecticide lindane increased from pH 5 to

pH 7, but decreased at pH 9, and in Kumar and Phillip (2006), degradation of endosulfan in aerobic systems was lowest at pH 4 and 10, but greatest at pH 6-8, though in anaerobic systems, degradation efficiency increased with increasing pH.

This effect of pH on the degradation rate of CPPs could be caused by the strong selective effect that pH has on soil microbial communities (Lauber *et al.* 2009). In a comprehensive study of bacterial community structure of soil across the UK, Griffiths *et al.* (2011) showed that α diversity (sample variance within a site) was positively related to pH, whereas β diversity (between sample variance in α diversity) was negatively related to pH. Highly acidic soils were dominated by a few taxa, with clear selection for Acidobacteria and Alphaproteobacteria.

pH can also modulate the sorption and hydrolysis of many pesticides, especially ionizable compounds where pH governs speciation (Franco *et al.* 2009). Yang *et al.* (2004) showed a 14-21% and 5.5% decrease in sorption per unit increase in pH for nitrile herbicide bromoxynil and herbicide diuron, respectively, with reduction in sorption thought to be a result in the deprotonation of functional groups at higher pH values.

1.3.4.2 The effect of soil organic matter on the degradation of crop protection products

Soil organic matter (SOM) refers to living soil biomass, fresh and partially decomposed organic residues, and humus. Depending on soil type, SOM makes up 1-12% of soil by volume (Sims *et al.* 1990; Kästner *et al.* 2014), and although in most cases comprises the smallest part of the soil solid phase, it is of dominating importance as it affects all physical, chemical, and biological soil properties due to its role as a carrier of biotic catalytic activity (Kästner 2008; Kästner *et al.* 2014). SOM is also important in controlling soil structure and plant growth, and as a source of carbon for microbial communities (Fontaine *et al.* 2003), and microbial activity and biomass have been shown to be correlated with SOM content (Schürner *et al.* 1985; Gaultier *et al.* 2008; Voos and Groffman 1997).

Voos and Groffman (1997) investigated the degradation of the systemic herbicide 2,4-dichlorophenooxyacetic acid (2,4-D) and the organochloride herbicide dicamba in soils from five different land uses. They found microbial biomass and SOM were correlated with the dissipation of both compounds. Similarly, Gaultier *et al.* (2008) investigated representative soils from seven eco-regions and found that microbial activity and biomass was greater in soil with a higher SOM content. However, it was also found that CPP degradation declined as SOM content increased. This could be due to increased sorption of the compounds, decreasing bioavailability and bioaccesibility, so decreasing degradation of CPPs.

1.3.4.3 The effect of clay on the degradation of crop protection products

Whilst SOM is generally the principal edaphic factor controlling CPP bioavailability and degradation in soil (Gevao *et al.* 2000; Kästner *et al.* 2014), clay content has also been linked to both processes. Clay interacts with SOM in the presence of polyvalent cations, resulting in the formation of stable clay-organic complexes and microaggregates (Bronick and Lal 2005; Kästner *et al.* 2014). These complexes are formed within macroaggregates, and play a role in the shaping of the soil system, providing a matrix for sorption and formation of NERs (Tisdall 1996; Kästner *et al.* 2014).

Different clay minerals also have different interactions with CPPs. For example, Chen *et al.* (2009) showed that carbamate insecticide carbaryl showed the strongest sorption and lowest biodegradation when associated with montmorillonite, relative to kaolinite and goethite.

1.3.4.4 The effect of moisture on the degradation of crop protection products

Moisture content has been shown to accelerate rate of degradation of many CPPs, including: organochlorine pesticide 1,3-dichloropropene (1,3-D) (Dungan *et al.* 2001) 2,4-D (Cattaneo *et al.* 1997; Bouseba *et al.* 2009), organochlorine insecticides aldrin, dieldrin, endrin, chlordane (Ghadiri *et al.* 1995), substituted urea herbicide isoproturon (Alletto *et al.* 2006; Schroll *et al.* 2006), thiazolinone herbicide benazolin-ethyl and herbicide glyphosate (Schroll *et al.* 2006), semicarbazone insecticide metaflumizone

(Chatterjee *et al.* 2013), and strobilurin fungicide kresoxim-methyl (Khandelwal *et al.* 2014).

The influence of soil moisture content on CPP degradation rates is greatest when soil moisture content is low. For example, in García-Valcárcel and Tadeo (1999) degradation of triazine herbicides hexazinone and simazine became faster when moisture content (by mass) increased from 4% to 10%, and from 10% to 18%. However, the increase in degradation was more pronounced in the increase from 4% to 10%, with the half-life of hexazinone decreasing from 572 days at 4% moisture, to 23 days at 10%, and 20 days at 18%. Similarly, the half-life of simazine decreased from 126 days at 4% moisture, to 33 days at 10% moisture, and 27 days at 18%.

1.3.4.5 The effect of temperature on the degradation of crop protection products

A 10°C increase in temperature typically doubles the rate of CPP degradation (Dungan *et al.* 2001; Alletto *et al.* 2006; Arshad *et al.* 2008), though in the environment this is not always the case (Bouseba *et al*. 2009). Temperature has been shown to impact the rate of degradation of a wide range of CPPs, including: 1,3-D (Dungan *et al.* 2001), 2,4-D (Bouseba *et al.* 2009), α- and β-endosulfan (Arshad *et al.* 2008), lindane (Benimeli *et al.* 2007), isoproturon (Alletto *et al.* 2006), aldrin, dieldrin, endrin and chlordane (Ghadiri *et al.* 1995).

1.4 CROP PROTECTION PRODUCT FATE ASSESSMENT

1.4.1 OECD regulatory laboratory study

Section three of the OECD Guidelines for the Testing of Chemicals is composed of 22 tests designed to investigate the degradation and accumulation characteristics of a chemical. One such test, OECD Guideline 307 (OECD 307) investigates the aerobic and anaerobic transformation of chemicals in soil. The method is designed to evaluate the rate and nature of transformation of the test compound and its transformation products, to which plants and soil organisms may be exposed.

Soil samples are treated with a [^{14}C]-labelled CPP, and are incubated in the dark in a flow-through system, under controlled temperature and moisture conditions (shown in Figure 2.2). At appropriate time intervals, in an experimental timeline not normally exceeding 120 d, samples are destructively harvested. The CPP is solvent-extracted from the sample, and parent and transformation products are quantified by chromatography. Mineralisation of the test CPP is quantified by continuously trapping any evolved $^{14}CO_2$ in NaOH or KOH. Finally, any NERs are quantified by combustion, and a mass balance is calculated. The time taken for 50% ($DegT_{50}$) and/or 90% ($DegT_{90}$) of the CPP to degrade is calculated by fitting appropriate degradation models, provided that they comply with the FOrum for the Coordination of pesticide fate models and their USe (FOCUS) guidelines (FOCUS 2006). These $DegT_{50}$ and $DegT_{90}$ values inform if further assessments are needed (OECD 307).

This test is repeated in multiple soil types with differing edaphic properties (classification/texture, pH, SOM content, moisture holding capacity) and the degradation rate at different temperatures calculated using the Arrhenius equation to assess the persistence of the CPP in a range of ecoregions and climatic conditions.

The introduction of OECD 307 standardised the assessment of CPP degradation and persistence within soil, allowing comparisons across a range of representative soil types and CPPs. Reproducibility between test systems is good as confounding environmental variables, such as fluctuations in temperature and moisture are kept constant. However, in standardising these variables, the test does not accurately represent the dynamic agricultural environment it is simulating. Soil that is used in the test is first sieved to ≤2 mm. This destroys any established soil structure, and breaks up fungal hyphal networks that have been shown to be functionally important in promoting soil aggregation (Tisdall *et al.* 2012). During the test, temperature and moisture content are maintained within a constrained range, which is not representative of the diurnal shifts in temperature and the random, dynamic rainfall events experienced in a true agricultural environment.

Maintaining constant moisture content in a closed system prevents the gravimetric movement of water through soil pores and channels, and the upward flow of water from evaporation is not simulated. The guideline also stipulates that soil used for the test must be taken from the top 15 cm of soil, so variability in the rate of CPP degradation associated with soil depth is omitted (Rodríguez-Cruz *et al.* 2006, 2008 & 2010). Tests are carried out in continuous

darkness, and so any impact of phototrophic degrading organisms, which develop in the top millimeter of soil, is ignored (Jefferey *et al.* 2009).

1.4.2 Regulatory field trials

Different regulatory bodies, such as the Environmental Protection Agency (EPA) in the United States (EPA 2008), and the European Food Safety Authority (EFSA 2010) in the EU, define guidelines for the assessment of CPP degradation using field trials.

In EU guidelines, a representative CPP formulation is applied to recently tilled soil and a time course of degradation is taken with cores sampled from several areas of the field site. In the lab, cores are divided into several depths and solvent-extracted. Extracts are analysed to quantify parent compound and transformation products. At the end of the time course, $DegT_{50}$ and $DegT_{90}$ values are calculated. Trials are performed in several different ecoregions that are representative of the CPP's intended use.

Field trials provide a more environmentally realistic assessment of the fate of CPPs in different soils and climatic conditions. Formulations are exposed to diurnal fluctuations in temperature, rainfall events, and indigenous microbial communities. However, field trials are principally targeted at obtaining a $DegT_{50}$ value associated with the soil matrix (1 cm to 30 cm; $DegT50_{MATRIX}$), and attempt to actively mitigate the effect of soil surface processes (volatilisation, photodegradation, runoff etc.). Suggested approaches to mitigate the influences of soil surface processes include mixing the top 10 cm of soil post-application,

injection of the substance into the soil matrix, and covering of the surface with sand.

1.4.3 Bridging the gap between the laboratory and the field

Whilst the aim of OECD 307 is to determine the rate and route of CPP degradation within soil, studies typically overestimate the persistence of CPPs relative to the field, which may be due to the absence of spatial and temporal variability in edaphic and climatic variables typically found in the field. Beulke *et al.* (2000) reviewed 178 studies, and compared the $DegT_{50}$ values obtained from field studies with those simulated using persistence models based on laboratory data. In 44% of studies models overestimated persistence by a factor of >1.25, whereas an underestimation of persistence by a factor of >1.25 was only found in 17% of the studies.

Since 61% of laboratory studies either over or under-estimated the degradation rate observed in the field by a factor of 1.25, there is clearly a need to gain a better understanding of what factors influence degradation in the field that are not accounted for in the laboratory test systems. Due to the design of the laboratory test system, fluctuations in temperature, moisture and nutrient status that would be present in the field are not investigated (OECD 307). These may influence both the adsorption of a compound to the soil surface and, therefore, its bioavailability/bioaccessibility, and may also impact on the microbial communities present, all of which may influence the degradation rate.

Beulke *et al.* (2005) later investigated the effect of varying edaphic and climatic variables on the degradation of the thiadiazine herbicide bentazone and the triazine herbicide cyanazine in lab based soil systems. They investigated the effect of soil aggregates of different sizes (<3 mm or 3-5 mm), fluctuating vs. constant temperature and moisture conditions, and static water vs. flowing water conditions. The rate of degradation of the two CPPs was not significantly impacted by the different treatments, and it was concluded that the assumptions underlying the extrapolation of laboratory data in different conditions were acceptable in the laboratory systems tested (Beulke *et al.* 2005).

Although these investigations by Beulke *et al.* (2005) have demonstrated that fluctuations in temperature and moisture did not alter the laboratory degradation rates for two compounds, the same may not be true for all compounds, nor in comparisons to field data. Likewise, the effect of soil structure is currently unknown. Laboratory experiments are conducted with 2 mm sieved soil (according to the OECD guidelines), which severely disrupts soil structure. Under field conditions, the soil will have a defined 3D structure where large areas are linked by macro- and micro-pores, as well as an intact fungal hyphae network, enabling the distribution of water and nutrients over a much larger area than would be possible in the 2 mm sieved, non-structured soil. Therefore, the processing of soil for laboratory tests may significantly impact the microbial communities present and subsequently the degradation rate of a CPP.

Other factors that are present in the field, and which are absent in laboratory studies, and which may have an impact on the microbial communities present in soil, and subsequently the degradation of CPPS, include (a) the

presence of plants and, therefore, an active rhizosphere and (b) the presence of sunlight, which can not only result in the degradation of compounds by photolysis but which can also have a large impact on the soil microbial communities due to the presence of phototrophic microorganisms.

Hence, accurate predictions of environmental fate using laboratory studies cannot be made if all possible routes of degradation that are present in the field are not fully investigated and understood.

1.4.3.1 Inclusion of non-UV light in test systems

OECD and EFSA guidance for CPP transformation studies attempts to mitigate the confounding effects of soil surface processes. One of these processes, photodegradation, can occur directly or indirectly (see Section 1.3.1), and all light is excluded from laboratory tests, and steps taken to mitigate its influence and effects in field trials. Photodegradation occurs at wavelengths <400 nm, and a soil photolysis study is required to be submitted for AI registration to determine whether photolysis is an important route of degradation for a compound. However, non-UV sunlight (>400 nm) can influence the microbial communities present at the soil surface, which in turn may influence CPP degradation. These phototrophs require photosynthetically active radiation (PAR) that is not accounted for in either OECD guideline 307 or soil photolysis studies.

Several CPPs have been shown to be transformed in axenic algal cultures, including atrazine (Kabra *et al.* 2014), aryloxyphenoxypropionate herbicide diclofop-methyl (Cai *et al.* 2007), fenamiphos (Caceres *et al.* 2008),

phenylpyrazole insecticide fipronil (Qu *et al.* 2014), and isoproturon (Mostafa and Helling 2001). Thomas and Hand (2011) investigated the influence of non-UV light in a regulatory-like water-sediment system containing algae and macrophytes. They reported reductions in the persistence of six CPPs relative to standard dark systems. Further work isolated eukaryotic and prokaryotic algae from the system, before exposing them to the phenylpyrrole fungicide fludioxonil to test for degrading competency. Eight green algae within the division Chlorophyta, including two *Scenedesmus* spp. and a *Chlorella* spp., and four cyanobacteria, including *Nostoc punctiforme* and *Anabaena cylindrica*, were shown to degrade fludioxonil (Thomas and Hand 2012).

The impact of phototrophs on degradation of CPPs within soil systems is less well established, though it was shown that inoculation of soil with *Chlorococcum* sp. or *Scenedesmus* sp. resulted in an increase in the rate of α-endosulfan degradation (Sethunathan *et al.* 2004). Davies *et al.* (2013) also concluded that the inclusion of non-UV light in an OECD 307 regulatory-like system influenced the degradation rates of CPPs. In a single time point screen of eight CPPs of varying modes of action and classes of chemistry, five exhibited higher rates of degradation when the systems were exposed to non-UV light/dark cycles, while one compound exhibited a lower rate of degradation. In further work, $DegT_{50}$ and $DegT_{90}$ were halved in the triazole fungicide benzovindiflupyr and the herbicide chlorotoluron, respectively.

Phototrophs have the ability to directly degrade CPPs, though they could also have indirect effects by altering the soil environment. This could be through input of carbon produced by photosynthesis (Yoshitake *et al.* 2010), input of

nitrogen from diazotrophic cyanobacteria (Belnap 2002; Abed *et al.* 2010; Zhao *et al.* 2010), or increasing soil pH resulting from phototrophs taking up CO_2 for use in photosynthesis (Davies *et al*. 2013a). Phototrophs are most likely to be found at the soil surface, which acts as the interface between the atmosphere and terrestrial environment and, therefore, may be important in understanding the fate of CPPs in a field scenario.

1.5 THE BIOLOGICAL SOIL CRUST

Soil is a complex system comprised of several discrete functional compartments. The Biological Soil Crust (BSC) is comprised of the top few millimeters of the soil surface and acts as the interface between the atmosphere and the terrestrial environment. It is functionally distinct from bulk soil as it is exposed to light and other environmental factors such as wind and splash/wash erosion. The community structure of the BSC has been shown to differ from the underlying bulk soil, primarily due to the development of photosynthetic communities such as cyanobacteria, algae, mosses and lichens (Abed *et al.* 2010; Langhans *et al.* 2009a; Garcia-Pichel *et al.* 2001; Li *et al.* 2011; Redfield *et al.* 2002; Yeager *et al.* 2004 & 2007; Zhang *et al.* 2009a & 2011). Research has mainly focused on the development and ecology of BSCs in dryland systems where they are estimated to cover 70% of the soil surface (Pointing and Belnap 2012), including the Colorado plateau and the Sonoran desert in the U.S. (Garcia-Pichel *et al.* 2001; Nagy *et al.* 2005; Redfield *et al.* 2002; Yeager *et al.* 2004 & 2007), the Gurbantunggut desert in

China (Li *et al.* 2015; Zhang *et al.* 2009a, 2009b & 2011), the Negev desert in Israel (Kidron *et al.* 2010), and the Sultanate of Oman (Abed *et al.* 2010). Although the majority of research has focused on arid lands, BSCs have also been shown to be ubiquitous in temperate soils, including under agricultural crops (Veluci *et al.* 2006; Knapen *et al*. 2007; Langhans *et al.* 2009a & 2009b).

1.5.1 Successional development of biological soil crusts

In arid lands, succession from early pioneer species can be an extended process. In a long-term study of succession at the surface of a bare sand dune in the Tengger desert, China, Li *et al.* (2002) highlighted three stages of development between 1956 and 1981. Initial colonisation of the surface occurred within one year, particularly by Cyanobacteria such as *M. vaginatus*. After eight years, mosses began to appear within the system, and after 25 years the BSC was dominated by algae, mosses, and liverworts. These successional stages have been shown in multiple arid lands, including the eastern Negev desert (Lange *et al.* 1992), Arches National Park, Utah (Belnap 1993) and the Gurbantunggut (Li *et al.* 2015) and Tengger deserts, China (Li *et al.* 2010).

1.5.2 Microbial community structure

1.5.2.1 Photosynthetic communities

The filamentous cyanobacterium *Microcoleus vaginatus* has been shown to be a dominant colonising bacterium (Belnap 1993), abundant in geographically-distinct dryland systems, including the Gurbantunggut desert (Zhang *et al*. 2009a & 2011; Li *et al.* 2015) and Shapotou region of China (Lan *et al.* 2012), the Sultanate of Oman (Abed *et al.* 2010), the northwestern Negev desert, Israel (Kidron *et al.* 2010), xeric shrubland in Florida (Hawkes and Flechtner 2002), the Chihuahuan desert, New Mexico (Yeager *et al.* 2004), and the Colorado plateau (Garcia-Pichel *et al.* 2001; Redfield *et al.* 2002; Yeager *et al.* 2004).

Following scalping events (removal of the top 3 cm of soil), the inoculation of soil with *M. vaginatus* has been shown to improve the rate of biological and physical recovery, highlighting its role as an effective pioneer species in the formation of BSCs (Belnap 1993).

Whilst BSC communities are dominated by *M. vaginatus* during early colonisation and establishment, the stage of succession influences Cyanobacteria community composition and structure. In both the Chihuahuan desert in New Mexico and the Colorado plateau, Yeager *et al.* (2004) showed a shift in dominance from *M. vaginatus* in the early stages of BSC formation to *Nostoc* and *Scytonema* spp. in late successional BSCs. This change in dominance is discernible visually, with several studies categorising BSCs in early successional stages as light, and BSCs in later successional stages as dark. This is based on

cyanobacterial dominance, with the early-dominating *M. vaginatus* being light green in colour, and the later dominating *Nostoc* spp. being dark green/black in colour (Garcia-Pichel *et al.* 2003; Darby *et al.* 2007; Bates and Garcia-Pichel 2009; Soule *et al.* 2009; Bates *et al.* 2012).

Culturing organisms that are part of BSCs has revealed the presence in soil crusts of a wide range of algae, such as *Chlamydomonas ovalis, Chlorococcum humicols, Chlorella vulgaris*, and *Synechococcus parvus* (Zhang *et al*. 2011). Late-successional BSCs have been shown to be dominated by moss, such as *Syntrichia ruralis* (Darby *et al.* 2007) and the *Bryophyta* clade (Li *et al.* 2015), and lichens, such as *Collema tenax* (Darby *et al.* 2007).

1.5.2.2 Heterotrophic communities

Whilst phototrophic communities dominate in arid land BSCs, they also harbour fungi, nematodes, archaea, and bacteria (Nagy *et al.* 2005; Darby *et al.* 2007; Soule *et al.* 2009; Liu *et al.* 2011; Bates *et al.* 2012). Garcia-Pichel and Bates (2009) showed that early and late successional BSCs of the Colorado plateau were dominated by the fungal division Ascomycota, and the free-living fungal genera *Alternaria*. Further, Bates *et al.* (2012) showed that Ascomycota were dominant in early and late cyanobacteria-dominated BSCs, and in lichen dominated BSCs of the Sonoran desert and Colorado Plateau.

Archaea have been shown to be common and abundant members of BSC communities, representing around 5% of the prokaryotic population (Soule *et al.* 2009). In a large-scale study across a wide biogeographic area of

North America of BSCs at different successional stages (*M. vaginatus-, Nostoc* spp.-, lichen-, or moss-dominated), archaeal populations were shown to be constant, regardless of the stage of microbial community development. Furthermore, only six different phylotypes, all within the phylum Crenarchaea, were found across all sites, three of which were highly dominant (Soule *et al.* 2009).

Research has also investigated the role of BSCs on nematode abundance and diversity, and has shown that nematode abundance is greater at the soil surface, relative to underlying bulk soil, in BSCs of the Chihuahuan desert and Colorado plateau (Darby *et al.* 2007). Moreover, community structure was influenced by the successional stage of BSCs, with a greater abundance of predators and omnivores in late stage compared to early stage BSCs (Darby *et al.* 2007). Similarly, later research in the Tengger desert of northern China showed that whilst nematode abundance and diversity was greater under BSC colonised relative to non-colonised soil, differences in nematode communities were seen at different successional stages, with a greater abundance and diversity of nematodes under later stage moss-dominated crusts when compared to communities under cyanobacteria- and lichen-dominated crusts (Liu *et al.* 2011).

The composition and structure of heterotrophic bacterial communities in BSCs is not well understood. Several culture-independent studies have, instead, focused on the 16S rRNA gene of cyanobacteria (Redfield *et al.* 2002), or the nitrogen fixation gene *nifH* in diazotrophic cyanobacteria (Yeager *et al.* 2004). Abed *et al.* 2010 investigated the diversity of 16S rRNA of bacteria, and found

clone libraries were dominated by sequences with close homology to cyanobacteria. However, sequences with close homology to β-proteobacteria, Actinobacteria, Chloroflexi, Bacteroidetes and Acidobacterium have been detected in BSCs in the Sonoran desert (Nagy *et al.* 2005).

1.5.3 Soil structure and water infiltration rates

The BSC acts as an interface between the atmosphere and the terrestrial environment, and its development has been shown to affect physical characteristics of the soil, such as structure and, subsequently, water infiltration rates (Belnap and Gillette 1997; Kidron *et al.* 2003; Zhang *et al.* 2006). The presence of a BSC is unequivocally effective at reducing soil erosion by wind and water in arid conditions where vegetative cover is sparse. Belnap and Gillette (1997) showed that BSC development improved soil stability in sandy desert soils of southeastern Utah. In BSCs undisturbed for one, five, ten, and 20 years, there was a commensurate increase in the friction threshold velocity (the velocity at which soil particles are blown away by wind) relative to bare sand with time since disturbance. When these crusts were subsequently disturbed, the friction threshold velocities were reduced by 73%-92%. Later work in the Gurbantunggut desert in China showed similar results (Zhang *et al.* 2006), with increased soil stability attributed to the intricate network of filamentous cyanobacteria and associated exopolysaccharides binding sandy soil together, increasing soil aggregation. The ability of several filamentous cyanobacteria to self-assemble to macroscopic yarns was used to taxonomically define several genera, notably *Microcoleus*, before this ability was recognised as a mechanism to colonise physically unstable

environments (Garcia-Pichel and Wojciechowski 2009). It is thought that this is the mechanism used by early colonising species in BSC development to biostabilise the soil surface, promoting succession of less pioneering species. Increases in soil stability are not restricted to the action of cyanobacteria and algae. Several fungal species have also been shown to improve soil stability by increasing soil aggregate size by cross-linkage and entanglement of particles (Tisdall *et al.* 2012).

BSCs have, confusingly, been shown to improve and reduce water infiltration rates relative to bare soil (Kidron *et al.* 1999, 2003 & 2012; Xiao *et al.* 2011; Chamizo *et al.* 2012). However, contrasting results can be attributed to the successional age of the crust and their taxonomic composition. Kidron *et al.* (2003) showed that in early-stage BSCs dominated by cyanobacteria, chlorophyll *a* concentration (used as a proxy for phototroph abundance) was linearly and positively related to increased surface runoff, but that the inclusion of a moss-dominated BSC reduced surface runoff (Kidron *et al.* 2003). This phenomenon has further been shown by Xiao *et al*. (2011), Chamizo *et al.* (2012), and Kidron *et al.* (2012).

A further study by Zaady *et al.* (2013) showed that in semi-arid lands, agricultural practices have long-term impacts on hydrological processes. Four agricultural practices from the area were simulated, and 16 years later the long-term impact of these practices relative to control plots was investigated. Scraping (the removal of the top 2 cm of soil to simulate tillage) and spraying (of herbicide to kill phototrophic organisms) led to decreased hydraulic conductivity and increased overland flow relative to bare control plots. However, mowing

(spreading of mown perennial vegetation to simulate grazing practices) and simulated vehicle tracks increased hydraulic activity and decreased overland flow relative to control plots.

1.5.4 The biological soil crust of temperate environments

Whilst there is a large body of work relating to the distribution, development, diversity and ecology of BSCs in arid and semi-arid lands (Garcia-Pichel *et al.* 2001; Redfield *et al.* 2002; Yeager *et al.* 2004; Abed *et al.* 2010; Zhang *et al.* 2011), the lack of knowledge regarding BSCs in temperate soils represents a significant research gap. However, the few studies that have been carried out in temperate environments do show consistency with arid land research. Initially, Jeffery *et al.* (2007) showed that when undisturbed for six months, microbial community phenotypic profiles changed markedly with depth in the first centimetre of an arable soil. Later work (Jeffery *et al.* 2009) revealed that spectral quality of light influenced the temporal development of the microbial phenotype at the surface of an arable soil, hypothesised to be driven by the presence of photoautotrophs at the soil surface. Furthermore, phototrophic community structure and successional development in a temperate system in the upper Rhine valley was shown to be similar to that seen in arid lands (Langhans *et al.* 2009a; Yeager *et al.* 2004). Phototrophic organisms were investigated by culture enrichment and direct determination, identifying cyanobacteria and eukaryotic algae commonly found in arid systems. These included *Chlamydomonas* sp., *Chlorella* sp., *Nostoc* sp., *Microcoleus* sp., and *Tolypothrix* sp. (Langhans *et al.* 2009a). The pattern of temperate BSC succession

was similar to arid lands, dominated by cyanobacteria and algae in early successional stages, developing into moss-dominated systems in late successional BSCs (Langhans *et al.* 2009a).

BSCs form a physical crust at the soil surface, and in temperate climates were shown to adversely affect the germination and emergence of a range of perennials, and have a species-dependent effect on a range on annuals (Langhans *et al.* 2009b). This is similar to arid lands, where lichen-dominated BSCs have been shown to adversely affect the germination, emergence and survival of desert grasses (Deines *et al.* 2007), and short moss-dominated BSCs have been shown to adversely affect the germination efficiency of seeds of four desert grasses (Serpe *et al.* 2006). However, though emergence, survival, and establishment were inhibited in temperate environments, the plants that did survive profited from a crust-associated increase in nitrogen, increasing growth, height and biomass (Langhans *et al.* 2009b).

1.5.5 Why study the agricultural importance of the BSC and phototrophs?

Loss of soil via erosive overland flow is a major route of pesticide loss in the agricultural environment (particularly the particle-associated flow), and a study into the occurrence of phototrophs in cropland soil and their impact on soil erosion highlighted the potential importance of phototrophs in reducing this loss (Knapen *et al*. 2007). Phototroph presence and surface coverage was determined by visual assessment in 62 fields covering 300 ha, comprised of winter wheat, maize, and sugar beet. A phototrophic layer was present in 74% of fields, and

16% of those fields had a surface cover of between 75% and 100%. It was further determined in laboratory flume experiments that soil detachment rates were reduced by 37% and 79% in the presence of algal- and moss-dominated crusts, respectively, relative to bare soil (Knapen *et al.* 2007). Whilst it has been shown that phototrophic communities form readily under temperate agricultural cropping systems, their community structure, development, and ecological importance are not well understood. Knapen *et al.* (2007) did distinguish three stages of BSC formation in cropland soils, from; (i) development of a physical surface seal by raindrop action, (ii) colonisation of the soil by algae (iii) establishment of mosses as the dominant life form. Further to this, Davies *et al.* (2013b) showed that after 80 days incubation under non-UV light/dark cycles, phototrophic communities in a temperate pasture soil were dominated by the diazotrophic cyanobacterium *Nostoc punctiforme,* consistent with observations of late successional crusts in BSCs in arid and semi arid lands (Garcia-Pichel *et al*. 2001; Yeager *et al.* 2004; Abed *et al.* 2010; Zhang *et al.* 2011; Nagy *et al.* 2005). It was also shown that phototrophic, bacterial, and fungal community structure was significantly different in light incubated systems relative to dark (Davies *et al.* 2013b).

Understanding the agricultural importance of phototrophs and their potential effects on soil structure could help inform better management practices. If the presence of phototrophs and associated crusts under cropping systems has such a profound effect on erosive reduction in the field, then a shift to no- or minimum-tillage strategies could be appropriate for farms at risk from erosive runoff. However, this may be counteracted by the ability of BSCs to impact the

germination efficiency and establishment of plants, so a tillage regime may be more appropriate.

Phototrophs, and associated BSCs, could play a role in the fate of CPPs in agricultural systems. When established, these CPPs act as the interface between the terrestrial environment and the atmosphere, and so their interaction with CPPs should not be ignored. Laboratory tests designed to deduce the rate and route of transformation, and the persistence and accumulation of a CPP should aim to simulate the physical, chemical, and biological properties of the soil as accurately as possible.

Whilst it is known that non-UV light impacts the rate of CPP degradation in a regulatory-like laboratory system (Davies *et al.* 2013a), it is not known if this effect of degradation is soil specific. Similarly, it is known that photrophic BSCs develop under cropping systems in temperate agricultural environments (Knapen *et al.* 2007), though it is unknown whether this affects the degradation or movement of CPPs in the environment, and if crop canopy cover has an effect on the BSCs forming under cropping systems.

1.6 AIMS AND OBJECTIVES

The overall aims of the work described in this thesis were two-fold. The first aim was to determine if non-UV light influenced the degradation rate and fate of CPPs in a different soil used to Davies *et al.*, in both laboratory and field systems, in order to ensure that effects observed previously were not an artefact of the soil type used. The second aim was to investigate the influence of light on the development of soil surface bacterial and phototrophic communities in simulated agricultural systems.

The thesis has been divided into six sections, with the general introduction (Chapter 1) preceding four self-contained experimental chapters (Chapters 2-5), each comprised of their own aims, methods, results, and discussion sections, followed by a general discussion (Chapter 6).

Chapter 2 aimed to determine if the effects of non-UV light on CPP degradation previously seen in an OECD 307-like test system were replicated in a novel soil. The question addressed was:

(i) Are there soil-to-soil differences in the non-UV light effect on CPP biodegradation?

Chapter 3 aimed to determine the effect of the spectral quality of light on the environmental fate of two CPPs. The questions addressed were:

(i) *Is the effect of light on degradation observed previously in a regulatory-like study also seen in a more environmentally realistic setting?*

(ii) *Does the spectral quality of light affect the biodegradation of two CPPs in soil cores incubated in the field?*

(iii) *Does the spectral quality of light affect the movement of parent compound in the soil?*

Chapter 4 aimed to determine if the spectral quality of light influenced the development of microbial communities at the soil surface treated with two different pesticides. The questions addressed were:

(i) *Does treatment of the soil with different CPPs influence bacterial and phototrophic community structure?*

(ii) *Does the spectral quality of light influence bacterial community structure at the soil surface?*

(iii) *Does the spectral quality of light influence phototrophic community structure at the soil surface?*

(iv) *Are there temporal/successional changes in phototroph and bacterial communities?*

Chapter 5 aimed to determine if crop canopy characteristics influenced the development of microbial communities in soil. The questions addressed were:

(i) *Does the soil surface harbour bacterial and phototroph communities that are distinct from underlying bulk soil?*

(ii) *Do crop canopy characteristics affect the development of bacterial communities in soil?*

(iii) *Do crop canopy characteristics affect the development of phototrophic communities in soil?*

CHAPTER 2: THE IMPACT OF NON-UV LIGHT ON CPP FATE IN AN OECD 307 REGULATORY-LIKE SYSTEM

2.1 INTRODUCTION

OECD Guideline 307 details the protocols to be used for investigating the aerobic and anaerobic transformation of a test chemical within the soil environment (OECD Guideline 307). The guideline states that the soil used within such a system should be sieved to ≤2 mm, maintained at constant moisture (pF2-2.5) and that samples be kept in constant darkness at a temperature of 20°C ±2°C for the duration of the test. These conditions are not comparable to those that test chemicals may encounter within the field environment (Davies *et al.* 2013a). The differences in conditions such as soil structure, and variable temperature and moisture, could influence the microbial populations present in the soil, affecting community composition and structure, and overall biomass. As the studies are conducted in the dark, the development of photoautotrophic communities, which are known to form readily at the surface of the soil in temperate arable systems, may be affected (Knapen *et al.* 2007). It is therefore likely that the OECD 307 guidelines lead to estimates of biodegradability of test substances that deviate from degradability observed in the environment.

Previous work within an adapted OECD 307 regulatory-like system (Davies *et al.* 2013a) concluded that non-UV light, used to exclude the possibility of photodegradation, influences the degradation rate of crop protection products (CPP). In a single time point screen of eight compounds of varying modes of action and classes of chemistry, five exhibited faster rates of degradation when the systems were exposed to non-UV light relative to samples kept in standard dark conditions, while one compound, cinosulfuron, exhibited a slower rate of degradation. In further work, time taken for half of the amount of benzovindiflupyr to degrade ($DegT_{50}$) was halved, and $DegT_{90}$ for chlorotoluron was also halved, in samples kept in non-UV light conditions. This phenomenon has also been observed in a similarly-adapted OECD guideline 308 (OECD Guideline 308) regulatory-like system investigating CPP transformation in water/sediment systems (Thomas and Hand 2011). Compared to a standard test system, the inclusion of non-UV light cycles in (separate) algal and macrophyte compartments resulted in increased rates of degradation, though no direct role could be attributed to the phototrophic communities. Further work (Thomas and Hand 2012) isolated sub-communities and species from these systems, and demonstrated significant degradation of the fungicide fludioxonil in their presence, demonstrating the potential role that phototrophic communities could play in xenobiotic degradation in the environment.

Previous work on the effect of non-UV light on the degradation of CPPs in soil used a single soil only, and it is unclear whether non-UV light has similar effects on CPP biodegradation in different soils. The main purpose of this study was to investigate if there were soil-to-soil differences in the non-UV light effect

on the biodegradation of CPPs previously reported by Davies *et al.* (2013a). This study was carried out using the same regulatory-like system, with a contrasting soil.

2.1.1 Question to be addressed

(i) Are there soil-to-soil differences in the non-UV light effect on CPP biodegradation?

2.2 MATERIALS AND METHODS

2.2.1 Soil

A clay loam (CL) soil was sourced from Boughton Loam Ltd (Northampton) in spring 2010, and is referred to subsequently as 'Boughton Loam' (BL). The properties of BL are shown in Table 2.1, alongside Gartenacker, a silt-loam pasture soil used in previous Warwick-Syngenta work (Davies *et al.* 2013a). The soil was installed in a 4 x 3.5 metre glasshouse plot at Syngenta Limited (Jealott's Hill International Research Centre, RG42 6EY, UK). In the growing season prior to use in this experiment, linseed was grown as a green manure crop. Soil used in the laboratory based degradation studies was sampled from the top 10 cm of this installed soil. Soil for use in the first tranche of regulatory-like degradation studies (pesticide A, fludioxonil, cinosulfuron) was sampled and processed in late November 2011. Soil for use in the second tranche of degradation studies (benzovindiflupyr and paclobutrazol) was sampled and processed in early July 2013. Soil was sieved to ≤ 2mm and used within 3 months of collection, in line with OECD guideline 307.

Soil was characterized at NRM laboratories (Bracknell, Berkshire). pH was measured potentiometrically in deionised water and calcium chloride (0.01M) using a (dry)soil:water ratio of 1:2.5 by mass. Organic matter (OM) and water holding capacity were reported as % w/w on a dry soil basis, with OM determined by loss on ignition, and water holding capacity (WHC) by mass by pressure plate at field capacity (0.33 Bar) and wilting point (15 Bar). Cation exchange capacity was determined by sodium saturation, and reported as meq/100g on a dry soil

basis. The particle size distribution was determined by a Pipette sedimentation method, and textural class assigned using the UK classification scheme. Results are reported as % w/w mineral fraction.

2.2.2 Test chemical/CPPs

Studies were performed using [^{14}C]-radiolabelled CPPs. The compounds used were; (i) [^{14}C]-pesticide A (specific activity (spec ac) 2.02 MBq/mg); (ii) [pyrrole-4-^{14}C]-fludioxonil (spec ac 1.469 MBq/mg); (iii) [triazinyl-U-^{14}C]-cinosulfuron (spec ac 2.327 MBq/mg); (iv) [triazolyl-U-^{14}C]-paclobutrazol (spec ac 4.281 MBq/mg); (v) [Pyrazole-5-^{14}C]-benzovindiflupyr (spec ac 5.62 MBq/mg). The structures of the compounds and positioning of [^{14}C]-labelling are shown in Figure 2.1. A summary of relevant characteristics is presented in Table 2.2. The rationale for choosing the CPPs used in this study was based on their contrasting responses to the inclusion of light in the regulatory-like system. In previous work in the same regulatory-like system (Davies *et al*. 2013a), benzovindiflupyr and fludioxonil displayed increased rates of degradation, and cinosulfuron a decreased rate of degradation. The response of paclobutrazol degradation to non-UV light was previously investigated in a soil core test system internally at Syngenta, with preliminary evidence suggesting a difference between persistence in light and dark treatments (Hand pers. comms). Pesticide A was previously investigated in a regulatory-like test system, displaying increased rates of degradation under light conditions relative to dark, but the structure and physical characteristic information cannot be given due to commercial sensitivity.

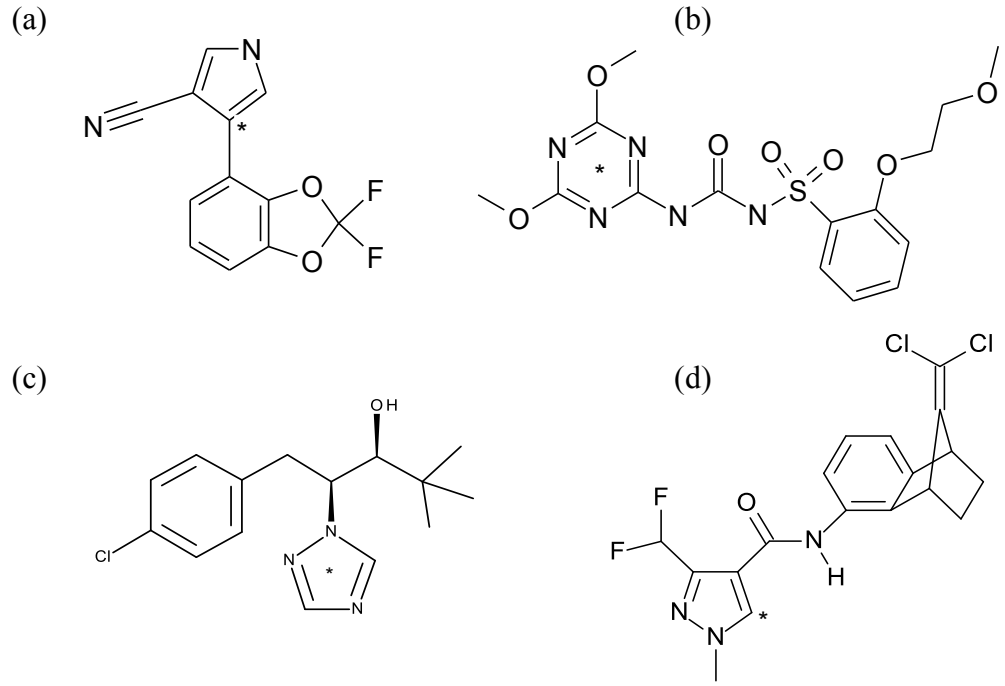

Figure 2.1: Structures of CPPs used in lab degradation studies: (a) Fludioxonil (b) Cinosulfuron, (c) Paclobutrazol, (d) Benzovindiflupyr. Radiolabel position is denoted by an asterisk. The structure of pesticide A is not shown.

Table 2.1: A comparison of physical soil characteristics between Gartenacker and Boughton Loam soils.

Soil	Classification	pH		% OM	CEC	Particle size analysis (%)			Water Holding Capacity (%)	
		H_2O	0.01M $CaCl_2$		meq/100 g	Sand (2.00-0.063mm)	Silt (0.063-0.002mm)	Clay (<.002mm)	1/3 bar	15 bar
Gartenacker	Silt Loam	6.9	6.6	4.1	10.1	34	52	14	29.6	16
Boughton Loam	Clay Loam	7	6.7	4.2	24.3	40	28	32	24.4	15.3

Table 2.2: Selected information of the CPPs investigated. Information was taken from EFSA conclusions for fludioxonil, paclobutrazol, and benzovindiflupyr (EFSA Journal 2007, 2010 & 2015), and from Tomlin (2006) for cinosulfuron.

Name	Type	Formula	K_{OC} (mL/g)	Henry's Law Constants (Pa m^3 $mol^{-1)}$	$DegT_{50}$ In Lab (Days)	$DegT_{50}$ In Field (Days)	Mode of Action
Fludioxonil	Phenylpyrrole fungicide	$C_{12}H_6F_2N_2O_2$	12000-385000	5.4×10^{-5}	119->365	8 - 43	Inhibits a protein kinase involved in a regulatory step of cell division
Cinosulfuron	Sulfonylurea herbicide	$C_{15}H_{19}N_5O_7S$	ca. 20	$<1 \times 10^{-6}$	ca. 20	ca. 3	Inhibits biosynthesis of essential amino acids valine and isoleucine
Paclobutrazol	Azole plant growth regulator (PGR)	$C_{15}H_{20}ClN_3O$	37.4 - 665.3	2.39×10^{-5}	27 - 618	14 - 202	PGR taken into xylem. Translocated to apical meristems. Produces more compact plants
Benzovindiflupyr	Triazole fungicide	$C_{18}H_{15}Cl_2F_2N_3O$	3172 - 4507	1.3×10^{-6}	596 - 1216	25 - 304	Succinate dehydrogenase inhibitor. Prevents ergosterol production

2.2.3 The transformation of [^{14}C]-labelled CPPs in an aerobic environment

2.2.3.1 Test system

The system design was based upon OECD guideline 307, represented diagrammatically in Figure 2.2. Approximately 100 g dry weight equivalent (dwe) of BL soil at 27-30% (pF 2-pF 2.5) moisture content by mass was transferred to 250 ml test vessels. Samples were pre-incubated for 7 d under experimental conditions. Soil moisture content was monitored once every two weeks (by weight) and maintained at starting weight by the addition of UltraPure Water (UPW). The system was closed, with air drawn by a pump from the environment, and bubbled through a bottle containing UPW to provide a continuous moist airflow through the system. Air passed through the test vessel and into an outlet trap (containing X ml 2M NaOH) to capture any mineralised [^{14}C]-compound. Samples were incubated under a light/dark cycle or continuous dark conditions. Those kept in the dark were placed in a controlled temperature (CT) room, maintained at 20 ±2°C. Samples exposed to 16:8 hour non-UV light/dark cycles were kept incubated in a Sanyo Gallenkamp Environmental Chamber (Model no. ML350) at 20 ± 2°C.

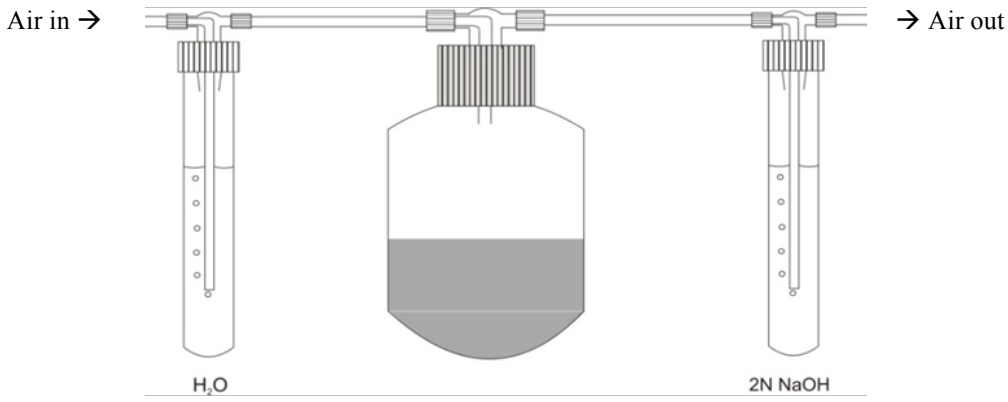

Figure 2.2: A schematic of the OECD 307 regulatory-like system used.

2.2.3.2 Light spectra

Light was produced in the Sanyo cabinet by Philips Master fluorescent lights (>360 nm) TLD 36Q/840. A spectral profile of the light produced was recorded using a Bentham Instruments Ltd photomultiplier DH-3 (DM150 double monochromator) with a Bentham cone diffuser sn 9941 probe. The profile obtained was compared against spectral profiles of natural sunlight from spring (April) and summer (June), shown in Figure 2.3. The majority of light was at wavelengths >380 nm, non-UV light/visible light. The Sanyo cabinet produced a small peak of UV-A between 360-380 nm, however this was only 1.65% of the total energy in the system, and <2.3% of the UV energy present in April and June readings. It was important that UV light was not present in the regulatory-like test system, as it has the potential to both affect microorganisms (Lin *et al.* 1997), and to photodegrade CPPs (Burrows *et al.* 2002).

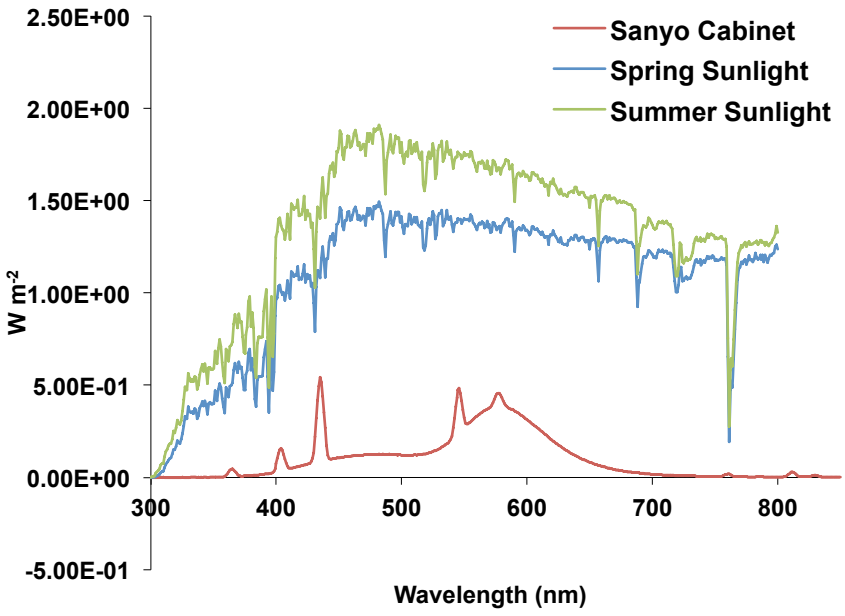

Figure 2.3: Spectral profile comparison between spring, summer, and Sanyo cabinet light.

2.2.3.3 Moisture and temperature

OECD Guideline 307 stipulates that temperature should be maintained at 20°C ± 2°C for the duration of the test. Temperature was recorded using CoMark N1001 Thermometer logging systems with probes inserted into test vessels containing soil with no test chemical applied, maintained alongside the experimental series. Temperature was monitored during the tests involving pesticide A, fludioxonil, and cinosulfuron, with no perturbations recorded. Moisture was maintained at 29.8% on a mass basis every two weeks.

For the paclobutrazol and benzovindiflupyr tests, the temperature of the CT room containing the dark kept samples was monitored by an inbuilt system. The temperature of the Sanyo cabinet was monitored using a CoMark N1001 Thermometer logging system, with the temperature probe placed in a test vessel containing soil with no test chemical applied. The average temperature of the CT room was 20.9°C, and the Sanyo cabinet 20.5°C. There were 19 days where the daily average temperature of dark-kept samples exceeded 22°C ≥76 days after treatment (DAT), with an average daily temperature of 24.47°C, and a maximum average daily temperature of 27.48°C. Temperature spikes were determined not have had an effect on degradation rates of either benzovindiflupyr or paclobutrazol. Moisture was maintained at 27.5% on a mass basis every two weeks.

2.2.4 Application of CPPs

Compounds were applied at, or close to, field application rates to ensure environmental relevance, with example calculations shown in Appendix I, Section I.1. Target and actual application rates are summarised in Table 2.3. Cinosulfuron was applied at 127% desired application rate; however, this was believed to have no impact on the study and was, therefore, deemed acceptable.

Test compounds were dissolved from stock solutions in acetonitrile at a desired nominal concentration. Triplicate pre-application checks were taken and analysed by liquid scintillation counting (LSC) (see Section 2.2.6). The application volume required to apply at the desired rate was calculated. The compound was applied drop wise onto the soil surface using a micropipette. After the final application, triplicate post-application checks were taken, and the results of the pre and post-application checks averaged to determine the average application rate (see Appendix I, Section I.2).

Table 2.3: Target and actual application rates of CPPs in OECD 307-like lab degradation study.

Compound	Target Application Rate (µg g^{-1})	Actual Application Rate (µg g^{-1})	Target Field Application Rate (g ai/ha)	Actual Field Application Rate (g ai/ha)
Pesticide A	0.267	0.266	200	199.8
Fludioxonil	0.267	0.247	200	185.8
Cinosulfuron	0.133	0.168	100	126.7
Paclobutrazol	0.133	0.138	100	103.6
Benzovindiflupyr	0.100	0.102	75	76.1

Post-application, vessels were hand-rolled to distribute the compound throughout the soil. Soil attached to the vessel sides was dislodged, and visible clumps of soil broken up with a spatula.

2.2.5 Sampling and extraction of CPPs

Samples were taken destructively, in triplicate, at six time points, across a compound-appropriate time course (detailed below), which was determined by assessing the previous work of Davies *et al*. (2013a) and published $DegT_{50}$ values (see Table 2.2). 0 DAT samples were taken within 30 minutes of compound application. Sampling times were as follows:

Pesticide A and fludioxonil: 0, 14, 30, 59, 90, 120 DAT

Paclobutrazol and benzovindiflupyr: 0, 14, 30, 61, 90, 118 DAT

Cinosulfuron: 0, 3, 7, 14, 30, 60 DAT

All compounds were extracted from soil using three rounds of solvent extraction, comprising 150 ml of 80:20 solvent:UPW (v/v). Following addition of solvent, samples were shaken at 300 rpm for 1 hour, centrifuged at 2000 rpm for 10 minutes; with extract decanted and pooled with successive extractions (Thomas and Hand 2011; Davies *et al*. 2013). Pesticide A, fludioxonil, cinosulfuron, and benzovindiflupyr were extracted using acetonitrile:UPW, and paclobutrazol with methanol:UPW. The third round of solvent extraction was adjusted to pH 3 with formic acid, except for cinosulfuron.

2.2.6 Analysis of crop protection product fate

Total [^{14}C]-activity recovered in solvent extracts and $^{14}CO_2$ traps was quantified by LSC. All extracts were quantified gravimetrically (i.e. concentration expressed per unit mass of soil extracted). Duplicate, weighed 1 ml samples were added directly to 5 ml of ScintSafe Gel™ scintillation cocktail. The amount of radioactivity present was then quantified using a Packard Tri-Carb 2910 TR or 3100 TR liquid scintillation analyser with automatic quench correction (Perkin-Elmer, Boston, MA). Each extract was counted for 5 mins. Prior to calculation of each result, a background count rate was determined and subtracted from each sample count rate. The total mass of the solvent extract was measured, and the total activity in the solvent extract solution calculated.

The amount of $^{14}CO_2$ present in the NaOH traps was quantified by volume. The volume of each trap was recorded, and duplicate 2 ml aliquots were combined with 10 ml Hionic Fluor LSC gel (Perkin-Elmer), and quantified as above. Total activity in each trapping solution was then calculated.

The [^{14}C]-activity remaining in the soil fraction after solvent extraction was termed non-extractable residue (NER), and was quantified by sample oxidation using a Packard Oximate 80 Model 307 (PerkinElmer). Samples were dried to constant mass, and homogenised to a fine powder using a Gyro-mill (Glen Creston Ltd; Pulverisette 5, Fritsch). Triplicate aliquots (approx. 0.25 g) were prepared in cardboard cups, and two drops of Combustaid (Perkin-Elmer) was added to the sample from a 5 ml plastic pasteur pipette immediately prior to oxidation. The combustion products were absorbed in Carbo-Sorb®, mixed with

Permafluor®E+ and the radioactivity determined by LSC using automatic quench correction. Each sample was counted for 5 mins with background correction. Dried soil mass was measured, and the total activity remaining as NER in the soil calculated.

The total [^{14}C] activity recovered from each fraction was quantified as a percentage of total applied radioactivity (AR), and summed to give a mass balance for each vessel (example shown in Appendix I, Section I.3). For samples to be included in the full analysis, mass balance was required to be within 90-110% of applied radioactivity, in accordance with acceptable criteria outlined in OECD guideline 307.

Solvent extracts were analysed using High Performance Liquid Chromatography (HPLC) to determine percentage parent remaining in the sample. Aliquots were concentrated to at least 1 000 Bq ml^{-1} prior to analysis using a sample concentrator, a Dri-Block DB-3D (Techne), incorporating a continuous dry and filtered air flow. Samples were concentrated to dryness and re-suspended in 1 ml of 50:50 (v/v) solvent (as used in extraction):UPW. Recoveries of 90-110% of were deemed acceptable, and were checked by LSC. An example is shown in Appendix I, Section I.4.

Pesticide A, cinosulfuron, and fludioxonil samples were analysed by HPLC using an Agilent HP1100 HPLC system connected to a LabLogic β-RAM radio-HPLC detector, in conjunction with LAURA software v4.04.101. Paclobutrazol and benzovindiflupyr were analysed using an Agilent HP1200 HPLC system connected to a flow scintillation analyser Radiomatic 625TR (PerkinElmer) in conjunction with LAURA software v4.1.14.96. Reverse phase

gradient elution was used, with samples run on a Hichrom ACE5 C18 column. Pesticide A, cinosulfuron, and fludioxonil were analysed on a column of 250 mm x 4.6 mm with 5 µm particle size. Paclobutrazol and benzovindiflupyr were analysed on a column of 250 mm x 4 mm with 5 µm particle size.

Pesticide A samples were analysed using a linear gradient starting at 95% 0.1% aqueous formic acid: 5% acetonitrile, progressing to 65% acetonitrile: 35% 0.1% aqueous formic acid over 30 mins, then progressing to 99% acetonitrile: 1% 0.1% aqueous formic acid by 31 mins, with conditions maintained through to 35 mins.

Fludioxonil samples were analysed using a gradient starting at 95% 0.1% aqueous formic acid: 5% acetonitrile for 5 mins, before progressing on a linear gradient to 100% acetonitrile at 25 mins. Conditions then reverted to starting conditions on a linear gradient over 2 mins.

Cinosulfuron samples were analysed by starting with a linear gradient at 95% 0.1% aqueous formic acid: 5% acetonitrile, progressing to 50% acetonitrile: 50% 0.1% aqueous formic acid over 35 mins. The final conditions were maintained until 37 mins.

Paclobutrazol samples were analysed on a linear gradient starting at 75% 0.1% aqueous formic acid: 25% acetonitrile, progressing to 95% acetonitrile: 5% 0.1% aqueous formic acid over 10 mins. The final conditions were maintained until 25 mins.

Benzovindiflupyr samples were analysed on a linear gradient starting at 95% 0.1% aqueous formic acid: 5% acetonitrile, progressing to 95% acetonitrile:

5% 0.1% aqueous formic acid over 25 mins, with the final conditions maintained through to 30 mins.

Resulting chromatograms were analysed using LAURA software (LabLogic, Sheffield, UK). Background subtraction was applied, and automatic peak detection employed. Chromatograms were individually assessed to quality check the peak detection, and any missing peaks attributed. Region Of Interest (ROI) was automatically calculated and presented as part of the chromatogram report. Example chromatogram traces for all compounds are shown in Appendix I, Section I.5. The levels of parent compound remaining were determined with the calculation below.

$$\text{Remaining Parent} = \frac{(\%\ Applied\ Radioactivity\ Extracted \times ROI\ \ (\%))}{100}$$

2.2.7 Degradation kinetics

The $DegT_{50}$ and degradation rates of the test compounds were estimated using Computer Aided Kinetic Evaluation (CAKE) v2.0, a modelling program that conforms to FOCUS (Forum for the Co-ordination of pesticide fate models and their Use) requirements (FOCUS 2006). ANOVA was used to determine if there were significant differences between the remaining parent compound by treatment and time, and if there was a significant interaction effect between treatment and time.

Two different kinetic models were used for assessing the degradation of the compounds investigated in this test, single first order (SFO) and hockey-stick (HS). The following explanations are taken from FOCUS guidelines (2006). SFO refers to first order kinetics. The time taken for a decrease in the concentration by a certain percentage is constant and it assumes that the number of pesticide molecules is small relative to the number of degrading microorganisms and their enzymes. It is a simple exponential equation with only two parameters, M_0 and k. The model is shown below.

$M = M_0 \exp^{(-kt)}$

M = Total amount of chemical present at time t

M_0 = Total amount of chemical present at time = 0

k = Rate constant [d^{-1}]

The HS model consists of two sequential first order curves. Initially there is degradation according to first-order kinetics (k_1), but at a certain time point (referred to as the 'break point') the rate constant changes to a different value (k_2). For typical bi-phasic patterns, the rate constant k_1 is usually larger than k_2. The model has four parameters, M_0, k_1, k_2 and t_b. The model is shown below.

$M = M_0 \exp^{(-k1\ t)}$ For $t \leq t_b$

$M = M_0 \exp^{(k1\ tb)} \exp^{-k2(t-tb)}$ For $t > t_b$

M = Total amount of chemical present at time t

M_0 = Total amount of chemical present at time = 0

k_1 = Rate constant until break point ($t = t_b$)

k_2 = Rate constant from $t = t_b$

t_b = Breakpoint (time at which rate constant changes)

Several acceptance requirements had to be met before accepting the model fit relating to visual assessment, goodness of fit (χ^2 <15%), assessment of whether degradation rate >0 (t-test, Prob ≤0.05), and correlation between observed and expected values (r^2 ≥0.7).

Pesticide A, benzovindiflupyr and cinosulfuron were analysed using the HS model, with the break point set at 14 DAT for all compounds and conditions. Paclobutrazol and fludioxonil were analysed using SFO.

2.2.8 Statistical Analysis

Where possible, parametric tests were performed on non-transformed data. If assumptions of homoscedasticity (variance of the data within groups) were not met, large residuals (identified in initial ANOVA analysis) were investigated and, where appropriate, data were log transformed. Two-way ANOVA (with treatment, time, and treatment*time) was used to compare time course data sets, and t-tests were performed on single time points for comparison to previous work that had used single time point sampling. Errors are presented ±1 Standard Error (S.E). All analyses were performed using Genstat v.13.2 (VSN International) and figures were plotted using Sigmaplot v.12.5.

Mineralisation data were analysed by ANOVA without data transformation. As mineralisation represents such a low percentage of total applied radioactivity (AR), the mineralisation data sets can contain a large number of 0 values and low variation. This reduces the residual mean squares, meaning

that background variability is decreased, and so significance can be overestimated. To account for this over-estimation of significance, results were pragmatically assessed to determine whether or not significance attributed from the ANOVA is real. This was done by looking at graphed data and assessing any differences subjectively.

2.3 RESULTS

2.3.1 Pesticide A

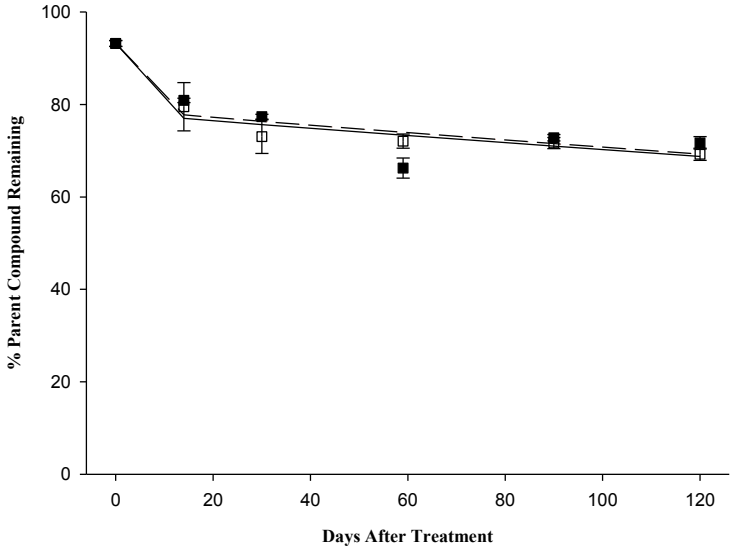

Figure 2.4: Extractable parent compound for pesticide A under light (□) and dark (■) conditions. The fitted hockey-stick models are shown as (——) for light predicted, and (- - -) for dark predicted kinetics.

Transformation of pesticide A is shown in Figure 2.4, and parent levels shown in Table 2.4. Parent declined from 93.20% at 0 DAT, to 69.24% and 71.71% under light and dark conditions, respectively, at 120 DAT. Time to $DegT_{50}$ was calculated as 487 d under both light and dark conditions. However as parent levels only declined to ~70% for both treatments at 120 DAT, these values should be taken with caution, as any error in the fitted model is extrapolated over time (kinetic model breakdown for all compounds is displayed in Table 2.9 at the end of the results section; HS - BP 14 DAT; $\chi 2 \leq 4.1\%$; $r^2 > 0.8$). There were no significant differences in pesticide A transformation between light and dark

conditions (p=0.652), and no significant treatment*time interaction was seen (p=0.323). There was a highly significant (p≤0.001) decline in parent compound over time.

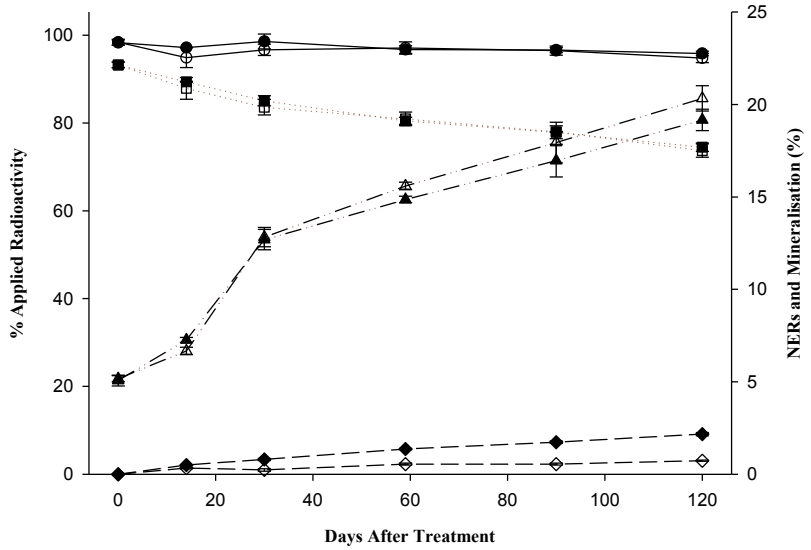

Figure 2.5: Mass balance for pesticide A under light (open symbols) and dark (closed symbols) conditions. Overall mass balance (—●—), and solvent extractable radioactivity (·····■·····) are shown on y-axis one. NERs (—·▲·—), and mineralization (—◆—) are shown on y-axis 2.

Average mass balance of pesticide A, and a breakdown of the fractions summed to give the mass balance, are shown in Figure 2.5 and detailed in Table 2.4. Mass balances were between 90% and 102% for all samples. There was no significant effect of light treatment (p=0.222) or sampling time (p=0.141), and no significant treatment*time interaction was seen (p=0.794).

The percentage of applied radioactivity recovered in the solvent extract declined in both treatments from an average of 93.23% at 0 DAT, to 73.73% and 74.50% at 120 DAT, under light and dark conditions respectively. Sampling time had a

highly significant ($p \leq 0.001$) effect on solvent-extractable radioactivity, although light treatment had no significant effect ($p=0.469$), and there was no treatment* time interaction ($p=0.948$).

NERs increased from 5.12% at 0 DAT, to 20.33% and 19.17% at 120 DAT, under light and dark conditions, respectively. There was a trend of higher NER formation under light relative to dark at 59, 90, and 120 DAT, though these differences were not significant ($p=0.077$, $p=0.523$, $p=0.262$). Overall, time was highly significant in NER formation ($p \leq 0.001$), light treatment ($p=0.247$) was not a significant factor, and there was no significant treatment*time interaction ($p=0.323$).

Mineralisation of pesticide A progressed to 0.73% and 2.17% under light and dark conditions respectively at 120 DAT. Treatment, sampling time, and treatment*time had highly significant effects on mineralization ($p \leq 0.001$), which was higher under dark relative to light conditions from ≥30 DAT.

Table 2.4: A breakdown of the average radioactivity present in the fractions summed to give the overall mass balance of pesticide A under light and dark conditions. Parent compound remaining is also shown. Errors, in brackets, represent ±1 S.E.

LIGHT

DAT	Solvent Extract (% AR)	NERs (% AR)	Mineralisation (% AR)	Mass Balance (% AR)	% Parent Compound
0	93.23 (0.64)	5.17 (0.17)	0.00 (0.00)	98.40 (0.67)	93.20 (0.63)
14	87.90 (2.48)	6.67 (0.20)	0.33 (0.03)	94.90 (2.28)	79.52 (5.23)
30	83.60 (1.77)	12.83 (0.52)	0.23 (0.07)	96.67 (1.28)	73.05 (3.64)
59	80.95 (1.55)	15.60 (0.21)	0.55 (0.05)	97.10 (1.40)	72.08 (1.54)
90	78.00 (0.10)	17.95 (1.10)	0.55 (0.05)	96.50 (1.05)	71.67 (1.20)
120	73.73 (1.51)	20.33 (0.68)	0.73 (0.03)	94.80 (1.04)	69.24 (1.32)

DARK

DAT	Solvent Extract (% AR)	NERs (% AR)	Mineralisation (% AR)	Mass Balance (% AR)	% Parent Compound
0	93.23 (0.64)	5.07 (0.29)	0.00 (0.00)	98.30 (0.60)	93.20 (0.63)
14	89.40 (0.10)	7.27 (0.13)	0.50 (0.00)	97.17 (0.03)	80.90 (0.47)
30	85.07 (1.16)	12.70 (0.55)	0.80 (0.06)	98.57 (1.69)	77.37 (0.53)
59	80.50 (0.81)	14.87 (0.18)	1.37 (0.03)	96.73 (0.86)	66.26 (2.17)
90	77.90 (1.47)	16.97 (0.88)	1.73 (0.07)	96.60 (0.57)	72.81 (0.69)
120	74.50 (0.95)	19.17 (0.58)	2.17 (0.09)	95.83 (0.50)	71.71 (1.34)

2.3.2 Benzovindiflupyr

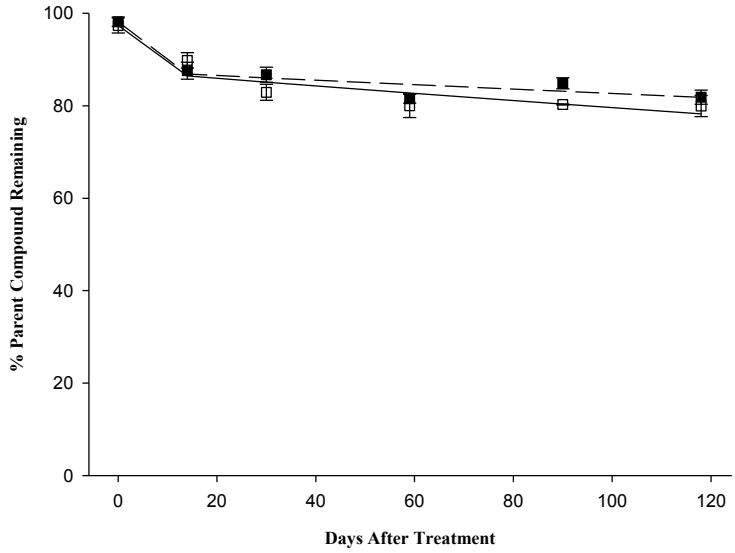

Figure 2.6: Extractable parent compound for the fungicide benzovindiflupyr under light (□) and dark (■) conditions. The fitted hockey-stick models are shown as (——) for light predicted, and (- - -) for dark predicted kinetics.

Transformation of benzovindiflupyr is shown in Figure 2.6, and parent levels shown in Table 2.5. Parent declined from 97.37% and 98.19% at 0 DAT under light and dark, to 79.94% and 81.85% at 120 DAT. Time to $DegT_{50}$ calculated under light conditions was 615 d, and 1020 d under dark conditions. However parent levels only declined to ~80% for both treatments by 118 DAT, and although parent levels were slightly lower under light conditions for ≥30 DAT, there is no certainty the trend would continue past 120 DAT (HS - BP 14 DAT; $\chi 2$ ≤2.2%; r^2 >0.73). There were no significant differences in benzovindiflupyr transformation between light and dark conditions (p=0.076), and no significant treatment*time interaction was seen (p=0.381). Time had a highly significant (p≤0.001) on benzovindiflupyr transformation.

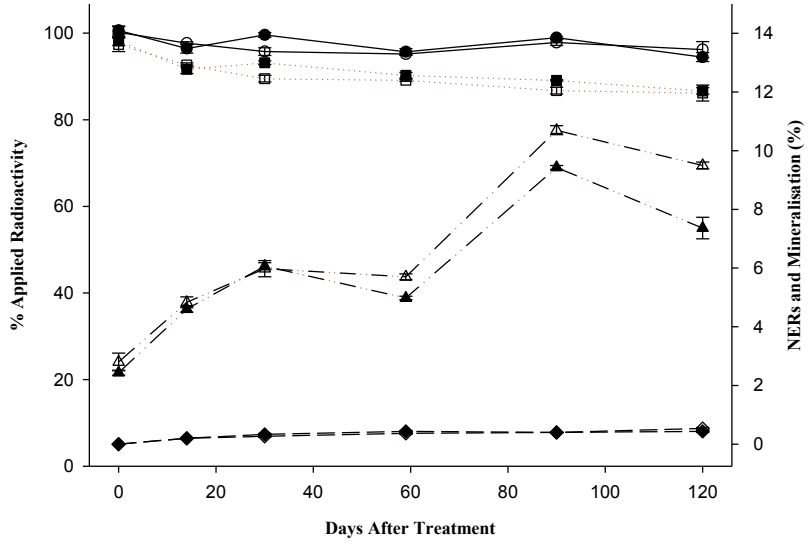

Figure 2.7: Mass balance for the fungicide benzovindiflupyr under light (open symbols) and dark (closed symbols) conditions. The partitioned radioactivity is shown for overall mass balance (——●——), and solvent extract (·····■·····) on y-axis one. NERs (—··▲··—), and mineralization (— —◆— —) are shown on y-axis 2.

Average mass balance of benzovindiflupyr, and a breakdown of the fractions summed to give mass balance, are shown in Figure 2.7 and detailed in Table 2.5. Mass balances were between 92% and 102% for individual samples. There was no significant effect of light treatment on mass balance ($p=0.337$), and no significant treatment*time interaction was seen ($p=0.077$). Time ($p<0.001$) significantly affected mass balance.

The percentage of applied radioactivity recovered in the solvent extract declined over the time course for both treatments, from 97.37% and 98.19% at 0 DAT under light and dark respectively, to 86.17% and 86.67% at 118 DAT, with a greater percentage recovered under dark conditions for four of five sampling points (excluding 0 DAT). Light treatment ($p=0.018$) and time ($p\leq0.001$)

significantly affected solvent extractable radioactivity, though treatment*time interaction did not (p=0.182).

NERs increased from 2.80% and 2.43% at 0 DAT under light and dark respectively, to 9.50% and 7.37% at 118 DAT. A greater % AR was recovered as NERs under light conditions relative to dark ≥ 59 DAT, significantly so at 90 and 118 DAT ($p \leq 0.05$, $p \leq 0.01$). Light treatment ($p \leq 0.001$) and time ($p \leq 0.001$) significantly affected NER formation, and a significant treatment*time interaction was seen (p=0.012).

Mineralisation levels were characteristically low, progressing to 0.53% and 0.43% at 118 DAT under light and dark conditions, with no significant effect of treatment (p=0.693). Time ($p \leq 0.001$) significantly affected mineralisation, and there was a significant treatment*time interaction (p=0.024), although pragmatically, this is probably an overestimation of significance.

Table 2.5: A breakdown of the average radioactivity present in the fractions summed to give the overall mass balance of benzovindiflupyr under light and dark conditions. Parent compound remaining is also shown. Errors, in brackets, represent ±1 S.E.

LIGHT

DAT	Solvent Extract (% AR)	NERs (% AR)	Mineralisation (% AR)	Mass Balance (% AR)	% Parent Compound
0	97.37 (1.62)	2.80 (0.30)	0.00 (0.00)	100.17 (1.32)	97.37 (1.62)
14	92.65 (0.47)	4.83 (0.19)	0.20 (0.00)	97.69 (0.33)	89.83 (1.66)
30	89.50 (0.76)	5.98 (0.27)	0.27 (0.03)	95.75 (0.89)	82.92 (1.74)
61	89.23 (0.24)	5.70 (0.10)	0.37 (0.03)	95.19 (0.24)	80.01 (2.55)
90	86.73 (0.77)	10.70 (0.15)	0.40 (0.00)	97.83 (0.67)	80.28 (0.12)
118	86.17 (1.84)	9.50 (0.12)	0.53 (0.03)	96.20 (1.86)	79.94 (2.29)

DARK

DAT	Solvent Extract (% AR)	NERs (% AR)	Mineralisation (% AR)	Mass Balance (% AR)	% Parent Compound
0	98.19 (1.01)	2.43 (0.09)	0.00 (0.00)	100.62 (1.03)	98.19 (1.01)
14	91.64 (0.97)	4.60 (0.10)	0.20 (0.00)	96.44 (1.06)	87.59 (1.83)
30	93.18 (0.45)	6.06 (0.12)	0.33 (.03)	99.57 (0.55)	86.73 (1.62)
61	90.28 (0.66)	4.98 (0.06)	0.43 (0.03)	95.70 (0.76)	81.53 (0.96)
90	89.10 (0.15)	9.43 (0.07)	0.40 (0.00)	98.93 (0.20)	84.87 (1.19)
118	86.67 (0.73)	7.37 (0.37)	0.43 (0.03)	94.47 (1.04)	81.85 (1.52)

2.3.3 Cinosulfuron

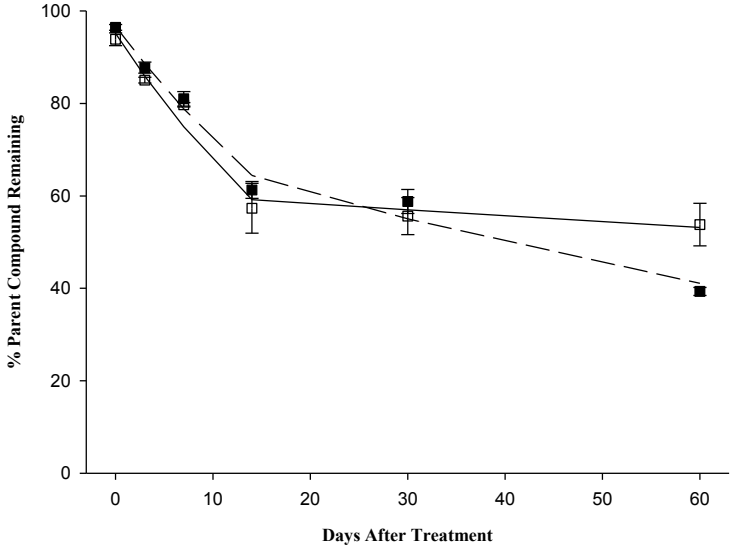

Figure 2.8: Extractable parent compound for the herbicide cinosulfuron under light (□) and dark (■) conditions. The fitted hockey-stick models are shown as (——) for light predicted, and (- - -) for dark predicted kinetics.

Transformation of cinosulfuron is shown in Figure 2.8, and parent levels shown in Table 2.6. After an initial, comparable, degradation phase to 14 DAT, the parent compound declined faster in the dark- than in the light-incubated treatment following the break point. Parent levels reached 53.81% and 39.32% at 60 DAT under light and dark respectively. Although there was no significant effect by treatment overall (p=0.931), parent remaining was significantly higher under light conditions at 60 DAT ($p \leq 0.05$). As a result, calculated time to $DegT_{50}$ of cinosulfuron was over twice as fast in dark relative to light incubated samples, at 43 days and 111 days, respectively (HS - BP 14 DAT; $\chi 2 \leq 2.9\%$; $r^2 > 0.89$). This outcome is dependent on the final sampling point, and further time points would have helped determine confirm its validity. There was a significant decline

in parent over time ($p \leq 0.001$), and there was a significant treatment*time interaction ($p=0.014$).

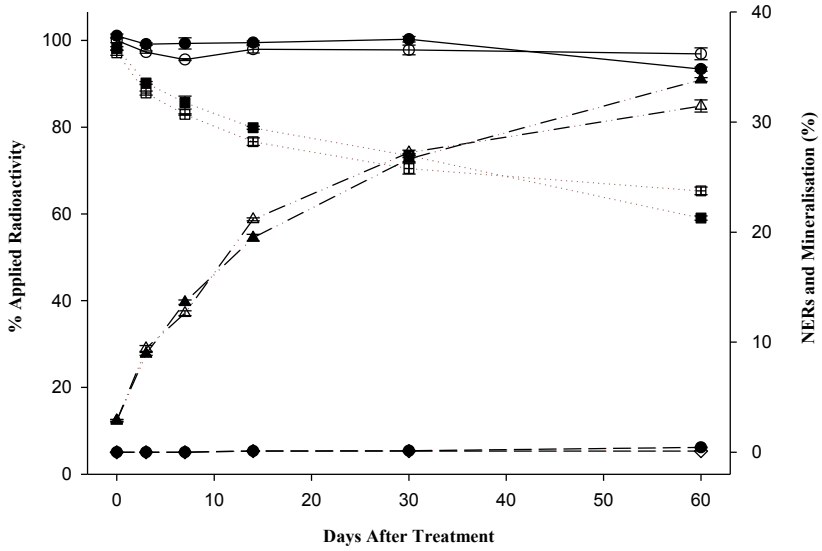

Figure 2.9: Mass balance for the herbicide cinosulfuron under light (open symbols) and dark (closed symbols) conditions. The partitioned radioactivity is shown for overall mass balance (—●—), and solvent extract (·····■·····) on y-axis one. NERs (—▲—), and mineralization (— ◆ —) are shown on y-axis 2.

Average mass balance of cinosulfuron, and a breakdown of the fractions summed to give mass balance, are shown in Figure 2.9 and detailed in Table 2.6. Mass balances were between 92% and 102% for all samples. Dark samples had a higher average mass balance at 0, 3, 7, 14, and 30 DAT. There was a significant effect of light treatment ($p=0.016$), and time ($p \leq 0.001$) on mass balance, and the treatment*time interaction was significant ($p=0.002$).

In light samples, the percentage applied radioactivity recovered in the solvent extract decreased from 97.13% at 0 DAT to 65.33% at 60 DAT, and in the dark samples from 98.17% at 0 DAT to 59.07% at 60 DAT. There was a higher

percentage of applied radioactivity recovered from dark samples at 0, 3, 7, 14, and 30 DAT relative to light samples, with 60 DAT being the only sampling point where a greater percentage of applied radioactivity was recovered in the solvent extract from the light samples. Light treatment ($p=0.028$) and time ($p\leq0.001$) significantly affected recovery of applied radioactivity, and there was a significant treatment*time interaction ($p\leq0.001$).

NER formation increased over time from 2.87% under both conditions at 0 DAT, to 31.47% and 33.87% at 60 DAT under light and dark, respectively. Although there was no overall significant effect of light treatment on NER formation ($p=0.682$), NER was significantly higher under dark conditions at 60 DAT ($p\leq0.05$). Time had a highly significant effect on NER formation ($p\leq0.001$), and there was a significant treatment*time interaction ($p=0.014$).

Cinosulfuron mineralisation was low, rising to 0.43% of applied radioactivity at 60 DAT under dark conditions, and just 0.10% under light conditions. Light treatment ($p\leq0.001$) and time ($p\leq0.001$) had highly significant effects on mineralisation, and there was a significant treatment*time interaction. However, pragmatically, this is probably an overestimation of significance due to the low values involved.

Table 2.6: A breakdown of the average radioactivity present in the fractions summed to give the overall mass balance of Cinosulfuron under light and dark conditions. Parent compound remaining is also shown. Errors, in brackets, represent ±1 S.E.

LIGHT

DAT	Solvent Extract (% AR)	NERs (% AR)	Mineralisation (% AR)	Mass Balance (% AR)	% Parent Compound
0	97.13 (0.55)	2.87 (0.09)	0.00 (0.00)	100.00 (0.52)	93.89 (1.38)
3	87.87 (0.46)	9.43 (0.27)	0.00 (0.00)	97.30 (0.25)	85.05 (0.62)
7	82.93 (0.17)	12.63 (0.22)	0.00 (0.00)	95.57 (0.22)	79.72 (0.47)
14	76.67 (0.86)	21.17 (0.13)	0.10 (0.00)	97.93 (0.84)	57.33 (5.38)
30	70.47 (1.27)	27.23 (0.22)	0.10 (0.00)	97.80 (1.11)	55.65 (4.01)
60	65.33 (0.87)	31.47 (0.55)	0.10 (0.00)	96.90 (1.37)	53.81 (4.58)

DARK

DAT	Solvent Extract (% AR)	NERs (% AR)	Mineralisation (% AR)	Mass Balance (% AR)	% Parent Compound
0	98.17 (0.38)	2.87 (0.12)	0.00 (0.00)	101.03 (0.43)	96.46 (0.61)
3	90.20 (0.31)	8.93 (0.13)	0.00 (0.00)	99.13 (0.29)	87.75 (1.20)
7	85.67 (1.49)	13.63 (0.20)	0.00 (0.00)	99.30 (1.29)	81.01 (1.57)
14	79.87 (0.34)	19.50 (0.31)	0.10 (0.00)	99.47 (0.42)	61.30 (1.82)
30	73.47 (0.47)	26.67 (0.28)	0.13 (0.03)	100.27 (0.63)	58.81 (2.60)
60	59.07 (0.50)	33.87 (0.18)	0.43 (0.03)	93.37 (0.47)	39.32 (0.85)

2.3.4 Paclobutrazol

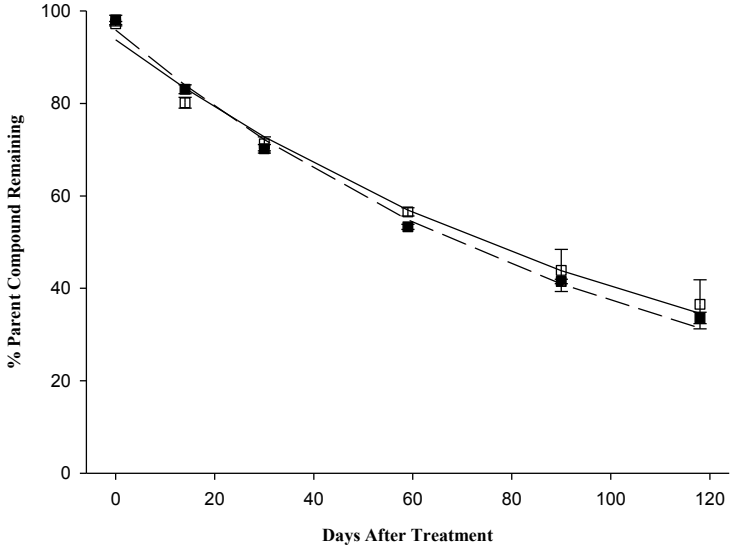

Figure 2.10: Extractable parent compound for the plant growth regulator paclobutrazol under light (□) and dark (■) conditions. The fitted single first order models are shown as (——) for light predicted, and (- - -) for dark predicted kinetics.

Transformation of paclobutrazol is shown in Figure 2.10, and parent levels shown in Table 2.7. Parent declined across the 118 DAT time course from 97.25% and 98.07% under light and dark, to 36.54% and 33.59%. Time to $DegT_{50}$ calculated under light and dark treatments were similar, at 82 d and 73 d under light and dark treatments respectively (SFO; $\chi 2 \leq 2.7\%$; $r^2 > 0.95$). There were no significant differences in paclobutrazol transformation between light and dark treatments ($p=0.45$), nor a significant treatment*time interaction ($p=0.099$). There was a highly significant ($p \leq 0.001$) decline in parent compound over time.

Average mass balance of paclobutrazol, and a breakdown of the fractions summed to give mass balance, are shown in Figure 2.11 and detailed in Table 2.7.

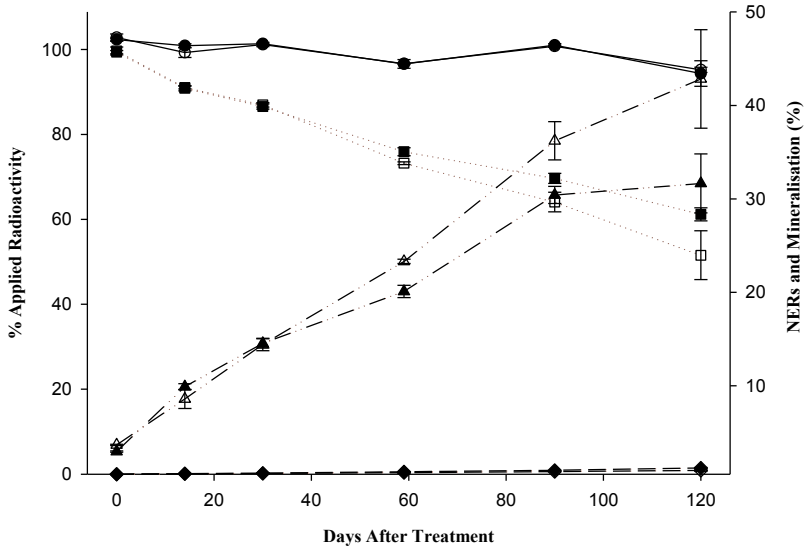

Figure 2.11: Mass balance for the plant growth regulator paclobutrazol under light (open symbols) and dark (closed symbols) conditions. The partitioned radioactivity is shown for overall mass balance (—●—), and solvent extract (·····■·····) on y-axis one. NERs (—·▲·—), and mineralization (— —◆— —) are shown on y-axis 2.

Mass balances of individual samples were between 90% and 105%, Average mass balance fluctuated across the time course, and declined slightly at 118 DAT to 95.20% and 94.33% under light and dark respectively. There was no significant effect of light treatment ($p=0.876$), and no significant treatment*time interaction was seen ($p=0.780$). Time ($p\leq0.001$) had a highly significant effect on mass balance.

The percentage of applied radioactivity recovered in the solvent extract decreased across the time course, with a lower percentage recovered under light conditions at 61, 90, and 118 DAT. At 0 DAT, 99.65% and 99.37% of applied radioactivity was recovered under light and dark conditions, and this reduced to 51.57% and 61.20% at 118 DAT. Light treatment ($p=0.019$) and time ($p\leq0.001$) significantly

affected solvent extractable radioactivity, though a significant treatment*time interaction was not seen ($p=0.088$).

NER formation increased over the time course and was slightly higher in samples incubated in the light relative to dark. Formation of NERs rose from 3.17% and 2.97% respectively under light and dark at 0 DAT, to 42.76% and 31.66% at 118 DAT. Light treatment was a significant factor in the formation of NERs ($p=0.023$), although time did significantly ($p\leq0.001$) affect NER formation, and a significant treatment*time interaction was observed ($p=0.026$).

Rate of mineralisation levels were low, rising to 1.47% at 118 DAT under dark, and 0.87% under light. Light treatment ($p\leq0.001$) and time ($p\leq0.001$) significantly affected mineralisation, and a significant treatment*time interaction was seen ($p=0.002$). However, as levels of paclobutrazol mineralisation are so low, it is unclear if this difference in mineralisation is truly significant.

Table 2.7: A breakdown of the average radioactivity present in the fractions summed to give the overall mass balance of paclobutrazol under light and dark conditions. Parent compound remaining is also shown. Errors, in brackets, represent ±1 S.E

LIGHT

DAT	Solvent Extract (% AR)	NERs (% AR)	Mineralisation (% AR)	Mass Balance (% AR)	% Parent Compound
0	99.65 (0.93)	3.17 (0.07)	0.00 (0.00)	102.81 (0.82)	97.25 (0.47)
14	91.05 (0.32)	8.13 (1.03)	0.10 (0.00)	99.28 (1.16)	80.15 (1.17)
30	86.98 (0.52)	14.03 (0.67)	0.17 (0.03)	101.17 (0.50)	71.26 (1.50)
61	73.23 (0.32)	23.03 (0.24)	0.37 (0.03)	96.63 (0.16)	56.56 (0.88)
90	64.10 (2.30)	36.07 (2.07)	0.60 (0.00)	100.77 (0.25)	43.86 (4.58)
118	51.57 (5.76)	42.76 (5.33)	0.87 (0.20)	95.20 (0.61)	36.54 (5.30)

DARK

DAT	Solvent Extract (% AR)	NERs (% AR)	Mineralisation (% AR)	Mass Balance (% AR)	% Parent Compound
0	99.37 (0.38)	2.97 (0.07)	0.00 (0.00)	102.33 (0.37)	98.07 (1.02)
14	90.87 (0.60)	9.90 (0.32)	0.10 (0.00)	100.87 (0.49)	83.09 (0.96)
30	86.57 (0.62)	14.54 (0.49)	0.23 (0.03)	101.34 (0.11)	70.20 (0.92)
61	75.93 (0.93)	20.09 (0.65)	0.57 (0.03)	96.59 (1.03)	53.32 (0.54)
90	69.67 (1.19)	30.43 (0.91)	0.90 (0.00)	101.00 (0.37)	41.48 (0.49)
118	61.20 (1.54)	31.66 (3.15)	1.47 (0.12)	94.33 (3.01)	33.59 (1.23)

2.3.5 Fludioxonil

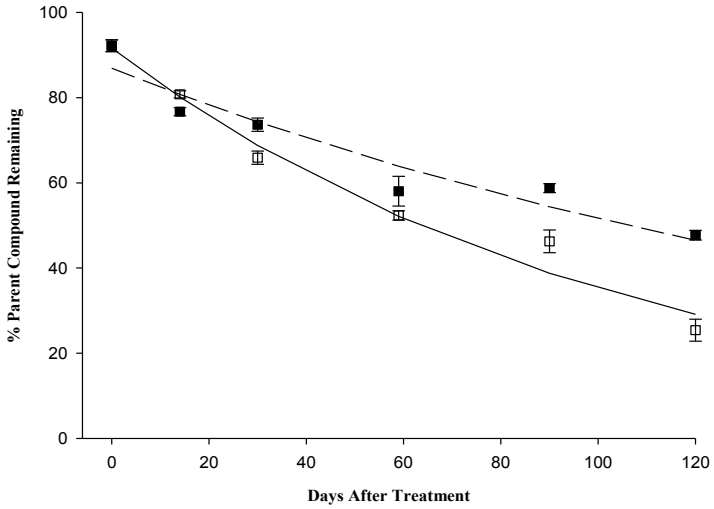

Figure 2.12: Extractable parent compound for the fungicide fludioxonil under light (□) and dark (■) conditions. The fitted single first order models are shown as (——) for light predicted, and (- - -) for dark predicted kinetics.

Transformation of fludioxonil is shown in Figure 2.12, and parent levels shown in Table 2.8. Fludioxonil transformation was more rapid under light conditions than dark. Parent declined from 92.19% at 0 DAT, to 25.41% and 47.73 % at 120 DAT, under light and dark conditions respectively. Calculated time to $DegT_{50}$ was 1.84 times slower under dark than light conditions, at 133 d and 73 d respectively (SFO; $\chi 2 \leq 4.8\%$; $r^2 > 0.89$). Both light treatment ($p \leq 0.001$) and time ($p \leq 0.001$) significantly affected transformation, and the treatment*time interaction seen was also significant ($p \leq 0.001$).

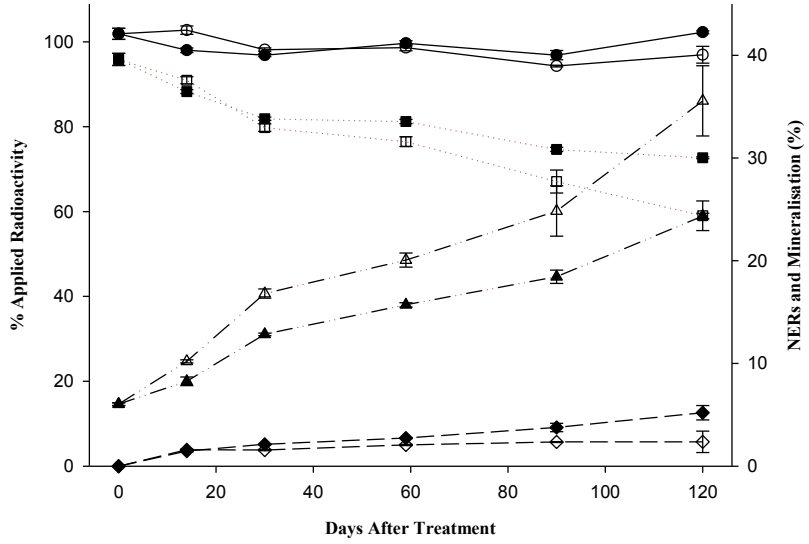

Figure 2.13: Mass balance for the fungicide fludioxonil under light (open symbols) and dark (closed symbols) conditions. The partitioned radioactivity is shown for overall mass balance (——●——), and solvent extract (·····■·····) on y-axis one. NERs (—··▲··—), and mineralization (— —◆— —) are shown on y-axis 2.

Average mass balance of fludioxonil, and a breakdown of the fractions summed to give mass balance, are shown in Figure 2.13 and detailed in Table 2.8. Mass balances were between 94% and 105%, and generally fluctuated over time, from 101.90% at 0 DAT to 96.97% and 102.27% at 120 DAT under light and dark conditions respectively. Light treatment did not significantly affect mass balance ($p=0.444$), although time did ($p\leq0.001$), and there was a significant treatment*time interaction ($p=0.002$).

The percentage of applied radioactivity recovered in the solvent extract decreased over time, with less applied radioactivity recovered under light relative to dark conditions. Percentage applied radioactivity declined from 95.87% at 0 DAT to 59.03% and 72.70% under light and dark conditions respectively. Light treatment

($p<0.001$) and time ($p<0.001$) significantly affected solvent extractable radioactivity, and there was a significant treatment*time interaction ($p<0.001$).

NER formation increased over the time course for both treatments, although formation was higher in light relative to dark conditions. Formation increased from 6.03% at 0 DAT, to 35.37% and 24.37% under light and dark respectively at 120 DAT. Light treatment ($p\leq0.001$) and time ($p\leq0.001$) significantly affected fludioxonil NER formation, and there was a significant treatment*time interaction ($p=0.005$).

Mineralisation of fludioxonil rose to 5.20% and 2.37% at 120 DAT under light and dark conditions, respectively. Light treatment ($p\leq0.001$) and time ($p\leq0.001$) significantly affected mineralisation, and the observed treatment*time interaction was significant ($p=0.010$).

Table 2.8: A breakdown of the average radioactivity present in the fractions summed to give the overall mass balance of fludioxonil under light and dark conditions. Parent compound remaining is also shown. Errors, in brackets, represent ±1 S.E.

LIGHT

DAT	Solvent Extract (% AR)	NERs (% AR)	Mineralisation (% AR)	Mass Balance (% AR)	% Parent Compound
0	95.87 (1.43)	6.03 (0.13)	0.00 (0.00)	101.90 (1.30)	92.19 (1.39)
14	90.97 (0.83)	10.20 (0.15)	1.60 (0.06)	102.77 (0.98)	80.78 (0.83)
30	79.80 (0.90)	16.80 (0.45)	1.57 (0.07)	98.17 (0.42)	65.93 (1.55)
59	76.50 (1.15)	20.07 (0.70)	2.07 (0.07)	98.63 (0.72)	52.36 (1.19)
90	67.10 (2.70)	24.85 (2.45)	2.35 (0.05)	94.30 (0.20)	46.27 (2.69)
120	59.03 (3.49)	35.57 (3.41)	2.37 (1.04)	96.97 (1.97)	25.41 (2.58)

DARK

DAT	Solvent Extract (% AR)	NERs (% AR)	Mineralisation (% AR)	Mass Balance (% AR)	% Parent Compound
0	95.87 (1.43)	6.03 (0.13)	0.00 (0.00)	101.90 (1.30)	92.19 (1.39)
14	88.30 (0.46)	8.27 (0.42)	1.47 (0.09)	98.03 (0.57)	76.72 (0.94)
30	81.90 (0.38)	12.83 (0.12)	2.13 (0.03)	96.87 (0.33)	73.66 (1.57)
59	81.23 (0.49)	15.70)0.21)	2.73 (0.03)	99.67 (0.62)	58.05 (3.49)
90	74.67 (0.50)	18.43 (0.65)	3.77 (0.41)	96.87 (1.09)	58.76 (1.04)
120	72.70 (0.21)	24.37 (0.27)	5.20 (0.70	102.27 (0.35)	47.73 (1.14)

Table 2.9: Kinetic models used for analysis of parent degradation in an OECD 307 regulatory-like system. Key parameters included are goodness of fit (χ^2), correlation of between observed and expected (r^2), probability that degradation rate > 0 (Prob > t), and $DegT_{50}$ values. The break point of the Hockey-Stick kinetics was set at 14 DAT for all analyses.

	Model	χ^2 (%)	r^2	Prob. > t	$DegT_{50}$ (days)
Pesticide A - Light	Hockey Stick	1.84	0.7797	k1, 3.15E-16; k2, 0.01017	487
Pesticide A - Dark	Hockey Stick	4.10	0.7935	k1, 6.83E-05; k2, 0.009724	487
Benzovindiflupyr - Light	Hockey Stick	2.17	0.7316	k1, 0.001197; k2, 0.003762	615
Benzovindiflupyr Dark	Hockey Stick	1.52	0.8236	k1, 1.39E-05; k2, 0.01022	1020
Cinosulfuron – Light	Hockey Stick	2.80	0.8983	k1, 2.99E-07; k2, 0.107	111
Cinosulfuron – Dark	Hockey Stick	2.86	0.9730	k1, 2.30E-09; k2, 2.30E-09	43
Paclobutrazol – Light	SFO	2.69	0.9507	k1, 2.39E-11	82
Paclobutrazol – Dark	SFO	2.12	0.9915	k1, 3.60E-17	73
Fludioxonil - Light	SFO	4.78	0.9685	k1, 8.20E-12	73
Fludioxonil - Dark	SFO	4.78	0.8950	k1, 3.43E-09	133

2.4 DISCUSSION

The inclusion of light in an adapted OECD 307 regulatory-like system using a clay-loam (CL) soil had a compound-specific effect on the rate of CPP degradation. Light significantly altered the rate of degradation of two out of five compounds, and increased the rate of NER formation for three out of five compounds. The effects seen were generally similar to those observed previously in a silt-loam (SL) soil (Davies *et al*. 2013a), suggesting a generic, rather than a soil specific, effect. Whilst the observed effects were generally similar, there were differences in the magnitude of the effect between studies. A variety of mechanisms could be responsible for the observed effects and the differences between soils, including the proliferation of phototrophic communities, pH shifts, and the physical characteristics of the soils.

Previously, non-UV light was shown to affect the persistence of certain CPPs within an adapted regulatory like system (Davies *et al.* 2013a), with four of the compounds from this study, fludioxonil, cinosulfuron, pesticide A and benzovindiflupyr, investigated previously by Davies *et al.* (2013a). The same effects on persistence were seen in a CL soil for two of the four compounds previously investigated, fludioxonil and cinosulfuron.

In Davies *et al.* (2013a), fludioxonil was sampled at a single time point at 69 DAT. Parent compound was significantly lower under light conditions relative to dark ($p \leq 0.01$), reaching 42% and 66% under light and dark, respectively. This effect was also seen here in CL soil with differences in parent transformation

between light and dark from 30 DAT onwards, evident by the generated $DegT_{50}$ values of 73 d and 133 d.

Cinosulfuron was included in this study in order to investigate its degradation kinetics in a different soil as it had behaved atypically in the previous compound screen, with higher persistence under light compared to dark conditions (Davies *et al.* 2013a). In the SL soil, sampled at 34 DAT, significantly less parent compound ($p \leq 0.05$) remained under dark conditions (28%) relative to light (42%). In the CL soil used in this study, ANOVA of parent degradation revealed no significant overall differences in cinosulfuron degradation between light and dark treatments. However, the atypical effect was also observed in the CL soil at 60 DAT ($p \leq 0.05$), with remaining parent compound significantly higher under light conditions relative to dark (54% and 39% respectively). As the Davies *et al.* (2013a) study only reported single time points, it is unclear if the same degradation profile would also have been seen in the SL soil. Additional data points beyond 60 DAT in this study to further investigate the nature of cinosulfuron behaviour would have been useful, though it can be concluded that the atypical effect was seen across soil types.

In the SL soil the $DegT_{50}$ of benzovindiflupyr almost halved under light conditions from 373 d to 183 d (Davies *et al*. 2013). While the $DegT_{50}$ values were markedly higher in this study, the calculated $DegT_{50}$ values showed a similar pattern in this CL soil, with $DegT_{50}$ roughly halving from 1020 d in the dark to 615 d under light conditions. However, ANOVA of the parent compound remaining shows that light treatment was not a significant factor ($p=0.076$). The main issue with deriving $DegT_{50}$ values from the models when compounds have

not degraded close to, or past, 50% AR is that when extrapolating, any error in the fitted model is exacerbated. As the data sets are so close to one another, it is not possible to state whether the effect seen is the same as observed previously. This issue of extrapolation also arises in the analysis of the degradation of pesticide A, although as the calculated $DegT_{50}$ is the same under both light and dark conditions (487 d), it is the accuracy of the generated $DegT_{50}$ values that is of concern, not whether any differences observed between treatments, are real.

These observed differences in transformation rates are not restricted to this test system. A similar impact of light on the rate of CPP transformation was observed in a non-UV light adapted water/sediment system based on OECD guideline 308 (Thomas and Hand 2011). In the sediment/water system, fludioxonil showed a 20-fold enhancement in transformation compared to dark controls, with persistence reduced considerably under light conditions for chlorotoluron (four-fold enhancement), prometryn (five-fold enhancement), and propiconazole (seven-fold enhancement). Several mechanisms have been mooted to try and explain these differences in CPP transformation across systems. A number of studies (Sethunathan *et al.* 2004; Cai *et al.* 2007; Caćeres *et al.* 2008; Mostafa and Helling 2011) have demonstrated the ability of phototrophic organisms to directly degrade CPPs in axenic culture. Fludioxonil was later shown to be directly degraded by eight green algae and four cyanobacteria isolated from the regulatory systems used by Thomas and Hand in 2011, confirming a direct involvement of certain green algae and cyanobacteria in CPP degradation (Thomas and Hand 2012).

Soil pH could also influence the transformation of CPPs indirectly, by impacting both physical properties of CPPs and microbial communities within the soil. The introduction of light/dark cycles could cause pH to rise within the test system, as actively photosynthesising communities within the soil take up acidic CO_2 during the light phase. This effect was seen previously for benzovindiflupyr in Davies *et al.* (2013a), with pH increasing over time in light conditions but not under dark conditions, with the soil in light kept samples 0.4 pH units higher relative to dark at 120 DAT. A similar effect was also seen in Davies *et al.* (2013a) in the chlorotoluron time course, with soil pH 0.2 units higher under light conditions relative to dark at 60 DAT.

Inclusion of non-UV light into the test system also affected the pattern of NER formation. In the SL soil, NER formation was significantly higher under light conditions for benzovindiflupyr and fludioxonil (Davies *et al*. 2013a). In the CL soil used here NER formation was also significantly higher under light conditions for benzovindiflupyr ($p \leq 0.001$) and fludioxonil ($p \leq 0.001$), and although not previously investigated by Davies *et al.* (2013a), paclobutrazol NER formation was significantly higher under light conditions relative to dark ($p=0.023$)

Fludioxonil NER formation reached between 30-35% in the SL soil, and 35% in the CL. Whilst the magnitude of NER formation was similar between soils, the differences between light and dark were distinct, with a 3.5 fold increase in the SL soil in light compared to dark, and a 1.45 fold increase in the CL soil. Light had the same effect on benzovindiflupyr NER formation in both soil types. NER formation in the SL was similar between treatments until 24 DAT, before

increasing under light conditions at later time points. Formation was higher under light relative to dark at 59 DAT, and significantly higher at 90 and 120 DAT ($p \leq 0.05$, $p \leq 0.01$). A similar effect was seen in the CL soil, with NER formation similar between treatments until 30 DAT, and then higher under light conditions at 59, 90, and 120 DAT ($p \leq 0.01$, $p \leq 0.01$, $p \leq 0.01$). As with its degradation effect, cinosulfuron NER formation was atypical, significantly higher under dark conditions ($p \leq 0.05$) at 60 DAT, though there was no overall effect of treatment.

Davies *et al.* (2013a) showed that the increase in NERs seen under light conditions could not be attributed to the assimilation of $^{14}CO_2$ into the biomass of phototrophs. This was done by accounting for the potential uptake by phototrophs of the additional $^{14}CO_2$ found in dark systems by phototrophs within the light systems, by subtracting the difference between the dark and light mineralisation values from the corresponding light NERs. Using this approach it was found that NERs were still significantly higher under light conditions for fludioxonil ($p \leq 0.01$), imidacloprid ($p \leq 0.01$), and benzovindiflupyr ($p \leq 0.001$). In this study, it was found using the same approach, that NERs were still significantly higher under light conditions for benzovindiflupyr ($p \leq 0.001$) across the time course. Treatment was no longer a significant factor in NER formation across the full time course for fludioxonil ($p = 0.165$), although NER formation was still higher under light conditions at 59, 90, and 120 DAT by 3.7%, 5%, and 8.4% respectively.

In this study, there was a trend towards higher NER formation under light conditions for pesticide A ≥14 DAT, however the difference between dark and light mineralisation was greater than the difference between NER formation

between the treatments at all time points, and so increase in NERs could potentially be explained by the differences in mineralisation between treatments.

The inclusion of non-UV light in the system also impacted the mineralisation profiles of the compounds. In the CL, CPP mineralisation was significantly higher under dark conditions for pesticide A and cinosulfuron. With benzovindiflupyr, there was also a trend for elevated mineralization rates in the dark treatment, although this was not significant.

Conversely, the fludioxonil mineralisation pattern in the SL soil was atypical, with mineralisation levels higher under light conditions relative to dark (12% and 14%; $p \leq 0.01$). This effect was not seen in the CL soil, with mineralisation significantly higher under dark (5.2%) compared to light (2.4%). This was the only instance where an effect of light observed in the test system was in disagreement to that previously reported by Davies *et al.* (2013a).

The effects of light observed previously in Davies *et al.* (2013a) were generally seen in this CL soil. However there were variations in the magnitude of the difference between light and dark treatments, and the overall magnitude of the effects. This could be attributable to differences between the physical characteristics of the soils (Table 2.1) affecting CPP fate. The soils used were similar in pH and organic matter content but had differing textural classes.

The CL soil contained 32% clay, whereas Gartenacker is classed as silt loam, comprised of 14% clay and 52% silt. This increase in clay content is evident in the differences in the cation exchange capacity (CEC) between the two soils, with the CEC of the CL (24.3 meg/100g) being almost 2.5 fold higher than

that of Gartenacker (10.1 meq/100g). These differences could explain the smaller differences in NER formation between the light and dark treatments in the CL soil relative to the SL. The CEC represents the capacity of the soil to hold exchangeable cations, and an increased CEC in one soil relative to another would suggest a greater ability for CPP residues to bind to the solid soil phase, increasing the NER fraction of the CPP. In the SL soil, there was a 3.5 fold increase in fludioxonil NER formation under light conditions, compared to a 1.45 fold increase in the CL soil. Though the magnitude of NER formation under light conditions was similar between soils, reaching 30-35% in SL and 35% in the CL, NER formation under dark conditions was much higher in the CL soil, reaching ~10% in the SL soil, and 24% in the CL.

CHAPTER 3: THE SPECTRAL QUALITY OF LIGHT INFLUENCES THE BEHAVIOUR OF TWO CPPS WITHIN SOIL CORES IN A FIELD SYSTEM

3.1 INTRODUCTION

A primary aim of laboratory-based regulatory studies is to investigate the behaviour of compounds under simulated environmental conditions, keeping variables (e.g. soil temperature and moisture content) that may confound results constant in an effort to catalogue the fundamental routes and rates of transformation. However, a lack of spatial and temporal variability of edaphic and climatic variables within regulatory systems can lead to the over-estimation of CPP persistence within a field environment. A review by Beulke *et al.* (2000) investigated 178 studies to compare the $DegT_{50}$ of CPPs from field studies to those obtained from modeled laboratory data, and demonstrated that persistence was over-estimated by a factor of >1.25 in 44% of studies.

The inclusion of non-UV light in a regulatory-like system based on OECD guideline 307 has been shown to influence the persistence and fate of CPPs in two classes of soil (Davies, *et al.* 2013a; Chapter 2), with light also affecting persistence in an adapted OECD guideline 308 water/sediment system (Thomas and Hand 2011). Whilst this light effect has been observed in laboratory studies, the maintenance of moisture content (pF 2-2.5), temperature (20°C ±2°C), and disruption of the soil matrix/architecture (sieved ≤2 mm) in such systems means that conditions that a compound would experience in the field are not

accurately replicated. Because of these disparities, it is unknown whether or not this effect of light would be replicated in a more environmentally relevant system.

Several hypotheses to explain the light effect on pesticide biodegradation have been mooted, including direct degradation by phototrophic microbial communities that are known to develop at the soil surface under the influence of light (Davies *et al.* 2013a; Knapen *et al.* 2007). However, current field study guidance from the European Food Standards Agency (EFSA 2010) stipulates incorporating CPPs below the soil surface by mixing of the topsoil post-application, or covering the surface with sand. All suggestions eliminate the possibility of measuring the impact and influence of soil surface processes on the degradation and movement of CPPs within field systems.

The main aim of this study was to investigate if the spectral quality of light influenced the degradation of two CPPs in a field system. Intact soil cores were pre-incubated for 60 days under three different light filters: (i) allowing all wavelengths of light through (CLEAR); (ii) restricting UV light (UV-Limited/UV-L); (iii) restricting photosynthetically active radiation (PAR-Limited/PAR-L). Two [^{14}C]-radiolabelled CPPs were applied to independent sets of cores within the semi-field system, and compound fate determined over time. $DegT_{50}$ was calculated from experimental data, and by extracting CPPs from different sections of the core, an assessment of the movement of parent compound within the core could also be made.

3.1.1 Questions to be addressed

(i) Is the effect of light on degradation observed previously in a regulatory-like study also seen in a more environmentally realistic system?

(ii) Does the spectral quality of light affect the biodegradation of two CPPs in soil cores incubated in the field?

(iii) Does the spectral quality of light affect the movement of parent compound in the soil?

3.2 MATERIALS AND METHODS

3.2.1 Soil

Refer to Section 2.2.1 for details.

3.2.2 Semi-field plot

A plot located at Jealott's Hill International Research Centre (Syngenta Limited) was used for both field experiments completed in this thesis. The plot was located in the west-end section of a glasshouse, enclosed by a 1 m high solid wall, and continued with netting to the roof on the north, west, and south faces. The net roof and sides had retractable coverings that automatically deployed PVC walls to provide cover when rain was detected. The east-facing wall was the solid wall attachment to the glasshouse. For details of experimental set up and plot set up, please see photos in Appendix II, Section II.1.

The crop canopy cover experiment detailed in Chapter 5 was conducted in 2011-2012, and therefore preceded this experiment. Between the end of the crop canopy cover experiment (October 2012) and the start of plot preparation for the field degradation study described in this Chapter (May 2013), the plot was left bare and weeds were allowed to grow. There were no anthropogenic additions to the plot during this fallow period.

3.2.3 Plot preparation

In May 2013, prior to marking out, the plot was weeded, manually turned over (using spade and fork), watered, left for a week to allow regrowth, before being weeded and turned over once more. The surface was tilled and flattened to reduce aggregate size, and leveled.

The plot was laid out with twine and pegs. Nine experimental plots, each 700 x 700 mm, were laid out in a grid design, with 300 mm spacing between adjacent plots. Within each of the 700 x 700 mm plots an external 150 mm buffer region was left, leaving a central 400 x 400 mm area. This was marked out with twine into 16, 100 x 100 mm squares. Within these 16 squares, 13 were randomly selected for core insertion (1 for environmental monitoring, 6 amended with paclobutrazol, and 6 amended with benzovindiflupyr, see Section 3.2.6). The plot was fenced off with radiochemical warning tape to comply with local radiochemical rules.

3.2.4 Light filters

The spectral quality of light transmitted to the soil surface was regulated using filters (LEE Filters, Andover, UK). Plots were covered with either: (i) DS130 – CLEAR (transmission of all wavelengths); (ii) DS 226 – UV (0% transmission of wavelengths <400 nm); (iii) DS124 – PAR (transmission of wavelengths 450-600 nm). Frames to hold the filters in place were constructed from wood (700 x 700 mm, with legs of 100 mm length and secured inside the

frame). Filters were affixed to the frames with double sided tape and staples. 50 mm wide strips of filter were secured flush to the bottom edge of the frame.

3.2.5 Light Spectra

The spectral profiles of the light wavelengths transmitted by the filters were characterised using the equipment described previously in Section 2.2.3.2. Full spectra readings were taken at three points underneath each filter, and averaged. Readings were taken from 1000-1500 on 1st August 2013, when the average air temperature was 27.21°C. The spectral profiles were then combined by treatment, to give the average treatment spectral profile.

Figure 3.1 shows the spectral profile recorded from under the CLEAR, UV-limiting (UV-L), and PAR-limiting (PAR-L) filters. The CLEAR and UV-L filters transmitted 155.50 $W.m^{-2}$ and 159.21 $W.m^{-2}$ respectively. The PAR-L filter transmitted 20.61 $W.m^{-2}$, <14% of the total energy of the CLEAR and UV-L filters.

Reduced transmission of wavelengths of light in the UV spectrum < 400 nm under the UV-L and PAR-L filters is evident. A comparison of total energy transmitted under each filter from 300–400 nm reveals that just 7.71% and 1.22% of energy was transmitted under UV-L and PAR-L filters, respectively, relative to CLEAR, significantly reducing the possibility of CPP degradation by photolysis. Comparison of the energy transmitted between wavelengths 400-700 nm, taken as the range of PAR wavelengths, reveals that the PAR-L filter

transmitted < 11.20% of the energy of both the CLEAR and UV-L filters. Over half (55%) of the total energy transmitted under the PAR-L filter was between 480 - 550 nm, outside of the range of efficient Chl *a* photosynthesis, preventing the proliferation of photosynthetic communities at the soil surface.

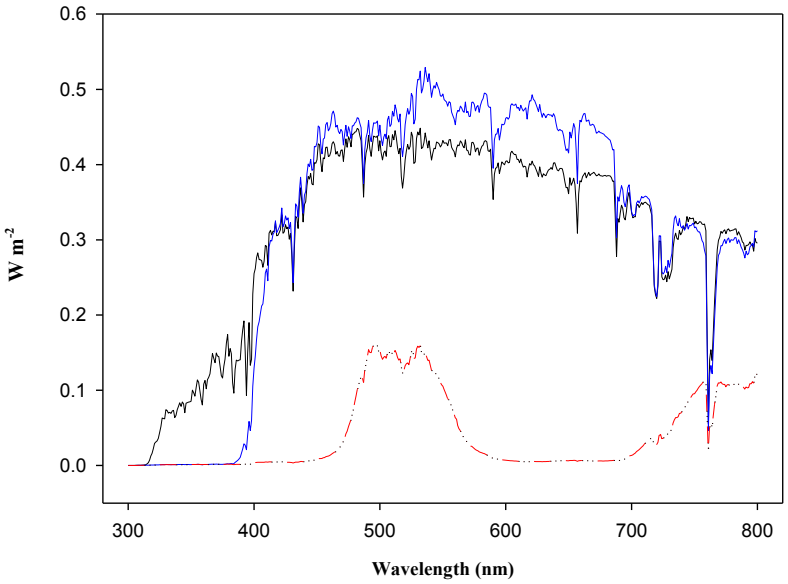

Figure 3.1: Spectral profile of light transmitted through CLEAR (black), UV-limiting (blue), and PAR-limiting (red) filters.

3.2.6 Cores

Cores were constructed of adonised aluminium, 75 x 75 mm (www.cookingmarvellous.com).. Cores were pushed almost fully into the soil, leaving a lip of several millimetres between the soil surface and the top of the core to prevent compound migration following application (See Appendix II, Figure II.2c).

They were installed in a randomised design ~2 months (60 days) before compound application, and soil surface microbiology was allowed to develop under the appropriate light filters (CLEAR, UV-L, PAR-L).

3.2.7 Moisture and Temperature

Irrigation was calculated from the average rainfall per day from July - November was taken from historical (2006-2012) meteorological office data collected at the Heathrow weather station, 20 km west of Jealott's Hill. The rate was 2.218 mm day^{-1} (1 mm rainfall equates to 1 L of water over 1 m^2). The experimental plots were 0.49 m^2, resulting in a daily watering rate of 1.087 litres $plot^{-1}$ day^{-1}. Daily watering was carried out, as it was determined that smaller, more frequent watering events would have less of an impact on compound migration than larger, less frequent events. Watering was carried out by hand, using a watering can with a fine rose applicator.

High temperatures were experienced between 16/07/13 - 15/08/13, with an average soil temperature of 17.75°C, and the plot dried quickly. A double rate of

water application was used for all plots during this period to maintain the moisture content of the soil.

Soil moisture (volumetric water content) and surface temperature was recorded in each plot from a monitoring core, with probes placed at the soil surface away from the edge of the soil core and each other. Data points were recorded every 30 mins and a daily average taken. Readings were taken using the WatchDog 1000 series micro-logging systems (Spectrum Technologies Inc.).

3.2.8 Compounds

The test compounds used in this study were also used in the Chapter 2 laboratory degradation experiments (described in Chapter 2). The compounds were [^{14}C]-labelled benzovindiflupyr and [^{14}C]-labelled paclobutrazol (see Section 2.2.2 for details). Benzovindiflupyr was chosen as it had displayed differences in degradation between light and dark conditions in both Davies, *et al.* (2013a), and internal Syngenta studies. Paclobutrazol was chosen as it had been shown to degrade relatively rapidly in several soils, and showed potential differences in degradation when exposed to light/dark cycles in internal Syngenta studies.

3.2.9 Application

Benzovindiflupyr was applied on 5th August 2013, and paclobutrazol applied one week later on the 12th August 2013. Test compounds were dissolved

in a UPW:acetonitrile mix prior to application to the soil core. Benzovindiflupyr was applied in a 75:25 v/v mix, and paclobutrazol in an 80:20 v/v mix. Compounds were applied to cores using a multi-dispensing pipette (Multipette® pro, Eppendorf). Benzovindiflupyr was applied in a 2.1 ml volume with 10 x 210 µl applications spread evenly across the core surface. Paclobutrazol was applied in a 2 ml volume with 10 x 200 µl applications spread evenly across the core surface.

Compound	Target Application Rate (µg core^{-1})	Actual Application Rate (µg core^{-1})	Target Field Application Rate (g ai/ha)	Actual Field Application Rate (g ai/ha)
Paclobutrazol	44.16	45.15	100	102.2
Benzovindiflupyr	33.12	33.44	75	75.7

Table 3.1: Target and actual application rates of Paclobutrazol and benzovindiflupyr in field degradation study

Triplicate 100 µl aliquots of the application solutions were taken pre- and post-treatment, and the application rates calculated as a percentage of target application rate, as detailed in Table 3.1. Application rates were chosen to be environmentally relevant, for an example calculations please see Appendix II, Section II.2. Paclobutrazol was applied at 102.24 g ai/ha (102.24% target). Benzovindiflupyr was applied at 75.67 g ai/ha (100.98% of target).

3.2.10 Sampling

Cores were destructively sampled according to a randomised design. Cores were taken on their designated sampling days. Cores were twisted *in situ* to physically detach the core from the surrounding soil, and the soil contained within the core from the soil below. The samples were pulled gently from the ground and transferred to the lab. Cores were split into three layers. The soil core was extruded from below using a custom made plunger, and sectioned into pre-labelled weighing boats using a sharp edge. The top 5 mm was taken as surface, 5 -30 mm taken as top bulk, and 30-55 mm taken as lower bulk.

Benzovindiflupyr cores were sampled at 0, 14, 30, 59, 90, 120 days after treatment.

Paclobutrazol cores were sampled at 0, 14, 30, 50, 70, 106 days after treatment.

3.2.11 Soil processing

Surface samples were transferred to pre-weighed beakers and frozen at -20 °C. Once frozen, samples were freeze-dried (Edwards High Vacuum International, Crawley, UK) overnight, before being transferred to storage at -20°C.

After freeze-drying, surface samples were homogenised so that aliquots of soil could be taken for downstream microbial analysis. Samples were transferred to pre-weighed beakers to determine surface soil mass. Surface samples were

homogenised using a Fritch pulverisette 5 system (30 ml bowls, 10 x 5 mm balls). Samples were run at 300 rpm for 1 minute. After homogenization samples were put through a 5 mm sieve to remove the beating balls and stones from the sample. Aliquots of soil were taken from the homogenised sample for subsequent Chl *a* (2 g), pH analysis (2 g) and DNA analysis (2 g). The mass of aliquots taken was recorded, and later used to correct the mass balance to account for the removed soil. Approximately 6 g of dry soil was removed per sample. The remaining sample was transferred to a pre-weighed extraction vessel, and the mass of the combined soil and extraction vessel recorded.

The beating balls were removed from the sieve, placed in the beaker that the sample had come from, and soaked in the appropriate extraction solvent (see Section 2.2.5) to remove any remaining CPP residue.

Stones (>2 mm) were removed from the sieve and placed in pre-weighed glassware. To check that none of the test compound had adsorped to the stones, the mass of the stones was calculated and deducted from the overall soil mass. The stones were soaked in approx. 25 ml appropriate extraction solvent (taken by mass) for half an hour, and radioactivity quantified by liquid scintillation counting (LSC) in terms of percentage applied radioactivity (AR).

Extraction solvent from the homogenising balls, and washings from the homogenisation bowl, were added to the extraction vessel, and the extraction solvent made up to approximately 100 ml. Cold solvent extraction was carried out as detailed in Section 2.2.5, using 100 ml extraction solvent, and the amount of compound in the solvent extract quantified by LSC. The percentage AR

remaining at the surface was determined by calculating a recovery per gram figure from the extracted surface soil, and multiplying by the total surface soil mass.

Top and lower bulk fractions were transferred to extraction vessels immediately after core splitting, and underwent cold solvent extraction, as detailed in Section 2.2.5 (with 175 ml of extraction solvent used instead of 150 ml). Recovery from the two fractions was then quantified gravimetrically by LSC as a percentage of AR.

3.2.12 Parent compound quantitation

Paclobutrazol and benzovindiflupyr solvent extracts containing ≥5% of applied radioactivity were concentrated for HPLC analysis, as detailed in Section 2.2.6. Any fraction containing <5% applied radioactivity (AR) was not concentrated and assumed to contain no parent compound.

Concentrated extracts were analysed by HPLC using the methods detailed in Section 2.2.6. Following HPLC analysis the surface, upper bulk, and lower bulk, 'percentage parent remaining' values were combined to give an overall value for parent compound remaining within each core as a percentage of AR (see Appendix II, Section II.5). For example chromatograms, please see Appendix II, Section II.7.

3.2.13 Non-extractable residues (NERs)

Following compound extraction, soils were initially air dried in their extraction bottles, before transfer to large weigh boats. When dried, samples were homogenised using the Fritsch pulverisette 5 system (150 ml bowls, 8 x 100 mm balls). Samples were run for 45 seconds, allowed to come to rest, and then run for a further 45 seconds. To quantify NERs, homogenised soils were analysed according to Section 2.2.6. Soil sections (e.g. lower bulk) whose associated primary extracts contained less than 5% of AR were not combusted. Applied radioactivity from solvent extracts and NERs were combined to give a mass balance (example shown in Appendix II, Section II.4)

3.2.14 Degradation kinetics

For details of calculating remaining parent compound, fitting of appropriate degradation kinetic models, and generating DT_{50} values, please refer to Section 2.2.7. All data were analysed by Hockey-Stick kinetics with the break point set at 30 DAT, the best-fit break point parameter from investigative model fitting.

A complete mass balance could not be derived, due to the experiment being an open system, so time taken for 50% of the parent compound to dissipate (DT_{50}) was calculated, rather than time taken to degrade to 50% of applied ($DegT_{50}$).

3.2.15 Data analysis

Two way ANOVA was performed on mass balance, percentage applied radioactivity remaining at the surface of the core, and parent remaining in the core. Samples identified as having large residuals during ANOVA were compared against corresponding samples (same time point, same filter treatment), and then across all filters. If the identified samples had low overall mass balance compared to corresponding replicates, they were discarded from the analysis. If samples had obviously lower percentage AR remaining at the surface, the apportioning of the extractable fraction between surface, top bulk, and lower bulk was investigated compared to similar samples. If the compound displayed characteristics of preferential flow through the core (i.e low mass balance in relation to comparable samples, large percentage of applied radioactivity/or parent compound present in the lower bulk), it was removed from the analysis. In total, two paclobutrazol and ten benzovindiflupyr treated cores were removed from analysis. For more detail see Appendix II, Section II.6.

Where possible, parametric tests were performed on non-transformed data. If normality assumptions were not met, data was either log or arcsine transformed prior to ANOVA. Treatment structure was light treatment (LIGHT (i.e. CLEAR and UV-limiting filters combined) and PAR limiting filter) by DAT, and blocking structure was the coordinates of the cores within the overall plot. Errors are ±1 Standard Error (S.E). All analyses were performed using Genstat v.13.2 (VSN International) and figures were plotted using Sigmaplot v.12.5 and Microsoft Excel (Microsoft).

3.2.16 Combination of CLEAR and UV treatments

Visual assessment of the time series of parent loss of paclobutrazol and benzovindiflupyr showed minimal difference in degradation between the CLEAR and UV-limiting filters. To confirm this statistically, parent data from under the CLEAR and UV-L filters for all time points excluding 0 DAT were pooled by filter (CLEAR or UV-L). An unpaired two-way t-test was performed on the data under the null hypothesis that the mean degradation under CLEAR filters over the time course (excluding 0 DAT) was equal to the mean degradation under UV-L over time (excluding 0 DAT). The null hypothesis was accepted for both paclobutrazol ($p=0.946$) and benzovindiflupyr ($p=0.943$), proving that there was no difference between CLEAR and UV-L data sets. The CLEAR and UV-L data sets were, therefore, analysed as a combined 'LIGHT' treatment for both compounds.

3.3 RESULTS

3.3.1 Soil temperature and moisture

Soil temperature and moisture content was recorded in all plots across the full 120-day experiment (with CLEAR and UV combined as LIGHT) for benzovindiflupyr (Figure 3.2). The paclobutrazol experiment ran from 7 to 113 DAT.

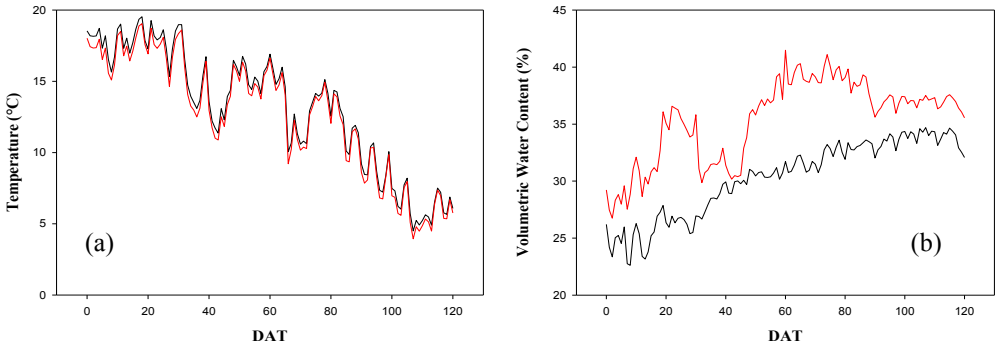

Figure 3.2: A comparison of (a) soil temperature, and (b) moisture recorded across a 120 day time course under LIGHT (black), and PAR limiting (red) conditions.

Soil temperature in paclobutrazol and benzovindiflupyr time courses was 0.46°C and 0.83°C higher under LIGHT conditions (paclobutrazol, 13.15°C; benzovindiflupyr, 13.25°C) relative to PAR-L conditions (12.79°C; 12.31°C). Soil temperature ranged from 19.54°C to 4.49°C under LIGHT conditions, and 19.03°C to 3.94°C under PAR-L conditions. Treatment ($p \leq 0.001$) and time ($p \leq 0.001$) were significant factors, and there was a significant treatment*time interaction ($p \leq 0.001$).

Average soil moisture content was 5.35% higher under PAR-L conditions (35.75%) than under LIGHT conditions (30.40%) in paclobutrazol treated cores, and 5.05% higher under PAR-L (35.32%) relative to LIGHT (30.27%). Soil moisture content in benzovindiflupyr treated cores ranged from 22.61% to 34.69% under LIGHT, and 25.77% and 42.45% under PAR-L conditions. Treatment ($p \leq 0.001$) and time ($p \leq 0.001$) were significant factors in moisture development. The treatment*time interaction was not significant ($p=1.00$).

3.3.2 Paclobutrazol

3.3.2.1 Parent transformation

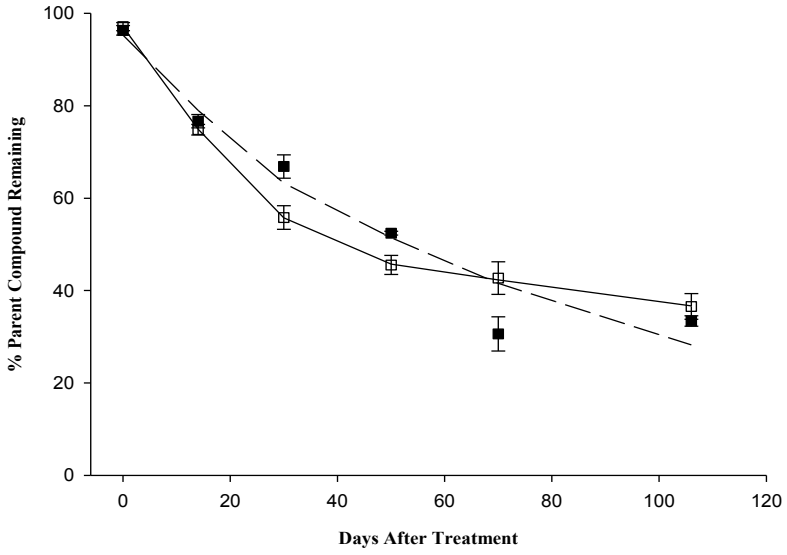

Figure 3.3: Extractable parent compound for paclobutrazol under LIGHT (□) and PAR-limited (■) conditions. The fitted hockey-stick models are shown as (—) for LIGHT predicted, and (- - -) for PAR-limited predicted. Error bars represent ±1 S.E.

The transformation of paclobutrazol (Figure 3.3) was similar between LIGHT and PAR-L conditions. Parent declined from 97.13% and 96.33% under

LIGHT and PAR-L conditions at 0 DAT, to 36.55% and 33.40% at 106 DAT, respectively. Degradation under LIGHT conditions was slightly faster relative to PAR-L at 30 and 50 DAT, but at 106 DAT there were no significant differences between the filter treatments. Filter treatment ($p=0.731$) was not a significant factor in the transformation of paclobutrazol, though time ($p<0.001$) was, and a significant filter treatment*time interaction was seen ($p=0.006$).

DT_{50} was calculated as 38 d, and 57 d under LIGHT and PAR-L treatments respectively. (HS – BP 30 DAT; χ^2 <9%; r^2 >0.94). A breakdown of the kinetic model fits is shown in Table 3.4 at the end of the results section.

3.3.2.2 Mass balance, solvent extract, NERs

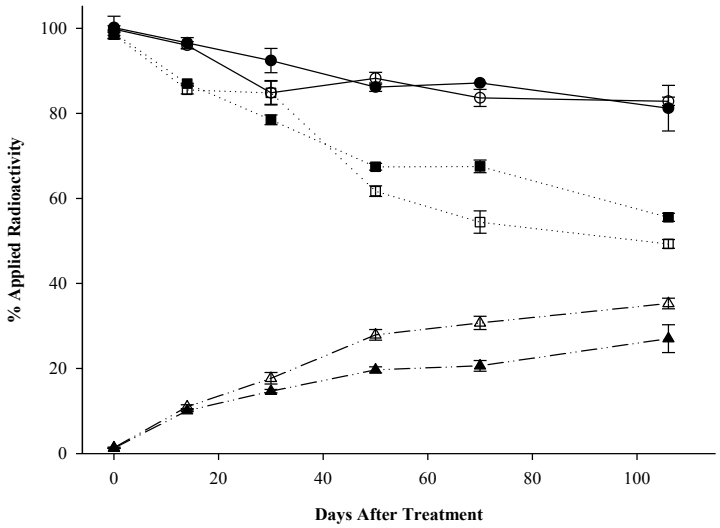

Figure 3.4: Mass balance for paclobutrazol under LIGHT conditions (open symbols) and PAR-limited conditions (closed symbols). The partitioned radioactivity is shown for overall mass balance (——●——), and solvent extract (·····■·····), and NERs (—·▲·—·) Error bars represent ±1 S.E.

Paclobutrazol mass balance, primary solvent extract and NER formation are shown in Figure 3.4. Mass balances declined across the 106 day time course from 99.82% and 100.17% under LIGHT and PAR-L conditions, respectively, at 0 DAT, to 82.85% and 81.23% at 106 DAT, respectively. Mass balance was not significantly affected by filter treatment ($p=0.328$) or filter treatment*time interaction ($p=0.263$), but time was highly significant ($p<0.001$).

The percentage of applied radioactivity recovered in the solvent extract was similar between treatments at 0 DAT (98.50% and 98.97% under LIGHT and PAR-L, respectively) and 14 DAT (85.85% and 87.00% under LIGHT and PAR-L). At 50, 70, and 106 DAT, percentage of applied radioactivity recovered was 5.8%, 13.4%, and 6.3% lower under LIGHT conditions relative to the PAR-L filter. Filter treatment ($p=0.003$) and time ($p<0.001$) significantly affected the percentage of applied radioactivity recovered in the solvent extract, and a significant filter treatment*time interaction was seen ($p=0.021$).

NER formation was similar between treatments at 0 and 14 DAT, but was higher under LIGHT conditions relative to PAR-L filter at all time points ≥30 DAT. At 106 DAT, NER formation was >7% higher under LIGHT compared to PAR-L conditions, with NERs accounting for 33.52% and 25.67% of applied radioactivity under LIGHT and PAR-L, respectively. Filter treatment ($p=0.005$) and time ($p<0.001$) were significant factors in NER formation, and a significant filter treatment*time interaction was seen ($p=0.001$).

3.3.2.3 Paclobutrazol movement

The influence of filter treatment on the movement of paclobutrazol parent compound from the soil surface was investigated by determining the average percentage of parent remaining at the soil surface and in the bulk soil fractions at each time point. Partitioning of remaining paclobutrazol is shown Figure 3.5, and values are shown in Table 3.2.

At 0 DAT, 97.13% and 96.33% of applied parent compound was recovered under LIGHT and PAR-L conditions respectively. Under LIGHT conditions, 77.50% of applied parent compound was recovered from the soil surface fraction, and 19.63% from the top bulk. In contrast, 93.40% of parent recovered under PAR-L conditions was resident at the soil surface, with 2.93% of parent recovered from the top bulk fraction.

A similar effect as also seen at 14 DAT, where 77.18% and 76.67% of applied parent was recovered under LIGHT and PAR-L conditions. A greater percentage of parent compound was recovered from the top bulk under LIGHT relative to PAR-L, 23.08% and 18.97%, respectively, and under LIGHT conditions 2.35% of applied parent compound was quantified in the lower bulk fraction. Addition of percentage parent found in the top bulk and lower bulk gave a combined bulk figure of 25.43% under LIGHT and 18.97% under PAR-L.

The pattern of a greater percentage of parent compound recovered from the bulk fractions under LIGHT relative to PAR-L was seen at all remaining time points.

Treatment ($p=0.025$) and time ($p<0.001$) were significant factors in the development of paclobutrazol parent compound in the combined bulk. No significant treatment*time interaction was seen ($p=0.284$).

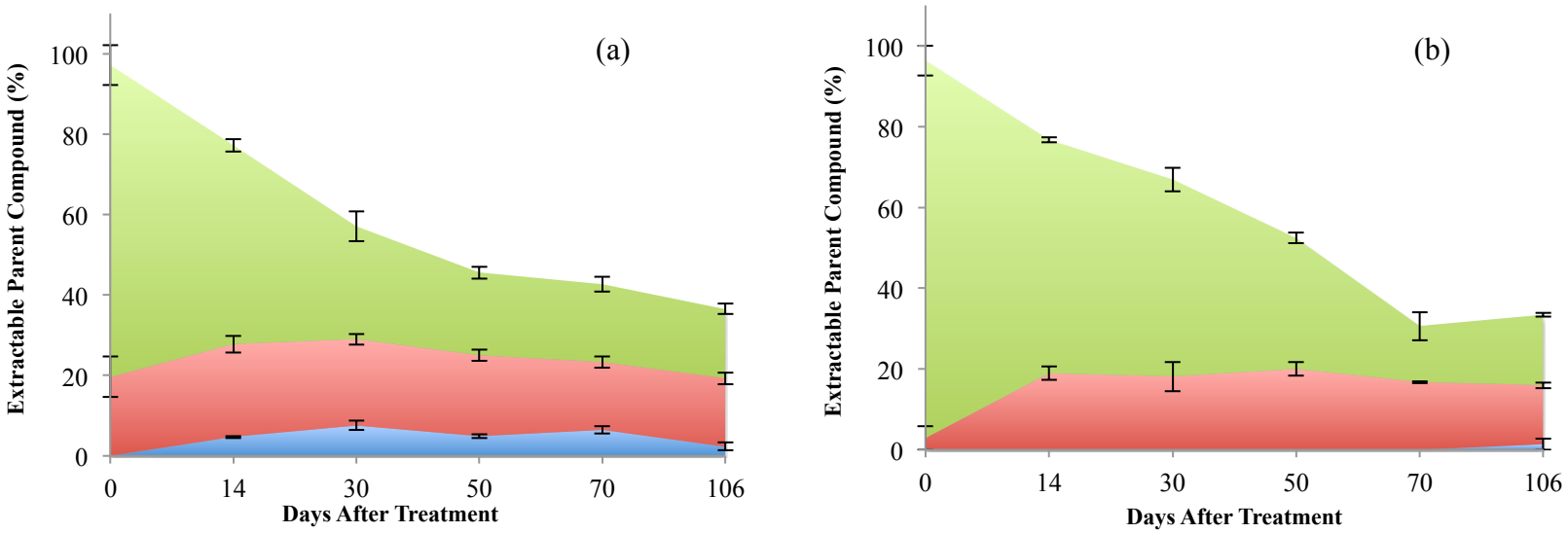

Figure 3.5: Graphs displaying the position of extractable paclobutrazol under (a) LIGHT and (b) PAR-L conditions. Amount of parent compound, as a percentage of applied, is shown in the surface (green), top bulk (red), and lower bulk (blue). Error bars represent ±1 S.E.

Table 3.2: The percentage of applied paclobutrazol remaining in the surface, top bulk, lower bulk, and combined bulk (top + lower bulk) of treated cores under LIGHT and PAR-L conditions. Errors, in brackets, are ±1 S.E.

DAT	Surface		Top Bulk		Lower Bulk		Combined Bulk	
	LIGHT	PAR-L	LIGHT	PAR-L	LIGHT	PAR-L	LIGHT	PAR-L
0	77.50 (4.95)	93.40 (3.69)	19.63 (5.04)	2.93 (2.93)	0.00	0.00	19.63 (5.04)	2.93 (2.93)
14	49.40 (1.52)	57.70 (0.61)	23.08 (2.09)	18.97 (1.66)	2.35 (1.16)	0.00	25.43 (2.16)	18.97 (1.66)
30	28.10 (3.70)	48.73 (2.89)	21.40 (1.31)	18.13 (3.64)	7.58 (1.14)	0.00	28.98 (2.47)	18.13 (3.64)
50	20.55 (1.40)	32.37 (2.89)	20.07 (1.38)	20.07 (1.71)	4.93 (0.51)	0.00	25.00 (1.13)	20.07 (1.71)
70	19.38 (1.85)	13.90 (3.50)	16.82 (1.42)	16.70 (0.20)	6.50 (0.93)	0.00	23.32 (1.85)	16.70 (0.20)
106	17.28 (1.27)	17.43 (0.50)	16.92 (1.45)	14.60 (0.72)	2.35 (0.94)	1.37 (1.37)	19.27 (1.70)	15.97 (1.59)

3.3.3 Benzovindiflupyr

3.3.3.1 Parent transformation

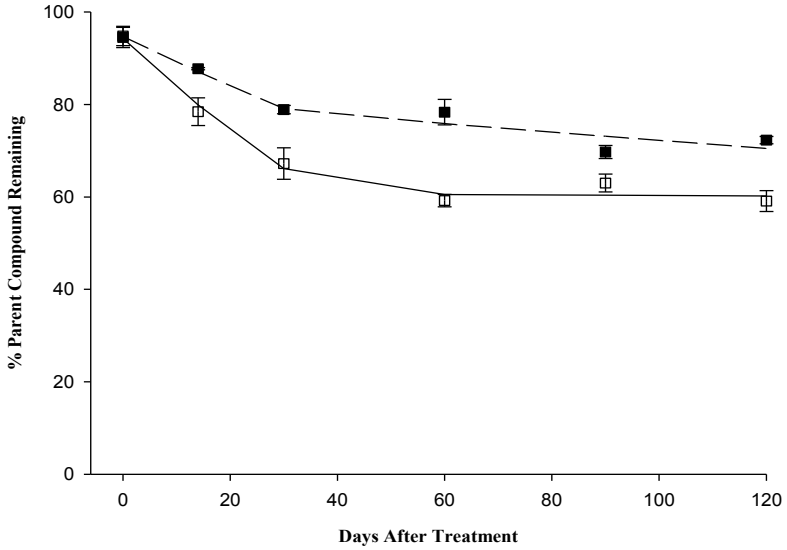

Figure 3.6: Extractable parent compound for benzovindiflupyr under LIGHT (□) and PAR-limiting (■) conditions. The fitted hockey-stick models are shown as (—) for LIGHT predicted, and (- - -) for PAR-limited predicted. Error bars represent ±1 S.E.

The transformation of benzovindiflupyr was faster under LIGHT conditions relative to PAR-L conditions (Figure 3.6). Under LIGHT conditions, parent declined from 94.82% at 0 DAT to 67.23% at 30 DAT. Rate of transformation slowed for the remainder of the test, reaching 59.12% at 120 DAT. Transformation under PAR-L conditions followed a similar biphasic pattern of degradation with an initial faster phase of degradation to 30 DAT, followed by a slower phase between 30 DAT and 120 DAT. Under PAR-L conditions benzovindiflupyr declined over the first 30 days of the test, from 94.50% to 78.90%. Rate of transformation slowed for the remainder of the test, with parent

declining to 72.30% at 120 DAT. Light filter treatment (p=0.013) was a significant factor in the transformation of benzovindiflupyr, as was time (p<0.001), and a significant filter treatment*time interaction was seen (p=0.003).

DT_{50} was calculated as >1000 d under LIGHT conditions (2930 d), and 447 d under PAR-L conditions (HS – BP 30 DAT; χ^2 <2.4%; r^2 >0.89) (see Table 3.4 for further details). However as levels of parent compound only declined to 60-70% at 120 DAT and had entered a slow phase of degradation, calculated values should be taken with caution, as any error in the fitted model is extrapolated over time.

3.3.3.2 Mass balance, solvent extract, and NERs

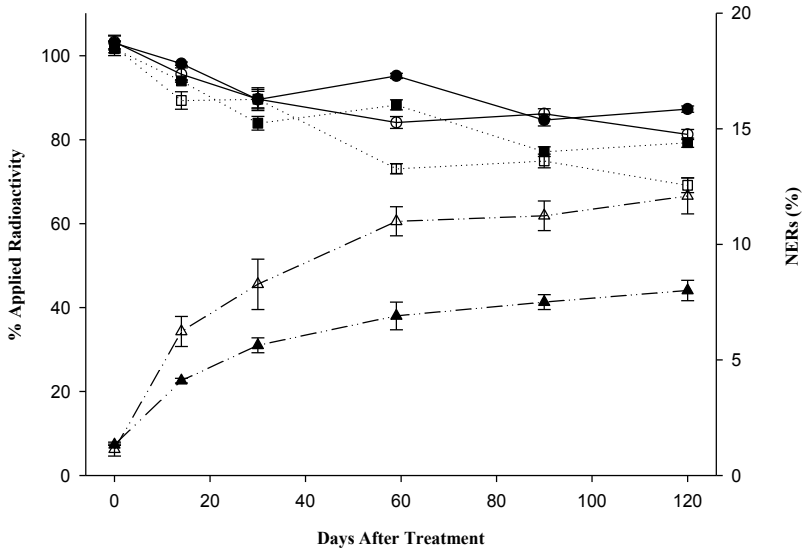

Figure 3.7: Mass balance for benzovindiflupyr under LIGHT (open symbols) and PAR-limiting conditions (closed symbols). The partitioned radioactivity is shown for overall mass balance (——●——), and solvent extract (·····■·····) on y-axis one. NERs (—·▲·—) are shown on y-axis 2. Error bars represent ±1 S.E.

Benzovindiflupyr mass balance, solvent extract and NER formation are shown in Figure 3.7. Mass balances were between 81% and 104%. Mass balance was highest at 0 DAT and generally declined across the 120 day time course, from 103.26% and 103.3% at 0 DAT, to 81.25% and 87.30% at 120 DAT under LIGHT and PAR-L conditions, respectively. There was no significant effect of filter treatment on mass balance ($p=0.309$). Time ($p<0.001$) significantly affected mass balance, and there was a significant filter treatment*time interaction ($p=0.004$).

Percentage of applied radioactivity recovered in the solvent extract declined under LIGHT and PAR-L across the time course. No clear pattern had emerged between treatments by 14 or 30 DAT, but at 59 (73.10% and 88.30%), and 120 DAT (69.15% and 79.30%), the percentage of applied radioactivity recovered in the solvent extract was lower under LIGHT conditions relative to PAR-L conditions. Filter treatment ($p=0.040$), and time ($p<0.001$) were both significant factors in determining percentage of applied radioactivity recovered in the solvent extract, and a significant filter treatment*time interaction was seen ($p<0.001$).

NER formation was comparable between treatments at 0 DAT, at 1.14% and 1.33% under LIGHT and PAR-L conditions. NER formation was higher under LIGHT conditions relative to PAR-L conditions at all remaining time points, reaching 12.10% and 8.00% at 120 DAT, respectively. Filter treatment ($p=0.008$) and time ($p<0.001$) were significant factors in the formation of NERs, and a significant filter treatment*time interaction was seen ($p=0.002$).

3.3.3.3 Benzovindiflupyr movement

The influence of light treatment on the movement of benzovindiflupyr parent compound from the soil surface was investigated as in Section 3.3.2.3. The average percentage of parent remaining at the soil surface and in the bulk soil fractions at each time point was determined. The partitioning of recovered benzovindiflupyr is shown Figure 3.8, and values are shown in Table 3.3.

At 0 DAT, 94.82% and 94.50% of parent compound was recovered under LIGHT and PAR-L condition respectively. Under LIGHT conditions 82.22% applied parent compound was resident at the soil surface, and under PAR-L conditions, 92.53% of applied compound was resident at the surface. The percentage of applied compound resident in the top bulk of the cores was greater under LIGHT conditions relative to PAR-L, with 12.60% and 1.97% of applied compound resident in the top bulk under LIGHT and PAR-L, respectively.

The average percentage of compound applied present in the top bulk applied was higher under LIGHT at all time points relative to PAR-L, and similarly, the percentage of parent compound present in the combined bulk was greater at all time points under LIGHT conditions relative to PAR-L.

Time ($p<0.001$) was a significant factor in the development of benzovindiflupyr parent compound in the combined bulk. Treatment ($p=0.083$) was not significant, and no significant treatment*time interaction was seen ($p=0.899$).

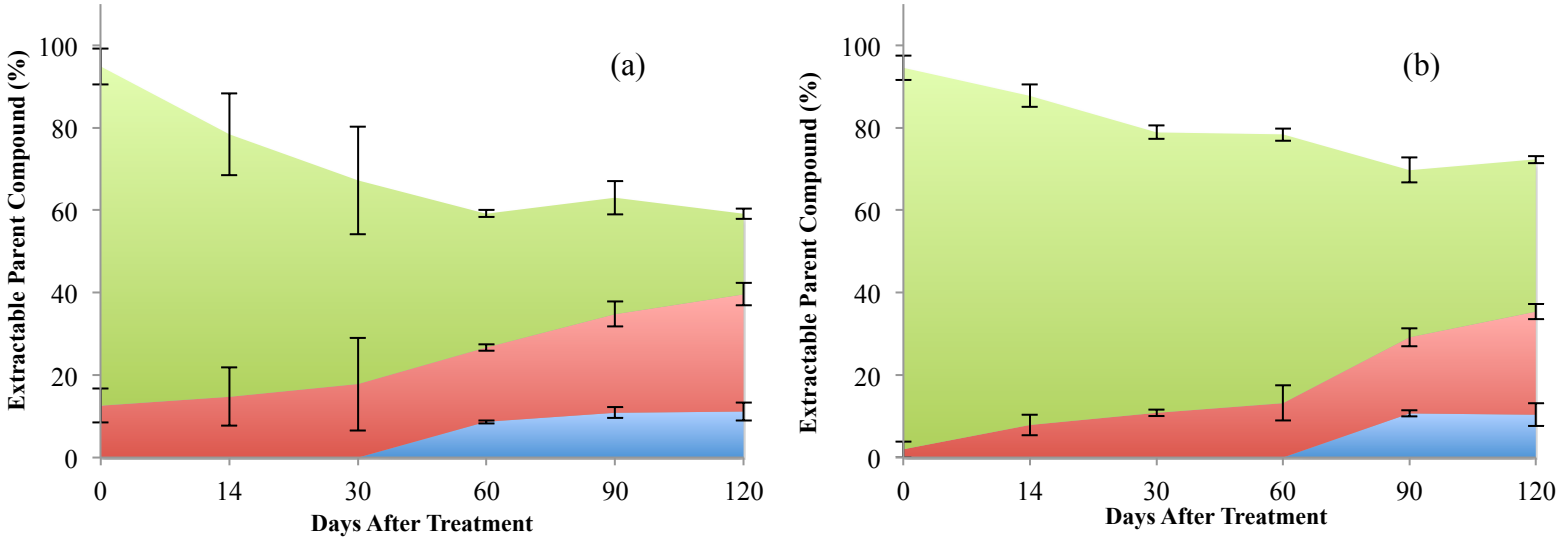

Figure 3.8: Graphs displaying the position of extractable benzovindiflupyr under (a) LIGHT and (b) PAR-L conditions. Amount of parent compound, as a percentage of applied, is shown in the surface (green), top bulk (red), and lower bulk (blue). Error bars represent ±1 S.E.

Table 3.3: The percentage of applied benzovindiflupyr remaining in the surface, top bulk, lower bulk, and combined bulk (top + lower bulk) of treated cores under LIGHT and PAR-L conditions. Errors, in brackets, are ±1 S.E.

DAT	Surface		Top Bulk		Lower Bulk		Combined Bulk	
	LIGHT	PAR-L	LIGHT	PAR-L	LIGHT	PAR-L	LIGHT	PAR-L
0	82.22 (4.33)	92.53 (2.95)	12.60 (4.11)	1.97 (1.97)	0.00	0.00	12.60 (4.11)	1.97 (1.97)
14	63.68 (9.94)	79.85 (2.75)	14.78 (7.04)	7.90 (2.50)	0.00	0.00	14.78 (7.04)	7.90 (2.50)
30	49.43 (13.06)	68.03 (1.60)	17.80 (11.24)	10.87 (0.83)	0.00	0.00	17.80 (11.24)	10.87 (0.83)
59	32.56 (0.90)	65.10 (1.50)	18.04 (0.82)	13.25 (4.25)	8.62 (0.35)	0.00	26.66 (1.12)	13.25 (4.25)
90	28.18 (4.09)	40.57 (3.03)	23.92 (3.08)	18.40 (2.19)	10.92 (1.30)	10.77 (0.78)	34.84 (4.07)	29.17 (1.62)
120	19.47 (1.24)	36.87 (0.88)	28.48 (2.71)	25.00 (1.85)	11.17 (2.19)	10.43 (2.77)	39.65 (2.81)	35.43 (0.92)

Table 3.4: Kinetic model parameter used for analysis of parent degradation in cores incubated in the field. Parameters included are goodness of fit (χ^2), correlation between observed and expected (r^2), rate constants for degradation (k), probability that degradation rate > 0 (Prob > t), and DT_{50} values.

Filter	χ^2 (%)	r^2	Rate constants [d^{-1}]	Prob. > t	DT_{50} (days)
Paclobutrazol LIGHT	1.01	0.9475	k1, 0.01849 k2, 0.003942	k1, 2.76E-014; k2, 0.0032	38
Paclobutrazol PAR-Limited	8.79	0.9489	k1, 0.01337 k2, 0.01074	k1, 5.10E-06; k2, 1.07E-05	57
Benzovindiflupyr LIGHT	2.14	0.8917	k1, 0.01182 k2, 8.73E-05	k1, 0.00234; k2, 0.6	2 930
Benzovindiflupyr PAR-limited	2.36	0.9070	k1, 0.005994 k2, 0.001218	k1, 3.48E-005; k2, 0.0406	447

3.4 DISCUSSION

The spectral quality of light reaching the soil surface in soil cores incubated in soil subject to outdoor conditions appeared to have a compound specific effect on the degradation rate of two CPPs. Light appeared to alter the rate of degradation for benzovindiflupyr but not paclobutrazol, and increased the rate of NER formation for both compounds, although the magnitude of NER formation was CPP specific. The effects seen were similar to those previously observed in a silt-loam (SL) soil in an OECD 307 regulatory-like laboratory system (Davies *et al.* 2013a) suggesting that the previously observed effects of non-UV light on CPP degradation and fate are not an artefact of the inclusion of light in a laboratory test system. Rather they appear to reflect real effects seen in a more environmentally realistic system.

The spectral quality of light appeared to significantly affected the vertical movement of both CPPs from the soil surface (top 5mm), with a greater percentage of applied parent compound moving away from the soil surface in cores exposed to LIGHT relative to cores from which photosynthetically active radiation was restricted (PAR-L). Most of the translocation appears to occur at 0 DAT, upon application, and a variety of mechanisms could be responsible for the observed effect. They include increased porosity in cores exposed to LIGHT, resulting in better infiltration and movement of water through the soil, and reduced sorption of CPPs resulting from exudation of organic compounds from the roots of eukaryotic phototrophic communities present at the soil surface in LIGHT exposed cores, discussed later.

The main question asked in this work was whether the spectral quality of light affected the biodegradation of two CPPs in soil cores incubated in a field system. Davies *et al.* (2013a) showed that the presence of non-UV light affected the biodegradation of several CPPs in a sandy-loam soil within a laboratory system. A single time point screen of eight CPPs revealed a general effect of non-UV light. Five compounds exhibited faster rates of degradation when the systems were exposed to non-UV light compared to when they were incubated in the dark, one compound exhibited a slower rate of degradation, and two compounds exhibited no difference in degradation rate. A complete time course of degradation for two compounds, benzovindiflupyr and chlorotoluron, was carried out under the contrasting conditions (non-UV light and dark). Degradation was faster under non-UV light conditions for both compounds.

In the Davies *et al.* (2013a) lab study, the rate of degradation of benzovindiflupyr increased under light conditions, roughly halving the $DegT_{50}$ relative to dark-incubated samples from 373 d to 183 d. The degradation followed a biphasic pattern, with a fast initial phase of degradation, succeeded by a slower phase, in which the degradation rate under light conditions was faster than in the dark.

The work described in this chapter aimed to see whether similar effects were seen in a more environmentally realistic system. We have shown that, for paclobutrazol and benzovindiflupyr, the presence or absence of UV light (<400 nm) did not significantly alter degradation rates, with no significant difference between the two LIGHT filter treatments. However, the presence or absence of PAR light significantly affected NER formation of paclobutrazol and

benzovindiflupyr, with increased NER formation in LIGHT conditions relative to PAR-L, and increased degradation of benzovindiflupyr in LIGHT conditions relative to PAR-L.

Whilst the calculated DT_{50} values in this study were higher than previously observed, 477 d under PAR-L conditions in the field (this study) compared to 373 d in the dark in the laboratory (Davies *et al.* 2013a), the same general effect was observed. Initial transformation of benzovindiflupyr was greater under LIGHT conditions relative to PAR-L, and a biphasic degradation pattern was observed, although with differences between LIGHT and PAR-L in the rate of the first phase of degradation (not seen previously in the laboratory). Degradation in this first phase was faster under LIGHT conditions, with remaining parent compound declining to 67.23% and 78.90% at 30 DAT under LIGHT and PAR-L, respectively. Calculation of DT_{50} using the rate of degradation from the first phase of the kinetics only revealed DT_{50} times of 59 d and 116 d under LIGHT and PAR-L conditions, respectively (data not shown).

The DT_{50} value of benzovindiflupyr under LIGHT conditions was calculated as >1000 d. However, it should be noted that this fit would have failed FOCUS (2006) fitting requirements, with a Prob. >t value of 0.6 for the second phase of degradation. Due to the biphasic kinetics of benzovindiflupyr, a DT_{25} may be a more appropriate indicator of biodegradation rate (~ 24 d under LIGHT, and ~ 90 d under PAR-L). Though the second phase of degradation was faster under PAR-L (k2 = 1.2E-03 d^{-1}) conditions relative to LIGHT (k2 = 8.73E-05 d^{-1}), it is unclear how representative such rates would be beyond the end of the observed time period.

As well as affecting transformation rates, the inclusion of non-UV light in a laboratory test system (Davies *et al.* 2013a) increased the formation of NERs relative to dark incubation for benzovindiflupyr, chlorotoluron and five other CPPs as part of the single time point screen. In the current study, using CL soil in a field system, the same general effect was seen, with NER formation significantly higher in the LIGHT relative to the PAR-L treatments for both benzovindiflupyr and paclobutrazol. This increased NER formation when non-UV light is included in the system has previously been attributed to several potential mechanisms, such as an increase in soil organic matter (SOM) in light kept samples, or shifts in pH of the soil (Davies *et al.* 2013a). Davies *et al.* (2013a) suggested that increased NER formation could be due to increases in the soil pH. in light conditions driven by the presence of phototrophs. CPPs bind to SOM in the soil matrix, which has been shown to be of dominating importance in the formation of NERs. The presence of a biological soil crust (BSC) in arid lands has been shown to increase carbon input and cycling within a soil system (Housman *et al.* 2006; Yoshitake *et al.* 2010; Zaady *et al.* 2000), with increases in this temperate system also due to the presence of mosses, and this light driven increase of carbon within the soil could aid the irreversible binding of CPPs within the soil matrix.

Significantly, the current study suggests an increase in movement of parent CPP away from the soil surface (top 5 mm) in the LIGHT relative to the PAR-L treatment, evidenced by the greater percentage of parent compound resident in the bulk fraction under LIGHT conditions relative to PAR-L This suggests that the development of a BSC in agricultural soils may have wider

impacts for the environmental fate of CPPs There are several mechanisms that could account for this phenomenon.

For both compounds there was a higher percentage of applied parent compound in the sub-surface layers under LIGHT conditions relative to PAR-L. This effect was also seen at later time points in the experiment, though the difference was not as pronounced as at 0 DAT. This suggests that the differences between LIGHT and PAR-L conditions in the translocation of parent compound from the soil surface occurs at 0 DAT, upon application. Prior to CPP application, the cores were incubated under the light filters for ~60 days to allow the microbial communities at the soil surface to develop under each of the conditions (CLEAR, UV-L and PAR-L). These results suggest that this pre-incubation period may responsible for the differences in the translocation of parent compound.

The increased movement of parent compound could be due to increased porosity at the soil surface in treatments under the influence of light, resulting in better drainage from the soil surface. Studies in arid lands have shown that BSCs can affect the infiltration rate both positively and negatively dependent on the dominant biota (Kidron *et al.* 2003; Zaady *et al.* 2013; Kidron *et al.* 1999). However, BSCs found in agricultural systems are more similar to later-stage BSCs found in arid lands (Davies *et al.* 2013b) that have been shown to increase water infiltration rates (Kidron *et al.* 2003 & 2012; Xiao *et al.* 2011), and are characterised by higher abundance of diazotrophic cyanobacteria, lichen and moss.

For example, Xiao *et al.* (2011) demonstrated that moss-dominated BSCs cultured in the laboratory significantly increased water infiltration and decreased overland

flow, with the increase in infiltration positively correlated with the extent of the soil coverage of the crust. In experiments where the moss crusts were horizontal, with no slope simulated, overland flow was still seen when crusts covered 0% and 29% of the soil surface, and represented 46% and 30% of the simulated rainfall. However, when there was 61% surface coverage, no runoff was observed. Similarly, with a slope gradient of 9%, when moss surface area covered 0%, 40%, and 78%, overland flow represented 67%, 39%, and 29% of the simulated rainfall events.

Another potential mechanism for enhanced movement of CPP from the soil surface in LIGHT relative to PAR-L treatments could be due to reduced sorption of parent compound resulting from production of root/rhizoid exudates and low-molecular-weight-organic-acids (LMWOAs) by phototrophs present at the soil surface. Luo *et al.* (2006) showed that presence of oxalate and root exudates enhanced the desorption of *p,p'*-DDT from soils. In seven soils representing four soil types, the addition of oxalate significantly increased desorption of *p,p'*-DDT, by between 11% and 59%. Further, addition of root exudates collected from solution cultures of maize, wheat, and ryegrass significantly increased desorption of *p,p'*-DDT. Relative to water, exudates increased desorption from 8.4% to 35.8% in maize, 9.7% to 36.8% in wheat, and 3.1% to 23.7% in ryegrass (Luo *et al.* 2006). Increased desorption by root exudates has also been seen with other xenobiotics in soil, such as polycyclic aromatic hydrocarbons (PAHs) (Ling *et al.* 2015). In a laboratory batch experiment, the addition of three LMWOAs to phenanthrene and pyrene contaminated soils enhanced desorption by up to 285% and 299% respectively.

Once desorbed from the soil solid phase, CPPs associated with dissolved- or colloidal organic carbon are present in the aqueous phase, allowing them to move vertically through the soil.

However, it seems unlikely that exudates played any major role in the movement of paclobutrazol and benzovindiflupyr in this experiment because differences in the positioning of parent compound were seen early experiment at 0, 14, and 30 DAT. Furthermore, there is little evidence in the literature to suggest that mosses have major exudation pathways.

A higher percentage of parent compound was detected in the bulk soil under the LIGHT treatment from 0 DAT. If root exudates were a main driver in desorption and movement of CPP into the core, it might be expected to be a continuous process and would be more likely to be seen later in the time course when mosses were observed. For benzovindiflupyr the rate of dissipation from the surface was similar between LIGHT and PAR-L treatments, and it is more probable that increased porosity of the soil surface of LIGHT cores at application resulted in an increase in the percentage of applied parent compound moving from the soil surface into the top bulk upon application.

A secondary factor that may influence the movement of CPP residues in the soil is bioturbation, the reworking of soils and sediments by animals or plants. This could involve the physical relocation of CPP residues sorbed to soil particles by earthworms and other macro-fauna. However, as previously discussed, differences in translocation between treatments in this study were observed at the application stage, suggesting a limited role of translocation by bioturbation in this system.

Whilst the differences observed between treatments may be due primarily to the different light treatments, secondary factors, such as soil moisture content, may also influence the differences observed between treatments. Differences in soil moisture content can influence the degradation rate of CPPs (Cattaneo *et al* 1997; Schroll *et al.* 2006; Chatterjee *et al.* 2013), and low soil moisture content can inhibit microbial activity, and therefore CPP biodegradation, by reducing hydration and activity of enzymes (Stark and Firestone 1995). In this study, the differences in soil moisture content between the LIGHT and PAR-L treatments may influence the fate of CPP residues in the environment by affecting bioavailability of residues, competency/reaction rate of degradation pathways, and taxonomic composition of microorganism communities in the soil.

Differences between treatments in the type of crust at the soil surface may affect drainage characteristics and moisture retention between treatments. Knapen *et al.* (2007) identified three stages of crust formation in a temperate cropland system. In the first stage, a non-biological surface seal developed by raindrop impact. This could help to explain the reduced movement of the compound from the soil surface in cores under PAR-L conditions relative to LIGHT, and contribute to the increased soil moisture observed under PAR-L relative to LIGHT. The absence of a BSC would decrease porosity at the soil surface, allowing greater kinetic impact from raindrops at the soil surface, thereby increasing physical sealing and decreasing the rate of evaporative loss from the soil surface. The presence of a BSC at the soil surface would increase the rate of evapotranspiration under the LIGHT treatment, with bioturbation from plants/mosses, bacteria and fungi increasing porosity, increasing drainage.

Currently, EU guidance on field trials do not account for the interaction of CPPs with the soil surface and the processes that occur there (EFSA 2010). However, the presence or absence of a BSC could have several implications for the terrestrial fate of CPPs. It is clear that the soil surface provides a discrete sphere of influence within soil, and that more research is needed to better understand the influence of soil surface processes on the environmental fate of CPPs.

The availability of photosynthetically active radiation in a field test degradation system appeared to increase the rate of CPP transformation for one of the two CPPs examined, and increased the NER formation for both CPPs tested. The CPPs also exhibited increased movement of parent compound away from the soil surface under LIGHT conditions, with a higher percentage of parent compound recovered from the bulk soil in LIGHT conditions relative to PAR-L cores. These effects may have been driven by the presence of a biological soil crust in LIGHT treated cores, representing the first point of contact of CPPs applied to the soil surface. It is important to further investigate the mechanisms responsible with a wider variety of CPPs, to further understand the role of the soil surface in the fate and behaviour of CPPs within the terrestrial environment.

CHAPTER 4: THE SPECTRAL QUALITY OF LIGHT INFLUENCES MICROBIAL COMMUNITY STRUCTURE AT THE SOIL SURFACE IN SOIL CORES INCUBATED IN THE FIELD

4.1 INTRODUCTION

Work presented in Chapter 3 showed that the spectral quality of light appeared to influence the degradation and movement of two CPPs in soil cores incubated in the field. This suggests that the impacts of non-UV light on CPPs observed within an adapted laboratory test system may also be relevant in a more environmentally realistic system (Davies *et al.* 2013a; Chapter 3). Work presented in this Chapter investigated the effect of the spectral quality of light and time on the development of bacterial and phototrophic communities present at the soil surface.

Biological soil crusts (BSCs) have been studied extensively in arid lands, and have been shown to harbour photosynthetic communities that are distinct spatially, from the underlying bulk soil, and temporally, at different successional stages of development. These phenomena have been observed across wide geographical scales, from the Gurbantunggut and Tengger deserts of China, to the Sultanate of Oman (Abed *et al.* 2010), and the Colorado Plateau of the United States (Garcia-Pichel *et al.* 2001; Yeager *et al.* 2004). However, most investigations have focused on studying phototrophic diversity using culture-dependent methods, with their associated biases

(Hawkes and Fletcher 2002; Li *et al.* 2002; Langhans *et al* 2009a; Li *et al* 2010; Zhang *et al.* 2011), or molecular methods targeting the 16S rRNA gene of bacteria to investigate dominantly abundant cyanobacteria, ignoring the diversity of eukaryotic phototrophs (Garcia-Pichel *et al.* 2001; Redfield *et al.* 2002; Nagy *et al.* 2005; Abed *et al* 2010; Zaady *et al.* 2010; Steven *et al.* 2012).

Phototrophic communities have also been shown to be widespread in temperate environments (Veluci *et al.* 2006; Langhans *et al.* 2009a), and are known to readily form under agricultural cropping systems (Knapen *et al.* 2007). Knapen *et al.* (2007) observed that BSCs in temperate agricultural environments went through three distinguishable phases of development: (i) development of a physical seal by raindrop action, (ii) colonization of the soil surface by algae and, (iii) establishment of a well-developed crust dominated by moss, similar to the successional development of BSCs observed in arid environments.

In a microcosm experiment, Jeffery *et al.* (2009) used PLFA analysis to show that the spectral quality of light resulted in the development of phenotypically distinct microbial communities 8 weeks post-disturbance, diverging for a further 24 weeks. Alongside increases in biomass and chlorophyll *a* concentration at the soil surface relative to bulk, it was hypothesised that the differences were driven by the development of photoautotrophs at the soil-air boundary. Later work by Davies *et al.* (2013b) investigated the development of fungal, bacterial and phototrophic communities in a temperate pasture soil under dark and non-UV light in laboratory conditions. It was found that the presence of light promoted the development of distinct communities relative to samples kept in the dark.

This chapter reports the development of bacterial and phototrophic communities at the soil surface under filters modulating the spectral quality of light in soil cores incubated in the field. Cores were installed under appropriate filters ~60 days before application of two CPPs to independent core sets. A timeline of degradation was taken for the applied CPPs (see Chapter 3), and at each time point, representative samples were taken from the soil surface (top 5 mm). Bacterial primers targeting the V4 region of the 16S rRNA gene (Caporaso *et al.* 2012) and universal phototroph primers designed to target prokaryotes and eukaryotes (Sherwood and Presting 2007) were used to create target amplicon libraries to investigate soil surface community differences by treatment and by time. Illumina MiSeq pyrosequencing of PCR amplicons, and chlorophyll *a* measurements were used to answer the following questions:

4.1.1 Questions/Aims to be addressed

(i) Does treatment of the soil with different CPPs influence bacterial and phototrophic community structure?

(ii) Does the spectral quality of light influence bacterial community structure at the soil surface?

(iii) Does the spectral quality of light influence phototrophic community structure at the soil surface?

(iv) Are there temporal/successional changes in phototroph and bacterial communities?

4.2 MATERIALS AND METHODS

4.2.1 Experimental outline

The body of work in this chapter covers the microbial analysis of the surface samples generated in Chapter 3. For details of experimental design and soil processing, please refer to Sections 2.2.1 through to 2.2.11 for details.

4.2.2 pH

The method used for pH analysis was as detailed in Emmett *et al.* (2008). Briefly, soil (2 g) was shaken with 5 ml UPW for 15 minutes at 200 rpm. Soil was allowed to settle, and pH was measured using a Mettler Toledo SevenEasy pH meter, with an InLab® SG 413 electrode (Mettler Toledo, Leicester, UK).

4.2.3 Chlorophyll *a*

Chlorophyll *a* was extracted using a modified version of Ritchie (2006). Two grams of soil sample was combined with 10 ml of 90:10 acetone/UPW (v/v) in a foil-wrapped 15 ml falcon tube. Samples were shaken at 200 rpm for five hours at 20°C. Following shaking, the samples were allowed to settle for at least 15 mins. The absorbance of 1 ml of the solvent extract was measured at 664 nm and 750 nm. The solution was acidified by the addition of 200 µl of 3M HCl, to convert chlorophyll *a* to pheophytin. Absorbance was measured at 665 nm and

750 nm at 30 seconds after acidification. Absorbance readings at 750 nm were deducted from absorbance at 664 nm and 665 nm as appropriate, and chlorophyll *a* was calculated according to the formula given from APHA in Castle *et al.* (2011).

4.2.4 DNA isolation

DNA was isolated from samples using the FastDNA™ SPIN Kit for Soil and the FastPrep® Instrument (MP Biomedicals, Santa Ana, CA). Samples were isolated according to the manufacturer's protocol. All centrifuge steps were performed at 14 000 x *g*.

500 mg of thawed sample was added to the Lysing Matrix E tube. To this, 978 µl of sodium phosphate buffer and 112 µl of MT buffer were added. Samples were homogenised using the FastPrep® Instrument for 40 seconds at speed setting 6.0. The samples were centrifuged for 10 minutes to pellet debris, and the supernatant transferred to a clean 2.0 ml micro-centrifuge tube. To this, 250 µl of PPS (Protein Precipitation Solution) was added, and the tube inverted by hand 10 times to mix. Samples were centrifuged for 5 minutes to pellet the precipitate, and the supernatant transferred to a clean 15 ml tube. Following re-suspension of the binding matrix, 1 ml was added to the supernatant. Tubes were rotated end over end for 2 minutes to allow binding of DNA, then placed in a rack for 3 minutes to allow the silica matrix to settle. An aliquot (500 µl) of supernatant was discarded, and the binding matrix re-suspended in the remaining supernatant. Approximately 700 µl of the mixture was added to a SPIN™ Filter, and centrifuged for 1 minute.

Catch tubes were emptied, and the process repeated. Resulting pellets were gently re-suspended by adding 500 µl of SEWS-M, using the force of the liquid from the pipette tip. Samples were centrifuged for 1 minute, and the catch tubes emptied. Samples were centrifuged for a further two minutes to dry the matrix, and the catch tube discarded and replaced. SPIN™ Filters were left to air dry for 5 minutes at room temperature. The binding matrix was gently re-suspended by adding 60 µl of DES, allowing it to soak, followed by light vortexing. Samples were centrifuged for 1 minute, and eluted DNA was collected in the catch tube.

Samples were diluted 10-fold in water (Just Water, double distilled microbiology grade water; Microzone Ltd, West Sussex) prior to quantitation and stored at -20°C.

4.2.5 DNA quantitation

DNA samples were quantitated using the Qubit® 2.0 (Invitrogen) broad range (BR) fluorometric quantitation protocol according to the manufacturers' guidelines. Briefly, a master mix of 199 µl of dsDNA BR buffer and 1 µl of dsDNA BR reagent per sample was made up in a clean tube. The mixture was vortexed, and 195 µl added to clean Qubit sample tubes. To this, 5 µl of sample DNA was added per sample tube. Two standards were made using 190 µl of master mix and 10 µl of appropriate standard (Standard #1, Standard #2). The samples were vortexed and incubated at room temperature for 2 minutes. Samples were then inserted into the Qubit® 2.0 fluorometer, and results recorded.

4.2.6 Illumina MiSeq amplicon library preparation

The methods below describe the combined library preparations for samples from Chapters 4 (108 samples) & 5 (168 samples). Libraries were prepared from the soil surface DNA isolations of all 108 cores from this study. Details of the samples from Chapter 5 are given in Sections 5.2.6 & 5.2.9.

Two library preparations were carried out. One library was constructed to target 16S rRNA to investigate bacterial community structure and diversity. The second library targeted the 23S rRNA gene to investigate phototrophic community structure and diversity.

Water used in the library preparation was Just Water double distilled microbiology grade water. Q5® refers to Q5® Hot Start High-Fidelity DNA polymerase 2x Master Mix (New England Biolabs, Inc).

4.2.6.1 Normalisation

At the start of library preparation, DNA samples were normalised to 5 ng/µl using a 96 well plate. This was achieved by diluting 5 µl of each DNA sample with the appropriate volume of water. Following normalisation, plates were spun briefly to collect the samples in the bottom of the wells. Between stages, plates were stored at -20°C.

4.2.6.2 Amplicon PCR

Primers were designed by addition of the Nextera XT transposase sequence to the published amplicon primer sequences. Bacterial primer sets were as used in Caporaso *et al.* (2012), and phototrophic primer sets detailed used in Sherwood and Presting (2007). Primer sequences are detailed in Table 4.1, below. All primers were ordered, HPLC purified, from Sigma-Aldrich.

Table 4.1: Primers and adapters used for MiSeq library construction.

Target	Region	Primer Sequence	Fragment Size (bp)
Bacterial	16S	515f - 5' - GTGCCAGCMGCCGCGGTAA 806r - 5' –GGACTACHVGGGTWTCTAAT	291
Phototrophic	23S	rV f1 - 5' - GGACAGAAAGACCCTATGAA rV r1 – 5' –TCAGCCTGTTATCCCTAGAG	410
Transposase sequences	-	F – 5' – TCGTCGGCAGCGTCAGATGTGTATAAGAGACAG R – 5' – GTCTCGTGGGCTCGGAGATGTGTATAAGAGACAG	32/33

A master mix of 2X Q5® master mix, water, and an appropriate primer set was prepared (for reaction number, plus 10%), see Table 4.2. Aliquots (22 µl) of master mix were added to the required number of wells across three 96 well plates. Template DNA sample (3 µl at 5 ng/µl) was added to the appropriate well, resulting in a final reaction volume of 25 µl. PCR plates were sealed with a foil lid (StarLab).

Samples were amplified using a GeneAmp 9700 thermocycler (Applied Biosystems, California) using the following temperature programme: 98°C for 30 seconds, followed by 25 cycles of 98°C for 10 seconds, 50°C for 15 seconds, and 72°C for 20 seconds. This was followed by a final hold stage of 72°C for 5 minutes, before cooling to 4°C.

To ensure amplification had been achieved, 5 µl aliquots of selected libraries were run on a gel (1.1% agarose, 40 minutes at 90V). A 100 bp DNA ladder (Invitrogen) was run in parallel to confirm product size.

Table 4.2: Reaction components of amplicon PCR.

Master Mix Components	Volume (µl)
Water	7
2X Q5	12.5
Forward Primer (10 µM)	1.25
Reverse Primer (10 µM)	1.25

4.2.6.3 PCR clean up I

The PCR clean up stage used AMPure XP beads (Agencourt, High Wycombe, UK) to separate free primers and primer dimer species from the amplicons.

AMPure XP beads were brought to room temperature and vortexed for 30 seconds to re-suspend magnetic beads. AMPure beads (35 µl) were added to each well of a MIDI plate (Thermo Scientific), at 1.4 times the volume of the amplicon PCR reaction volume. Amplicon PCR plates were centrifuged to collect all

product at the bottom of the well (1,000 x g, 1 minute), and the entire reaction volume transferred to the corresponding MIDI plate well. The plate was sealed with a Microseal 'B' film (Bio-Rad), and vortexed for 2 minutes on a plate vortex (IKA, North Carolina), at speed setting 4.5 (1 800 rpm). The plate was incubated at room temperature without shaking for 5 minutes, and then transferred to a magnetic stand (Ambion, Life Technologies) for 4 minutes, or until the supernatant had cleared. Once the supernatant had cleared, it was removed and discarded. With the MIDI plate remaining on the magnetic stand, samples were washed with a prepared solution of 80:20 (v/v) ethanol (200 proof, Sigma-Aldrich):sterile nuclease free water (Fisher Scientific). An aliquot (200 µl) of this solution was added per well, incubated for 30 seconds, then carefully removed and discarded. The ethanol wash step was repeated, with care taken to remove any excess ethanol from each well. With the plate remaining on the magnetic stand, samples were allowed to air dry for 10 minutes. The plate was removed from the magnetic stand, and 27.5 µl of 10 mM Tris pH 8.5 (Qiagen Buffer EB) was added to each well, and the magnetic bead pellet was re-suspended by gently pipetting up and down. The plate was sealed with a Microseal 'B' film (Bio-Rad), and vortexed for 2 minutes on a plate vortex (IKA, North Carolina), at a speed setting of 4.5 (1,800 rpm). The plate was incubated at room temperature for 2 minutes, and then transferred to a magnetic stand (Ambion, Life Technologies) for 4 minutes, or until the supernatant had cleared. Using a multi-channel pipette, 25 µl of library was carefully transferred to the corresponding well of a new 96 well PCR plate. The PCR plate was checked on a white background to ensure no magnetic beads had been transferred. Any wells that looked brown had the contents transferred back to the corresponding well of

the MIDI plate and were left until the supernatant had cleared. The contents were then individually transferred to the new 96 well plate. Once all libraries had been transferred, the plate was sealed with a foil lid (StarLab), and the plate centrifuged to collect the entire library at the bottom of the wells.

Selected libraries were run on a gel to check that the clean up was successful. A random selection of at least 5 libraries were quantitated by Qubit to ensure there was sufficient product (≥7.0 ng/µl) to progress to the next stage.

4.2.6.4 Index PCR

At this stage Illumina sequencing adapters and unique dual indices were added to the bead cleaned amplicon PCR products using index primers from the Nextera XT Index Kit v2 (Oligonucleotide sequences © 2007-2013 Illumina, Inc. All rights reserved).

A master mix of 13 µl of 2X Q5 master mix and 5 µl of water was prepared (for library number, plus 10%). Aliquots (18 µl) of master mix were added to 276 wells across three 96 well plates. The index primers were arranged in racks (TruSeq Index Plate Fixture), with forward i5 index primers aligned by row, and reverse i7 primers aligned by column. An aliquot (2.5 µl) of the forward i5 index primer was added to wells 1-12 of the appropriate row, and 2.5 µl of the reverse i7 index primer was added to wells A-H of the appropriate column. Template DNA (3 µl) from the AMPure amplicon PCR clean up was added to the

corresponding well, leaving a final reaction volume of 26 µl. PCR plates were sealed with a foil lid (StarLab).

Libraries were amplified using a GeneAmp 9700 thermocycler (Applied Biosystems, California) using the following temperature programme: 95°C for 3 minutes, followed by 8 cycles of 98°C for 20 seconds, 55°C for 15 seconds, and 72°C for 15 seconds. This was followed by a final hold stage of 72°C for 5 minutes, before cooling to 4°C.

4.2.6.5 PCR clean up II

PCR products were cleaned by the method described in Section 4.2.6.3.

4.2.6.6 Library quantitation

DNA concentration of all libraries was quantitated by the Qubit BR assay (Section 4.2.5), with a minimum DNA concentration of ≥7 ng/µl required to pass to the next stage. Any libraries with a concentration below this threshold were investigated. The corresponding libraries were checked at the 'PCR clean up I' stage by visualising product on gels and, if present, libraries quantitated to check for suitable concentration to continue to index PCR. If there was not a suitable product concentration to re-run from this stage, library preparation was started from the amplicon PCR stage.

4.2.6.7 Normalisation to 10 nM

Before final pooling, samples were normalised to 10 mM, using 5 µl of DNA sample and an appropriate volume of 10 mM Tris buffer, pH 8.5 (Qiagen Buffer EB). DNA concentration in nM was calculated based on the average expected amplicon size, with the equation detailed in the Illumina library preparation literature (Oligonucleotide sequences © 2007-2013 Illumina, Inc. All rights reserved).

4.2.6.8 Pooling

Following normalisation to 10 nM, libraries were pooled. Using a multichannel pipette, 5 µl of each library was transferred to the first column of a new 96 well plate. At the end of this process, the pooled libraries were transferred to a 1.5 ml micro-centrifuge tube, vortexed to mix, and spun down. DNA concentration of the pooled library was quantitated using the Qubit BR assay (Section 4.2.5). Finally, the pooled libraries were split into 3 x 1.5 ml micro-centrifuge tubes. One containing 100 µl of pooled libraries for sequencing, with the remaining pooled libraries split between micro-centrifuge tubes two and three, stored separately.

4.2.6.9 Sequencing details

Samples were shipped on dry ice to The Genome Analysis Centre, Norwich Research Park, NR4 7UH, UK on 19th April 2014.

The provided library pool was diluted to 2 nM with NaOH and 5 µL transferred into 995 µl HT1 (Illumina) to give a final concentration of 10 pM. An aliquot (600 µl) of the diluted library pool was spiked with 10% PhiX Control v3 and placed on ice before loading into an Illumina MiSeq cartridge following the manufacturer's instructions. The sequencing chemistry utilised was MiSeq Reagent Kit v2 (500 cycles) with run metrics of 250 cycles for each paired end read using MiSeq Control Software.

4.2.7 Bioinformatic Analyses

Samples described in Chapters 4 and 5 were multiplexed together for sequencing, and were also processed together.

Sequences were processed using a pipeline combination of UPARSE (Edgar 2013), and QIIME v.1.8.0-20140103 (Caporaso *et al.* 2010). A custom Java program was used to combine paired end reads with a minimum overlap of 20 bp, maximum mismatch of 3 bp, and a minimum length of 100 bp. Sequences were clustered at 97% identity (representing an operational taxonomic unit (OTU)), sequences de-replicated and singletons discarded, and a representative sequence set chosen. For 16S rRNA genes, chimeras were identified using the Greengenes gold database. For 23S rRNA genes, chimeras were identified using

the *de novo* chimera check in the UPARSE pipeline. Taxonomy was assigned by BLAST (Altschul *et al.* 1990) with default settings. 16S rRNA sequences were assigned against the Greengenes 13_5 database, and 23S rRNA sequences using the ARB SILVA 119 LSU Ref database (Quast *et al.* 2013). The resulting taxonomically assigned OTU tables were abundance-filtered at 0.005% (Bokulich *et al.* 2013), discarding any OTUs containing less than 0.005% of the total sequence count.

The method of processing 16S rRNA and 23S rRNA reads differed from this point. For 16S rRNA reads, the OTU table was split by taxonomy, retaining the bacterial sequences only. The OTU table was further filtered to remove any sequences assigned as bacterial, but of mitochondrial or chloroplast origin. At this point any unassigned OTUs were also removed.

For 23S rRNA reads, there were 58 OTUs assigned as 'No Blast Hit' post-abundance filtering, with some of these OTUs contributing as much as 5% of sequences per sample. Taxonomy was assigned to these OTUs by aligning sequences in ARB (Ludwig *et al.* 2004). Sequences were extracted from the representative set and imported into ARB. Sequences were aligned against *E.coli* 0157, with 50/58 sequences suitably aligned, and inserted into a tree of SILVA 119 LSU Ref using parsimony criteria. For a more accurate placement on the tree, organisms of close phylogenetic distance were selected from the tree, and the unassigned sequences' alignment refined against these. This tree construction can be seen in Appendix III, Section III.1. Taxonomy was then assigned to the OTUs that had previously been assigned as 'No Blast Hit' based on their position within the tree. The resulting OTU table was filtered to retain sequences of

cyanobacterial or eukaryotic origin, removing non-target organisms from the analysis. Finally, the OTU table was filtered to remove any eukaryotic samples assigned as 'Metazoa'.

Samples were rarefied at the same level for both compounds for both 16S rRNA and 23S rRNA sequences. The level of rarefaction was set at ten percent of the average sequence per sample value. Samples containing fewer sequences per sample than this value were discarded, and the level of rarefaction set at the next highest sequence per sample value above the cut off. Illumina data were rarefied at 1 196 for bacterial samples, and 725 for phototrophic samples. Sequence processing results are detailed in Section 4.3.3, Tables 4.3 & 4.4, and details of samples lost from rarefaction are detailed in Appendix III, Section III.2.

4.2.8 Statistical analyses

Parametric tests on non-transformed data were performed where possible. If assumptions of heteroscedacity were not met, data were log- or arcsine-transformed. Two-way ANOVA (with treatment, time, and treatment*time) was performed on pH and chlorophyll *a* concentration. Analyses were performed using Genstat v.13.2 (VSN International) and figures were plotted using Sigmaplot v.12.5.

Alpha (α) diversity was analysed by Student's t-test in QIIME using the *Observed Species* rarefaction measure.

Beta (β) diversity was visualised using Bray Curtis similarity matrices with non-metric multidimensional scaling (NMDS). ANalysis Of SIMilarities (ANOSIM) was used to evaluate beta diversity. ANOSIM reports the level of dissimilarity between sample groups (global R) and the associated level of significance (P). R values are within the range +1 to -1. A positive R value indicates that dissimilarity is greater between groups than within groups. A negative R value indicates that samples are more dissimilar within groups than between groups. Significance values (P) were obtained by permutation tests. Similarity Percentages (SIMPER) analysis was used to quantify the relative contribution (%) of each taxon to dissimilarity between groups, and the top five bacterial phyla and phototrophic taxa driving dissimilarity by treatment and time were further investigated. Two-way ANOVA tests were performed on selected taxa to investigate if there were significant effects of treatment and time, and if there were any significant treatment*time interactions. NMDS, ANOSIM and SIMPER analyses were run using Primer 6 (Plymouth, UK; Clarke 1993).

4.3 RESULTS

4.3.1 Soil surface pH

Two-way ANOVA revealed no significant differences in pH by CPP applied (p=0.589). Light treatment appeared to significantly affect pH (p=0.018), and Tukey's post-hoc test revealed the treatment mean of PAR-L (7.52, B) was significantly different to CLEAR (7.45, A), and UV-L (7.45, A).

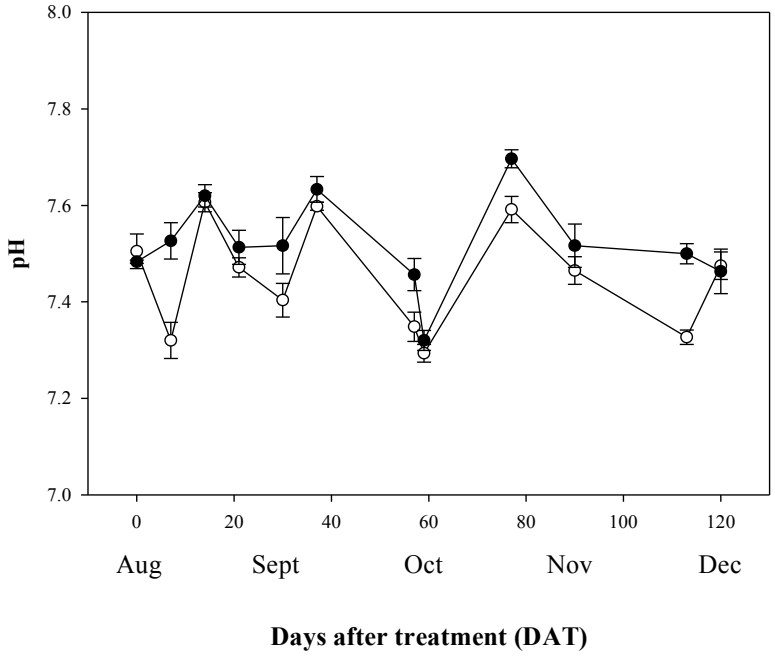

Figure 4.1: Time course of soil surface pH under LIGHT (open symbols) and PAR-L conditions (closed symbols). Error bars represent ±1 S.E.

CLEAR and UV-L were combined as a single treatment, 'LIGHT', shown in Figure 4.1. Average pH was significantly higher under PAR-L conditions, 7.52, relative to LIGHT, 7.45. The pattern of pH development was largely similar

between treatments, fluctuating over time. ANOVA revealed treatment and time (both $p \leq 0.001$) were significant factors in soil surface pH development, and a significant treatment*time interaction was seen ($p=0.009$).

4.3.2 Chlorophyll *a*

Two–way ANOVA revealed no significant difference in chlorophyll *a* concentration by CPP applied ($p=0.626$), and no significant CPP*treatment interaction was seen ($p=0.955$). Filter treatment ($p<0.001$) was a highly significant factor determining chlorophyll abundance, and Tukey's post-hoc test revealed that the treatment mean of chlorophyll *a* concentration under PAR-L (4.87 μg Chl *a*.g^{-1} soil, A) was significantly less than in the CLEAR (47.51 μg.g^{1}, B) and UV-L (47.56 μg.g^{-1}, B) treatments.

CLEAR and UV-L were combined as a single treatment 'LIGHT', shown in Figure 4.2. Average chlorophyll concentration in the PAR-L treatment was low over the whole experiment, rising from an average of 1.5 μg.g^{-1} at 0 DAT to a high of 9.3 μg.g^{-1} at 57 DAT. Average chlorophyll concentration rose under LIGHT from 12.5 μg.g^{-1} at 0 DAT to a high of 89.7 μg.g^{-1} at 57 DAT. Concentration declined to 27.5 μg.g^{-1} at 77 DAT, but increased across the remainder of the time course to 69.0 μg.g^{-1} at 120 DAT.

Filter treatment and time (both $p<0.001$) were significant factors in the development of chlorophyll *a* concentration, and a significant treatment*time interaction was observed ($p=0.009$).

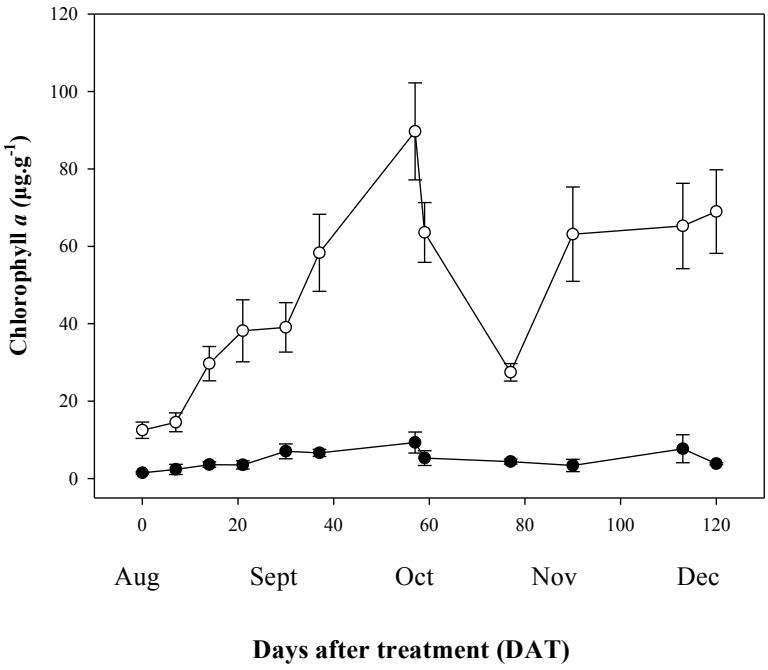

Figure 4.2: Time course of chlorophyll *a* development at the soil surface under LIGHT (open symbols) and PAR-L conditions (closed symbols). Error bars are ±1 S.E.

4.3.3 Sequence processing

A total of 16 449 460 reads were returned from sequencing targeting the 16S rRNA gene. A total of 610 599 (10.6%) sequences from 17 991 OTUs (87.9%) were discarded from the bacterial community composition analysis by abundance filtering at 0.005% (Table 4.3).

A total of 15 510 366 reads were returned from sequencing targeting the 23S rRNA gene. As part of the processing of phototrophic samples (Table 4.4), sequences with a close homology to heterotrophic bacterial sequences were discarded, removing 4 322 OTUs (85%) and 3 280 844 sequences (76%). The resulting OTU table was abundance-filtered at 0.005%, removing a further 609

(79.60%) OTUs and 30 364 sequences (2.9%). OTU tables were then split by experiment for further analysis.

Table 4.3: Bacterial OTU table summary before and after sequence-based OTU abundance filtering.

	16S rRNA sequence processing	
	Non-Abundance filtered	**Abundance filtered**
Number of OTUs	20 476	2 485
Total sequence count	5 765 217	5 154 618
Average sequences/sample	20 889	18 676
Max sequences/sample	69 082	61 397
Min sequences/sample	264	238

Table 4.4: Phototrophic OTU table summary, showing filtering of non-target sequences and sequence based abundance filtering of target sequences.

	23S rRNA sequence processing		
	All (Target & non-target)	**Eukaryotic/Cyano filtered**	**Abundance filtered**
Number of OTUs	5087	765	156
Total sequence count	4 316 280	1 035 436	1 005 072
Average sequences/sample	15 696	3 765	3 655
Max sequences/sample	39 940	21 333	21 268
Min sequences/sample	984	77	75

4.3.4 Chemical comparison

Table 4.5 shows the effect of rarefaction on sample count and number of OTUs remaining in 16S rRNA and 23S rRNA data sets.

Table 4.5: Bacterial and phototrophic OTU table summary (non-rarefied and rarefied).

	16S rRNA	**23S rRNA**
	OTU table summary (rarefied)	**OTU table summary (rarefied)**
Sample count	108 (102)	108 (106)
Number of OTUs	2 425 (2 365)	156 (146)
Average sequences/sample	11 953	7 070
Rarefaction level	1 196	725

Non-metric multidimensional scaling analysis of Bray-Curtis similarities revealed that bacterial (Figure 4.3a) and phototrophic communities (Figure 4.3b) under CLEAR and UV-L conditions clustered together, and were distinct from those under PAR-L filters, and that no effect of CPP treatment was seen. This was confirmed by ANOSIM (Table 4.6).

Pairwise comparisons revealed no significant differences in bacterial or phototrophic community structure at the soil surface between CPPs under the same light filter treatments (e.g. CLEAR), evidenced by low or negative R values, indicating low dissimilarity (Table 4.6, 1.), and significance levels $P>0.05$.

There were also no significant differences in bacterial or phototrophic community structure between CLEAR and UV-L conditions in cores treated with different

CPPs (Table 4.6, 2.), with low or negative R values for all pairwise comparisons, and significance >0.05 for all comparisons.

Pairwise comparisons of filter treatments by CPP (Table 4.6, 3. & 4.) revealed no significant differences in community structure between CLEAR and UV-L, but significant differences between CLEAR and PAR-L and UV-L and PAR-L for both CPPs. Furthermore pairwise comparisons of communities under CLEAR and UV-L filters of paclobutrazol treated cores with communities under PAR-L filter of benzovindiflupyr treated cores, and vice versa (Table 4.6, 5.), showed significant differences with R values all ≥0.422, and significance of P≤0.001 for all comparisons.

Further analysis of bacterial and phototrophic community structure combined CPP treatments, and CLEAR and UV-L were combined as a single treatment, 'LIGHT'.

Table 4.6 Analysis of similarities (ANOSIM) evaluating the variation of soil surface bacterial and phototrophic community structure by CPP and filter treatment.

	16s rRNA	23S rRNA
TREATMENT*CPP - Global Effect	**R = 0.259, *P*≤ 0.001**	**R= 0.245, *P*≤ 0.001**
1. CLEAR – Paclo vs. CLEAR Benzo	R = -0.032, *P*= 0.762	R= -0.033, *P*= 0.894
1. UV – Paclo vs. UV – Benzo	R = -0.016, *P*= 0.594	R= -0.018, *P*= 0.667
1. PAR – Paclo vs. PAR – Benzo	R = 0.020, *P*= 0.248	R= 0.047, *P*= 0.120
2. CLEAR – Paclo vs. UV – Benzo	R= -0.024, *P*= 0.672	R= -0.024, *P*= 0.740
2. UV – Paclo vs. CLEAR Benzo	R= -0.017, *P*= 0.620	R= -0.021, *P*= 0.696
3. CLEAR – Paclo vs. UV - Paclo	R= -0.012, *P*= 0.553	R= -0.018, *P*= 0.628
3. CLEAR – Paclo vs. PAR – Paclo	R= 0.595, *P*≤ 0.001	R= 0.409, *P*≤ 0.001
3. UV – Paclo vs. PAR - Paclo	R= 0.450, *P*≤ 0.001	R= 0.419, *P*≤ 0.001
4. CLEAR – Benzo vs. UV – Benzo	R= -0.044, *P*= 0.920	R= -0.042, *P*= 0.967
4. CLEAR – Benzo vs. PAR – Benzo	R= 0.433, *P*≤ 0.001	R= 0.533, *P*≤ 0.001
4. UV – Benzo vs. PAR - Benzo	R= 0.488, *P*≤ 0.001	R= 0.593, *P*≤ 0.001
5. CLEAR – Paclo vs. PAR – Benzo	R = 0.531, *P*≤ 0.001	R= 0.549, *P*≤ 0.001
5. UV – Paclo vs. PAR – Benzo	R = 0.391, *P*≤ 0.001	R= 0.585, *P*≤ 0.001
5. PAR – Paclo vs. CLEAR – Benzo	R = 0.479, *P*≤ 0.001	R= 0.422, *P*≤ 0.001
5. PAR – Paclo vs. UV - Benzo	R = 0.553, *P*≤ 0.001	R= 0.485, *P*≤ 0.001

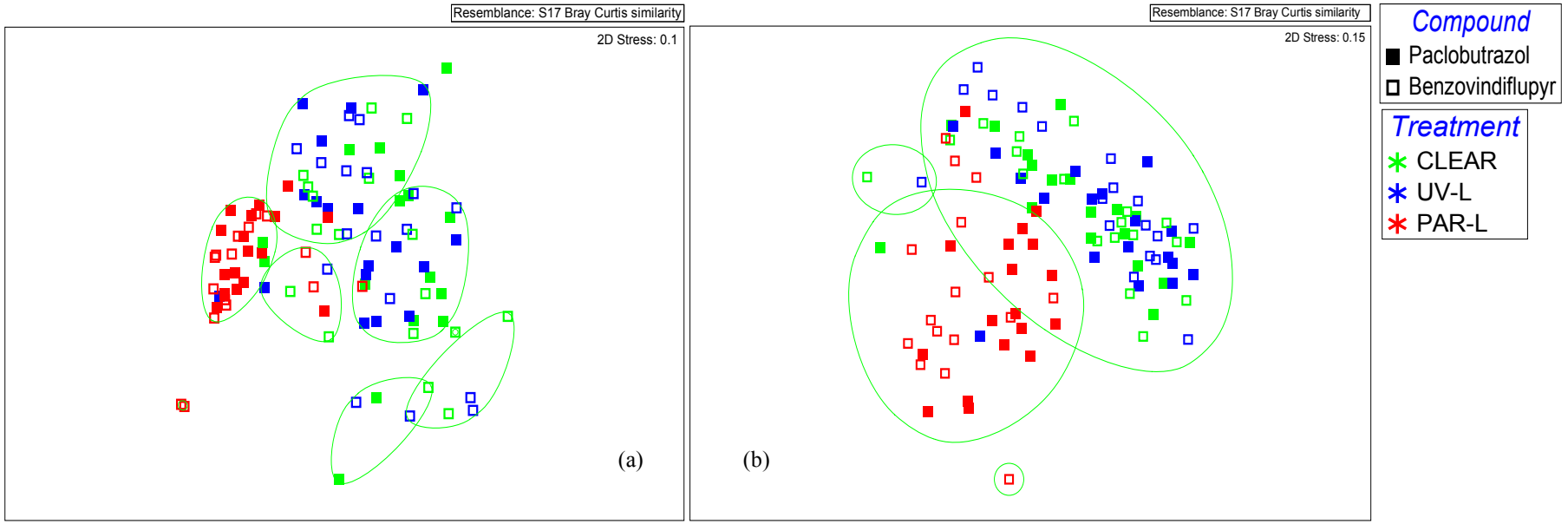

Figure 4.3: Non-metric multidimensional scaling analysis of Bray-Curtis similarities of community structure for (a) bacterial, and (b) phototrophic communities at the soil surface under CLEAR (green), UV-Limiting (blue), and PAR-Limiting (red) filters. Clustering is based on similarity of community structure. The green lines in (a) represent bacterial communities sharing 89% similarity. The greens line in (b) represent phototrophic communities sharing 40% similarity.

4.3.5 Bacterial community composition

4.3.5.1 Bacterial community structure

Analysis of *Observed Species* showed bacterial α diversity at the soil surface was significantly higher under PAR-L conditions relative to LIGHT ($p \leq 0.001$), with an average of 575 observed species under PAR-L and 535 under LIGHT. Figure 4.4a shows the rarefaction curves for bacterial sequences under LIGHT and PAR-L conditions. Diversity increased with sequencing depth, although a plateau in diversity was not seen under either of the filter treatments.

NMDS of Bray-Curtis similarities revealed PAR-L communities were more similar to each other across time than the communities under LIGHT conditions, shown by the closer clustering of samples (Figure 4.4b). The ordination plots reveal a light-mediated temporal development of bacterial communities, with greater development under LIGHT conditions relative to PAR-L. ANOSIM confirmed that light treatment was a significant factor in the differentiation between bacterial community development, see Table 4.7. Pairwise comparison of LIGHT to PAR-L revealed significant differences in community structure, with a global R value of 0.582 revealing greater similarity within groups than between groups. Time was also significant with a global R value of 0.436, and a significance value of $P \leq 0.001$.

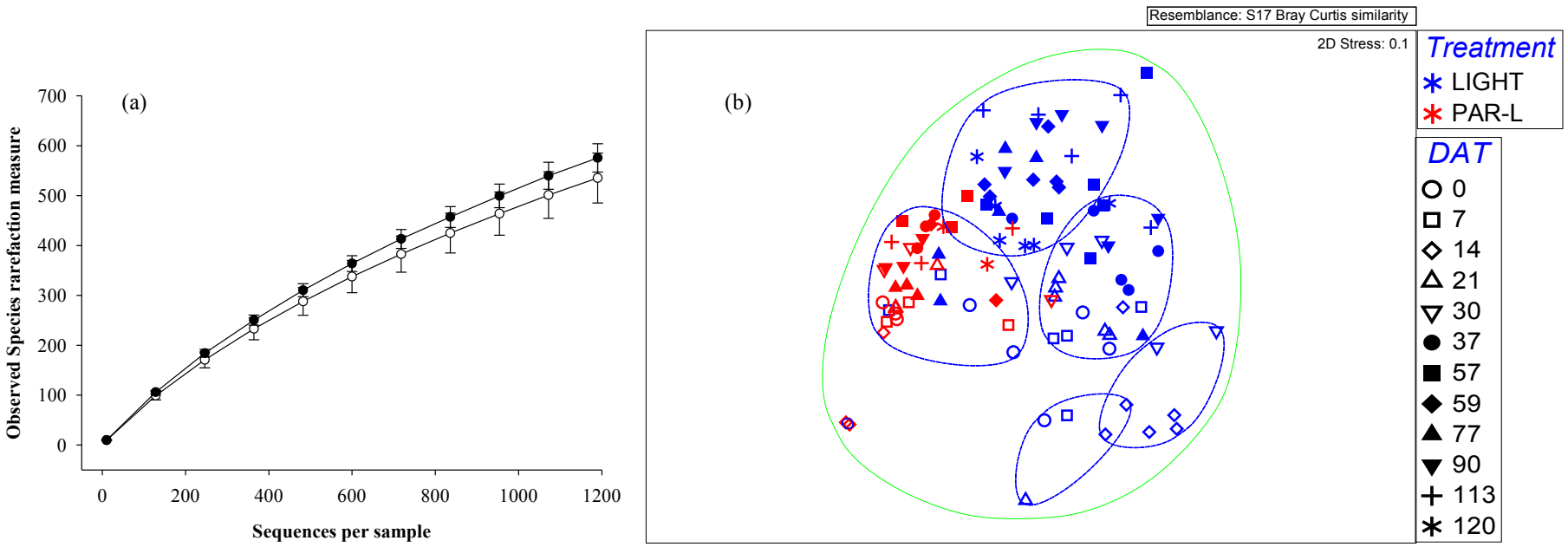

Figure 4.4: (a) Bacterial α diversity estimates of *Observed Species* for LIGHT (open circle) and PAR-L (closed circle) and; (b) Ordination plot from non-metric multidimensional scaling analysis of Bray-Curtis similarities of community structure for bacterial communities at the soil surface under LIGHT (blue) and PAR-L (red) conditions. Clustering is based on similarity of bacterial community structure: at 70% (green line), and 88% (blue lines).

Table 4.7: Analysis of similarities (ANOSIM) evaluating the variation of soil surface bacterial community structure by treatment and time.

	16S rRNA
TREATMENT - Global Effect	**R = 0.582, $P \leq 0.001$**
TIME – Global Effect	**R = 0.436, $P \leq 0.001$**

4.3.5.2 Bacterial community composition

At the phylum level (Figure 4.5), relative composition analysis showed that Actinobacteria and Proteobacteria dominated under both LIGHT and PAR-L conditions. Communities present under LIGHT filters were dominated by Actinobacteria, Proteobacteria, Cyanobacteria, and Chloroflexi. Under PAR-L conditions, Actinobacteria, Proteobacteria, and Chloroflexi dominated. Acidobacteria, Planctomycetes, Verrucomicrobia, Bacteroidetes, Gemmatimonadetes, and Firmicutes represented <10% relative abundance for all conditions, and Cyanobacteria under PAR-L conditions only.

Eleven phyla were represented at levels <1%, including Nitrospirae (0.6%), and Armatimonadetes (0.2%). Phyla representing <0.01% relative read abundance include Elusimicrobia, Chlorobi, Fibrabacteres, Spirochaetes, Thermi, and candidate phyla BRC1, OD1, TM7, and WS3 (data not shown).

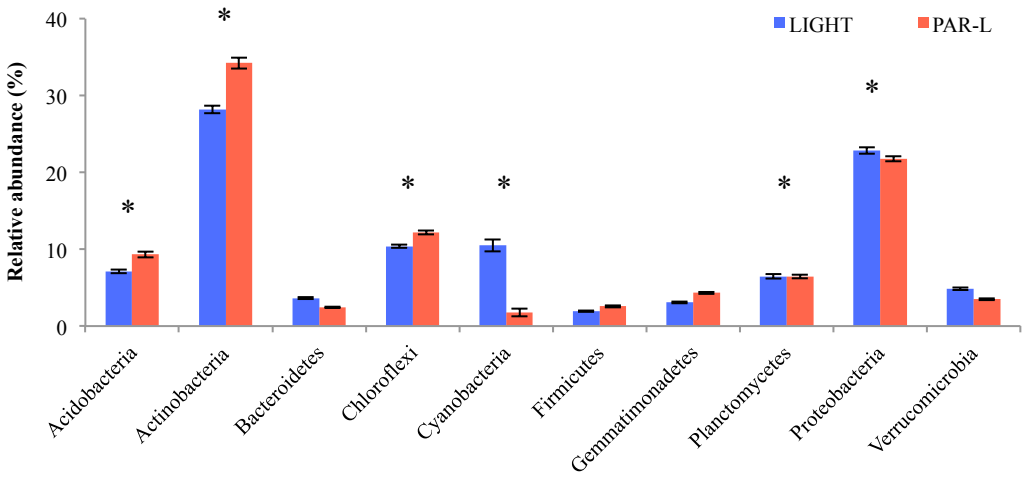

Figure 4.5: Comparison of the average relative abundance of bacterial phyla under LIGHT (blue) and PAR-L (red) conditions. Error bars represent ±1 S.E. Asterisks denote phyla identified by SIMPER analysis as main drivers of dissimilarity.

SIMPER analysis was used to identify the top five phyla driving dissimilarity by filter treatment, between LIGHT and PAR-L, and by time, between 0 and 120 DAT. Full results are shown in Appendix III, Table III.3. Average dissimilarity by filter treatment was 15.73%, and 13.82% by time. The six phyla contributing the greatest percentage difference to this dissimilarity were identified as Cyanobacteria, Actinobacteria, Proteobacteria, Acidobacteria, Planctomycetes and Chloroflexi.

Two-way ANOVA tests were performed on the top six phyla contributing to dissimilarity by treatment and time. The temporal development of bacterial phyla is shown in Figure 4.6.

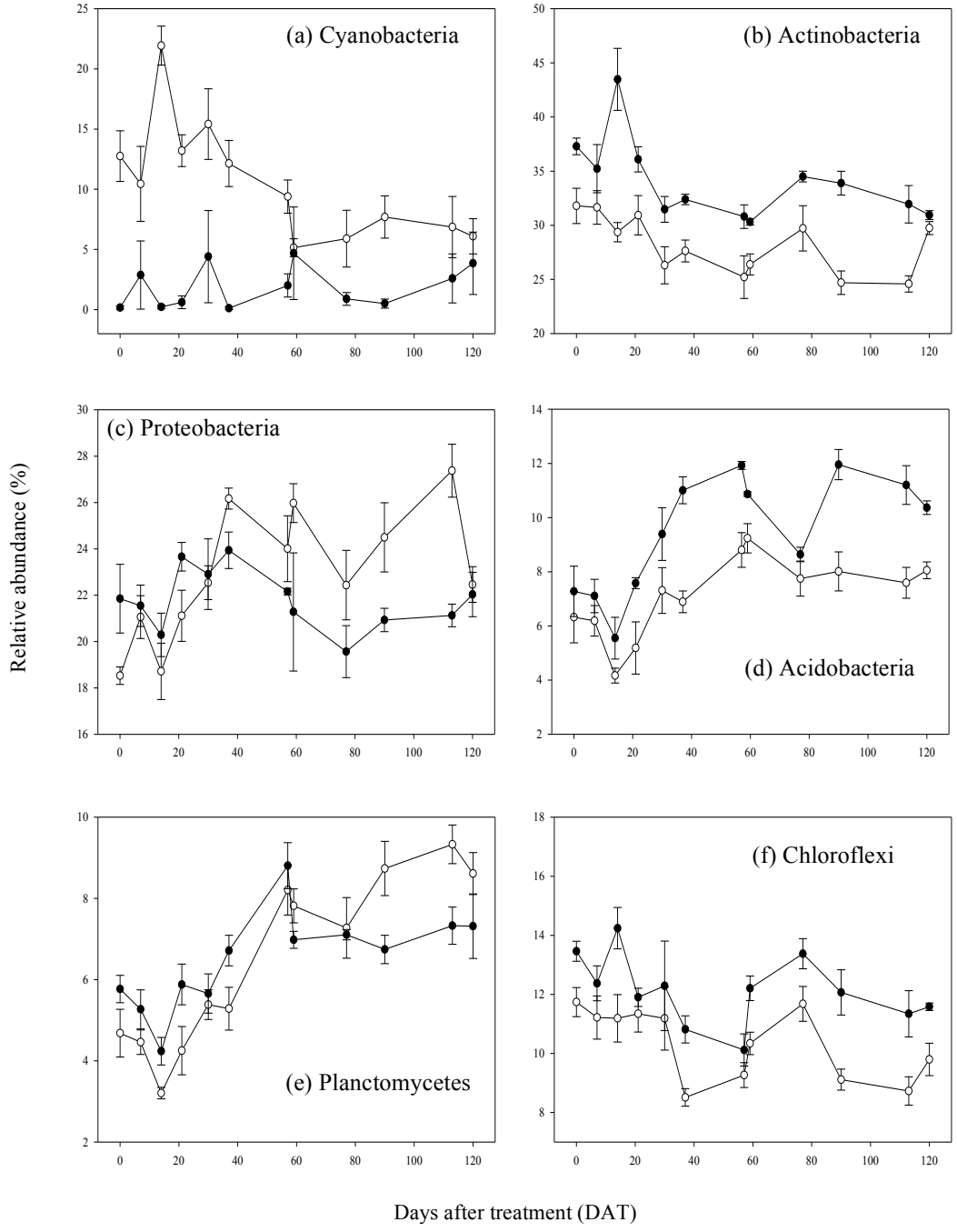

Figure 4.6: Graphs displaying the temporal development of the relative abundance of bacterial phyla identified by SIMPER analysis as driving dissimilarity by treatment and time. LIGHT samples are represented by open symbols, and PAR-L by closed symbols. Error bars represent ±1S.E.

Cyanobacteria (Figure 4.6a) was identified as the phylum making the greatest percentage contribution to the overall dissimilarity by filter treatment, (30.73%) and time (24.15%). Average relative abundance of Cyanobacteria was significantly higher under LIGHT (10.51%) relative to PAR-L (1.77%). Average relative abundance of Cyanobacteria was low under PAR-L, and fluctuated under 5% relative abundance over time. Relative abundance of Cyanobacteria under LIGHT conditions progressed from 12.76% at 0 DAT, to a high of 21.93% at 14 DAT, before generally declining over time, plateauing at ~6% from 59 DAT for the remainder of the experiment. Filter treatment ($p \leq 0.001$) and time ($p \leq 0.001$) were highly significant factors in the development of Cyanobacterial communities, and a highly significant treatment*time interaction was observed ($p < 0.001$).

The phylum Cyanobacteria was composed of two major classes, Oscillatoriophycideae and Nostocophycideae, representing 5.96% and 1.02% of overall relative abundance, respectively. Average relative abundance of Oscillatoriophycideae was higher under LIGHT conditions, 8.09%, relative to PAR-L, 1.71%. Relative abundance generally decreased over time under LIGHT, from 10.33% at 0 DAT to 3.16% at 120 DAT. Under PAR-L, average relative abundance was low, but generally rose from 0.14% at 0 DAT to 3.80% at 120 DAT. Average relative abundance of Nostocophycideae was higher under LIGHT, 1.51%, relative to PAR-L, 0.05%. Relative abundance rose over time under LIGHT from 0.13% at 0 DAT to a high of 4.10% relative abundance at 113 DAT. Relative abundance under PAR-L was low, representing 0.00% relative abundance at 0 DAT, reaching a high of 0.14% at 113 DAT. Treatment

(Oscillatoriophycideae, p≤0.001; Nostocophycideae, p≤0.001) and time (Oscillatoriophycideae p≤0.001, Nostocophycideae p=0.003) were significant factors in the development of both classes. A significant treatment time interaction was seen for Oscillatoriophycideae (p≤0.001), but not in Nostocophycideae (p=0.163).

Actinobacteria (Figure 4.6b) was identified as the phylum making the second greatest percentage contribution to the overall dissimilarity by treatment, (20.60%) and time (14.38%). The average relative abundance of Actinobacteria was significantly higher under PAR-L (34.23%) relative to LIGHT (28.20%). The pattern of development of Actinobacteria relative abundance was similar between PAR-L and LIGHT, though consistently higher under PAR-L. Relative abundance under both treatments generally declined, from 31.79% and 37.29% under LIGHT and PAR-L, respectively, at 0 DAT, to 29.74% and 30.94%, respectively, at 120 DAT. Filter treatment (p≤0.001) and time (p≤0.001) were significant factors in Actinobacteria community development, and a significant filter treatment*time interaction was seen (p=0.033).

Proteobacteria (Figure 4.6c) was identified as the phylum contributing the third greatest percentage difference to overall dissimilarity by treatment (10.16%) and time (13.01%). Average relative abundance of Proteobacteria was significantly higher under CLEAR (22.86%) relative to PAR-L (21.78%). Relative abundance fluctuated across the time course, and relative abundance was initially higher under PAR-L, though was higher under LIGHT ≥37 DAT. Filter treatment (p=0.024) and time (p≤0.001) were significant factors in the

development of Proteobacteria communities, and a significant treatment*time interaction was seen ($p=0.007$).

Acidobacteria (Figure 4.6d) was identified as the phylum making the fourth greatest percentage contribution to overall dissimilarity by treatment (8.03%) and the fifth greatest by time (8.53%). The average relative abundance of Acidobacteria was significantly higher under PAR-L (9.34%) relative to LIGHT (7.13%). Relative abundance rose across the time course under all treatments, and under PAR-L rose from 7.27% at 0 DAT to 10.37% at 120 DAT. The pattern of development of relative abundance under LIGHT was similar, though consistently lower under PAR-L, rising from an average of 6.32% at 0 DAT to 8.05% at 120 DAT. Filter treatment ($p\leq0.001$) and time ($p\leq0.001$) were significant factors in the development of Acidobacteria communities, although no significant filter treatment*time interaction was seen ($p=0.195$).

Planctomycetes (Figure 4.6e) was identified as the phylum making the fourth greatest percentage contribution to dissimilarity by time (12.78%). There was no significant difference in average relative abundance between treatments, and relative abundance rose across the time course under all treatments, from 5.09% at 0 DAT to 8.29% at 120 DAT. Time ($p\leq0.001$) was highly significant in Planctomycetes community development. Filter treatment ($p=0.839$) was not a significant factor, and no significant filter treatment*time interaction was seen ($p=0.230$).

Chloroflexi (Figure 4.6f) was identified as driving dissimilarity by treatment, making the fifth greatest percentage contribution to overall dissimilarity (6.67%). Average relative abundance of Chloroflexi was

significantly higher under PAR-L (12.15%) relative to LIGHT (10.34%). Relative abundance fluctuated across the time course, but generally decreased from 11.74% and 13.46% under LIGHT and PAR-L respectively at 0 DAT to 9.80% and 11.58% at 120 DAT. Filter treatment ($p \leq 0.001$) and time ($p \leq 0.001$) were significant factors in the development in Chloroflexi community development. No significant treatment*time interaction was seen ($p=0.739$).

4.3.6 Phototrophic community composition and structure

4.3.6.1 Phototrophic community structure

Analysis of *Observed Species* showed phototrophic α diversity at the soil surface was significantly higher under PAR-L conditions relative to LIGHT ($p \leq 0.001$), with an average of 52.8 observed species under PAR-L and 35.6 under LIGHT (rarefied at 725). Figure 4.7a shows the rarefaction curves for phototrophic sequences under LIGHT and PAR-L conditions. Diversity increased with sequencing depth, although a plateau in diversity was not seen under either of the filter treatments.

NMDS of Bray-Curtis similarity revealed a light-mediated, time-dependent development of phototrophic community structure (Figure 4.7b). ANOSIM revealed that light treatment was a significant factor driving the structural diversity (Table 4.8), with significant differences between PAR-L and LIGHT conditions. Time was also shown to be significant in the development of phototrophic community structure, with a global R value of 0.438 and a significance value of $P \leq 0.001$.

Table 4.8: Analysis of similarities (ANOSIM) evaluating the variation of soil surface phototrophic community structure by treatment and time.

	23S rRNA
TREATMENT - Global Effect	**R = 0.841, *P*≤ 0.001**
TIME – Global Effect	**R = 0.438, *P*≤ 0.001**

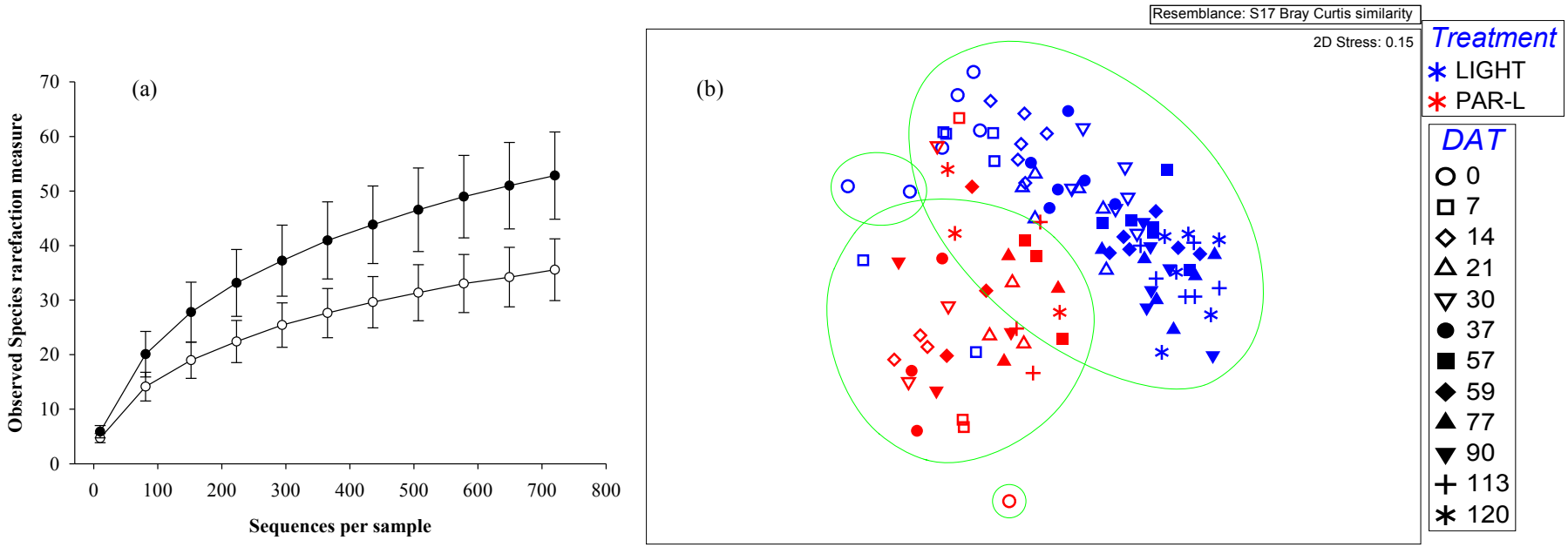

Figure 4.7: (a) Phototrophic α diversity estimates of *Observed Species* for LIGHT (open circles) and PAR-L (closed circles) and; (b) Ordination plot from non-metric multidimensional scaling analysis of Bray-Curtis similarities of community structure for phototrophic communities at the soil surface. Clustering is based on similarity of phototrophic community structure: green lines (40% similarity).

4.3.6.2 Phototrophic community composition

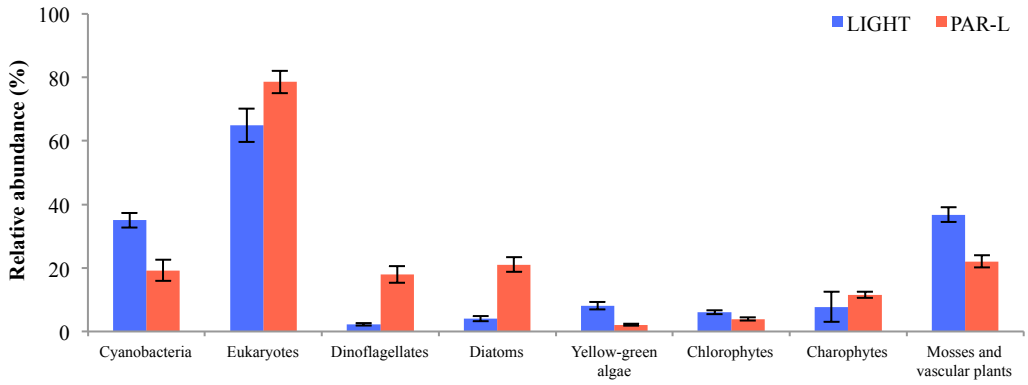

Figure 4.8: Comparison of the average relative abundance of cyanobacterial and eukaryotic phototrophic taxa, between LIGHT (blue) and PAR-L (red) conditions and a breakdown summary of the major taxa composing the eukaryotic phototrophs. Error bars represent ±1 S.E.

Sequencing revealed a phototrophic community structure dominated by eukaryotes, although cyanobacteria representation was significantly higher under LIGHT conditions relative to PAR-L (Figure 4.8). A wide range of eukaryotic phototrophs were detected, including dinoflagellates, diatoms, yellow-green algae, green algae (both chlorophytes and charophytes) and mosses.

SIMPER analysis was used to identify the top five taxa driving dissimilarity in phototrophic communities by filter treatment, between LIGHT and PAR-L, and by time between 0 and 120 DAT. Overall average dissimilarity was 61.19% by filter treatment, and 78.45% by time. Taxa identified as driving dissimilarity included the cyanobacteria *Microcoleus vaginatus and Nodosilinea nodulosa,* the sub-division of moss *Bryophytina,* the order of diatoms *Naviculales,* and the yellow-green algae family *Vaucheriaceae.* Full results are shown in Appendix III, Table III.4.

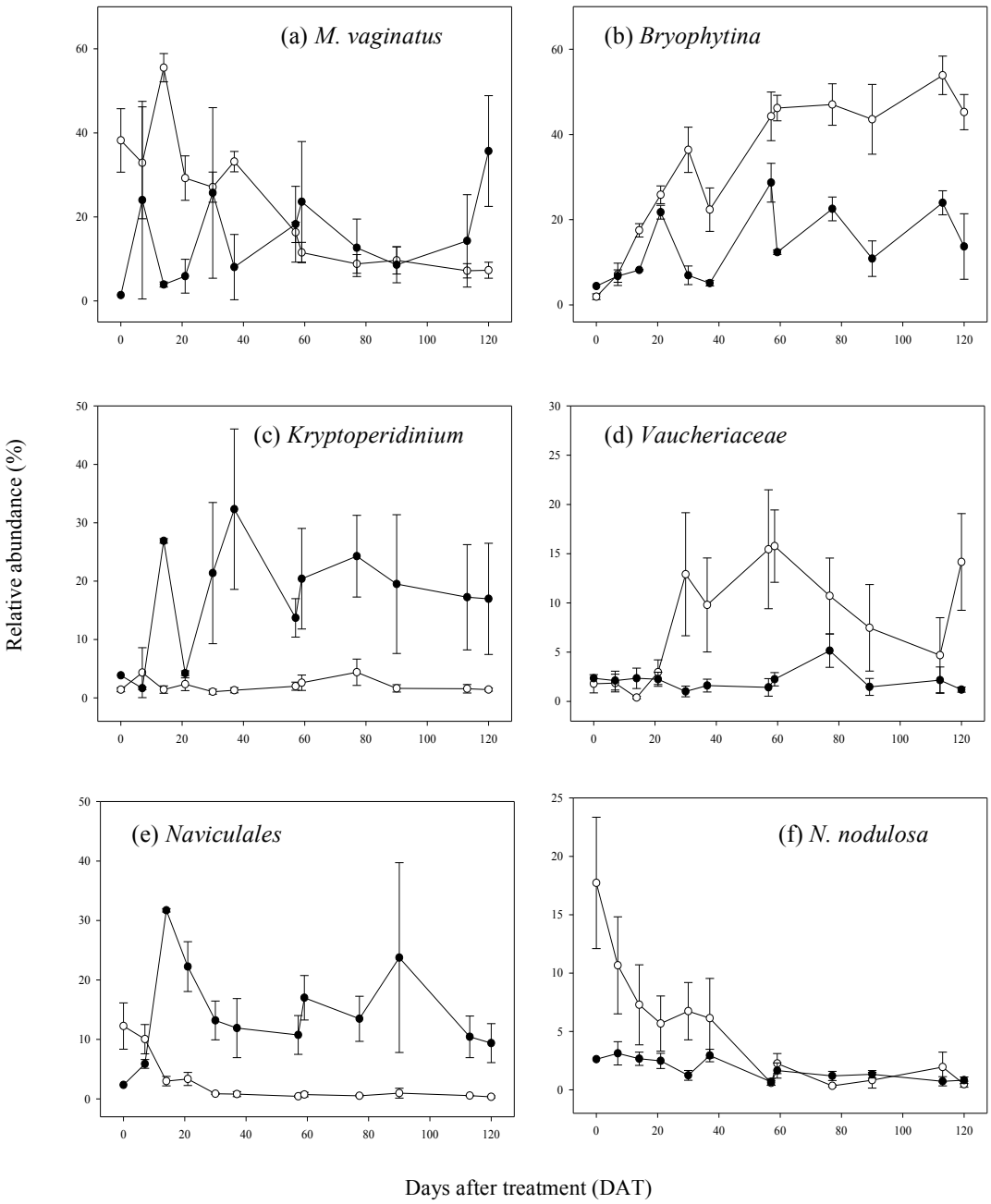

Figure 4.9: Graphs displaying the temporal development of the relative abundance of phototrophic taxa identified by SIMPER analysis as driving dissimilarity by treatment and time. LIGHT samples are represented by open symbols, and PAR-L by closed symbols. Error bars are ±1 S.E.

Two-way ANOVA tests were performed on the six taxa identified as contributing to the greatest percentage to dissimilarity by treatment and time. The temporal development of these taxa is shown in Figure 4.9.

The cyanobacterium *M. vaginatus* (Figure 4.9a) was identified as the taxon making the greatest percentage contribution to dissimilarity by treatment, (18.84%) and the second greatest contribution to dissimilarity by time (19.92%). Average relative abundance was highest under LIGHT (23.07%) relative to PAR-L (15.98%). There was high variability in relative abundance over time, although relative abundance generally declined under LIGHT conditions from an average of 38.20% at 0 DAT, reaching a high of 55.5% at 14 DAT, to 11.5% at 59 DAT. Relative abundance plateaued under light for the remainder of the time course, remaining <10% at all time points ≥77 DAT. Under PAR-L conditions, relative abundance was variable, and generally rose across the time course from an average of 1.5% at 0 DAT to 14.3% at 113 DAT, before a rise to a high of 35.7% at 120 DAT. Filter treatment ($p \leq 0.001$) and time ($p = 0.008$) were significant factors in *M. vaginatus* community development, and a significant filter treatment*time interaction was seen ($p \leq 0.001$).

The sub-division *Bryophytina* (Figure 4.9b) was identified as the taxon making the greatest percentage contribution to dissimilarity by time (25.95%), and the taxon making the second greatest percentage contribution to dissimilarity by treatment (17.05%). Average relative abundance was significantly higher under LIGHT (32.62%) relative to PAR-L conditions (14.32%). The pattern of development was similar under both treatments, and generally increased over time, although at a greater rate and magnitude under LIGHT relative to PAR-L.

Under LIGHT conditions relative abundance generally increased over time from 1.93% at 0 DAT to 46.21% at 59 DAT, and then plateaued for the remainder of the experiment. Under PAR-L relative abundance fluctuated across the time course, but reached 28.69% at 57 DAT. Filter treatment ($p \leq 0.001$) and time ($p \leq 0.001$) were significant factors in the development of *Bryophytina* communities, and a significant filter treatment*time interaction was seen ($p \leq 0.001$).

The genus *Kryptoperidinium* (Figure 4.9c) was identified as the taxon making the third greatest percentage contribution to dissimilarity by treatment, contributing 13.26% to the overall average dissimilarity of 61.19%. Average relative abundance was significantly higher under PAR-L conditions (17.63%), relative to LIGHT (2.12%). Relative abundance was low under LIGHT, representing <4.50% at all time points. Variation in relative abundance under PAR-L was high, and initially fluctuated from 3.99% at 0 DAT to a high of 32.32% at 37 DAT, before plateauing for the remainder of the experiment. Filter treatment ($p \leq 0.001$) was a significant factor in the development of Kryptoperidinium communities, and significant treatment*time interaction was seen ($p=0.002$). Time ($p=0.214$) was not a significant factor.

The family *Vaucheriaceae* (Figure 4.9d) was identified as the taxon making the fifth greatest contribution to dissimilarity by treatment (6.39%), and the fourth greatest contribution by time (7.57%). Average relative abundance was higher under LIGHT (8.16%) relative to PAR-L (2.10%). Relative abundance was generally low, representing <2.5% relative abundance at all time points excluding 90 DAT, where relative abundance was at a high of 5.15%. Under LIGHT,

relative abundance increased to 12.92% at 30 DAT and fluctuated across the remainder of the experiment. Filter treatment ($p \leq 0.001$) and time ($p=0.011$) were significant factors in the development of *Vaucheriaceae* communities, though no significant filter treatment*time interaction was seen ($p=0.140$).

The order *Naviculales* (Figure 4.9e) was identified as the taxon making the fourth greatest percentage contribution to dissimilarity by treatment (11.55%), and the fifth greatest contribution by time (7.35%). Average relative abundance was higher under PAR-L (15.05%), relative to LIGHT conditions (2.82%). Relative abundance under LIGHT declined from 12.25% at 0 DAT to 0.87% at 30 DAT, and remained at <1% relative abundance for the remainder of the experiment. Relative abundance under PAR-L increased to a high of 31.72% at 14 DAT, but declined to 13.20% at 30 DAT and remained generally steady for the remainder of the experiment. Filter treatment ($p \leq 0.001$) and time ($p \leq 0.001$) were significant factors in the development of *Naviculales* communities, and a significant filter treatment*time interaction was seen ($p \leq 0.001$).

The cyanobacterium *Nodosilinea nodulosa* (Figure 4.9f) was identified as the taxon making the third greatest percentage contribution to dissimilarity by time, contributing 10.23%. Average relative abundance was significantly higher under LIGHT (5.06%) relative to PAR-L (1.80%). Relative abundance under LIGHT decreased from 12.71% at 0 DAT to 2.25% at 59 DAT, and remained at <2% for the remainder of the experiment. Relative abundance was low under PAR-L, at <3.2% across the whole time course. Filter treatment ($p=0.014$) and time ($p \leq 0.001$) were significant factors in the development of *N. nodulosa*, though a significant filter treatment*time interaction was not seen ($p=0.089$).

4.4 DISCUSSION

The availability of photosynthetically active radiation (PAR) appeared to significantly affect bacterial and photrophic community structure and their temporal development at the soil surface. It also appeared to significantly affect the α diversity of phototrophic and bacterial communities, with species richness greater under PAR-Limited conditions. Exposure to UV light had no significant effect on bacterial or phototroph community structure and development relative to when UV light was limited. Availability of PAR light also enhanced soil surface chlorophyll *a* concentration, and increased soil pH.

Chlorophyll *a* concentration was used as a broad scale measure of phototroph community development. Phototroph community development was clearly restricted under PAR-L conditions compared to LIGHT conditions. Jeffery *et al.* (2009) observed that the restriction of UV-A (<380 nm) at the soil surface resulted in a four-fold increase in the concentration of chlorophyll *a*. No such effect was observed in this work, with Tukey's test revealing no significant difference in chlorophyll concentration between CLEAR and UV-L filter treatments.

Community composition analysis of phototrophic communities revealed dominance by eukaryotic algae, with an average relative abundance of 64.97% under LIGHT conditions and 78.59% under PAR-L. This dominance of eukaryotic phototrophs contrasted with the findings of Davies *et al.* (2013b), who observed that Cyanobacteria were dominant under both light and dark treatments

in a temperate agricultural soil, such that after 80 d incubation Cyanobacteria accounted for 63.8% and 82.7% of sequences under light and dark respectively.

Sequencing targeting the 23S rRNA gene revealed moss as the dominant phototrophic taxon at 30 DAT under LIGHT conditions. The development of phototroph communities under the LIGHT filters displayed temporal successional development, with the cyanobacterium *Microcoleus vaginatus* initially dominant, before the development and proliferation of mosses in the subdivision *Bryophytina.* This time-dependent successional shift in the dominant phototrophs present in BSCs has been well documented. Li *et al.* (2002) highlighted three main stages of development in a 25-year time course, from initial colonisation by Cyanobacteria, to the appearance of mosses within the system, leading to domination by eukaryotic algae, mosses, and liverworts. Similar patterns of successional development have been shown the world over in arid environments, such as the eastern Negev desert in Israel (Lange *et al.* 1992), and Arches National Park in Utah (Belnap 1993). However, development of crusts in arid environments is slow, and it has been observed that formation of crusts occurs much faster in temperate soils relative to those in arid environments. In Knapen *et al.* (2007), BSCs were seen to form readily in a sandy loess soil. Phototroph cover of 5% had developed by 50-80 days after tillage, cover of 5-25% by 105 days, and cover of 50-75% with abundant moss apparent 179 days after tillage. This timescale contrasts sharply with that of BSC development in the Tengger desert (Li *et al.* 2002) where the first stage of BSC development, colonisation of Cyanobacteria, occurred in the first year, and moss was not observed until year eight.

The dominant cyanobacterial taxon present within a BSC is influenced by several factors, including the type of BSC (Redfield *et al.* 2002), the successional stage (Yeager *et al.* 2004), temperature (Garcia-Pichel *et al.* 2013), and level of aridity (Zaady *et al.* 2010). Early stage BSC development is characterised by colonisation and dominance of pioneering species such as *M. vaginatus*, before a shift in dominance to diazotrophic cyanobacteria, such as *Nostoc punctiforme* and *Anabaena cylindrica,* in more mature later-stage crusts of arid lands (Garcia-Pichel *et al.* 2003; Yeager *et al.* 2004). In a temperate pasture soil incubated under light and dark conditions in a lab based system, Davies *et al.* (2013b) found that phototrophs of cyanobacterial origin, rather than eukaryotic phototrophs, were relatively more abundant under both light and dark conditions. Further, 65.1% of the cyanobacterial sequences were identified as having close homology to the diazotrophic cyanobacterium *N. punctiforme* PC73102. This dominance in relative abundance of *N. punctiforme* was not seen in dark kept soil, where 12.6% of cyanobacterial sequences were assigned as *N. punctiforme* PCC73102.

In this work a similar effect of late-stage dominance of diazotrophic cyanobacteria was seen. From 77 DAT onwards, sequences assigned to the Cyanobacteria family Nostocaceae, containing diazotrophic cyanobacteria characteristic of late-stage crusts such as *N. punctiforme* and *A. cylindrica,* were dominant under LIGHT conditions, representing 50.81% of all cyanobacterial sequences, rising to 63.08% at 113 DAT. Similarly to the dark kept samples in Davies *et al.* (2013b), this dominance of diazotrophic cyanobacteria was not seen under PAR-L, in which there was a maximum relative abundance of 29.17%

cyanobacterial sequences at 0 DAT, with proportional abundance decreasing over time.

The results of 16S rRNA sequencing complemented the pattern of successional development of Cyanobacteria observed in the 23S rRNA sequencing under LIGHT conditions, from filamentous colonising cyanobacteria to diazotrophic cyanobacteria. The order Oscillatoriales, of which the early colonising cyanobacterium *M. vaginatus* is a member, was initially dominant, representing 81.09% of cyanobacterial sequences, but relative abundance decreased over time as successional dominance shifted to the order Nostocales. This order, containing diazotrophic cyanobacteria such as *N. punctiforme* and *A. cylindrica*, is known to proliferate in mature crusts, and represented 58.72% and 43.54% of cyanobacterial sequences at 113 and 120 DAT, respectively. This late stage emergence of Nostocales was similar to the dominance characteristics seen in Davies *et al.* (2013b), and is typical of mature BSC composition (Garcia-Pichel *et al.* 2003; Yeager *et al.* 2004). These diazotrophic cyanobacteria are important ecosystem engineers in arid regions as they input N into the, usually, nutrient-poor environment (Belnap 2002; Zhao *et al.* 2010), allowing further development of the BSC, leading ultimately to increased productivity of vascular plants (Langhans *et al.* 2009b). However, the contribution of cyanobacterial communities to N_2 fixation in temperate agricultural soil is unknown, though if it were found to be agriculturally relevant, this could inform tillage practice and land management approaches relating to the application of N fertiliser.

In BSCs of arid regions, bacterial communities are dominated by Cyanobacteria (Garcia-Pichel *et al.* 2001; Redfield *et al.* 2002; Abed *et al.* 2010).

In a BSC in the Sultanate of Oman, Abed *et al* (2010) showed that 77-81% of 16S rRNA isolates belonged to the phylum Cyanobacteria, with remaining clones attributed to Alpha- and Deltaproteobacteria, Bacteroidetes, Gemmatimonas and Planctomycetes. However, Davies *et al.* (2013b) did not observe this dominance of Cyanobacteria in a laboratory incubated temperate pasture soil, although the inclusion of non-UV light was shown to have several effects. 454-pyrosequencing targeting 16S rRNA revealed that Cyanobacteria represented <4% of the relative abundance of bacterial reads, and the dominating phyla were Proteobacteria and Actinobacteria (Davies *et al.* 2013b). Furthermore, in the presence of light there was a selection for the phylum Firmicutes, representing an average of 19.39% relative abundance in soil exposed to non-UV light, and just 5.90% in the dark. Similarly, in the study reported here, the dominant phyla were Actinobacteria and Proteobacteria, although the relative abundance of reads assigned as Cyanobacteria was higher, averaging 10.51% in LIGHT conditions. However, the selective effect for the phylum Firmicutes was not seen, with Firmicutes representing an average of just 2.57% relative abundance under PAR-L conditions, and 1.93% under LIGHT. Bacterial community structure was also more variable in Davies *et al.* (2013b) with communities from 40 and 80 days incubation only sharing 40% similarity. In this study, community variability was much lower and all samples shared at least 70% community structure.

Davies *et al.* (2013b) also showed that the comparative reduction in bacterial diversity under light conditions was not due to selection for Cyanobacteria, as α diversity was still significantly lower under light conditions after OTUs assigned as Cyanobacteria were removed from the analysis. However,

when Cyanobacterial OTUs were removed from the analysis in this study, α diversity was still lower under LIGHT conditions relative to PAR-L, though not significantly so ($p=0.069$; results not shown).

The decrease in bacterial diversity at the soil surface under LIGHT conditions relative to PAR-L could be partly explained by direct selection pressures of LIGHT, however further differences could be due selection from other pressures, such as indirect selection of heterotrophic bacteria due to the input of C and N into the system, associated with growth of phototrophs (Belnap 2002; Zhao *et al.* 2010; Yoshitake *et al.* 2010; Davies *et al.* 2013b). This effect was described by Davies *et al.* (2013b) as analogous to the 'rhizosphere effect', where the rhizosphere can select for certain microbial communities in a plant-specific manner (Morgan *et al.* 2005), and suggested a new discrete zone of influence at the soil surface termed the 'crustosphere'.

The observed differences in microbial community composition may also be influenced to indirect factors, by differences in environmental parameters affecting community development other than light, including moisture, pH, and bioturbation. Soil moisture content was consistently and significantly higher under PAR-L conditions relative to LIGHT (Section 3.3.1), and this may also have influenced community composition at a treatment level.

A comprehensive UK-wide study of bacterial community structure of soil by Griffiths *et al.* (2011) showed that community dissimilarity was most strongly linked to differences in pH, and that acidic soils were dominated by a few taxa, with clear selection for Alphaproteobacteria and Acidobacteria. In this study, soil pH was consistently higher under PAR-L conditions relative to LIGHT. However,

the relative abundance of the phylum Acidobacteria was higher under PAR-L conditions relative to LIGHT across the experiment, and no significant difference was observed in the relative abundance of Alphaproteobacteria between filter treatments, which suggests that the observed differences in pH were not a main driver of differences in community structure.

Bioturbation, the reworking of soils by organisms, may also affect taxonomic composition of soil surface bacterial communities. Monard *et al.* (2011) showed that earthworm engineering modified the taxonomic composition of atrazine degraders in burrow linings and in casts, relative to bulk soil. However, whilst enhancing soil heterogeneity, such effects were localised, and unlikely to affect community composition on a treatment or time scale.

Sequencing revealed that the availability of photosynthetically active radiation (PAR) in soil cores incubated in the field appeared to significantly affect the diversity and structure of phototrophic and bacterial communities at the soil surface. It was also shown that effects seen previously in a temperate, lab-based, soil experiment are also seen in a more environmentally realistic system. Future work should focus on the significance of these community shifts and their roles within agricultural systems.

CHAPTER 5: CROP CANOPY COVER INFLUENCES THE TEMPORAL AND SPATIAL DEVELOPMENT OF MICROBIAL COMMUNITIES AT THE SOIL SURFACE

5.1 INTRODUCTION

Work presented in Chapter 4 showed that bacterial and phototrophic community structure at the soil surface developed temporally, and was significantly different when photosynthetically active radiation (PAR) was artificially restricted from reaching the soil surface. Work in this Chapter investigated the effect of differing crop canopy cover on the bacterial and phototrophic communities present in the soil.

The artificial modulation of the spectral quality of light reaching the soil surface has been shown to affect microbial community phenotype and structure at the soil surface in several systems. Jeffery *et al*. (2009) used filters to modulate the spectral quality of light reaching the soil surface of repacked cores, and subsequent PLFA analysis showed that phenotypically distinct communities had formed by eight weeks post-disturbance, accompanied by an increase in biomass relative to the underlying bulk soil and increased chlorophyll *a* content. Similar observations were made between non-UV light- and dark-kept systems (Davies *et al.* 2013b), where distinct bacterial and phototrophic communities were observed at the soil surface between light and dark systems. Bacterial soil surface communities were structurally distinct to those of the underlying bulk soil, and no significant difference was observed in phototrophic community structure between

bulk and surface soil, suggesting a greater influence of light than previously thought. Temporal development of soil surface communities was also observed, similar to the previous observations of temporal development of BSCs in arid and semi-arid environments (Abed *et al.* 2010; Garcia-Pichel *et al.* 2001; Yeager *et al.* 2004). In soil cores incubated in the field, this temporal development of soil surface communities was mediated by the presence of PAR (Chapter 4), though the light reaching the surface of the soil was still artificially restricted.

Knapen *et al.* (2007) observed that BSCs readily form *in situ* in a temperate agricultural environment, though it was unclear whether the type of crop or canopy characteristics affected the development of bacterial and phototrophic communities at the soil surface, and if any differences extended to communities present in the bulk soil.

Work presented in this chapter investigated the development of bacterial and phototrophic communities under crops exhibiting differing canopy characteristics. Cores were taken at regular intervals over a 150-day period, from planting to harvest, and were divided into surface and bulk components. Bacterial primers targeting the V4 region of the 16S rRNA gene (Caporaso *et al.* 2012) and universal phototroph primers designed to target prokaryotes and eukaryotes (Sherwood and Presting 2007) were used to create target amplicon libraries to investigate if there were differences in soil community structure by layer (surface vs. bulk), treatment (crop type) or across time. Illumina MiSeq pyrosequencing of PCR amplicons, and chlorophyll *a* measurements were used to answer the following questions.

5.1.1 Questions to be addressed

(i) Does the soil surface harbour bacterial and photosynthetic communities that are distinct from underlying bulk soil?

(ii) Do crop canopy characteristics affect the development of bacterial communities in soil?

(iii) Do crop canopy characteristics affect the development of phototrophic communities in soil?

5.2 MATERIALS AND METHODS

5.2.1 Soil

The soil used was the same as described in Section 2.2.1. Several weeks prior to the start of the experiment, ~60 kg of well-rotted calf manure was dug evenly into the plot as an organic fertiliser.

5.2.2 Plot preparation

The plot used for this experiment is the same as described previously in Chapters 3 and 4. In the weeks prior to planting, the plot was weeded regularly using a hoe, and the soil surface evened by raking. The plot was split in to a square comprised of nine 1 x 1 m subplots separated by 0.4 x 1 m dividing regions. Planting treatments were allocated to the nine subplots in a Latin square design, and three of the dividing regions taken as bare plots, shown in Appendix IV, Section IV.1. The plots were marked out with string, and planting lines were also laid out. The planting lines were kept in place until the crops began to shoot, to avoid pulling out the crops whilst weeding.

5.2.3 Planting patterns

Crops exhibiting differing canopy characteristics were chosen to provide different levels of shading. The crops chosen were onion (minimal shading), wheat (medium shading) and main crop potatoes (maximal shading). Planting patterns are shown in Figure 5.1.

Onion sets, *Alium cepa cv. Sturon*, were planted in two sets of three rows, with the rows 50 mm apart, a central gap of 400 mm between sets of rows, and a 200 mm gap left at either edge (Figure 5.1a). Sturon sets were planted every 50 mm along each row.

Spring wheat, *Triticum aestivum cv. Cobber,* was planted in seven rows, with the rows 120 mm apart, and an 80 mm gap at the edge of the plot (Figure 5.1b). Wheat seed (15 g) was spread evenly between the rows, with a seed every 30-50 mm.

Main crop potatoes, *Solanum tuberosum cv. Desiree*, were planted in two rows, with 330 mm between the edge of the plot and the rows. Seed potatoes were planted 300 mm apart in each row (Figure 5.1c).

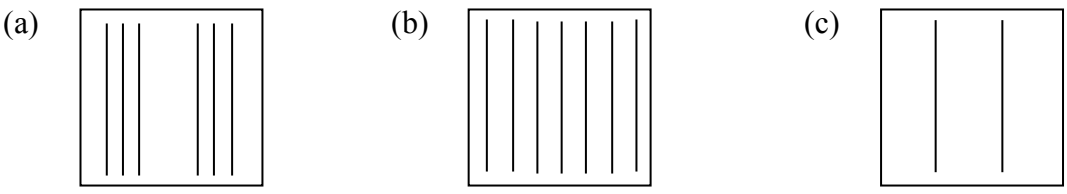

Figure 5.1: Planting patterns of: (a) onion, (b) wheat and (c) potato. All plots were 1 m^2.

5.2.4 Plot maintenance

Weeding was carried out by hand for the duration of the experiment to prevent unnecessary disturbance of the soil surface.

To minimise the risk of disease, such as powdery mildew (wheat) and late blight (potato), the plot was watered from ground level using leaker hoses, with two leaker hose lengths crossing each subplot. Watering was not on a set timer, rather determined by the glasshouse manager as required by the crops, with all crop types getting the same water addition. The wheat crop was treated for powdery mildew 53 days after planting (DAP) on 22nd June 2012, with the systemic foliar fungicide fenpropidin at 375 g ai/ha. The whole plot was treated for aphids 71 DAP on the 9th July 2012, with the carbamate insecticide primicarb at 280 g ai/ha.

5.2.5 Environmental monitoring

Soil temperature and soil moisture content (VWC) were recorded in one plot of each treatment (Bare, Onion, Wheat, Potato). Probes were positioned in the centre of the plot at a depth of 20 cm. Data were recorded every 30 mins and a daily average taken. Readings were taken using WatchDog 1000 series micro-logging systems (Spectrum Technologies Inc.).

5.2.6 Sampling and processing

Soil was sampled at; 0, 14, 30, 60, 91, 120, and 150 days after planting (DAP). Subplots were further divided in to 9 additional subplots, and samples taken in accordance with a randomised design. Cores were taken with a 50 mm diameter acrylic corer. The corer was inserted to 50 mm, rotated to break the connection of the sampled core with the soil beneath, and withdrawn carefully from the soil. A plunger (machined to fit the corer) was inserted beneath the core, extruding the core to the top of the corer. The top 5 mm of core was exposed, and a sharp edge (pallet knife) was used to firmly separate the layer into a pre-labelled weigh boat. The remaining 45 mm of core was extruded into a separate weigh boat. The corer was cleaned with distilled water, and the process repeated.

Soil samples were transferred to the lab, flash frozen, and homogenised. Surface soil samples were flash frozen in weigh boats by addition of liquid nitrogen. Samples were homogenised using a Gyro-Mill (Glen Creston Ltd) at 200 rpm for 40 seconds. Samples were then transferred to falcon tubes cooled with liquid nitrogen, and samples transferred to ice. Once all samples had been processed, they were transferred to -80°C for storage.

The same basic method was used for processing bulk soil samples. Following homogenisation one falcon tube of soil was filled with a sample of the homogenized soil and the remaining sample was discarded.

5.2.7 Chlorophyll *a*

Please refer to Section 4.2.3

5.2.8 DNA isolation and quantitation

DNA was isolated and quantitated by the methods described in Sections 4.2.4 & 4.2.5. DNA was isolated from surface and bulk samples from all plots across the full time course.

5.2.9 Library preparation, sequencing, and bioinformatic analyses

Libraries were prepared and sequencing completed as detailed in Section 4.2.6. Sequence processing and bioinformatic analyses were as detailed in Section 4.2.7

5.2.10 Statistical Analyses

Please refer to Section 4.2.8 for details of statistical analyses

5.3 RESULTS

5.3.1 Temperature and moisture

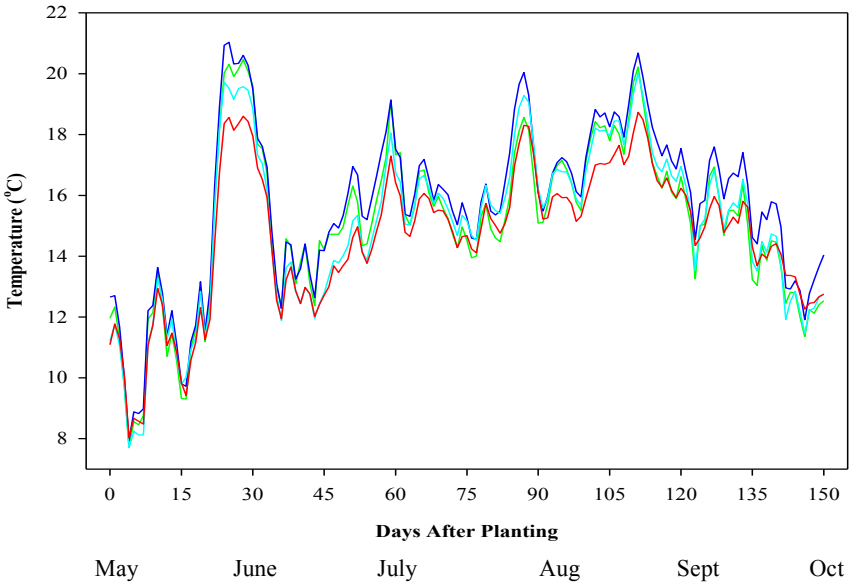

Figure 5.2: A comparison of average daily soil temperature recorded across a 150-day time course under Bare (green), Onion (blue), Wheat (cyan), and Potato (red) treatments.

Soil temperature (Figure 5.2) generally rose with time over the experiment to ca. 110 days (end of Sept) and then decreased. The average temperature was highest under Onion treatment (15.69°C) relative to Bare soil (15.11°C), Wheat (15.05°C), and Potato (14.66°C). The highest maximum temperature was 21.04°C under Onion, 20.46°C under Bare, 20.02°C under Wheat, and 18.73°C under Potato . Minimum daily average temperatures were 7.70°C under Bare, 7.71°C under Wheat, 7.94°C under Onion, and 8.02°C under Potato.

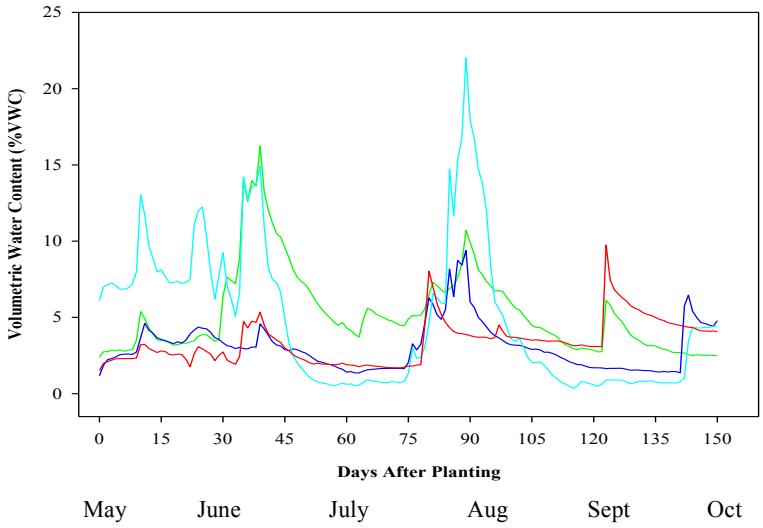

Figure 5.3: A comparison of average daily soil moisture content (VWC) across a 150-day time course under Bare (green), Onion (blue), Wheat (cyan), and Potato (red) treatments.

Soil moisture (Figure 5.3) fluctuated over time at varying magnitudes by treatment. The highest average moisture content was under Bare soil (5.27%), relative to Wheat (4.88%), Potato (3.40%), and Onion (3.09%). The highest recorded soil moisture was 22.04% under Wheat, relative to 16.24% under Bare, 9.75% under Potato, and 9.39% under Onion. Minimum recorded soil moistures were 0.35% under Wheat, 1.18% under Onion, 1.51% under Potato, and 2.39% under Bare soil.

5.3.2 Chlorophyll *a*

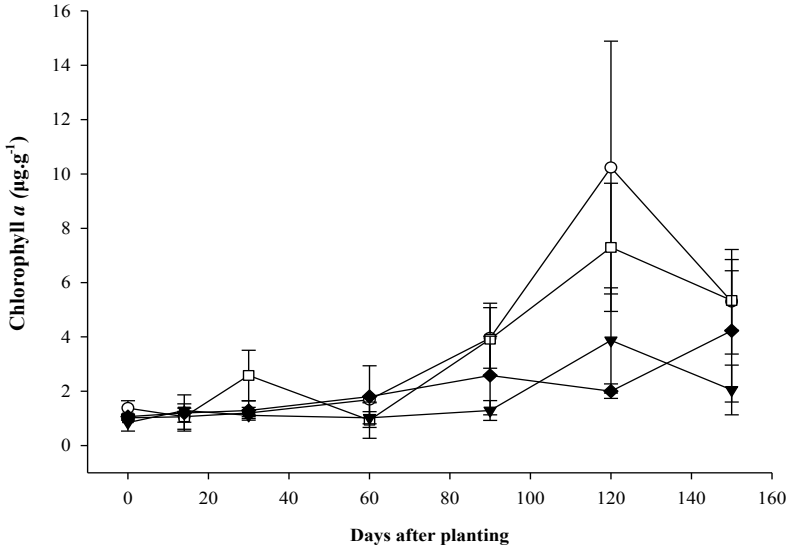

Figure 5.4: Time course of chlorophyll concentration at the soil surface under crops with differing canopy characteristics. Bare (—○—), Onion (—□—), Wheat (—◆—), and Potato (—▼—). Error bars represent ±1 S.E.

Chlorophyll *a* concentration at the soil surface was similar between treatments until 60 DAP, with concentration rising under Bare soil, Onion and Wheat treatments at 91 DAP. This trend continued to 120 DAP, where chlorophyll *a* concentration also rose under Potato, and average recorded concentration reached maximum levels for Bare soil (10.24 $\mu g.g^{-1}$), Onion (7.30 $\mu g.g^{-1}$), and Potato (3.87 $\mu g.g^{-1}$) treatments, before declining by 150 DAP. Concentration was highest for Wheat treatment at 150 DAP (4.23 $\mu g.g^{-1}$). Time ($p \leq 0.001$) was a significant factor in the development of chlorophyll *a* concentration. However, treatment was not a significant factor ($p=0.079$) and there was no significant treatment*time interaction ($p=0.631$).

5.3.3 Surface vs. bulk

Following processing described in Section 4.3.3, samples were analysed together to compare surface and bulk samples. Table 5.1 shows the OTU summary information for both 16S and 23S rRNA amplicon samples, the effect of rarefaction on sample count and number of OTUs is displayed. Bacterial and phototrophic data sets were rarefied at 2 231 and 147 sequences/sample, respectively. Details of samples lost due to rarefaction are included in Appendix IV, Section IV.2

Table 5.1: Bacterial and phototrophic OTU table summaries (non-rarefied and rarefied) for comparison of Surface and Bulk samples

	16S rRNA	**23S rRNA**
	OTU table summary (rarefied)	OTU table summary (rarefied)
Sample count	167 (165)	167 (162)
Number of OTUs	2 425 (2 410)	156 (142)
Average sequences/sample	20 566	1 446
Rarefaction level	2 231	147

Analysis of *Observed Species* rarefaction measure reveals that bacterial and phototrophic α diversity was significantly higher in bulk soil relative to the surface soil ($p \leq 0.001$ and $p=0.013$, respectively). Diversity increased with sequencing depth, though a plateau was not seen for surface or bulk samples in either analysis (Figure 5.5).

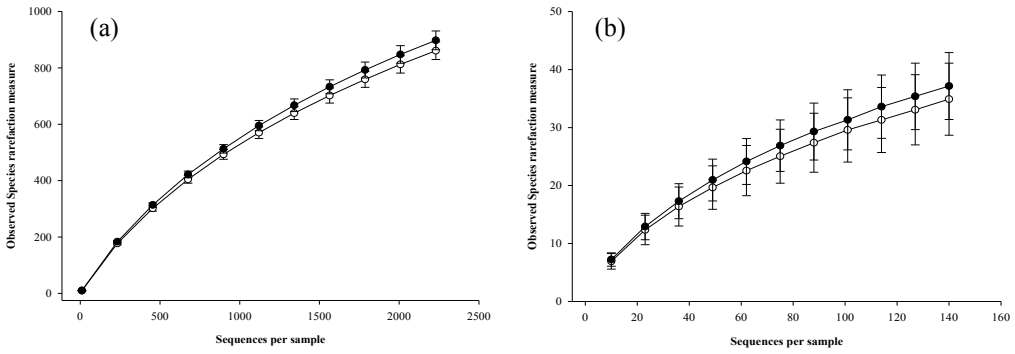

Figure 5.5: Observed Species α diversity estimates of (a) bacterial, and (b) phototrophic communities present in surface (open circles) and bulk (closed circles) samples. Error bars represent ±1 S.E.

NMDS ordination plots of Bray Curtis similarities are displayed in Figure 5.6. Bacterial communities showed high similarity, with all samples clustering within 85% similarity (Figure 5.6a). The ordination revealed a temporally mediated pattern of dissimilarity between surface and bulk bacterial communities, with surface and bulk layers becoming more dissimilar with the progression of time. ANOSIM confirmed the distinct nature of the layers, with an R statistic of 0.563, and a significance value $P \leq 0.001$.The temporal element of the community development is highlighted by ANOSIM, with an R statistic of 0.241, and a significance value of $P \leq 0.001$ (Table 5.2).

NMDS revealed that phototrophic community structure was more variable than that of bacteria, with clustering displayed at 70% similarity (Figure5.6b). Soil surface communities were more variable than those within the bulk, and there was clear temporal development of surface communities from 30 DAP onwards. ANOSIM revealed separation by layer with a global R of 0.250, and $P \leq 0.001$. Time was also significant, $P \leq 0.001$, although more variable than the layer effect, with an R statistic of 0.145.

Table 5.2: Results of analyses of similarity (ANOSIM) evaluating variation in the structure of Surface and Bulk soil samples by treatment and by time.

	16S rRNA	23S rRNA
LAYER - Global Effect	**R = 0.563, *P*= 0.001**	**R= 0.250, *P*= 0.001**
TIME – Global Effect	**R = 0.241, *P*= 0.001**	**R = 0.145, *P*=0.001**

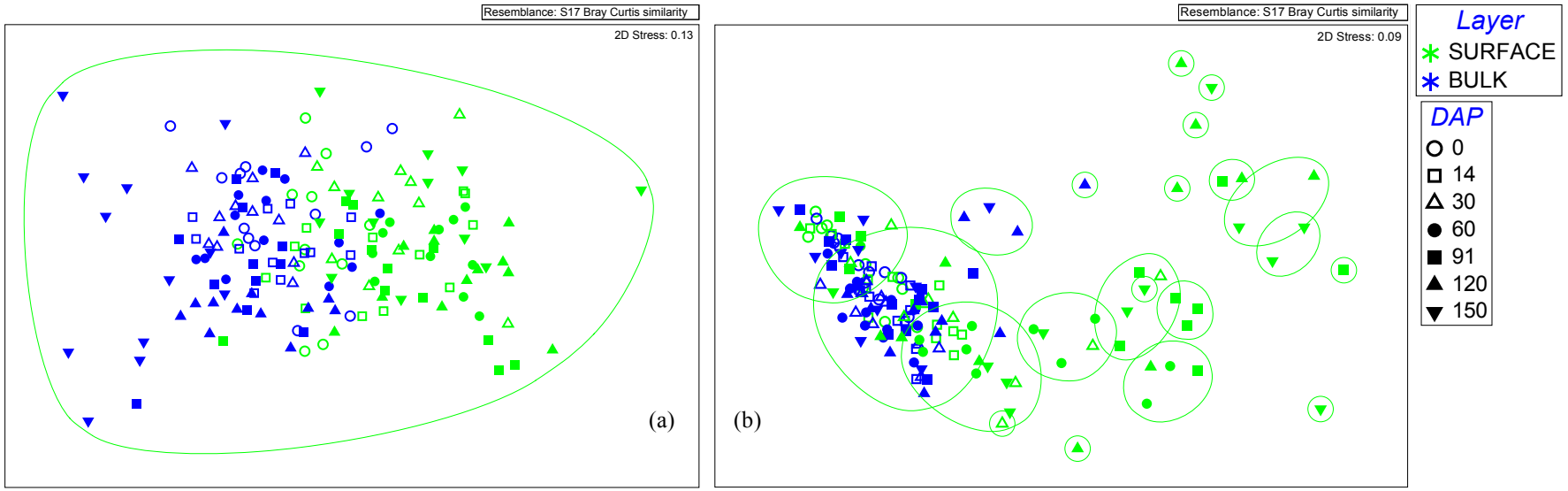

Figure 5.6: Ordination plots from non-metric multidimensional scaling analysis of Bray Curtis similarities of (a) bacterial, and (b) phototrophic community structure between bulk and surface soil samples. Green lines represent a similarity threshold of (a) 85%, and (b) 70%.

5.3.3.1 Phyla driving bacterial community dissimilarity between surface and bulk soil

SIMPER analysis was used to identify bacterial phyla driving dissimilarity between bulk and surface samples in 16S rRNA samples (full results shown in Appendix IV, Section IV.3, Table IV.3). The overall average dissimilarity between surface and bulk was 9.05%, and the overall dissimilarity by time (0 DAP vs. 150 DAP) was 9.05%. The five phyla contributing the greatest percentage difference to this dissimilarity were identified as Actinobacteria, Acidobacteria, Proteobacteria, Firmicutes and Chloroflexi. Two-way ANOVA tests were performed on the top five phyla contributing to dissimilarity by layer and time. A comparison of the temporal development of the relative abundance of these phyla is shown in Figure 5.7.

Actinobacteria (Figure 5.7a) was identified as the phylum making the greatest percentage contribution to the overall dissimilarity between surface and bulk (30.99%), and across time (26.41%). Relative abundance levels were similar at 0 DAP, at 35.01% and 36.00% in bulk and surface, before diverging for the remainder of the experiment. Average relative abundance of Actinobacteria was higher at the soil surface (39.41%) across the whole experimental period relative to bulk (34.08%). From 14 DAP to 120 DAP, the pattern of development of Actinobacterial abundance remained similar between surface (average 39.96%) and bulk (average 34.70%), before a decline in the bulk relative abundance at 150 DAP to 29.73%. Layer ($p \leq 0.001$) and time ($p \leq 0.001$) were significant factors in the development of Actinobacteria communities, and a significant layer*time interaction was seen ($p \leq 0.001$).

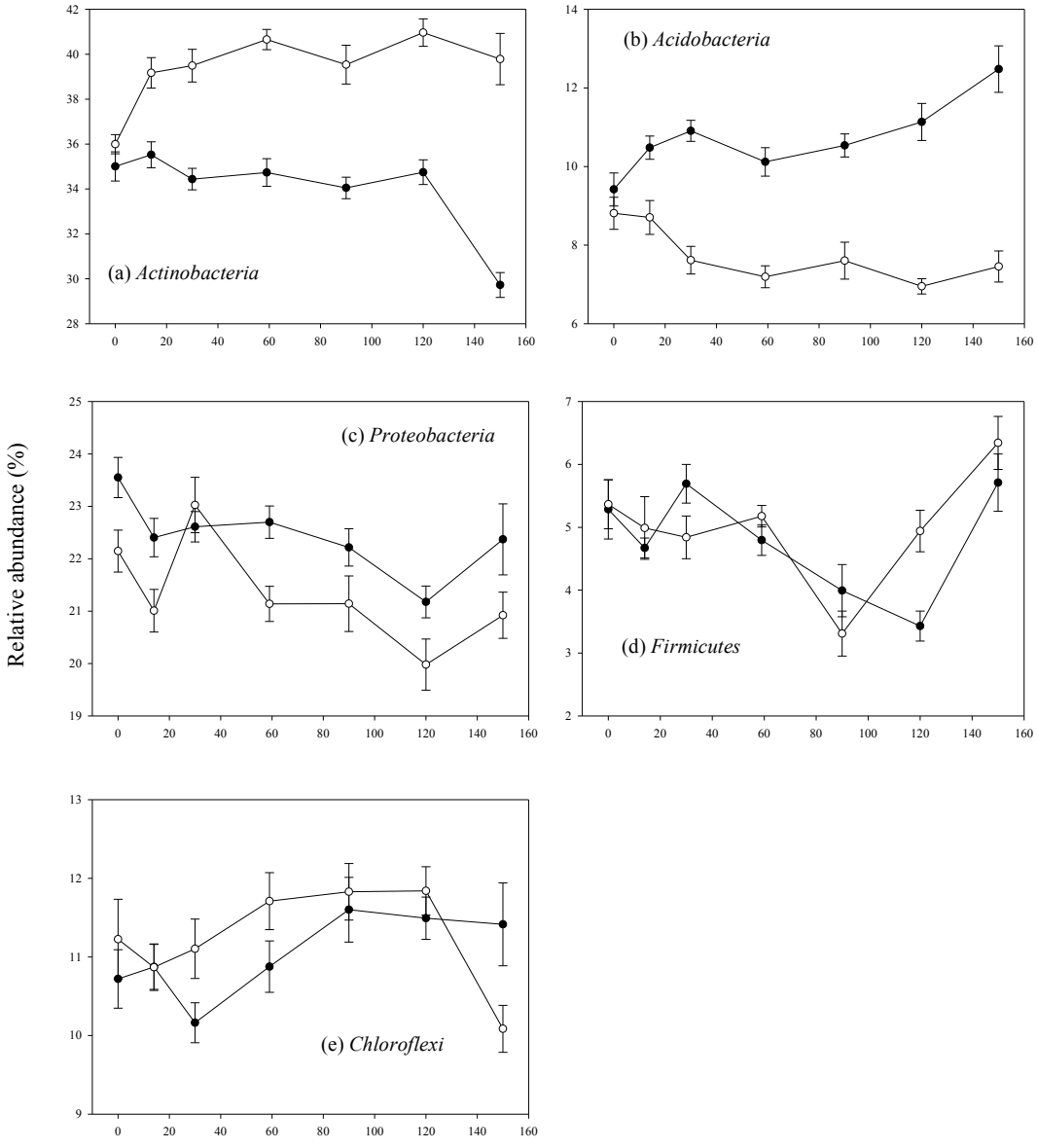

Figure 5.7: The temporal development of the relative read abundance of bacterial phyla identified by SIMPER analysis as driving dissimilarity by layer and time. Surface samples are represented by open symbols, and bulk by closed symbols. Error bars represent ±1 S.E.

Acidobacteria (Figure 5.7b) was identified as the phylum contributing the second most to dissimilarity by layer (17.56%) and time (14.37%). Average relative abundance was higher in bulk soil (10.68%) relative to surface (7.75%). Abundance levels were similar at 0 DAP, 9.42% and 8.81% in bulk and surface. Generally, relative abundance increased in bulk samples over time, with a final relative abundance of 12.48% at 150 DAP, while relative abundance decreased in surface samples, reaching 7.46% at 150 DAP. Layer ($p \leq 0.001$) and time ($p=0.029$) were significant factors in the development of Acidobacteria communities, and there was a significant treatment*time interaction ($p \leq 0.001$).

Proteobacteria (Figure 5.7c) was the third greatest contributor to dissimilarity between surface and bulk (10.59%) and by time (11.91%). Average relative abundance was higher in bulk soil (22.45%) relative to the surface layer (21.31%) across the time course. The pattern of development of the relative abundance of Proteobacteria across the time course was similar in bulk and surface soil, apart from at 30 DAP where relative abundance was higher in surface samples (23.03%) relative to bulk (22.61%). Layer ($p \leq 0.001$) and time ($p \leq 0.001$) were significant factors in the development of Proteobacteria communities, though no significant treatment*time interaction was seen ($p=0.260$).

Firmicutes (Figure 5.7d) were identified as the fourth greatest contributor to dissimilarity by layer (8.03%), and the fifth greatest by time (9.55%). Average relative abundance across the time course was higher in surface samples (4.99%) relative to bulk soil (4.80%). The development of Firmicute relative abundance was similar between layers. It was generally stable until 60 DAP before a general decrease in abundance to 91 DAP in surface samples and 120 DAP in bulk soil,

before increasing in abundance to 150 DAP. Layer ($p=0.298$) was not a significant factor in the development of Firmicute communities, although time ($p\leq0.001$) was. The layer*time interaction was also significant ($p=0.023$).

Chloroflexi (Figure 5.7e) was the fifth greatest contributor to dissimilarity by layer (8.00%) and the fourth greatest by time (9.86%). Average relative abundance was higher in surface samples (11.24%) relative to bulk (11.01%). Relative abundance was higher in surface samples at all time points expect at 14 DAP (both 10.87%), and 150 DAP, where relative abundance at the surface (10.09%), was lower than in bulk samples (11.42%). Layer ($p=0.259$) was not a significant factor in the development of Chloroflexi communities, although time ($p=0.009$) was, and there was a significant treatment*time interaction ($p=0.043$).

5.3.3.2 Taxa driving phototrophic community dissimilarity between surface and bulk soil

SIMPER analysis was used to identify phototroph (23S rRNA) taxa driving dissimilarity between bulk and surface samples (full results shown in Appendix IV, Section IV.3, Table IV.4). The overall dissimilarity between surface and bulk was 41.00%, and overall dissimilarity by time was 42.44%.

The five taxa contributing the greatest percentage difference were identified as Spermatophyta, Vaucheriaceae, Chaetosphaeridiaceae, Kryptoperidinium and Coleochaetaceae. Two-way ANOVA tests were performed on the top five taxa contributing to dissimilarity by layer and time. The temporal development of the phyla is shown in Figure 5.8.

The superdivision Spermatophyta (Figure 5.8a) was identified as contributing the greatest percentage difference to the overall dissimilarity between bulk and surface (32.82%), and time (37.73%), with average relative abundance higher in bulk (56.32%) relative to surface samples (38.44%). The relative abundance of reads assigned as Spermatophyta was similar between bulk and surface samples at 0 and 14 DAP, declining from 67% to 55%, respectively, and generally remained steady in bulk samples for the remainder of the experiment, with a decline at 120 DAP to 45.00%, before an increase at 150 DAP to 60.50%. In surface soil samples, relative abundance continued to decline for the remainder of the experiment, reaching 17.70% at 150 DAP. Layer ($p \leq 0.001$) and time ($p \leq 0.001$) were significant factors in the development of Spermatophyta communities, and there was a significant layer*time interaction ($p \leq 0.001$).

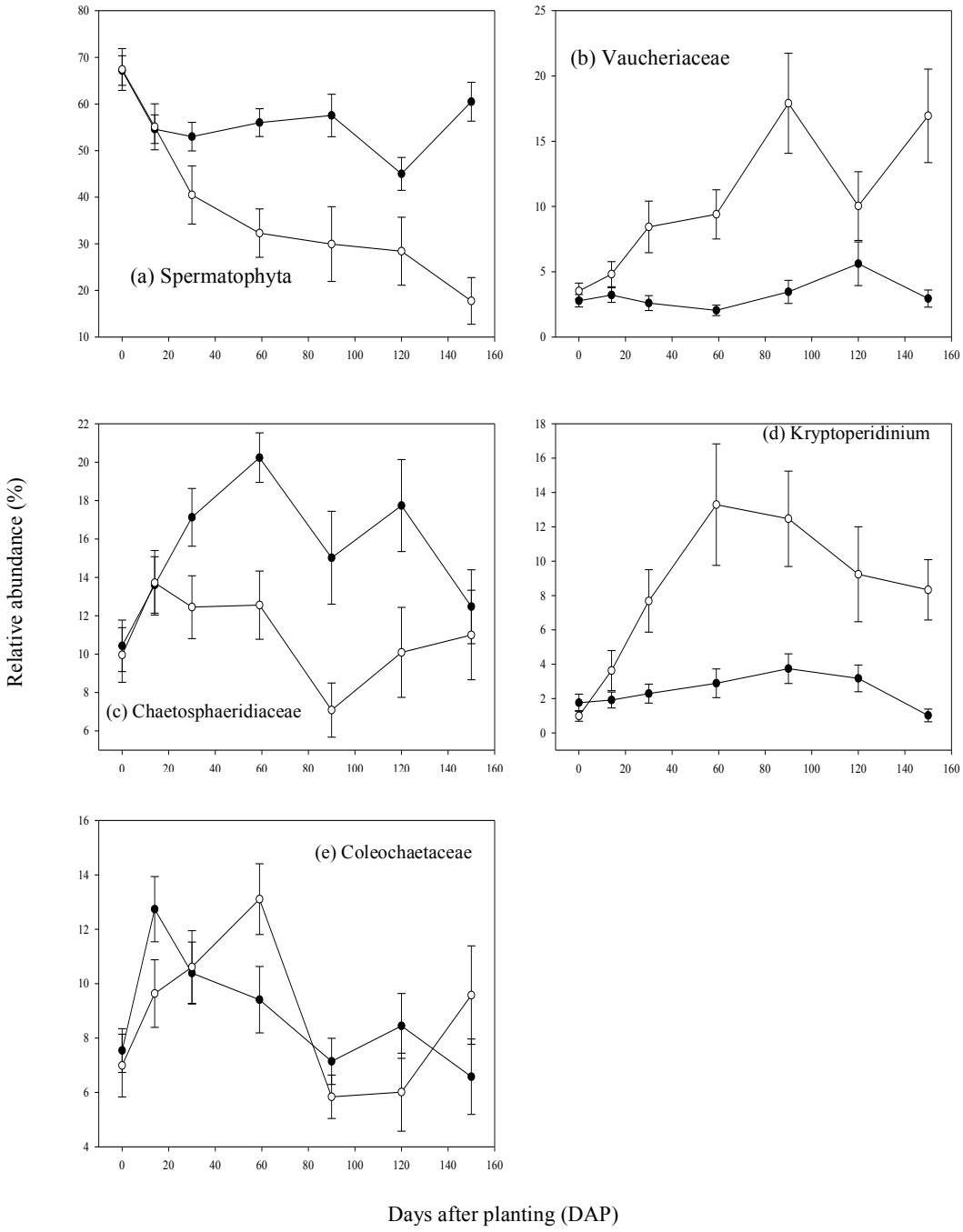

Figure 5.8: The temporal development of the relative read abundance of phototrophic taxa identified by SIMPER analysis as driving dissimilarity by layer and time. Surface samples are represented by open symbols, and bulk by closed symbols. Error bars represent ±1 S.E.

The family Vaucheriaceae (Figure 5.8b) was identified as the taxon contributing the second highest percentage to overall dissimilarity by layer (10.19%) and time (9.13%). Average relative abundance was higher in surface samples relative to bulk soil, 10.19% and 3.24% respectively. Relative abundance was similar at 0 DAP, 2.78% in bulk and 3.53% in surface samples, before diverging for the remainder of the experimental period. Relative abundance in bulk samples was generally low with levels similar to 0 DAP, with relative abundance at its highest level (5.61%) at 120 DAP. Relative abundance in surface samples generally rose over time, reaching a high of 17.91% at 91 DAP. Layer ($p \leq 0.001$) and time ($p \leq 0.001$) were significant factors in the development of Vaucheriaceae communities, and a significant layer*time interaction was seen ($p \leq 0.001$).

The family Chaetosphaeridiaceae (Figure 5.8c) contributed the third highest percentage to overall dissimilarity by layer (9.85%) and time (8.01%). Average relative abundance levels were higher in bulk samples relative to surface soil, at 15.23% and 10.94%, respectively. Relative abundance was similar between bulk and surface samples at 0 and 14 DAP, rising from 10% to ~14%, before diverging for the remainder of the experimental period. Relative abundance in bulk samples continued to rise, reaching a high of 20.24% at 60 DAP, before declining over the remainder of the experimental period, reaching 12.47% at 150 DAP. Relative abundance in surface samples remained steady at 30 DAP (12.45%) and 60 DAP (12.55%) before declining to a low of 7.09% at 91 DAP. Relative abundance rose for the remainder of the time course, reaching 11.00% at 150 DAP. Between 60 DAP and 120 DAP both surface and bulk followed a

similar pattern of development, with a decline in abundance to 91 DAP (bulk, 5.22%; surface, 5.46%) and a rise at 120 DAP (bulk, 2.72%; surface, 3.00%). Layer ($p \leq 0.001$) and time ($p=0.010$) were significant factors in the development of Chaetosphaeridiaceae communities, although a significant layer*time interaction was not seen ($p=0.075$).

The genus Kryptoperidinium (Figure 5.8d) made the fourth highest contribution to dissimilarity by layer (8.33%) and the fifth highest by time (5.29%). Average relative abundance was higher in surface samples relative to bulk, at 7.98% and 2.41% respectively. Relative abundance in surface samples rose from 0.99% at 0 DAP to a high of 13.30% at 60 DAP, before declining over the remainder of the experiment to 8.33% at 150 DAP. Relative abundance in bulk samples remained low, progressing from 1.76% at 0 DAP to 3.74% at 91 DAP, before declining to 1.02% at 150 DAP. Layer ($p \leq 0.001$) and time ($p \leq 0.001$) were significant factors in the development of Kryptoperidinium communities, and there was a significant interaction of layer*time ($p=0.011$).

The family Coleochaetaceae (Figure 5.8e) made the fifth highest contribution to dissimilarity by layer (5.97%) and the fourth by time (6.09%). Average relative abundance was similar between bulk and surface samples, at 8.83% and 7.75% respectively. Relative abundance generally rose in bulk samples from 7.28% at 0 DAP to a high of 12.74% at 14 DAP, before declining over time to 6.58% at 150 DAP, with a rise in relative abundance at 120 DAP the exception in the trend. The relative abundance in surface samples increased from 6.99% at 0 DAP to 13.11% at 60 DAP. Relative abundance declined to a low of 5.84% at 91 DAP, before increasing to 9.58% at 150 DAP. Layer ($p=0.918$) was not a

significant factor in the development of Coleochaetaceae communities, although time ($p \leq 0.001$) was, and there was a significant layer*time interaction ($p=0.040$).

5.3.4 Bulk soil

Post-processing and analysis are described in Sections 4.3.3 and 5.3.3. OTU tables were split into bulk and surface for further investigation from the rarefied table used for analysis in Section 5.3.3. All bulk samples targeting 16S rRNA and 23S rRNA were retained following rarefaction.

Analysis of the *Observed Species* rarefaction measure revealed no significant differences in the α diversity of bacterial communities within the bulk soil between treatments (p=1.0 for all comparisons). The α diversity of the phototrophic community within the bulk soil was higher under Bare and Onion relative to Potato, although not significantly so (detailed in Table 5.3). Rarefaction curves for bacterial and phototrophic communities by treatment are shown in Figure 5.9.

Table 5.3: Results of pairwise comparisons of the *Observed* Species rarefaction measure of phototrophic communities in bulk soil samples between treatments.

Pairwise comparison	P value
Bare vs. Onion	1
Bare vs. Wheat	1
Bare vs. Potato	0.084
Onion vs. Wheat	1
Onion vs. Potato	0.224
Wheat vs. Potato	1

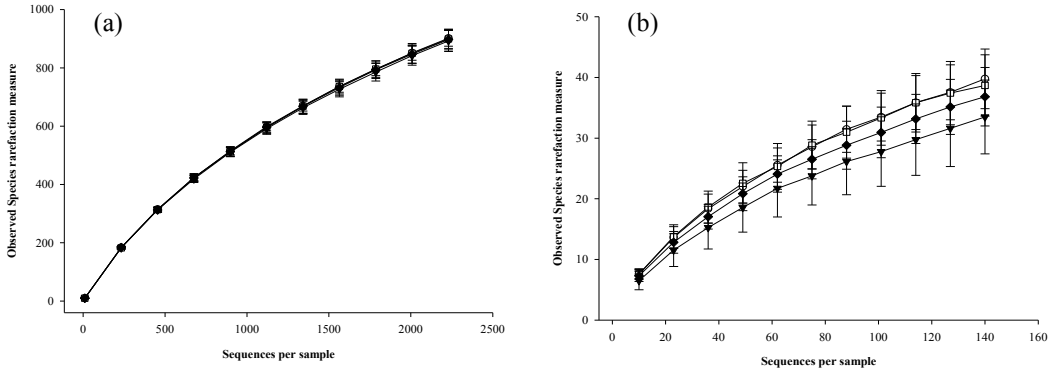

Figure 5.9: Observed Species α diversity estimates of (a) bacterial, and (b) phototrophic communities present in bulk soil under Bare (—○—), Onion (—□—), Wheat (—◆—), and Potato (—▼—) canopies. Error bars represent ±1 S.E.

NMDS ordination plots of Bray Curtis similarities are displayed in Figure 5.10. Bacterial communities (Figure 5.10a) within the bulk soil showed high similarity, with all samples clustered within 90% similarity. Limited differences were seen between treatments. ANOSIM (Table 5.4) revealed no significant effect of treatment (global R=0.038, P=0.259), although time (global R=0.198, P≤0.001) was significant in the development of communities, with further detail reported in Section 5.3.3.1.

Phototrophic community structure (Figure 5.10b) was more variable, although most samples clustered within 70% similarity, with five samples from 120 and 150 DAP clustering separately from the majority of samples. Treatment was a significant factor in the separation of communities (global R=0.151, P=0.010) with significant differences observed between Bare and Wheat, and Bare and Potato. Time (global R=0.180, P≤0.001), was also significant.

Table 5.4: Results of analyses of similarity (ANOSIM) evaluating variation in the structure of bacterial and phototrophic communities in bulk soil samples by treatment, and by time.

	16S rRNA – Bulk	**23S rRNA - Bulk**
Global – Treatment	R= 0.038, *P*= 0.259	R= 0.151, *P*= 0.010
Bare vs. Onion	R= -0.008, *P*= 0.525	R= 0.016, *P*= 0.400
Bare vs. Wheat	R= 0.122, *P*= 0.091	R= 0.283, *P*= 0.008
Bare vs. Potato	R= 0.021, *P*= 0.407	R= 0.254, *P*= 0.014
Onion vs. Wheat	R= 0.078, *P*= 0.215	R= 0.078, *P*= 0.213
Onion vs. Potato	R= 0.065, *P*= 0.276	R= 0.170, *P*= 0.078
Wheat vs. Potato	R= -0.048, *P*= 0.727	R= 0.103, *P*= 0.124
Global – Time	R= 0.198, *P*≤ 0.001	R= 0.180, *P*≤ 0.001

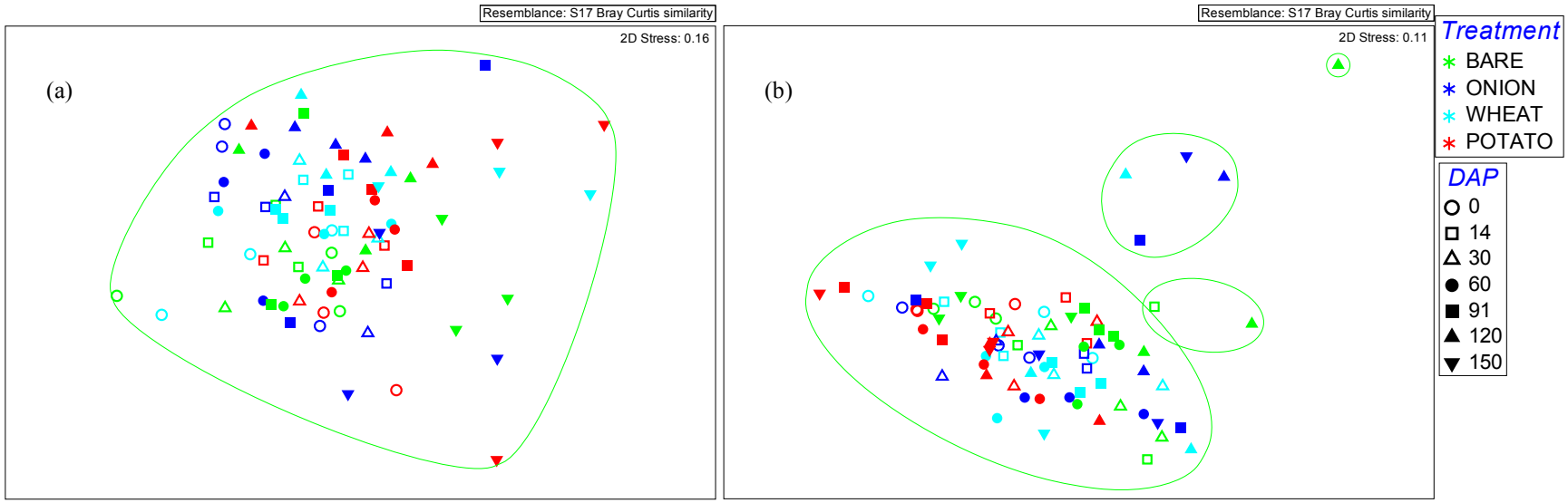

Figure 5.10: Ordination plots from non-metric multidimensional scaling analysis of Bray Curtis similarities of (a) bacterial, and (b) phototrophic community structure in bulk soil taken from under crops exhibiting differing canopy characteristics. Green lines represent a similarity threshold of (a) 90%, and (b) 70%.

5.3.4.1 Bacterial composition summary – Bulk soil

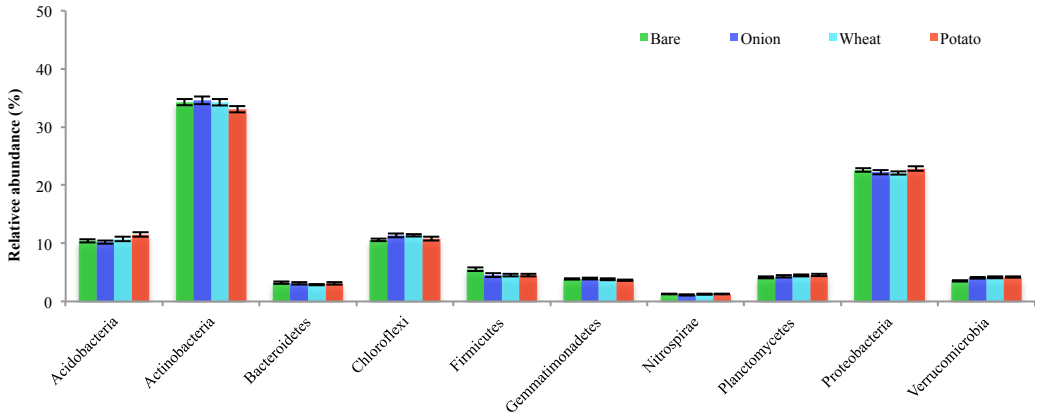

Figure 5.11: Comparison of the average relative abundance of bacterial phyla in bulk soil samples between crop canopy treatments. Errors bars represent ±1 S.E.

At the phylum level (Figure 5.11) Actinobacteria, Proteobacteria, Chloroflexi, and Acidobacteria dominated the bulk soil under all canopy conditions. Six phyla represented <10% relative abundance, ranked as follows; Firmicutes > Planctomycetes > Gemmatimonadetes > Verrucomicrobia > Bacteroidetes > Nitrospirae. Phyla representing <1% relative abundance included Armatimonadetes, Chlorobi, Cyanobacteria, Elusimicrobia, Fibrobacteres, Spirochaetes, Thermi, and candidate phyla BRC1, OD1, TM7, WS3 (data not shown).

5.3.4.2 Phototrophic composition summary – Bulk soil

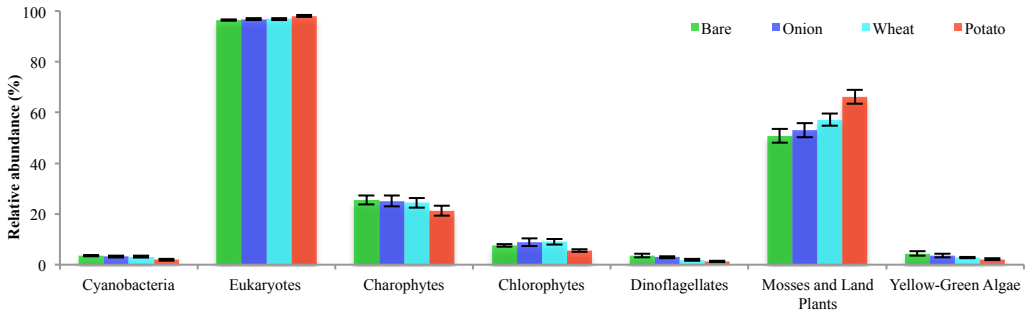

Figure 5.12: Comparison of the average relative abundance of phototrophic taxa between different crop canopy treatments in bulk soil samples. Error bars represent ±1 S.E.

Phototrophic communities in bulk soil samples were dominated by eukaryotes, representing > 96% relative abundance under all treatments (Figure 5.12). A range of eukaryotic phototrophs were detected, including charophytes, chlorophytes, dinoflagellates, yellow-green algae, mosses and land plants. Relative abundance of cyanobacteria was low, < 4% under all treatments. Three orders of cyanobacteria were represented, ranked by abundance as: Oscillatoriales > Nostocales > Chroococcales.

ANOVA showed that, for both cyanobacteria and eukaryotes, there was a significant difference by treatment ($p=0.010$) and time ($p=0.009$), although no significant treatment*time interaction was seen ($p=0.443$). Tukey's test revealed a significant difference in the average relative abundance of eukaryotes under Potato (98.06%, B) relative to Onion (98.86%, AB), Wheat (98.86%, AB) and Bare soil (96.47%, A). The reverse was true for cyanobacteria, with relative

abundance highest under Bare soil (3.53%, B) relative to Onion (3.14%, AB), Wheat (3.14%, AB), and Potato (1.94%, A).

SIMPER analysis was used to identify phototrophic taxa driving dissimilarity within the bulk soil samples, with full results shown in Appendix IV, Section IV.3, Table IV.5. Values of dissimilarity reported here by treatment, unless stated otherwise, are between Bare soil and Potato, and 0 DAP and 150 DAP by time. The overall dissimilarity by treatment was 25.47%, and the overall dissimilarity by time was 23.62%.

The six taxa contributing the greatest percentage difference to this dissimilarity were identified as Spermatophyta, Chaetosphaeridiaceae, Coleochaetaceae, Vaucheriaceae, Kryptoperidinium and Chlorellaceae. Two-way ANOVA with Tukey's post-hoc test (when a significant treatment effect was seen) was performed on the top five taxa contributing to dissimilarity by treatment and time. The temporal development of the taxa is shown in Figure 5.13.

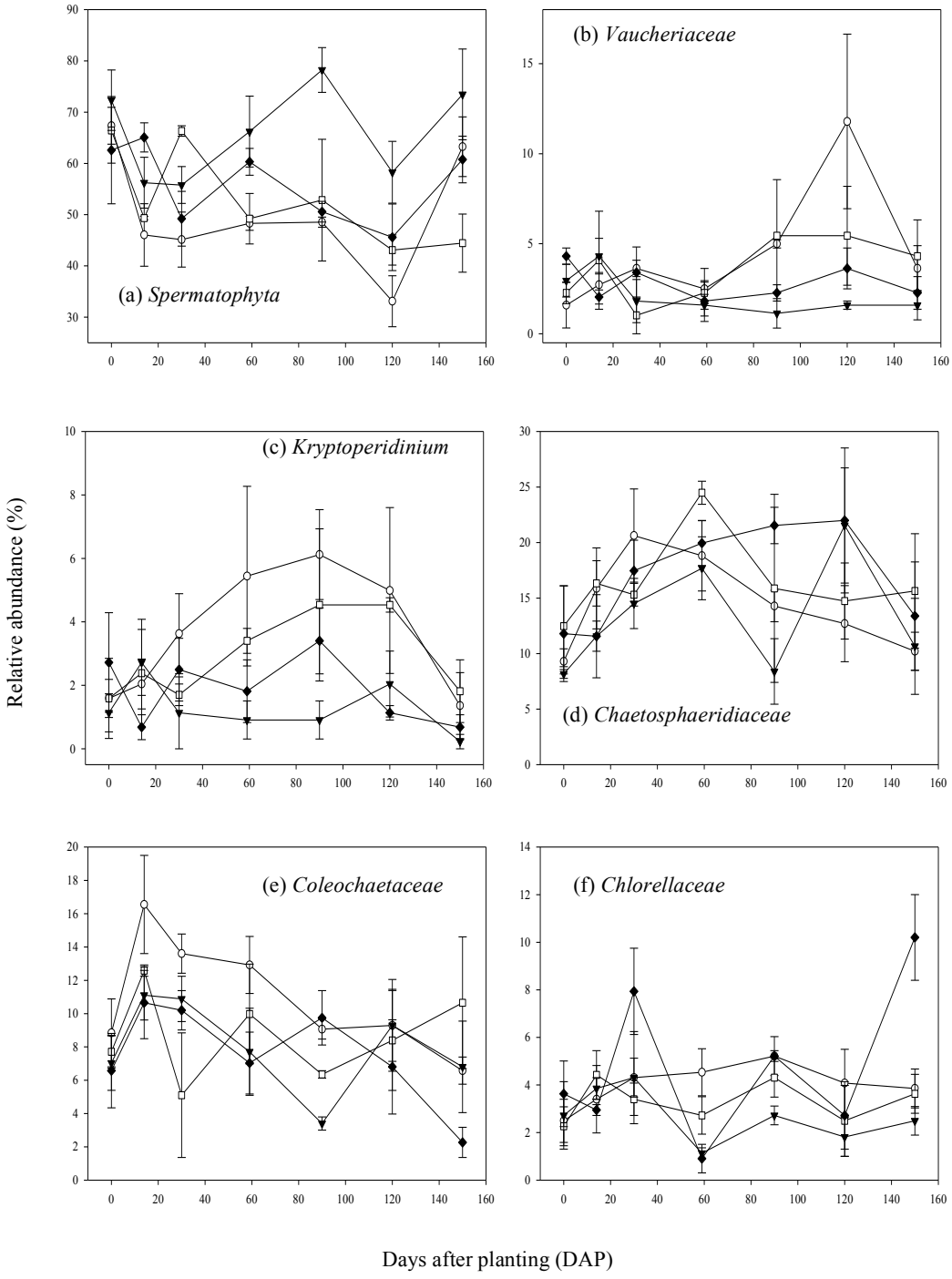

Figure 5.13: The temporal development of the relative read abundance of phototrophic taxa identified by SIMPER analysis as driving dissimilarity by treatment and time in bulk soil. Treatments are: Bare (—○—), Onion (—□—), Wheat (—◆—), and Potato (—▼—). Error bars represent ±1 S.E.

Spermatophyta (Figure 5.13a) was identified as the taxon making the greatest contribution to the overall dissimilarity by treatment (34.08%) and by time (30.56%). Average relative abundance was significantly higher under Potato (65.79%, B), relative to Wheat (56.30%, A), Onion (52.60%, A), and Bare soil (50.24%, A). Relative abundance averaged across all treatments generally declined across the time course from a treatment average of 67.20% at 0 DAP to 45.00% at 120 DAP, before increasing to 60.50% at 150 DAP. Treatment ($p \leq 0.001$) was a significant factor in the development of Spermatophyta communities in bulk soil, as was time ($p \leq 0.001$), and there was a significant treatment*time interaction ($p=0.030$).

Chaetosphaeridiaceae (Figure 5.13d) was identified as the taxon making the second greatest contribution to the overall dissimilarity by treatment (11.72%), and by time (13.12%). Average relative abundance was lowest under Potato (13.22%) relative to Bare soil (14.54%), Onion (16.47%) and Wheat (16.81%), though differences between treatment means were not significant. Average relative abundance rose across the time course from 10.43% at 0 DAP to a high of 20.24% at 60 DAP, before decreasing to 12.47% at 150 DAP. Treatment ($p=0.241$) was not a significant factor in the development of Chaetosphaeridiaceae communities in bulk soil, although time ($p=0.008$) was. There was no significant treatment*time interaction ($p=0.686$).

Coleochaetaceae (Figure 5.13e) was identified as the taxa making the third greatest contribution to overall dissimilarity by treatment, and by time, contributing 8.88% and 9.00% respectively. Average relative abundance was significantly higher under Bare soil (10.98%, B) relative to Onion (8.66%, AB),

Potato (8.03%, AB), and Wheat (7.61%, A). Relative abundance of Coleochaetaceae was higher under Bare soil relative to all other treatments to 60 DAP, reaching a high of 16.55% at 14 DAP, before following a general pattern of decline across the remainder of the experimental period to 6.58% at 150 DAP. Relative abundance under Onion, Wheat, and Potato followed a random pattern of development over time after an initial increase to 14 DAP. Treatment ($p=0.018$) and time ($p=0.002$) were significant factors in the development of Coleochaetaceae communities in bulk soil, although no significant treatment*time interaction was seen ($p=0.232$).

Vaucheriaceae (Figure 5.13b) was identified as the taxon making the fourth greatest contribution overall dissimilarity by treatment (6.74%), and the fifth by time (4.92%). Average relative abundance was significantly higher under Bare soil (6.74%, B) relative to Onion (3.65%, AB), Wheat (2.82%, AB), and Potato (2.14%, A). Relative abundance was similar between treatments to 60 DAP, developing from an average of 2.78% at 0 DAP to 2.04%. Relative abundance increased under Bare soil and Onion to an average of 5.22% at 91 DAP, with abundance plateauing under Onion for the remaining time points. Relative abundance continued to increase under Bare soil to a high of 11.79% at 120 DAP, before declining to 3.63% at 150 DAP. Treatment ($p=0.050$) was a significant factor in the development of Vaucheriaceae communities in bulk soil, although time ($p=0.053$) was not, and there was no significant interaction of treatment*time ($p=0.092$).

Kryptoperidinium (Figure 5.13c) was identified as the taxon making the fifth greatest contribution to dissimilarity by treatment (5.91%). Average relative

abundance was significantly higher under Bare soil (3.60%, B) relative to Onion (2.94%, AB), Wheat (2.82%, A) and Potato (1.30%, A). Relative abundance under Bare and Onion followed a similar pattern of development, generally increasing from 1.59% at 0 DAP, reaching a high of 6.12% at 91 DAP under Bare, before declining to an average of 1.59% at 150 DAP. Relative abundance under Wheat and Potato fluctuated over time, although it was consistently higher under Wheat from 30 to 91 DAP. Treatment ($p=0.004$) and time ($p=0.047$) were significant factors in the development of Kryptoperidinium communities in bulk soil, although no significant treatment*time interaction was seen ($p=0.611$).

Chlorellaceae (Figure 5.13f) was identified as the taxon contributing the fifth greatest percentage to the overall dissimilarity by time (4.92%). Average relative abundance was significantly higher in Wheat (4.79%, B) relative to Bare soil (3.98%, AB), Onion (3.32%, AB) and Potato (2.72%, A). The significance in the average relative abundance of Wheat relative to other treatments was due to high relative abundance at 30 DAP and 150 DAP, reaching 7.94% and 10.20% respectively. Relative abundance under Bare soil and Onion was generally higher relative to Potato after 14 DAP. Treatment ($p=0.005$) and time ($p\leq0.001$) were significant factors in the development of Chlorellaceae communities in bulk soil, and a significant treatment*time interaction was seen ($p=0.007$).

5.3.5 Surface soil

Post-processing and analysis are described in Sections 4.3.3 and 5.3.3. OTU tables were split into bulk and surface for further investigation from the rarefied table used for analysis in Section 5.3.3. As a result of rarefaction, two samples targeting 16S rRNA, and four targeting 23S rRNA, were removed from analysis.

Analysis of the *Observed Species* rarefaction measure revealed no significant differences in α diversity between treatments in either bacterial or phototrophic communities (p=1.0 for all comparisons). Diversity increased with sequencing depth, though a plateau in diversity was not seen under any of the crop treatments (Figure 5.14).

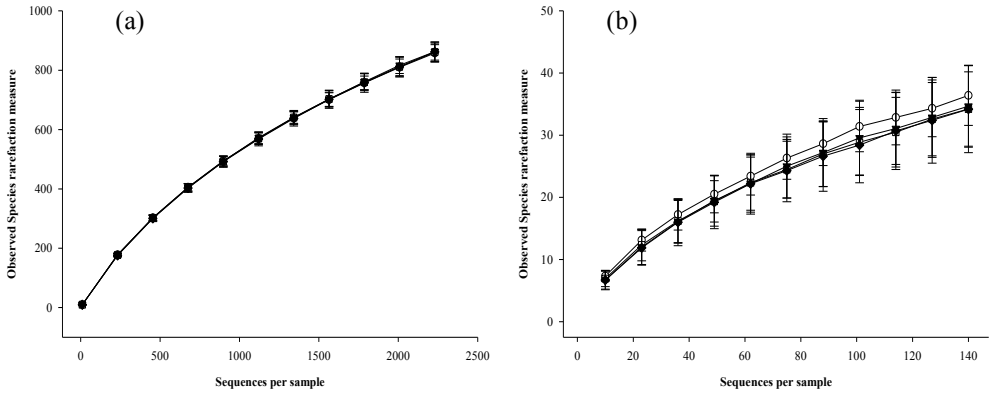

Figure 5.14: Observed Species α diversity estimates of (a) bacterial, and (b) phototrophic communities present in surface soil under Bare (—○—), Onion (—□—), Wheat (—◆—), and Potato (—▼—) canopies. Error bars represent ±1 S.E.

NMDS ordination plots of bacterial and phototrophic soil surface communities are shown in Figure 5.15. Bacterial communities showed high

similarity, with all but two samples clustering at 90% similarity. ANOSIM revealed that treatment had no significant effect on the β diversity of bacterial communities, with an R statistic of 0.019 suggesting limited similarity within treatments, and P value of 0.328. Whilst pairwise comparisons did not reveal any significant differences between treatments, comparisons of Bare soil against Onion, Wheat and Potato showed an increase in the dissimilarity between bacterial communities as canopy cover increased. This was shown by increasing R statistic values of 0.015, 0.106 and 0.116 in comparisons of the Bare soil treatment against Onion, Wheat and Potato, respectively, and decreasing P values of 0.427, 0.164, and 0.139. Time ($R=0.274$, $P\leq0.001$) was significant in the development of bacterial communities, with further detail reported in Section 5.3.3.1.

Phototrophic community structure was more variable, although most samples clustered within 64% similarity. The ordination revealed similarity of community structure between treatments at the beginning of the experimental period, with temporal development of communities under Bare soil and Onion driving dissimilarity between treatments later in the time course (≥60 DAP). ANOSIM results supported the visual assessment of a treatment based temporal development of phototrophic community structure. Pairwise comparison between treatments (Table 5.5) showed an increase in dissimilarity in comparisons of Bare soil and Onion against treatments of increasing crop canopy cover, shown by an increase in the R statistic and a decrease in the significance value.

Table 5.5 Results of analyses of similarity (ANOSIM) evaluating variation in the structure of Surface soil samples by treatment, and by time.

	16S rRNA – Surface	**23S rRNA - Surface**
Global – Treatment	R= 0.019, *P*= 0.328	R= 0.224, *P*= 0.004
Bare vs. Onion	R= 0.015, *P*= 0.427	R= 0.138, *P*= 0.113
Bare vs. Wheat	R= 0.106, *P*= 0.164	R= 0.183, *P*= 0.072
Bare vs. Potato	R= 0.116, *P*= 0.139	R= 0.479, *P*≤ 0.001
Onion vs. Wheat	R= -0.029, *P*= 0.594	R= 0.057, *P*= 0.313
Onion vs. Potato	R= -0.092, *P*= 0.805	R= 0.41, *P*= 0.004
Wheat vs. Potato	R= -0.042, *P*= 0.650	R= 0.081, *P*= 0.169
Global – Time	R= 0.274, *P*≤ 0.001	R= 0.341, *P*≤ 0.001

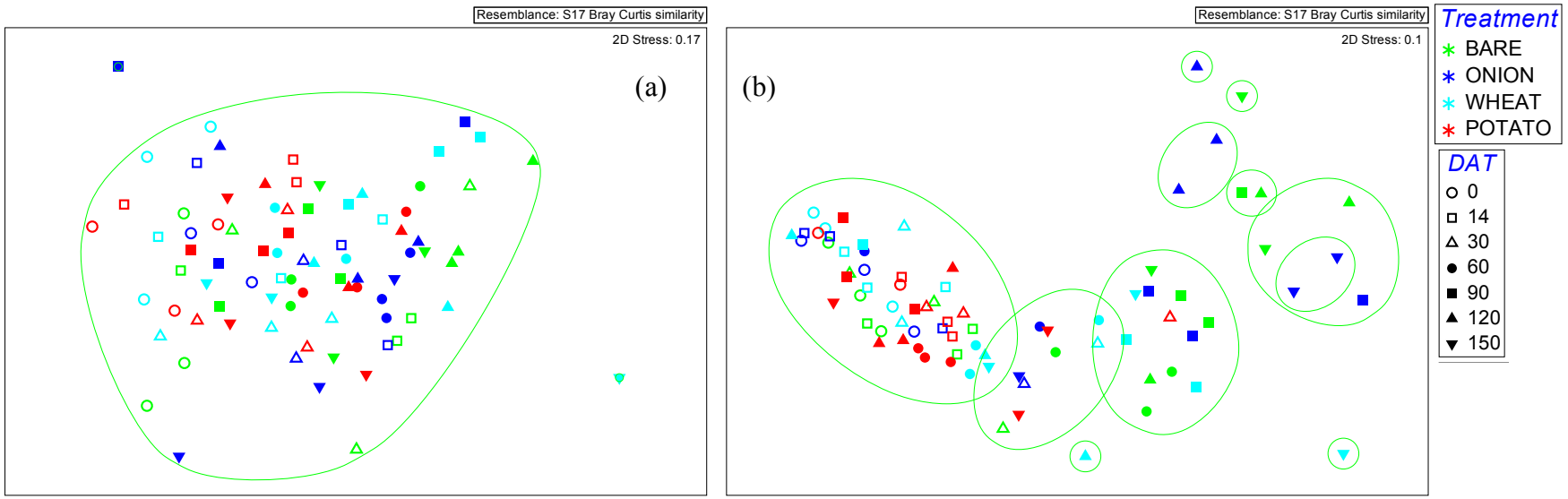

Figure 5.15: Ordination plots from non-metric multidimensional scaling analysis of Bray Curtis similarities of (a) bacterial, and (b) phototrophic community structure in surface soil taken from under crops exhibiting differing canopy characteristics. Green lines represent a similarity threshold of (a) 0%, and (b) 64%.

5.3.5.1 Bacterial community composition – soil surface

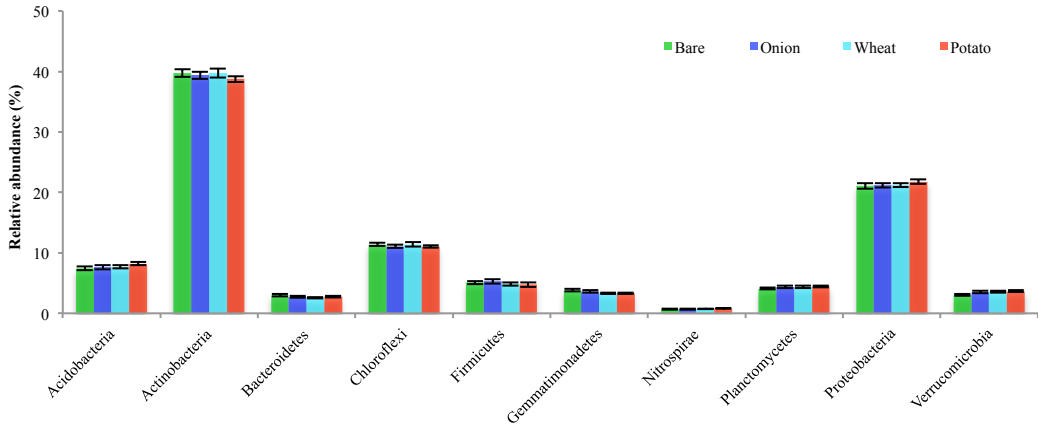

Figure 5.16: Comparison of the average relative abundance of bacterial phyla at the soil surface between crop canopy treatments. Errors bars represent ±1 S.E.

At the phylum level (Figure 5.16) Actinobacteria, Proteobacteria, and Chloroflexi dominated the soil surface under all canopy conditions. Six phyla represented <10% relative abundance, ranked as follows; Acidobacteria > Firmicutes > Planctomycetes > Gemmatimonadetes > Verrucomicrobia > Bacteroidetes. Phyla representing <1% relative abundance include Armatimonadetes, Chlorobi, Cyanobacteria, Elusimicrobia, Fibrobacteres, Nitrospirae, Spirochaetes, Thermi and candidate phyla BRC1, OD1, TM7, WS3 (data not shown).

5.3.5.2 Phototrophic community composition – soil surface

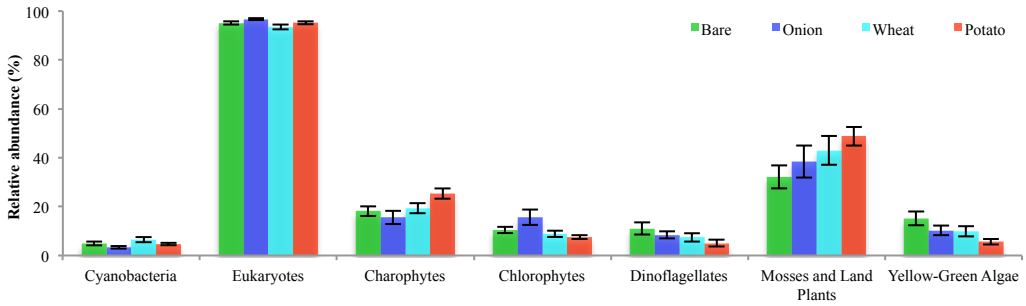

Figure 5.17: Comparison of the average relative abundance of phototrophic taxa between different crop canopy treatments. Error bars represent ±1 S.E.

Sequencing analysis revealed that phototrophic communities at the soil surface were dominated by eukaryotes, representing >93.50% relative abundance under all treatments. A range of eukaryotic phototrophs were detected, including charophytes, chlorophytes, dinoflagellates, yellow-green algae, and mosses and land plants (Figure 5.17). Relative abundance of cyanobacteria was low, ranging from a minimum of 3.44% under Onion to a maximum of 6.27% under Wheat. Three orders of Cyanobacteria were represented, ranked by abundance as; Oscillatoriales > Nostocales > Chroococcales.

ANOVA showed that for cyanobacteria and eukaryotes, there were no significant differences by treatment ($p=0.063$) or time ($p=0.154$), and no significant treatment*time interaction ($p=0.964$).

SIMPER analysis was used to identify phototrophic taxa driving dissimilarity between treatments within the surface soil samples (full results shown in Appendix IV, Section IV.3, Table IV.6). Values of dissimilarity reported by treatment are between Bare soil and Potato, and dissimilarity by time is between 0 DAP and 150 DAP. The overall dissimilarity by treatment was 48.51%, and the overall dissimilarity by time was 64.94%.

The six taxa contributing the greatest percentage to these differences were identified as Spermatophyta, Vaucheriaceae, Kryptoperidinium, Chaetosphaeridiaceae, Coleochaetaceae and Bryophytina. Two-way ANOVA with Tukey's post-hoc test was performed on the top six taxa contributing to dissimilarity by treatment and time. The temporal development of the phyla is shown in Figure 5.18.

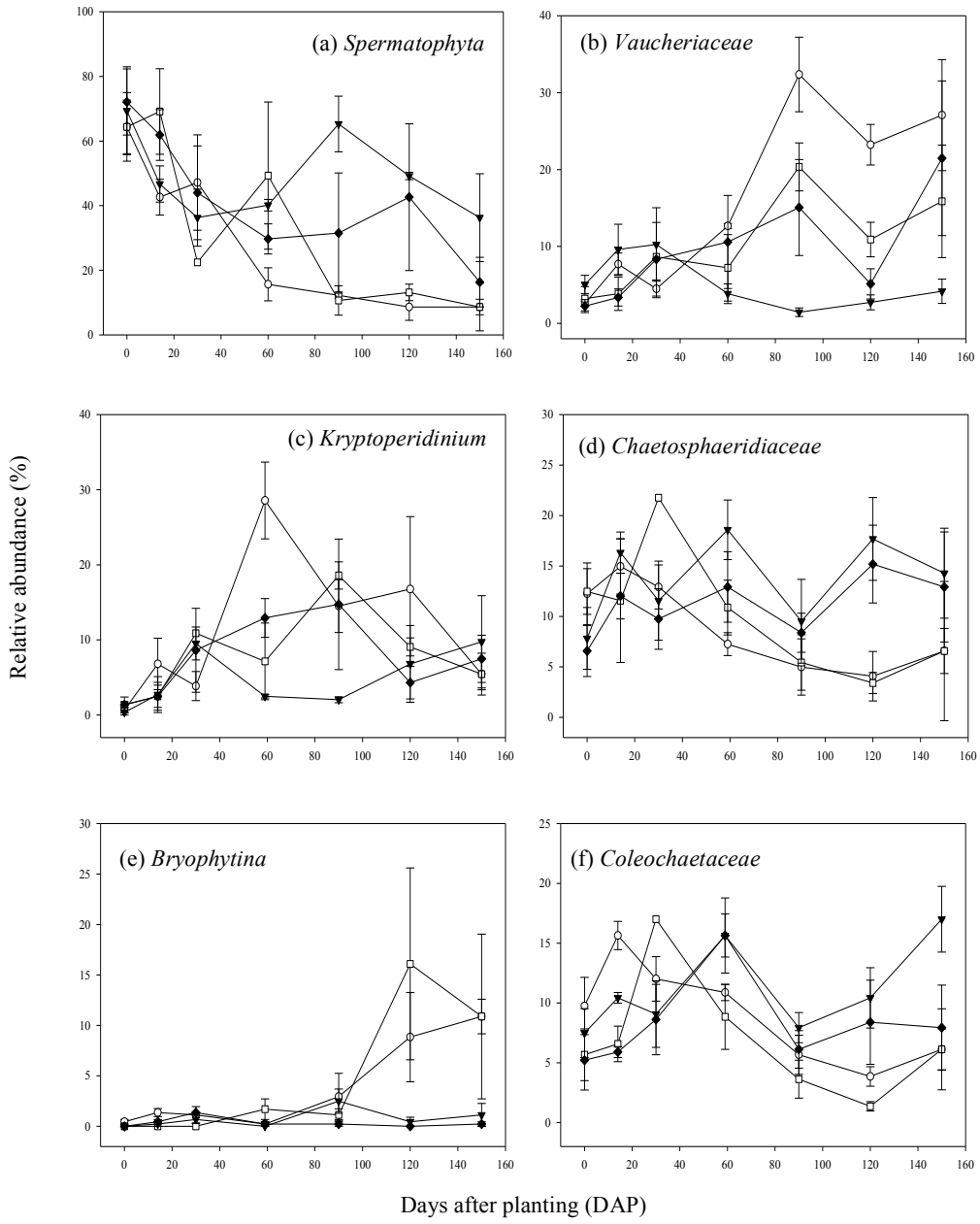

Figure 5.18: Graphs displaying the relative read abundance of phototrophic taxa in surface soil samples. Treatments are: Bare (—○—), Onion (—□—), Wheat (—◆—), and Potato (—▼—). Error bars represent ±1 S.E.

Spermatophyta (Figure 5.18a) was identified as the taxon making the greatest contribution to the overall dissimilarity by treatment (28.97%), and time (39.89%). Average relative abundance was significantly higher under Potato (48.03%, B) relative to Wheat (42.60%, AB), Onion (34.58%, A), and Bare soil (28.47%, A). Relative abundance under Bare soil and Onion generally decreased over time, from an average of 64.40% at 0 DAP, to 9.20% at 150 DAP. Relative abundance under Wheat and Potato decreased at a similar rate as under Onion to 30 DAP, before increasing to 65.30% under Potato at 91 DAP, and 42.60% under Wheat at 120 DAP. Relative abundance decreased under both Wheat and Potato at 150 DAP. Treatment ($p=0.002$) and time ($p\leq0.001$) were significant factors in the development of Spermatophyta communities in surface soil, and a significant treatment*time interaction was seen ($p=0.040$).

Vaucheriaceae (Figure 5.18b) was identified as the taxon making the seconded greatest contribution to dissimilarity by treatment (14.03%) and time (11.71%). Average relative abundance was significantly higher under Bare soil (15.13%, B) relative to Onion (10.28%, AB), Wheat (9.91%, AB), and Potato (5.61%, A). Relative abundance was similar between treatments until 30 DAP, rising from an average of 3.66% at 0 DAP to 8.63%. Relative abundance under Potato declined to a low of 2.49% at 91 DAP, rising to 4.99% at 150 DAP. Relative abundance under Bare soil, Onion, and Wheat followed a similar pattern of development, although at a greater magnitude under Bare soil. Relative abundance rose to a high of 33.79% at 91 DAP under Bare soil, before declining to 24.49% at 150 DAP. Treatment ($p\leq0.001$) and time ($p\leq0.001$) were significant factors, and there was a significant treatment*time interaction ($p=0.002$).

Kryptoperidinium (Figure 5.18c) was identified as the taxon making the third greatest contribution to dissimilarity by treatment (11.25%), and the fourth by time (5.59%). Average relative abundance was significantly higher under Bare soil (10.95%, B) relative to Onion (8.43%, AB), Wheat (7.42%, AB) and Potato (5.03%, A). The pattern of development of relative abundance was initially similar between treatments; rising from a treatment average of 0.94% at 0 DAP to 8.20% at 30 DAP. From 30 DAP, the relative abundance of Kryptoperidinium under Onion and Wheat generally rose to 91 DAP, before declining over remainder of the experimental period. The relative abundance under Potato decreased to 2.04% at 91 DAP before increasing to 9.75% at 150 DAP, similar to all other treatments. Relative abundance under Bare soil reached a high of 28.57% at 60 DAP, before generally declining to the end of the experiment. Treatment ($p=0.034$) and time ($p\leq0.001$) were significant factors in the development of Kryptoperidinium communities in surface soil, and a significant treatment*time interaction was seen ($p=0.020$).

Chaetosphaeridiaceae (Figure 5.18d) was identified as the taxon contributing the fourth greatest percentage difference to dissimilarity by treatment (8.26%), and the third by time (6.44%). Average relative abundance was highest under Potato (13.98%) relative to Wheat (11.11%), Onion (9.60%), and Bare soil (9.01%), although there were no significant differences between the treatment means. Relative abundance generally fluctuated under all treatments to 30 DAP, and declined under Onion and Bare soil for the remainder of the time course. Relative abundance rose under Wheat and Potato, following a similar development pattern to 150 DAP, reaching an average of 13.61%. Treatment

(p=0.101) was not a significant factor in the development of Chaetosphaeridiaceae communities in surface soil, nor was time (p=0.082). No significant treatment*time interaction was seen (p=0.112).

Coleochaetaceae (Figure 5.18f) was identified as the taxon contributing the fifth greatest percentage difference to dissimilarity by treatment (5.82%) and time (4.43%). Average relative abundance was significantly higher under Potato (11.33%, B) relative to Bare soil (9.14%, AB), Wheat (8.26%, AB) and Onion (6.60%, A). Relative abundance under Bare soil and Onion followed a similar pattern of development, initially increasing to 14 and 30 DAP, respectively, before declining across the rest of the time course to an average of 6.69% 150 DAP. Relative abundance under Wheat and Potato generally rose from 0 DAP to a high of 15.65% at 60 DAP, before fluctuating for the remainder of the experiment, reaching a high of 17.01% under Potato at 150 DAP, and 7.94% under Wheat. Treatment (p=0.010) and time ($p \leq 0.001$) were significant factors in the development of Coleochaetaceae communities in surface soil, and a significant treatment*time interaction was seen (p=0.002).

Bryophytina (Figure 5.18e) was identified as the taxon contributing the fifth greatest percentage difference to dissimilarity between Bare and Potato (6.07%). Average relative abundance was higher under Bare soil (3.69%) and Onion (3.74%) than Potato (0.71%) and Wheat (0.36%), although Tukey's test revealed this difference between the treatment averages was not significant. The pattern of development was similar under all treatments to 91 DAP, with low relative abundance for all treatments. Relative abundance under Bare soil and Onion rose for the remainder of the time course, reaching a high of 16.10% under

Onion at 120 DAP. Relative abundance remained low under Wheat and Potato for the rest of the time course. Treatment ($p=0.046$) and time ($p=0.014$) were significant factors, although a significant treatment*time interaction was not seen ($p=0.141$).

5.4 DISCUSSION

Light appeared to have a significant impact on the community structure of bacterial and phototrophic community structure in surface soil, which harboured increasingly distinct communities relative to the underlying bulk soil as time passed. Furthermore, crop canopy characteristics appeared to have a significant effect on phototroph community structure at the soil surface, with the effect further extending to impact phototrophic community structure in the bulk soil of Bare and Onion treatments. Conversely, canopy characteristics had no significant effect on bacterial diversity or community structure between treatments at the soil surface or in the bulk soil.

Chlorophyll *a* concentration, used as a broad-scale assessment of phototroph community development, indicated slow phototroph development over the experiment. Concentrations in surface soil had started to rise under Bare soil, Onion and Wheat treatments by 91 DAP. This delay in the development of chlorophyll *a* concentration was previously observed in Jeffery *et al.* (2009), where chlorophyll *a* concentration at the soil surface did not begin to increase relative to sub-surface soil until 16 weeks post-disturbance at a soil moisture content of 12% (by mass).

Analysis revealed that phototrophic communities present at the soil surface were significantly different to those of the underlying bulk soil. The main driver of the dissimilarity between the surface and bulk phototrophic communities was the light-driven, time-mediated decrease in the relative abundance of sequences assigned as Spermatophyta. This assignment of the majority of

sequences as vascular plants in the bulk soil shows limited development of active phototrophs until the end of the experimental period, with most sequences coming from the seed bank of the soil, in sharp contrast to the soil surface.

Community composition analysis of phototroph communities at the soil surface revealed domination by eukaryotic algae, with average relative abundance of 95.10% at the soil surface. This dominance of the relative abundance of eukaryotic algae contrasted with the findings of Davies *et al*. (2013b), in a laboratory-incubated soil, where a greater percentage of reads were assigned as Cyanobacteria, accounting for 63.8% and 82.7% of sequences under light and dark respectively. A dominance of eukaryotic phototrophs was seen previously in this soil (Chapter 4), where eukaryotic sequences represented 64.97% and 78.59% under LIGHT and PAR-L conditions, respectively.

In work presented in Chapter 4, the phototrophic community was initially dominated by the cyanobacterium *Microcoleus vaginatus,* before successional change to domination of the surface communities by moss, similar to the successional change observed in arid lands and previous lab based investigations (Li *et al.* 2002; Lange *et al.* 1992; Belnap 1993; Davies *et al.* 2013b). Whilst there was a temporal development of phototrophic communities at the soil surface in this system, it was driven predominantly by a decrease in the percentage of reads assigned as Spermatophyta. However, whilst the absence of *M. vaginatus* observed within this system is different to other studies in the literature, the increase in the relative abundance of moss (Bryophytina) at the soil surface in Bare soil and Onion treatments ≥ 120DAP is similar to other systems, generally seen as the final successional stage of BSC development.

Investigations into the successional development of cyanobacterial communities in arid lands (Li *et al.* 2002; Lange *et al.* 1992; Belnap 1993) and more recently, temperate agricultural systems (Davies *et al.* 2013b), have shown development from filamentous early colonising species of the order Oscillatoriales, to diazotrophic cyanobacteria of the order Nostocales. In our system, there was no clear pattern of development of the cyanobacterial community up to and including 60 DAP. However, from 91 DAP, Oscillatoriales was the most abundant order, although the proportion of reads assigned as Nostocales increased under Bare soil and Onion relative to Wheat and Potato. Furthermore, at 120 DAP there was a higher proportion of reads with close homology to the order Nostocales under Bare soil (46.80%) and Onion (41.70%) relative to Wheat (8.35%) and Potato (12.17%), similar to later stage BSCs (Garcia-Pichel *et al.* 2003; Yeager *et al.* 2004). With such a low abundance of reads assigned as Cyanobacteria, it is unclear how ecologically significant this would be to the soil environment.

Interestingly, the diversity of phototrophic communities in the bulk soil was generally higher under Bare soil and Onion treatments relative to Wheat and Potato. This was most likely to be due to the effect of light on the soil surface communities impacting beyond the soil surface, with similar effects observed previously by Davies *et al.* (2013b). In a laboratory test system of bare soil exposed to non-UV light/dark cycles, Davies *et al.* (2013b) observed that the effects of light on the photrophic community at the soil surface extended to the underlying bulk soil, and also affected soil nutrients and pH. This effect could be explained in several ways, from cracks at the soil surface allowing further

penetration of light, uneven soil surface and large aggregate size, or even the filamentous nature of BSC phototrophic organisms contributing DNA to the bulk soil. Within this experimental system, the proliferation and development of the phototrophic community at the soil surface would have been responsible for a decrease in the relative abundance of samples assigned as Spermatophyta from the seed bank within the bulk soil, increasing the *Observed Species* measure of diversity in bulk soil from Bare and Onion treatments, despite the selection pressure of light.

Community composition analysis of bacterial communities revealed significant differences between soil surface and bulk microbial communities, suggesting an influence of light on the development of bacterial communities (observed previously in Davies 2013b). The main drivers of dissimilarity between bulk and surface samples were the relative abundances of the phyla Actinobacteria, Acidobacteria, and Proteobacteria, which were established early in the time course (≤14 DAP).

The results of the 16S rRNA sequencing are similar to the 23S rRNA sequencing in that the relative abundance of Cyanobacteria was low throughout the experimental period, representing an average of 0.044% and 0.020% in the surface and bulk, respectively. However, the relative abundance of Cyanobacteria under Bare conditions was higher than under Potato at 150 DAP, at 0.30 % and 0.045% relative abundance respectively. In arid land BSCs, bacterial community structure tends to be dominated by Cyanobacteria (Abed *et al.* 2010), making up to 70% relative abundance. However, this dominance was has not been reported in temperate agricultural systems, with Cyanobacteria representing <4% of the

bacterial population in a light dark lab comparison system (Davies *et al.* 2013b), and an average of 10.51% in the same soil used in this study in the following year under LIGHT conditions (Chapter 4). This could suggest that the influence of Cyanobacteria on the structure of bacterial communities at the soil surface could be overestimated using artificial systems, although the difference could be explained by the differences in environmental variables. Knapen *et al*. (2007) has shown that BSCs form readily under agricultural cropping systems, and although soil moisture was not recorded, photos of the site show moist soil, and rainfall was recorded at ≥1 mm per day for all sites. BSCs also formed readily under the light filter system described in Chapter 4, where average volumetric moisture content of the soil was 33.10%, compared to just 4.16% in this study. It should be held in mind that the probes in this study were placed at 20 cm depth in the centre of the experimental plot. Such low moisture values could be a reflection of their positioning below, or within, the root systems of the crops. As a result, these moisture values are very low and should be taken with caution, with the moisture content at the soil surface where the plots were watered likely to be higher. However, an internal study at Syngenta of chlorophyll *a* concentration in agricultural fields of multiple cropping systems and seasons showed that chlorophyll *a* concentration was positively correlated to moisture (Marshall pers. comm). Clearly availability of water has an important role in the development of phototrophic communities.

Although light availability has been shown to affect the composition and structure of microbial communities, differences in microbial community structure

could also be affected by indirect factors in the experimental system, such as moisture content, application of CPP for powdery mildew and bioturbation.

The application of fenpropidin could have directly affected soil fungal community structure if any parent compound reached the soil surface after spraying. Any perturbation could have indirectly affected other microbial populations, such as bacteria and phototrophs, or could have acted as an energy source and been directly degraded.

Differences in microbial populations could also be caused indirectly by bioturbation, the reworking of soils by macro-invertebrates, such as worms and mites, and plants. Monard *et al.* (2011) showed that, locally, earthworm soil engineering greatly modified the taxonomic composition of atrazine degraders in burrow linings and in casts relative each other and bulk soil, increasing soil heterogeneity.

Sequencing revealed that under low-density canopies, phototroph community development was generally similar to other systems, although slower, possibly reflecting the low moisture content of the soil. There was little phototroph community development under high-density canopies, suggesting that communities may develop more slowly relative to low-density canopies.

CHAPTER 6: GENERAL DISCUSSION

6.1 Chemical fate

This work has shown that non-UV light can impact CPP degradation and fate in a laboratory-based regulatory-like aerobic soil system. Further, it has shown that availability of photosynthetically radiation (PAR) affects the degradation and movement of CPPs in soil cores incubated in the field. This has a range of implications for CPP regulatory studies conducted under both lab and field conditions.

Inclusion of non-UV light had a compound specific effect on the degradation behaviour of CPPs in a clay-loam soil when using an OECD 307 regulatory-like study, impacting the rate of degradation of two of the five CPPs studied (Chapter 2). Similar effects were observed in a silt-loam soil by Davies *et al.* (2013a), where light significantly impacted the degradation rate of six of the eight CPPs tested. In this study, non-UV light had similar impacts on two of the CPPs studied previously, fludioxonil and cinosulfuron, with similar direction of effects between soils. Degradation of the other three compounds was not affected by non-UV light in this study. The conservation of altered degradation rates between soils of different classes within the same system showed that the observed effects are not an artefact of the soil used, although there were soil-to-soil differences in the magnitude of the effects.

An effect of light on the fate of two CPPs, benzovindiflupyr and paclobutrazol, was also observed in soil cores incubated in the field. Degradation

of benzovindiflupyr was impacted by the restriction of PAR, and the initial degradation rate was faster in LIGHT conditions than when PAR was restricted. Dissipation, and calculated DT_{50} values, were generally faster in the field relative to the $DegT_{50}$ values calculated from the OECD 307 system. Paclobutrazol DT_{50}, when exposed to light, was faster in the field system (38 d) than the laboratory $DegT_{50}$ (82 d), and DT_{50} under PAR-L conditions in the field (57 d) was faster than the $DegT_{50}$ in the standard OECD 307 system (73 d).

Despite its recalcitrant nature, benzovindiflupyr degradation was faster under field conditions relative to the OECD 307 regulatory-like study. Benzovindiflupyr displayed bi-phasic kinetics in both the laboratory and the field. In the OECD 307 study, parent degraded to ~88% in the first phase of degradation in light and dark conditions, before entering an extremely slow phase of degradation for the remainder of the experiment. A similar effect was seen in the field, with benzovindiflupyr initially degrading under LIGHT and PAR-L conditions, before entering a slow phase of degradation. The initial rate of degradation under LIGHT was faster relative to PAR-L conditions, degrading to 67% and 79% respectively at 30 DAT, before entering the slow second phase of degradation. It is unclear how accurate the calculated DT_{50} values are due to the extrapolation necessary for the models to calculate the DT_{50}. There was more degradation under PAR restricted conditions in the field than in either treatment under lab conditions.

The inclusion of non-UV light in the OECD 307 regulatory like system was shown to increase the formation of NERs. In this clay-loam soil, NER formation was higher in light-incubated systems relative to those incubated in the

dark for three of the five compounds tested. Similar effects were shown in the OECD 307 regulatory like system in a silt-loam soil, where seven of the eight CPPs investigated had increased NER formation in light incubated samples relative to dark (Davies *et al.* 2013a). This effect of increased NERs was also seen in the field system examined in this thesis (Chapter 3), where NER formation was significantly higher under LIGHT conditions than when PAR was restricted. This suggests that it is wavelengths from within the PAR spectrum that drive the effects seen in both the lab and field systems. This could be due to increased C input from communities that develop under the influence of light, providing an increased pool of SOM, a key irreversible binding medium of CPPs in soil, therefore increasing the NER fraction (Yoshitake *et al.* 2010; Kästner *et al.* 2014). This NER fraction could be either parent compound or metabolites, although the nature of NERs makes this hard, if not impossible, to determine. For example, in the OECD 307 study of paclobutrazol there was little difference between degradation in light and dark conditions, with $DegT_{50}$ slightly faster in the dark (73 d) relative to light (82 d). Despite this, the NER fraction was still larger under light conditions, representing 42.76% of applied radioactivity compared with 31.66% in the dark. This could be due to increased binding of parent CPP or metabolites. However, the average percentage region of interest attributed to parent compound in the analysis of the HPLC chromatograms was higher in light-kept samples relative to dark ≥30 DAT, suggesting increased binding of metabolites under light conditions. This effect could also be explained by increased mineralisation under light conditions. Mineralisation was higher under dark conditions, which could be due to natural incorporation of $^{14}CO_2$ by the phototrophic community under light conditions, but may also suggest that

increased NER formation in paclobutrazol may be due to increased binding of metabolites in light conditions. However, it is unknown if this is the case with other CPPs tested.

An interesting effect of light, which was unobservable in the laboratory based system but which was observed in the field, was the influence of PAR at the soil surface (top 5 mm) in the movement/location of paclobutrazol and benzovindiflupyr. PAR appeared to increase the transfer of parent compound to the underlying bulk soil. It was previously postulated that the presence of a BSC could increase the retention time of CPPs at the soil surface, increasing the time available for CPPs to be co-metabolised by organisms at the soil surface (Davies *et al.* 2013b). In contrast, this work has shown that whilst the rate of CPP degradation at the soil surface could be increased when exposed to light, the percentage of parent compound in the sub-surface layer increased when PAR was not restricted. This suggests that the impact of light on CPP fate may not just be restricted to the influence and impact of phototrophic communities, but could extend to more general effects beyond the soil surface.

It is clear that light can impact the degradation and fate of some CPPs within field systems. Being able to accurately model or predict a CPP's fate in the environment requires an understanding of how that CPP behaves in all environmental compartments. This demonstration of a novel mechanism of the movement of CPPs away from the soil surface when a BSC is present highlights the need for further understanding of soil surface processes, the influence of which are negated by current EU regulatory field trial regulations (EFSA 2010). The cumulative effects of altered degradation rates of parent compound, increased

NER formation, and increased movement of parent compound away from the soil surface could combine to reduce erosive run off of CPPs at the soil surface during overland flow events. If a late stage successional BSC were present, this would act to reduce soil and CPP loss to watercourses. However, increased movement of CPP away from the soil surface could pose a risk in compounds that move easily through the soil matrix and have a propensity to leach, elevating the risk of environmental contamination. Further investigation with a wider range of CPPs is required to better understand the effect of CPPs physical properties on their behaviour at the soil surface when a BSC is present.

6.2 Soil surface microbiology

Work presented in Chapter 4 showed that the artificial restriction of photosynthetically active radiation (PAR) at the soil surface significantly affected bacterial and phototrophic community structure in a time dependent manner. More specifically, phototrophic communities under the influence of LIGHT developed in a manner seen in arid land soil systems around the world (Li *et al.* 2002; Garcia-Pichel *et al.* 2003; Yeager *et al.* 2004; Darby *et al.* 2007; Li *et al.* 2010; Li *et al.* 2015), and laboratory-based temperate test systems (Davies *et al.* 2013b). Dominance of the cyanobacterial community shifted from early colonising species, such as *Microcoleus vaginatus*, to diazotrophic cyanobacteria, such as *Nostoc punctiforme* and *Anabaena cylindrica*. More broadly, overall dominance of the phototrophic community shifted from Cyanobacteria to moss, previously observed across a longer timeline in arid

environments (Li *et al.* 2002; Yeager *et al.* 2004), where BSC development takes years rather than weeks.

Furthermore, in Chapter 5 it was shown that light had a significant impact on the structure of bacterial and phototrophic communities at the soil surface relative to the underlying bulk soil, with communities becoming increasingly distinct over time. In addition, crop canopy characteristics also appeared to have a significant effect on the development of photrophic communities at the soil surface, with greater development under low-density canopy systems.

6.3 Soil surface community comparisons

When designing standardised tests, such as those outlined by the OECD, it is important to try and replicate conditions as they are in the environment that a CPP would encounter. One of the aims of the PAR-L filter used in Chapter 4 was to simulate full crop canopy cover, and mimic any effects that it may have on microbial communities present at the soil surface. Therefore it is important to know if the soil surface communities in the Chapter 4 study were similar to those measured in the Chapter 5 study. Non-metric multidimensional scaling analysis of Bray-Curtis similarities revealed bacterial and phototrophic community structures at the soil surface were significantly different in experiments conducted in Chapters 4 and 5 (Figure 6.1) at the same location.

Bacterial community structure was less variable in the Chapter 5 study relative to the Chapter 4 study, shown by the closer grouping of samples

(Figure 6.1a). ANOSIM revealed significant differences between experiments, with a global R value of 0.468 and a significance value of p=0.001. However, the ordination plot shows that when PAR-L light was restricted, community structure was more similar to that observed in the Chapter 5 study under Wheat and Potato. SIMPER analysis revealed differences in the relative abundance of the phyla Actinobacteria and Cyanobacteria as driving dissimilarity between the communities.

Phototrophic community structure in Chapter 5 experiments was significantly different to community structure in Chapter 4 experiments (Figure 6.1b). ANOSIM revealed significant differences between experiments, with a global R value of 0.756 and a significance value of p=0.001. Clustering between treatments was similar in both experiments, with two main clusters of samples sharing 40% community structure, with PAR-L and high density crop canopy clustering separately from the LIGHT and low density crop canopy, respectively. SIMPER analysis revealed differences in the relative abundance of the taxa Spermatophyta, Bryophytina and *Microcoleus vaginatus* as driving dissimilarity between the communities.

For ANOSIM and SIMPER results, please see Appendix V, Sections V.1 and V.2.

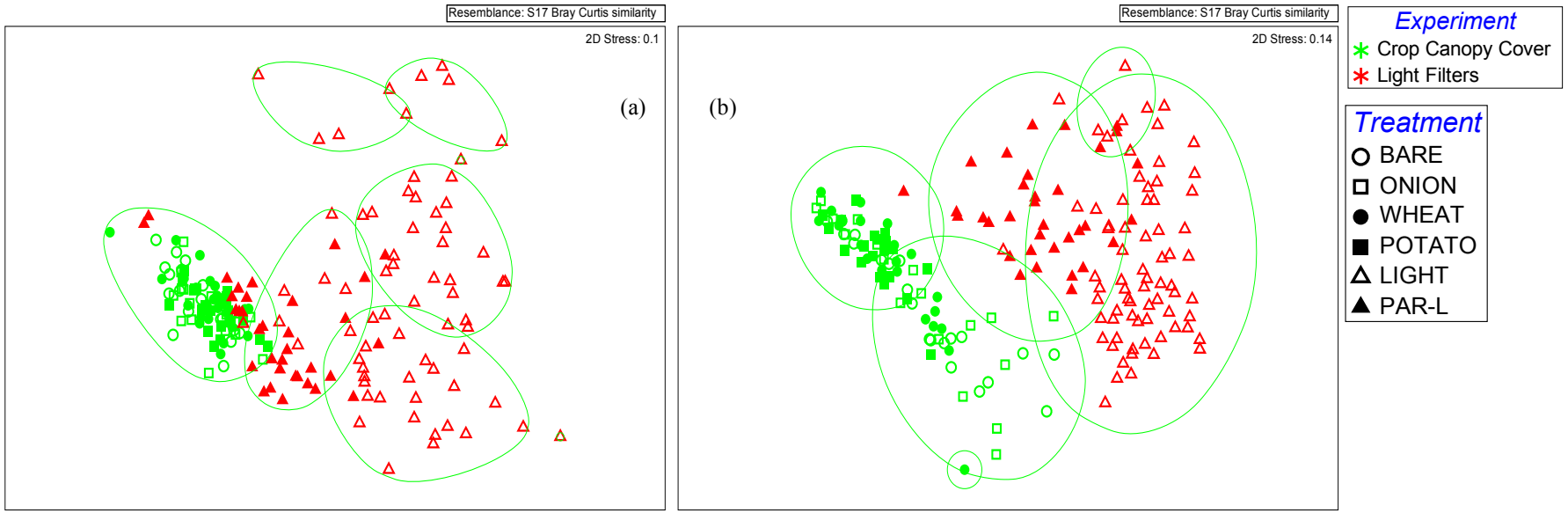

Figure 6.1:Ordination plot from non-metric multidimensional scaling analysis of Bray-Curtis similarities of community structure similarity for (a) bacterial, and (b) phototrophic soil surface communities from the semi-field degradation experiment (red symbols) and those found under crop canopy cover (green symbols). Clustering is based on similarity of phototrophic community structure: green lines represent (a) 89% similarity, and (b) 40% similarity.

The differences in community structure between the two experiments could reflect the contrasting soil moisture content between the experiments. An internal study at Syngenta showed that chlorophyll *a* concentration at the soil surface was positively correlated to moisture, suggesting a role of water availability in the development of phototrophic communities under cropping systems (Marshall pers. comms). The development of the phototrophic community was much greater in the Chapter 4 study relative to the Chapter 5 study, and average moisture content was higher, 32.96% in the Chapter 4 study compared to just 4.16% in the Chapter 5 study. Although the Chapter 5 value may be reported in error (discussed at the end of Chapter 5), the soil surface was visibly much moister in Chapter 4 relative to Chapter 5. This slow development of communities has also been observed in low moisture arid soils, where successional development can take tens of years (Li *et al.* 2002).

From a microbial ecology perspective it is of particular interest that the successional development of phototrophic communities follows the same general pattern between eco-regions, including arid soils (Li *et al.* 2002; Garcia-Pichel *et al.* 2003; Yeager *et al.* 2004; Darby *et al.* 2007), temperate lab systems (Davies *et al*. 2013b), field systems with high moisture (Chapter 4), and to an extent, under crop canopy systems with low moisture content (Chapter 5).

Overall, this work has shown that soil surface communities under the influence of light may impact CPP degradation, the movement of parent compound from the soil surface and NER formation. It has also shown that in a relatively water-limited system under crops with low-density canopy coverage, similar successional development of microbial communities is eventually seen,

and it is interesting to note from an environmental fate perspective that these impacts are not currently assessed as part of the regulatory framework for CPP registration.

6.4 Implications for industry

This work has provided a means to more realistically assess the environmental fate of CPPs in a regulatory-like laboratory study, and a more environmentally realistic field system. It offers further insight into non-standard tests that could be included in regulatory submissions as additional evidence of degradation of recalcitrant CPPs in conditions that better replicate the environment a CPP will encounter in the field.

This work also provides a framework to investigate the development of microbial communities within laboratory systems. Whilst similar trends are observed in the fate and degradation of CPPs when light is included in test systems in the lab and field, it is unknown if the microbial communities that develop in the lab do so in the same manner as in the field, as seen in Chapters 4 and 5. Knowing the composition of the microbial communities and any temporal/successional development would help us to understand if microbial community development in the light adapted OECD 307 test system is representative of the field environment, and if the mechanisms may be shared between systems.

The main aim of the tests required by regulatory bodies for CPPs is to understand the properties and behaviour of CPPs within certain environments, in order to accurately predict their fate. However, in order to accurately model, it is first necessary to understand the fate of the CPP in different environmental compartments. This work has shown that there is a need for the developers of CPPs to understand their products outside of current regulatory requirements in non-standard systems, in a bid to fully understand their environmental fate, and to drive forward the development of more environmentally realistic regulatory tests.

6.5 Future work

This work highlights a range of areas for future research to better understand the impact of light on the degradation and fate of CPPs at the soil surface, the role of edaphic and environmental variables in the development of microbial communities at the soil surface, and the impact of soil type on CPP degradation.

Are there shifts in the community structure of key phyla below the community level? Finer scale microbial analysis

Community level analysis work presented in Chapters 4 and 5 provides a high level, qualitative understanding of the bacterial and phototrophic communities by treatment and time. However, whilst such broad scale analysis provides an overview of the major shifts in community structure at the phylum

level, it can mask shifts in community development at lower taxonomic rank, such as class or family. Further work could use finer scale methods, such as RT-qPCR targeting Cyanobacteria at the family level, to quantitatively analyse the differences observed at community level in greater detail.

Are soil communities comparable between lab and field?

Whilst the impact of light on the degradation and fate of CPPs is largely conserved across systems, it is important to firstly understand the microbiology of the systems to fully understand the mechanisms driving these impacts. It is important to investigate how similar, compositionally and structurally, microbial communities that develop within the lab-based OECD 307 regulatory like system are to those that develop in a field environment, and whether or not the effects that are observed following the inclusion of light are as a result of indirect effects on the physical, chemical and biological properties of soil, or are related to direct effects of phototrophic organisms within the microbial environment.

What are the effects of processing and storage of soils used in lab studies?

OECD guideline 307 states that soil should be used within three months of collection, and it is important to understand how processing of soil (i.e. sieving), and the manner and length of soil storage before its use in laboratory studies, affects microbial community structure in both the regular OECD 307 study, and also in the adapted light-included study.

Are differences in degradation and transport of CPPs observed under light filters also observed under cropping systems?

This work has shown that the artificial modulation of light reaching the soil surface affects the degradation and movement of two CPPs in cores incubated in a field environment. Further work should focus on the role of crop canopy cover in the development of microbial communities, and whether and how the presence of a canopy influences the fate of organic compounds within the soil. Marchand *et al.* (2002) observed that 61% of atrazine mineralised under four-week old maize seedlings, compared to just 48% in non-planted soil, suggesting that the presence of a rhizosphere could further influence the degradation and fate of CPPs in the environment. This demonstrates influences on CPP fate that extend beyond a crop's impact on the soil surface. However, investigations should focus on a wide range of different CPPs to better understand the relevance of these effects on in a wider context.

How does the presence of a BSC affect nutrient cycling at the soil surface in an agricultural environment?

BSCs are important components of both nutrient input and cycling in arid environments. It would be of interest to better understand the role that BSCs play in nutrient cycling and input in a temperate, agricultural environment. Future work could investigate the development of key nutrients (e.g. carbon, nitrogen, phosphorous and potassium) in BSCs under the influence of light, and could also

investigate the role of specific edaphic factors on the nutrient cycling competency of BSCs.

How does soil type affect the influence of light on the degradation and transport of CPPs?

OECD 307 tests are carried out in multiple soil types chosen represent the varying eco-regions that a CPP may be used in. Edaphic characteristics can vary greatly, including the textural class of the soil, organic matter content and moisture holding capacity. It would be of interest to understand the effects that variations in such characteristics have on microbial community development and degrading competency, with and without light. This could be carried out in a systematic manner in soils from varying ecological regions to better understand the effects that physical soil characteristics have on microbial community development in the soil, degrading competency and the effects of PAR relative to standard OECD 307 tests carried out in the dark.

Current research into the effect of light on the biodegradation and fate of CPPs has, so far, not been carried out in an arable soil. Work by Davies *et al.* (2013a & b) was carried out using the silt-loam soil Gartenacker from Switzerland, which is a pasture soil as opposed to arable (although it is used in regulatory submissions in the EU and USA). Further, the work presented in this thesis was completed with blended soil, sourced from (a company called) Boughton Loam, not an agricultural soil, which may have impacted the degradation rates observed. For example, Krogh *et al.* (2009) investigated the

degradation of the veterinary pharmaceutical ivermectin in the OECD 307 system in four soils, three of which were agricultural from across Europe, and one artificial soil that satisfied OECD guideline criteria. It was observed that dissipation time in the three agricultural soils was much faster relative to that in the artificial soil, with calculated DT_{50} times of between 16.1-37.1 d in the three agricultural soils, and a DT_{50} of > 500 d in the artificial soil. A similar effect was seen in the faster degradation of benzovindiflupyr in Gartenacker relative to the soil used in this study.

However, as these general effects have been observed in an artificial soil where degradation is slow, the magnitude of these effects could be more pronounced in agricultural soils. This highlights a need to better understand the effect of light in agriculturally and ecologically relevant soil types, as stipulated by regulatory bodies, to better understand the role of soil type and edaphic factors in the magnitude of the observed effects.

7. REFERENCES

Abed, R. M., Al Kharusi, S., Schramm, A. and Robinson, M. D. (2010). Bacterial diversity, pigments and nitrogen fixation of biological desert crusts from the Sultanate of Oman. *FEMS Micro. Ecol.*, **72**, 418-28.

Alexander, M. (1981). Biodegradation of Chemicals of Environmental Concern. *Science*, **105**, 2713-2717.

Alexander, M. (1995). How toxic are toxic chemicals in the soil? *Environ. Sci. Tech.*, **29**, 2713-2717.

Alletto, L., Coquet, Y., Benoit, P. and Bergheaud, V. (2006). Effects of temperature and water content on degradation of isoproturon in three soil profiles. *Chemosphere*, **64**, 1053-61.

Altschul S. F., Gish W., Miller W., Myers E. W. and Lipman, D.J. (1990). Basic Local Alignment Search Tool. *Journal of Mol. Biol.*, **215**, 403-410.

Arias-Estévez, M., López-Periago, E., Martínez-Carballo, E., Simal-Gándara, J., Mejuto, J. C. and García-Río, L. (2008). The mobility and degradation of pesticides in soils and the pollution of groundwater resources. *Agric. Ecosyst. Environ.*, **123**, 247-260.

Arshad, M., Hussain, S. and Saleem, M. (2008). Optimization of environmental parameters for biodegradation of alpha and beta endosulfan in soil slurry by Pseudomonas aeruginosa. *J. Appl. Microbiol.*, **104**, 364-70.

Awasthi, N., Ahuja, R. and Kumar, A. (2000). Factors influencing the degradation of soil-applied endosulfan isomers. *Soil Biol. Biochem.*, **32**, 1697-1705.

Bates, S. T. and Garcia-Pichel, F. (2009). A culture-independent study of free-living fungi in biological soil crusts of the Colorado Plateau: their diversity and relative contribution to microbial biomass. *Environ. Microbiol.*, **11**, 56-67.

Bates, S. T., Nash, T. H. 3rd, and Garcia-Pichel, F. (2012). Patterns of diversity for fungal assemblages of biological soil crusts from the southwestern United States. *Mycologia*, **104**, 353-61.

Belnap, J. (2002). Nitrogen fixation in biological soil crusts from southeast Utah, USA. *Biol. Fert. Soils.*, **35**, 128-135.

Belnap, J. (1993). Recovery rates of cryptobiotic crusts: inoculant use and assessment method. *Great Basin Nat.*, **53**, 89-95.

Belnap, J. and Gillette, D. A. (1997). Disturbance of biological soil crusts: Impacts on potential wind erodibility of sandy desert soils in southeastern Utah. *Land Deg. Dev.*, **8**, 355-362.

Belnap, J., Hawkes, C. V. and Firestone, M. K. (2003). Boundaries in Miniature: Two examples from Soil. *BioScience*, **53**, 739-749.

Beltran, F. J., Ovejero, G. and Acedo, B. (1993). Oxidation of atrazine in water by ultraviolet radiation combined with hyfrogen peroxide. *Water Res.*, **27**, 1013-1021.

Benimeli, C. S., Gonzalez, A. J., Chaile, A. P. and Amoroso, M. J. (2007). Temperature and pH effect on lindane removal by Streptomyces sp. M7 in soil extract. *J. Basic Microbiol.*, **47**, 468-73.

Benvenuti, S. (1995). Soil light penetration and dormancy of Jimsonweed (Datura stramonium) seeds. *Weed Sci.*, **43**, 389-393.

Bernanke, J. and Köhler, H. R. (2009). The impact of environmental chemicals on wildlife vertebrates. *Rev. Environ. Contam. Toxicol.*, **198**, 1-47.

Beulke, S., Dubus, I. G., Brown, C. D. and Gottesbüren, B. (2000). Simulation of Pesticide Persistence in the Field on the Basis of Laboratory Data - A Review. *J. Environ. Qual.*, **29**, 1371-1379.

Beulke, S., van Beinum, W., Brown, C. D., Mitchell, M. and Walker, A. (2005). Evaluation of simplifying assumptions on pesticide degradation in soil. *J. Environ. Qual.*, **34**, 1933-1943.

Bokulich, N. A., Subramanian, S., Faith, J. J., Gevers, D., Gordon, J. I., Knight, R., Mills, D. A. and Caporaso, J.G. (2013). Quality-filtering vastly improves diversity estimates from Illumina aplicon sequencing. *Nat. Methods*, **10**, 57-60.

Bosso, C. J. (1988). Transforming adversaries into collaborators - Interest groups and the regulation of chemical pesticides. *Policy Sci.*, **21**, 3-22.

Bouseba, B., Zertal, A., Beguet, J., Rouard, N., Devers, M., Martin, C. and Martin-Laurent, F. (2009). Evidence for 2,4-D mineralisation in Mediterranean soils: impact of moisture content and temperature. *Pest Manage. Sci.*, **65**, 1021-1029.

Bravlavsky, S. E. (2007). Glossary Of Terms Used In Photochemistry 3rd Edition. *Pure Appl. Chem.*, **79**, 293-465.

Brekken, J. P. and Brezonik, P. L. (1998). Indirect photolysis of acetochlor: Rate constant of a nitrate-mediated hydrowyl radical reaction. *Chemosphere*, **36**, 2699-2704.

Bronick, C. J. and Lal, R. (2005). Soil structure and management: a review. *Geoderma*, **124**, 3-22.

Burrows, H. D., Santaballa, J. A. and Steenken, S. (2002). Reaction Pathways and mechanisms of photodegradation of pesticides. *J. Photochem. Photobiol.*, **67**, 1011-1344.

Caceres, T., Megharaj, M. and Naidu, R. (2008). Toxicity and transformation of fenamiphos and its metabolites by two micro algae Pseudokirchneriella subcapitata and Chlorococcum sp. *Sci. Total Environ.*, **398**, 53-9.

Cai, X., Liu, W., Jin, M. and Lin, K. (2007). Relation of diclofop-methyl toxicity and degradation in algae cultures. *Environ.Toxicol. Chem.*, **26**, 970-975.

Canty, M. N., Hagger, J. A., Moore, R. T., Cooper, L. and Galloway, T. S. (2007). Sublethal impact of short term exposure to the organophosphate pesticide azamethiphos in the marine mollusc Mytilus edulis. *Mar. Pollut. Bull.*, **54**, 396-402.

Caporaso JG, Kuczynski J, Stombaugh J, Bittinger K, Bushman FD, Costello EK, Fierer N, Gonzalez Pena A, Goodrich JK, Gordon JI, Huttley GA, Kelley ST, Knights D, Koenig JE, Ley RE, Lozupone CA, McDonald D, Muegge BD, Pirrung M, Reeder J, Sevinsky JR, Turnbaugh PJ, Walters WA, Widmann J, Yatsunenko T, Zaneveld J and Knight, R. (2010). QIIME allows analysis of high- throughput community sequencing data. *Nat. Methods*, **7**, 335-336.

Caporaso, J. G., Lauber, C. L., Walters, W. A., Berg-Lyons, D., Huntley, J., Fierer, N., Owens, S., Betley, J., Fraser, L., Bauer, M., Gormley, N., Gilbert, J., Smith, G. and Knight, R. (2012). Ultra-high-throughput microbial community analysis on the Illumina HiSeq and MiSeq platforms. *ISME J*, **6**, 1621-4.

Castle, S. C., Morrison, C. D. and Barger, N. N. (2011). Extraction of chlorophyll a from biological soil crusts: A comparison of solvents for spectrophotometric determination. *Soil Biol. Biochem.*, **43**, 853-856.

Cattaneo, M. V., Masson, M. and Greer, C. W. (1997). The influence of moisture on microbial transport, survival and 2,4-D biodegradation with a genetically marked Burkholderia cepacia in unsaturated soil columns. *Biodegradation*, **8**, 87-96.

Chamizo, S., Cantón, Y., Rodríguez-Caballero, E., Domingo, F. and Escudero, A. (2012). Runoff at contrasting scales in a semiarid ecosystem: A complex balance between biological soil crust features and rainfall characteristics. *J. Hydrol.*, **452-453**, 130-138.

Chatterjee, N. S., Gupta, S. and Varghese, E. (2013). Degradation of metaflumizone in soil: impact of varying moisture, light, temperature, atmospheric CO2 level, soil type and soil sterilization. *Chemosphere*, **90**, 729-36.

Chen, H., He, X., Rong, X., Chen, W., Cai, P., Liang, W., Li, S. and Huang, Q. (2009). Adsorption and biodegradation of carbaryl on montmorillonite, kaolinite and goethite. *Applied Clay Science*, **46**, 102-108.

Clarke, K. R. (1993). Non-parametric multivariate analyses of changes in community structure. *Aust. J. Ecol.*, **18**, 117-143.

Coat, S., Monti, D., Legendre, P., Bouchon, C., Massat, F. and Lepoint, G. (2011). Organochlorine pollution in tropical rivers (Guadeloupe): role of ecological factors in food web bioaccumulation. *Environ. Pollut.*, **159**, 1692-701.

Commission Regulation (EU) No. 283/2013 setting out the data requirements for active substances, in accordance with Regulation (EC) No. 1107/2009 of the European Parliament and of the Council concerning the placing of plant protection products on the market. *Official Journal of the European Union L*, **93**, 1-84.

Commission Regulation (EU) No. 284/2013 setting out the data requirements for plant protection products, in accordance with Regulation (EC) No. 1107/2009 of the European Parliament and of the Council concerning the placing of plant protection products on the market. *Official Journal of the European Union L*, **93**, 85-152.

Curran, W. S., Loux, M. M., Liebl, R. A. and Simmons, F. W. (1992). Photolysis of imidazolinone herbicides in aqueous solution and on soil. *Weed Sci.*, **40**, 143-148.

Darby, B. J., Neher, D. A. and Belnap, J. (2007). Soil nematode communities are ecologically more mature beneath late- than early-successional stage biological soil crusts. *Appl. Soil Ecol.*, **35**, 203-212.

Davies, L. O., Bramke, I., France, E., Marshall, S., Oliver, R., Nichols, C., Schafer, H. and Bending, G. D. (2013a). Non-UV light influences the degradation rate of crop protection products. *Environ. Sci. Tech.*, **47**, 8229-37.

Davies, L. O., Schafer, H., Marshall, S., Bramke, I., Oliver, R. G. and Bending, G. D. (2013b). Light structures phototroph, bacterial and fungal communities at the soil surface. *PLoS ONE*, **8**, e69048.

Deines, L., Rosentreter, R., Eldridge, D. J. and Serpe, M. D. (2007). Germination and seedling establishment of two annual grasses on lichen-dominated biological soil crusts. *Plant and Soil*, **295**, 23-35.

DeLorenzo, M. E., Scott, G. S. and Ross, P. E. (2001). Toxicity of pesticides to aquatic microorganisms: a review. *Environ.Toxicol. Chem.*, **20**, 84-98.

Directive 2009/128/EC of the European parliament and of the Council. Establishing a framework for Community action to achieve sustainable use of pesticides. *Official Journal of the European Union L*, 309-371.

Dungan, R. S., Gan, J. and Yates, S. R. (2001). Effect of temperature, organic amendment rate and moisture content on the degradation of 1,3-dichloropropene in soil. *Pest Manage. Sci.*, **57**, 1107-13.

Edgar, R. C. (2013). UPARSE: highly accurate OTU sequences from microbial amplicon reads. *Nat. Methods*, **10**, 996-8.

Emmett, B. A., Frogbrook, Z. L., Chamberlain, P. M., Griffiths, R. I., Pickup, R., Poskitt, J., Reynolds, B., Rowe, E., Spurgeon, D., Rowland, P., Wilson, J. and Wood, C. M. (2008). *Countryside Survey Technical Report No. 3/07*: Soils Manual. Swindon, UK.

European Food Safety Authority. (2010). Guidance for evaluating laboratory and field dissipation studies to obtain DegT50 values of plant protection products in soil. *EFSA Journal*, **8**, 1936.

European Food Safety Authority. (2015). Conclusion on the peer review of the pesticide risk assessment of the active substance benzovindiflupyr. *EFSA Journal*.

European Food Safety Authority. (2010). Conclusion on the peer review of the pesticide risk assessment of the active substance paclobutrazol. *EFSA Journal*, **8**.

European Food Safety Authority (2007). Conclusion regarding the peer review of the pesticide risk assessment of the active substance fludioxonil. *EFSA Journal*, **110**, 1-85.

Fantke, P., Wieland, P., Wannaz, C., Friedrich, R. and Jolliet, O. (2013). Dynamics of pesticide uptake into plants: From system functioning to parsimonious modeling. *Environ. Modell. Software.*, **40**, 316-324.

FERA (2013). Pesticide Usage Statisitics. FERA website: http://pusstats.csl.gov.uk/.

Fontaine, S., Mariotti, A. and Abbadie, L. (2003). The priming effect of organic matter: a question of microbial competition? *Soil Biol. Biochem.*, **35**, 837-843.

Food and Agriculture Organisation. (2002). International code of conduct of the distribution and use of pesticides. **Available: http://www.fao.org/docrep/005/y4544e/y4544e00.htm Accessed 20150228**.

Forum for the Coordination of Pesticide Fate Models and their Use. (2006). Guidance document on estimating persistence and degradation kinetics from environmental fate studies on pesticides in EU registration: Report of the focus work group on degradation kinetics, pp. 434. EC Document Reference Sanco/10058/2005 version 2.0.

Franco, A., Fu, W. and Trapp, S. (2009). Influence of soil pH on the sorption of ionizable chemcicals: modelling advances. *Environ.Toxicol. Chem.*, **28**, 458-464.

Garcia-Pichel, F., Johnson, S. L., Youngkin, D. and Belnap, J. (2003). Small-scale vertical distribution of bacterial biomass and diversity in biological soil crusts from arid lands in the Colorado plateau. *Microb. Ecol.*, **46**, 312-21.

Garcia-Pichel, F., Lopez-Cortes, A. and Nubel, U. (2001). Phylogenetic and morphological diversity of cyanobacteria in soil desert crusts from the Colorado Plateau. *Appl. Environ. Microbiol.*, **67**, 1902-1910.

Garcia-Pichel, F., Loza, V., Marusenko, Y., Mateo, P. and Potrafka, R. M. (2013). Temperature drives the continental-scale distribution of key microbes in topsoil communities. *Science*, **340**, 1574-1577.

Garcia-Pichel, F. and Wojciechowski, M. F. (2009). The evolution of a capacity to build supra-cellular ropes enabled filamentous cyanobacteria to colonize highly erodible substrates. *PLoS ONE*, **4**, e7801.

García-Valcárcel, A. I. and Tadeo, J. L. (1999). Influence of Soil Moisture on Sorption and Degradation of Hexazinone and Simazine in Soil. *J. Am. Chem. Soc.*, **47**, 3895-3900.

Gaultier, J., Farenhorst, A., Cathcart, J. and Goddard, T. (2008). Degradation of [carboxyl-14C] 2,4-D and [ring-U-14C] 2,4-D in 114 agricultural soils as affected by soil organic carbon content. *Soil Biol. Biochem.*, **40**, 217-227.

Gevao, B., Semple, K. T. and Jones, K. C. (2000). Bound pesticide residues in soils; a review. *Environ. Pollut.*, **108**, 3-14.

Ghadiri, H., Rose, C. W. and Connell, D. W. (1995). Degradation of organochlorine pesticides in soils under controlled environment and outdoor conditions. *J. Environ. Manage.*, **43**, 141-151.

Griffiths, R. I., Thomson, B. C., James, P., Bell, T., Bailey, M. and Whiteley, A. S. (2011). The bacterial biogeography of British soils. *Environ. Microbiol.*, **13**, 1642-54.

Grube, A., Donaldson, D., Kiely, T. and Wu, L. (2011). Pesticides Industry Sales and Usage - 2006 and 2007 Market Estimates. *US Environmental Protection Agency*.

Hawkes, C. V. and Flechtner, V. R. (2002). Biological soil crusts in a xeric Florida shrubland: composition, abundance, and spatial heterogeneity of crusts with different disturbance histories. *Microb. Ecol.*, **43**, 1-12.

Housman, D. C., Powers, H. H., Collins, A. D. and Belnap, J. (2006). Carbon and nitrogen fixation differ between successional stages of biological soil crusts in the Colorado Plateau and Chihuahuan Desert. *J. Arid Environ.*, **66**, 620-634.

International Union of Pure and Applied Chemistry. (2010). History of pesticides. **Available: http://agrochemicals.iupac.org/index.php?option=com_sobi2&sobi2Task=sobi2Details&catid=3&sobi2Id=31&Itemid=19 Accessed 20150228.**

Jeffery, S., Harris, J. A., Rickson, R. J. and Ritz, K. (2009). The spectral quality of light influences the temporal development of the microbial phenotype at the arable soil surface. *Soil Biol. Biochem.*, **41**, 553-560.

Kabra, A. N., Ji, M. K., Choi, J., Kim, J. R., Govindwar, S. P. and Jeon, B. H. (2014). Toxicity of atrazine and its bioaccumulation and biodegradation in a green microalga, Chlamydomonas mexicana. *Environ. Sci. Pollut. Res.*, **21**, 12270-8.

Karpouzas, D. G. and Walker, A. (2000). Factors influencing the ability of Pseudomonas putida strains epI and II to degrade the organophosphate ethoprophos. *J. Appl. Microbiol.*, **89**, 40-48.

Katagi, T. (2002). Abiotic hydrolysis of pesticides in the aquatic environment. In *Rev. Environ. Contam. Toxicol.*, pp. 79-261. Edited by G. W. Ware. New York: Springer.

Katagi, T. (2006). Behaviour of Pesticides in Water-Sediment Systems. In *Rev. Environ. Contam. Toxicol.*, pp. 133-251. Edited by G. W. Ware. New York: Springer.

Kelsey, J. W., Kottler, B. D. and Alexander, M. (1997). Selective chemical extractants to predict bioavailability of soil-aged organic chemicals. *Environ. Sci. Tech.*, **31**, 214-217.

Khandelwal, A., Gupta, S., Gajbhiye, V. T. and Varghese, E. (2014). Degradation of kresoxim-methyl in soil: impact of varying moisture, organic matter, soil sterilization, soil type, light and atmospheric CO2 level. *Chemosphere*, **111**, 209-17.

Kidron, G. J. (1999). Differential water distibution over dune slopes as affected by slope position and microbiotic crust, Negev Desert, Israel. *Hydrol. Process.*, **13**, 1665-1682.

Kidron, G. J., Monger, H. C., Vonshak, A. and Conrod, W. (2012). Contrasting effects of microbiotic crusts on runoff in desert surfaces. *Geomorphology*, **139-140**, 484-494.

Kidron, G. J., Vonshak, A., Dor, I., Barinova, S. and Abeliovich, A. (2010). Properties and spatial distribution of microbiotic crusts in the Negev Desert, Israel. *Catena*, **82**, 92-101.

Kidron, G. J., Yair, A., Vonshak, A. and Abeliovich, A. (2003). Microbiotic crust control of runoff generation on sand dunes in the Negev Desert. *Water Resources Research*, **39**, 1108.

Kislev, M. E., Weiss, E. and Hartmann, A. (2004). Impetus for sowing and the beginning of agriculture: ground collecting of wild cereals. *Proc. Nat. Acad. Sci. U.S.A.*, **101**, 2692-5.

Knapen, A., Poesen, J., Galindo-Morales, P., Baets, S. D. and Pals, A. (2007). Effects of microbiotic crusts under cropland in temperate environments on soil erodibility during concentrated flow. *Earth Surf. Proc. Land.*, **32**, 1884-1901.

Krogh, K. A., Jensen, G. G., Schneider, M. K., Fenner, K. and Halling-Sorensen, B. (2009). Analysis of the dissipation kinetics of ivermectin at different temperatures and in four different soils. *Chemosphere*, **75**, 1097-104.

Kumar, M. and Philip, L. (2006). Bioremediation of endosulfan contaminated soil and water -- optimization of operating conditions in laboratory scale reactors. *J. Hazard. Mater.*, **136**, 354-64.

Kästner, M. (2008). "Humification" Process or Formation of Refractory Soil Organic Matter. In *Biotechnology*, pp. 89-125. Edited by: Wiley-VCH Verlag GmbH.

Kästner, M., Nowak, K. M., Miltner, A., Trapp, S. and Schäffer, A. (2014). Classification and Modelling of Nonextractable Residue (NER) Formation of Xenobiotics in Soil – A Synthesis. *Crit. Rev. Environ. Sci. Tech.*, **44**, 2107-2171.

Lan, S., Wu, L., Zhang, D. and Hu, C. (2011). Successional stages of biological soil crusts and their microstructure variability in Shapotou region (China). *Environ. Earth Sci.*, **65**, 77-88.

Lange, O. L., Kidron, G. J., Budel, B., Meyer, A., Kilian, E. and Abeliovich, A. (1992). Taxonomic composition and photosynthetic characteristics of the 'Biological Soil Crusts' covering sand dunes in the western Negev desert. *Func. Ecol.*, **6**, 519-527.

Langhans, T. M., Storm, C. and Schwabe, A. (2009a). Biological soil crusts and their microenvironment: Impact on emergence, survival and establishment of seedlings. *Flora*, **204**, 157-168.

Langhans, T. M., Storm, C. and Schwabe, A. (2009b). Community assembly of biological soil crusts of different successional stages in a temperate sand ecosystem, as assessed by direct determination and enrichment techniques. *Microb. Ecol.*, **58**, 394-407.

Lauber, C. L., Hamady, M., Knight, R. and Fierer, N. (2009). Pyrosequencing-based assessment of soil pH as a predictor of soil bacterial community structure at the continental scale. *Appl. Environ. Microbiol.*, **75**, 5111-20.

Li, K., Bai, Z. and Zhang, H. (2015). Community succession of bacteria and eukaryotes in dune ecosystems of Gurbantunggut Desert, Northwest China. *Extremophiles*, **19**, 171-81.

Li, X.-R., He, M.-Z., Zerbe, S., Li, X.-J. and Liu, L.-C. (2010). Micro-geomorphology determines community structure of biological soil crusts at small scales. *Earth Surf. Proc. Land.*, **35**, 932-940.

Li, X.-R., Wang, X.-P., Li, T. and Zhang, J.-G. (2002). Microbiotic soil crust and its effect on vegetation and habitat on artificially stabilized desert dunes in Tengger Desert, North China. *Biol. Fert. Soils.*, **35**, 147-154.

Lin, L., Cook, D. N., Wiesehahn, G. P., Alfonso, R., Behrman, B., Cimino, G. D., Corten, L., Damonte, P. B., Dikeman, R., Dupuis, K., Fang, Y. M., Hanson, C. V., Hearst, J. E., Lin, C. Y., Londe, H. F., Metchette, K., Nerio, A. T., Pu, J. T., Reames, A. A., Rheinschmidt, M., Tessman, J., Isaacs, S. T., Wollowitz, S. and Corash, L. (1997). Photochemical inactivation of viruses and bacteria in platelet concentrates by use of a novel psoralen and long-wavelength ultraviolet light. *TRANFUSION*, **37**, 423-425.

Ling, W., Sun, R., Gao, X., Xu, R. and Li, H. (2015). Low-molecular-weight organic acids enhance desorption of polycyclic aromatic hydrocarbons from soil. *Eur. J. Soil Sci.*, **66**, 339-347.

Liu, Y., Li, X., Jia, R., Huang, L., Zhou, Y. and Gao, Y. (2011). Effects of biological soil crusts on soil nematode communities following dune stabilization in the Tengger Desert, Northern China. *Appl. Soil Ecol.*, **49**, 118-124.

Ludwig, W., Strunk, O., Westram, R., Richter, L., Meier, H., Yadhukumar, Buchner, A., Lai, T., Steppi, S., Jobb, G., Forster, W., Brettske, I., Gerber, S., Ginhart, A. W., Gross, O., Grumann, S., Hermann, S., Jost, R., Konig, A., Liss, T., Lussmann, R., May, M., Nonhoff, B., Reichel, B., Strehlow, R., Stamatakis, A., Stuckmann, N., Vilbig, A., Lenke, M., Ludwig, T., Bode, A. and Schleifer, K. H. (2004). ARB: a software environment for sequence data. *Nucleic Acids Res.*, **32**, 1363-71.

Luo, L., Zhang, S., Shan, X. Q. and Zhu, Y. G. (2006). Oxalate and root exudates enhance the desorption of p,p'-DDT from soils. *Chemosphere*, **63**, 1273-1279.

Madigan, M. T., Martinko, J. M. and Parker, J. (2003). Brock Biology of Microorganisms (USA: Pearson Education International).

Marchand, A-L., Piutti, S., Lagacherie, B. and Soulas, G. (2002). Atrazine mineralization in bulk soil and maize rhizosphere. *Biol. Fert. Soils.*, **35**, 288-292.

Miller, P. M. and Chin, Y. P. (2005). Indirect Photolysis Promoted by Natural and Engineered Wetland Water Constituents: Processes Leading to Alachlor Degradation. *Environ. Sci. Tech.*, **39**, 4454-4462.

Miller, P. M. and Chin, Y. P. (2002). Photoinduced Degradation of Carbaryl in a Wetland Surface Water. *Journal of Agricultural and Food Chemistry*, **50**, 6758-6765.

Monard, C., Vandenkoornhuyse, P., Le Bot, B. and Binet, F. (2011). Relationship between bacterial diversity and function under biotic control: the soil pesticide degraders as a case study. *ISME J*, **5**, 1048-56.

Mostafa, F. I. and Helling, C. S. (2001). Isoproturon degradation as affected by the growth of two algal species at different concentrations and pH values. *J. Environ. Sci. Health Part B.*, **36**, 709-27.

Müller, K., Magesan, G. N. and Bolan, N. S. (2007). A critical review of the influence of effluent irrigation on the fate of pesticides in soil. *Agric. Ecosyst. Environ.*, **120**, 93-116.

Nagy, M. L., Perez, A. and Garcia-Pichel, F. (2005). The prokaryotic diversity of biological soil crusts in the Sonoran Desert (Organ Pipe Cactus National Monument, AZ). *FEMS Micro. Ecol.*, **54**, 233-45.

Nowak, K. M., Girardi, C., Miltner, A., Gehre, M., Schaffer, A. and Kastner, M. (2013). Contribution of microorganisms to non-extractable residue formation during biodegradation of ibuprofen in soil. *Sci. Total Environ.*, **445-446**, 377-84.

Nowak, K. M., Miltner, A., Gehre, M., Schaffer, A. and Kästner, M. (2011). Formation and fate of bound residues from microbial biomass during 2,4-D degradation in soil. *Environ. Sci. Tech.*, **45**, 999-1006.

OECD Guidelines for the Testing of Chemicals. (2002). OECD Guideline 307: Aerobic and Anaerobic Transformation in Soil. *OECD Publishing*.

Pointing, S. B. and Belnap, J. (2012). Microbial colonization and controls in dryland systems. *Nat. Rev. Microbiol.*, **10**, 551-62.

Qu, H., Ma, R. X., Liu, D. H., Wang, P., Huang, L. D., Qiu, X. X. and Zhou, Z. Q. (2014). Enantioselective toxicity and degradation of the chiral insecticide fipronil in Scenedesmus obliguus suspension system. *Environ. Toxicol. Chem.*, **33**, 2516-21.

Quast, C., Pruesse, E., Yilmaz, P., Gerken, J., Schweer, T., Yarza, P., Peplies, J. and Glockner, F. O. (2013). The SILVA ribosomal RNA gene database project: improved data processing and web-based tools. *Nucleic Acids Res.*, **41**, D590-6.

Redfield, E., Barns, S. M., Belnap, J., Daane, L. L. and Kuske, C. R. (2002). Comparative diversity and composition of cyanobacteria in three predominant soil crusts of the Colorado Plateau. *FEMS Micro. Ecol.*, **40**, 55-63.

Ritchie, R. J. (2006). Consistent sets of spectrophotometric chlorophyll equations for acetone, methanol and ethanol solvents. *Photosynth. Res*, **89**, 27-41.

Rodríguez Cruz, M. S., Jones, J. E. and Bending, G. D. (2008). Study of the spatial variation of the biodegradation rate of the herbicide bentazone with soil depth using contrasting incubation methods. *Chemosphere*, **73**, 1211-5.

Rodríguez-Cruz, M. S., Jones, J. E. and Bending, G. D. (2006). Field-scale study of the variability in pesticide biodegradation with soil depth and its relationship with soil characteristics. *Soil Biol. Biochem.*, **38**, 2910-2918.

Rodríguez-Cruz, M. S., Bælum, J., Shaw, L. J., Sørensen, S. R., Shi, S., Aspray, T., Jacobsen, C. S. and Bending, G. D. (2010). Biodegradation of the herbicide mecoprop-p with soil depth and its relationship with class III tfdA genes. *Soil Biol. Biochem.*, **42**, 32-39.

Schaumann, G. E. and Bertmer, M. (2008). Do water molecules bridge soil organic matter molecule segments? *Eur. J. Soil Sci.*, **59**, 423-429.

Schroll, R., Becher, H. H., Döerfler, U., Gayler, S., Grundmann, S., Hartmann, H. P. and Ruoss, J. (2006). Quantifying the Effect of Soil Moisture on the Aerobic Microbial Mineralization of Selected Pesticides in Different Soils. *Environ. Sci. Tech.*, **40**, 3305-3312.

Schürner, J., Clarholm, M. and Rosswall, T. (1985). Microbial biomass and activity in an agricultural soil with different organic matter contents. *Soil Biol. Biochem.*, **17**, 611-618.

Semple, K. T., Doick, K. J., Jone, K. C., Burauel, P., Craven, A. and Harms, H. (2004). Defining bioavailability and bioaccessibility of contaminated soil and sediment is complicated. *Environ. Sci. Tech.*, **38**, 228A-231A.

Serpe, M. D., Orm, J. M., Barkes, T. and Rosentreter, R. (2006). Germination and seed water status of four grasses on moss-dominated biological soil crusts from arid lands. *Plant Ecol.*, **185**, 163-178.

Sethunathan, N., Megharaj, M., Chen, Z. L., Williams, B. D., Lewis, G. and Naidu, R. (2004). Algal Degradation of a Known Endocrine Disrupting Insecticide, r-Endosulfan, and Its Metabolite, Endosulfan Sulfate, in Liquid Medium and Soil. *J. Agric. Food Chem.*, **52**, 3030-3035.

Sharpless, C. M. (2012). Lifetimes of triplet dissolved natural organic matter (DOM) and the effect of NaBH(4) reduction on singlet oxygen quantum yields: implications for DOM photophysics. *Environ Sci Technol*, **46**, 4466-73.

Sherwood, A. R. and Presting, G. G. (2007). Universal primers amplify a 23S rDNA plastid marker in eukaryotic algae and cyanobacteria. *J. Phycol*. **43**, 605-608.

Sims, J. L., Sims, R. C. and Matthews, J. E. (1990). Approach to bioremediation of contaminated surface soils. *Hazard. Water. Hazard. Mater.*, **7**, 117-149.

Singh, B., Walker, A. and Wright, D. (2006). Bioremedial potential of fenamiphos and chlorpyrifos degrading isolates: Influence of different environmental conditions. *Soil Biol. Biochem.*, **38**, 2682-2693.

Singh, B. K., Walker, A., Morgan, J. A. W. and Wright, D. J. (2003). Effects of Soil pH on the Biodegradation of Chlorpyrifos and Isolation of a Chlorpyrifos-Degrading Bacterium. *Appl. Environ. Microbiol.*, **69**, 5198-5206.

Soule, T., Anderson, I. J., Johnson, S. L., Bates, S. T. and Garcia-Pichel, F. (2009). Archael populations in biological soil crusts from arid lands in North America. *Soil Biol. Biochem.*, **41**, 2069-2074.

Stark, T. and Firestone, M. K. (1995). Mechanisms for soil moisture effects on activity of nitrifying bacteria. *Appl. Environ. Microbiol.* **61**, 218-221.

Steven, B., Gallegos-Graves, L. V., Starkenburg, S. R., Chain, P. S. and Kuske, C. R. (2012). Targeted and shotgun metagenomic approaches provide different descriptions of dryland soil microbial communities in a manipulated field study. *Environ. Microbiol. Rep.*, **4**, 248-56.

Stoate, C., Boatman, N. D., Borralho, R. J., Carvalho, C. R., Snoo, G. R. d. and Eden, P. (2001). Ecological impacts of arable intensification in Europe. *J. Environ. Manage.*, **63**, 337-365.

Thayer, K. and Houlihan, J. (2004). Pesticides, Human Health, and the Food Quality Protection Act. *Wm. & Mary Envtl. L. & Pol'y Rev.*, **28**, 257-312.

Thomas, K. A. and Hand, L. H. (2012). Assessing the metabolic potential of phototrophic communities in surface water environments: fludioxonil as a model compound. *Environ. Toxicol. Chem.*, **31**, 2138-46.

Thomas, K. A. and Hand, L. H. (2011). Assessing the potential for algae and macrophytes to degrade crop protection products in aquatic ecosystems. *Environ.Toxicol. Chem.*, **30**, 622-31.

Tisdall, J. M. (1996). Formation of soil aggregates and accumulation of soil organic matter. In *Structure and organic matter storage in agricultural soils*, pp. 57-96. Edited by. Boca Raton, FL, USA: CRC Press.

Tisdall, J. M., Nelson, S. E., Wilkinson, K. G., Smith, S. E. and McKenzie, B. M. (2012). Stabilisation of soil against wind erosion by six saprotrophic fungi. *Soil Biol. Biochem.* **50**, 134-141.

Tomlin, C. D. S. (2006). *The pesticide manual,* 14th edn. Pp.1349. British Crop Protection Council: Hampshire, UK.

U.S. Environmental Protection Agency. (2008). Fate, transport, and transformation test guidelines. OPPTS 835.6100 Terrestrial Field Dissipation. *EPA*, 712-C-08-020.

U.S. Environmental Protection Agency. (1994). Physico-chemical properties and environmental fate of pesticides. Environmental hazards assessment of program. Edited by C. D. Linde, pp. 53. California: Environmental Protection Agency.

Veluci, R. M., Neher, D. A. and Weicht, T. R. (2006). Nitrogen fixation and leaching of biological soil crust communities in mesic temperate soils. *Microb. Ecol.*, **51**, 189-96.

Voos, G. and Groffman, P. M. (1997). Relationship between microbial biomass and dissipation of 2,4-D and dicamba in soil. *Biol. Fert. Soils.* **24,** 106-110.

Wallace, D. F., Hand, L. H. and Oliver, R. G. (2010). The role of indirect photolysis in limiting the persistence of crop protection products in surface waters. *Environ. Toxicol. Chem.*, **29**, 575-81.

Xiao, B., Wang, Q.-h., Zhao, Y.-g. and Shao, M.-a. (2011). Artificial culture of biological soil crusts and its effects on overland flow and infiltration under simulated rainfall. *Appl. Soil Ecol.*, **48**, 11-17.

Xin-Yu, L., Zhen-Cheng, S., Xu, L., Cheng-Gang, Z. and Hui-Wen, Z. (2010). Assessing the effects of acetochlor on soil fungal communities by DGGE and clone library analysis. *Ecotoxicology*, **19**, 1111-6.

Yang, Y., Chun, S., G. and Huang, M. (2004). pH-Dependence of Pesticide Adsorption by Wheat-Residue-Derived Black Carbon. *Langmuir*, **20**, 6736-6741.

Yeager, C. M., Kornosky, J. L., Housman, D. C., Grote, E. E., Belnap, J. and Kuske, C. R. (2004). Diazotrophic Community Structure and Function in Two Successional Stages of Biological Soil Crusts from the Colorado Plateau and Chihuahuan Desert. *Appl. Environ. Microbiol.*, **70**, 973-983.

Yeager, C. M., Kornosky, J. L., Morgan, R. E., Cain, E. C., Garcia-Pichel, F., Housman, D. C., Belnap, J. and Kuske, C. R. (2007). Three distinct clades of cultured heterocystous cyanobacteria constitute the dominant N2-fixing members of biological soil crusts of the Colorado Plateau, USA. *FEMS Micro. Ecol.*, **60**, 85-97.

Yoshitake, S., Uchida, M., Koizumi, H., Kanda, H. and Nakatsubo, T. (2010). Production of biological soil crusts in the early stage of primary succession on a high Arctic glacier foreland. *New Phytol.*, **186**, 451-60.

Younes, M. and Galal-Gorchev, H. (2000). Pesticides in Drinking Water - A Case Study. *Food Chem. Toxicol.*, **38**, 87-90.

Zaady, E., Abel, S., Barkai, D., Sarig, S. and Kesselmeier, J. (2013). Long-term impact of agricultural practices on biological soil crusts and their hydrological processes in a semi-arid landscape. *J Arid Environ.*, **90**, 5-11.

Zaady, E., Kuhn, U., Wilske, B., Sandoval-Soto, L. and Kesselmeier, J. (2000). Patterns of CO2 exchange in biological soil crusts of successional age. *Soil Biol. Biochem.*, **32**, 959-966.

Zhang, B., Zhang, Y., Downing, A. and Yulu, N. (2011). Distribution and composition of Cyanobacteria and microalgae associated with biological soil crusts in the Gurbantunggut Desert, China. *Arid Land Res. Manage.*, **3**, 275-293.

Zhang, B., Zhang, Y., Zhao, J., Wu, N., Chen, R. and Zhang, J. (2009a). Microalgal species variation at different successional stages in biological soil crusts of the Gurbantunggut Desert, Northwestern China. *Biol. Fert. Soils.*, **45**, 539-547.

Zhang, J., Zhang, Y.-m., Downing, A., Cheng, J.-h., Zhou, X.-b. and Zhang, B.-c. (2009b). The influence of biological soil crusts on dew deposition in Gurbantunggut Desert, Northwestern China. *J. Hydrol.*, **379**, 220-228.

Zhang, Y. M., Wang, H. L., Wang, X. Q., Yang, W. K. and Zhang, D. Y. (2006). The microstructure of microbiotic crust and its influence on wind erosion for a sandy soil surface in the Gurbantunggut Desert of Northwestern China. *Geoderma*, **132**, 441-449.

Zhao, Y., Xu, M. and Belnap, J. (2010). Potential nitrogen fixation activity of different aged biological soil crusts from rehabilitated grasslands of the hilly Loess Plateau, China. *J. Arid Environ.*, **74**, 1186-1191.

APPENDIX I: OECD 307 REGULATORY LIKE STUDY – FURTHER METHODS

I.1 Application rate calculations

Field application rates were derived from the Pesticide Manual (Tomlin 2006) or internal Syngenta data.

Example: Paclobutrazol

The desired application rate of paclobutrazol was 100 g ai/ha. This was converted to g ai/cm^2, and divided by five to give g ai/cm^3 if evenly distributed to 5 cm depth. This value was divided by the assumed bulk density of the soil, 1.5 g/cm^3, giving the application rate required as 0.133 μg/g. Each test vessel contained 100 g dwe soil, so each test system required 13.33 μg of paclobutrazol to be applied.

The specific activity (SpecAc; the activity, Bq, of the radiolabelled CPP by mass) of paclobutrazol (4 281 Bq/μg) was multiplied by the required mass of paclobutrazol to be applied (13.33 μg) to give the activity to be applied per test system (57 080 Bq).

I.2 Application checks

A treatment solution for the number of test systems to be applied + 10% (50) was made up. Application volume per test system was 100 µL. The concentration of the treatment solution was checked by liquid scintillation counting in triplicate before and after application Pre- and post-application values were averaged to give the average application per system, 59 134.88 Bq, 103.6% of desired.

I.3 Mass balance

Radioactivity in each analysed fraction was quantified by LSC as a percentage of applied radioactivity, and summed to give the mass balance of a sample. An example mass balance table for 30 DAT paclobutrazol light samples is shown in Table I.1 below.

Table I.1: An example of a mass balance table. Values shown are for 30 DAT paclobutrazol light samples.

DAT	Sample	Acetonitrile combined extracts	NERs	CO_2	Total % Applied
30	56	87.4	12.7	0.1	100.3
30	57	85.9	14.9	0.2	101.1
30	58	87.6	14.48	0.2	102.2

I.4 Concentration calculations – procedural recoveries

Solvent extract samples were concentrated to at least 1 000 Bq ml^{-1} prior to HPLC analysis. Having previously quantified the amount of radiochemical present in the solvent extracts, a Bq/g figure was known for each sample. The volume of solvent extract to be concentrated was calculated (8.70 g), and the sample blown down to dryness. The sample was re-suspended in 1 ml 50:50 Solvent:UPW and the mass recorded (1.02 g). A 50 µl aliquot was taken for LSC (0.0438 g), the Bq recorded (45.20 Bq) and divided by the aliquot weight to give a Bq/g figure (1032 Bq/g). Total Bq in the concentrated sample was calculated (1032*1.02 = 1054.90), and divided by the expected Bq figure (calculated from solvent extract Bq/g figure*extract mass) and multiplied by 100 to give the recovery (101.50%).

Table I.2: An example of a concentration step required prior to HPLC analysis. Example from 59 DAT paclobutrazol light sample.

Extract Mass (g)	Concentrated Mass (g)	Aliquot mass (g)	Bq	Bq/g	Total Bq	Expected Bq	Recovery (%)
8.70	1.02	0.0438	45.2	1032	1054.9	1039.1	101.5

I.5 Example HPLC chromatograms

Example chromatograms from ^{14}C-HPLC analysis of compounds investigated in Chapter 2.

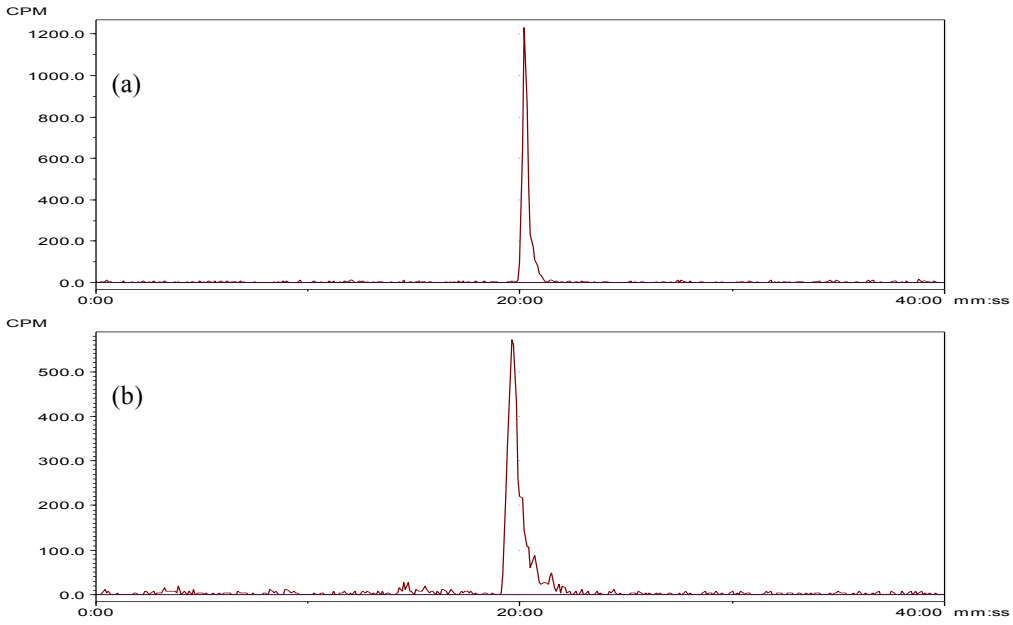

Figure I.1: HPLC chromatograms from analysis of [^{14}C]-pesticide A at (a) 0 DAT, and (b) 120 DAT in an OECD 307 regulatory like study.

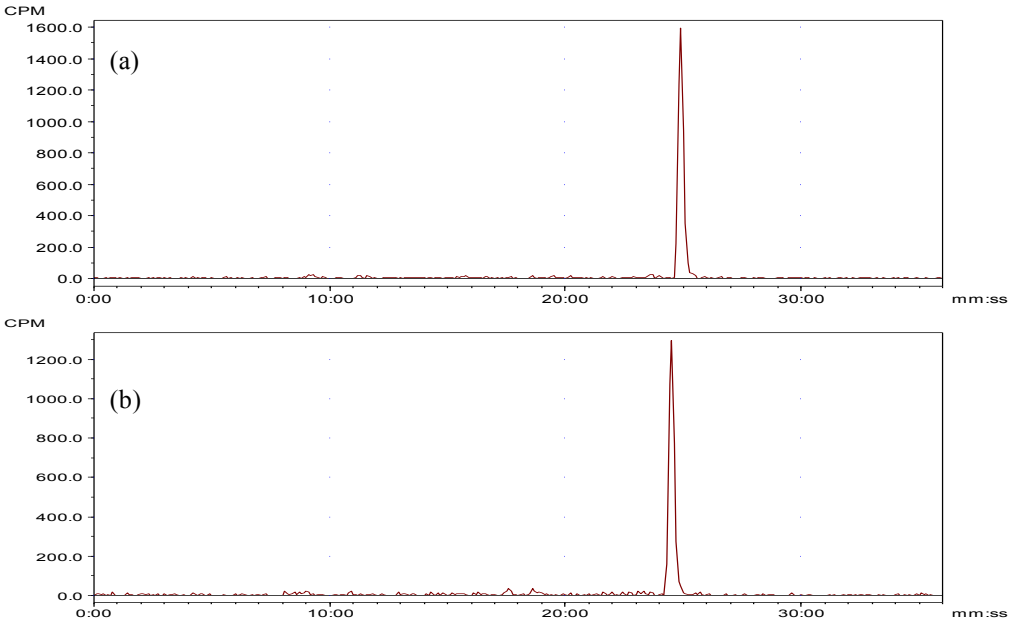

Figure I.3: HPLC chromatograms from analysis of [^{14}C]-benzovindiflupyr at (a) 0 DAT, and (b) 118 DAT in an OECD 307 regulatory like study.

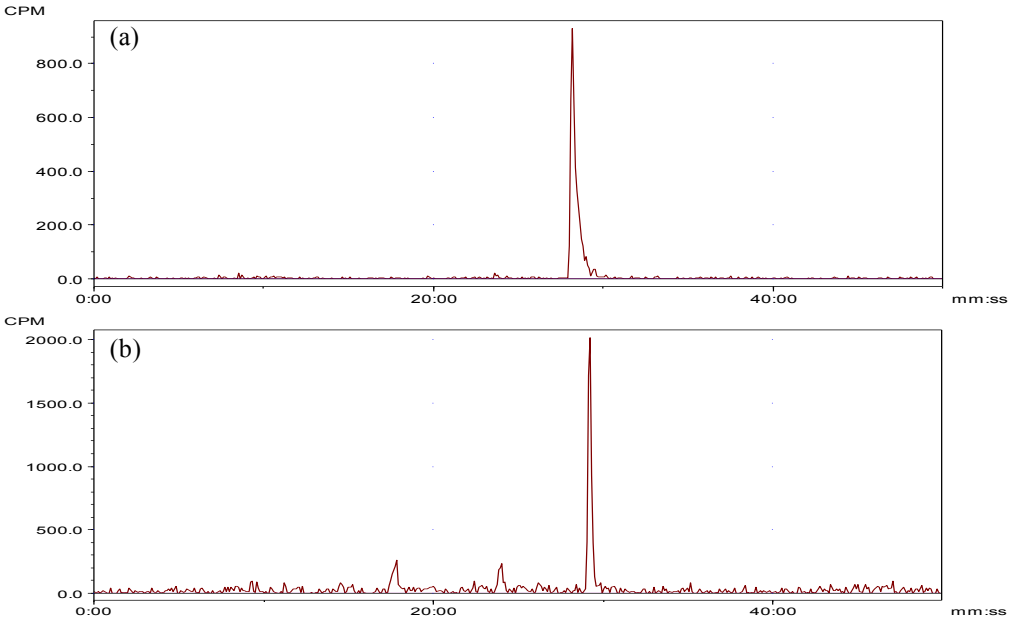

Figure I.4: HPLC chromatograms from analysis of [^{14}C]-cinosulfuron at (a) 0 DAT, and (b) 60 DAT in an OECD 307 regulatory like study.

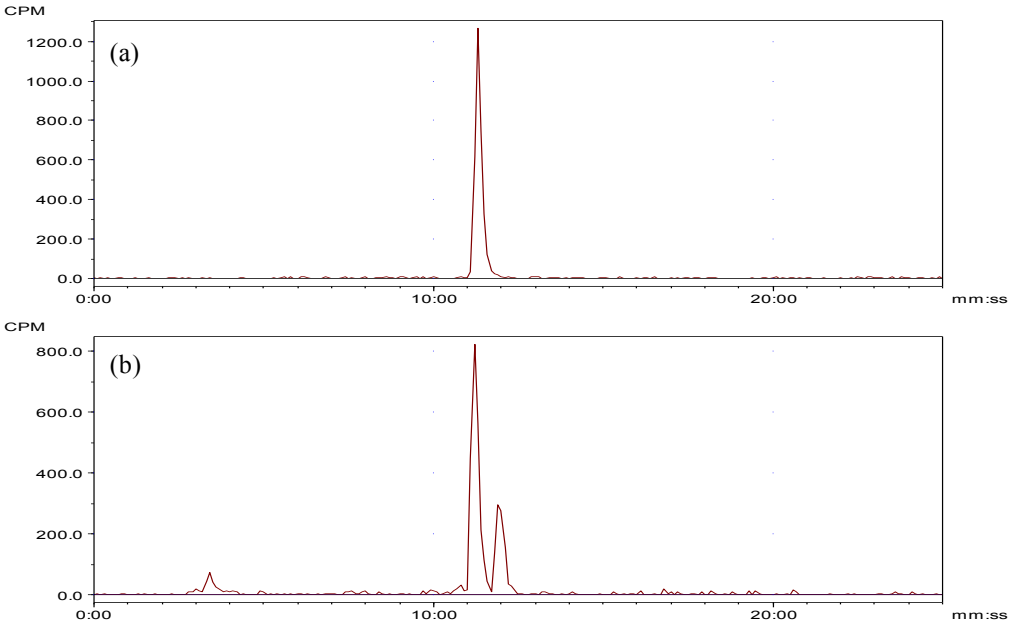

Figure I.4: HPLC chromatograms from analysis of [^{14}C]-paclobutrazol at (a) 0 DAT, and (b) 118 DAT in an OECD 307 regulatory like study.

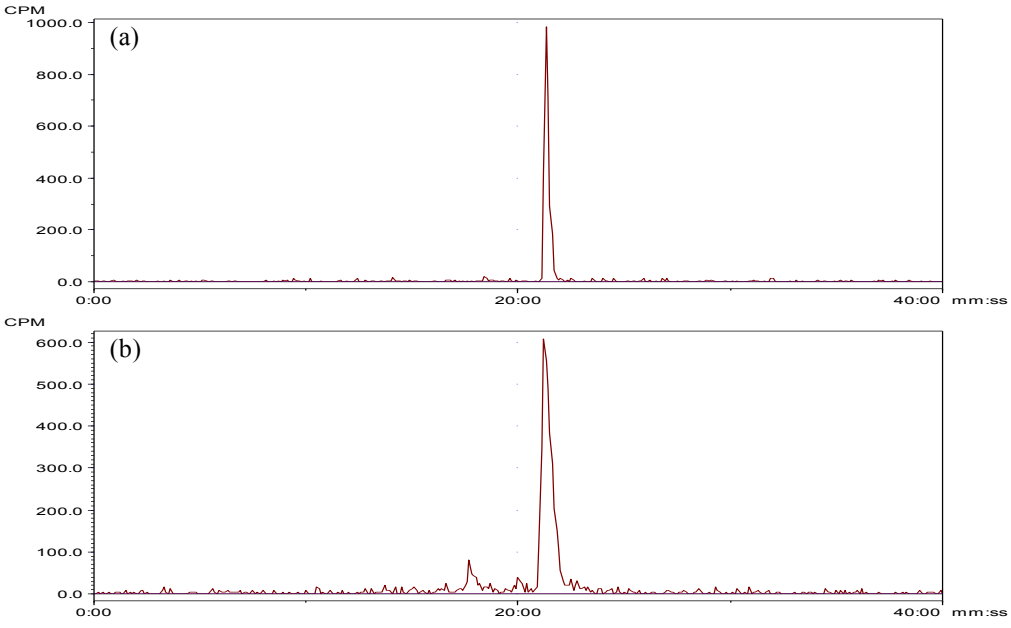

Figure I.5: HPLC chromatograms from analysis of [^{14}C]-fludioxonil at (a) 0 DAT, and (b) 120 DAT in an OECD 307 regulatory like study.

APPENDIX II: FIELD DEGRADATION – FURTHER METHODS

II.1 Plot layout

The plot layout for the filter degradation experiment detailed in Chapters 3 & 5 is shown in Figure II.1 and II.2a The areas was comprised triplicate light filter treatments arranged in a Latin square design. Cores were installed in a randomised design (Figure II.2b) with one monitoring core per plot. Figure II.2c shows cores extracted from the ground at 57 DAT.

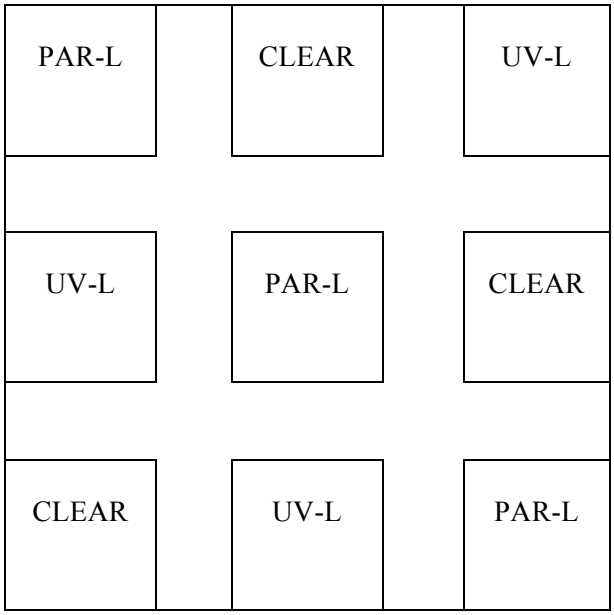

Figure II.1: The plot layout used in the field degradation experiment detailed in Chapters 3 & 5.

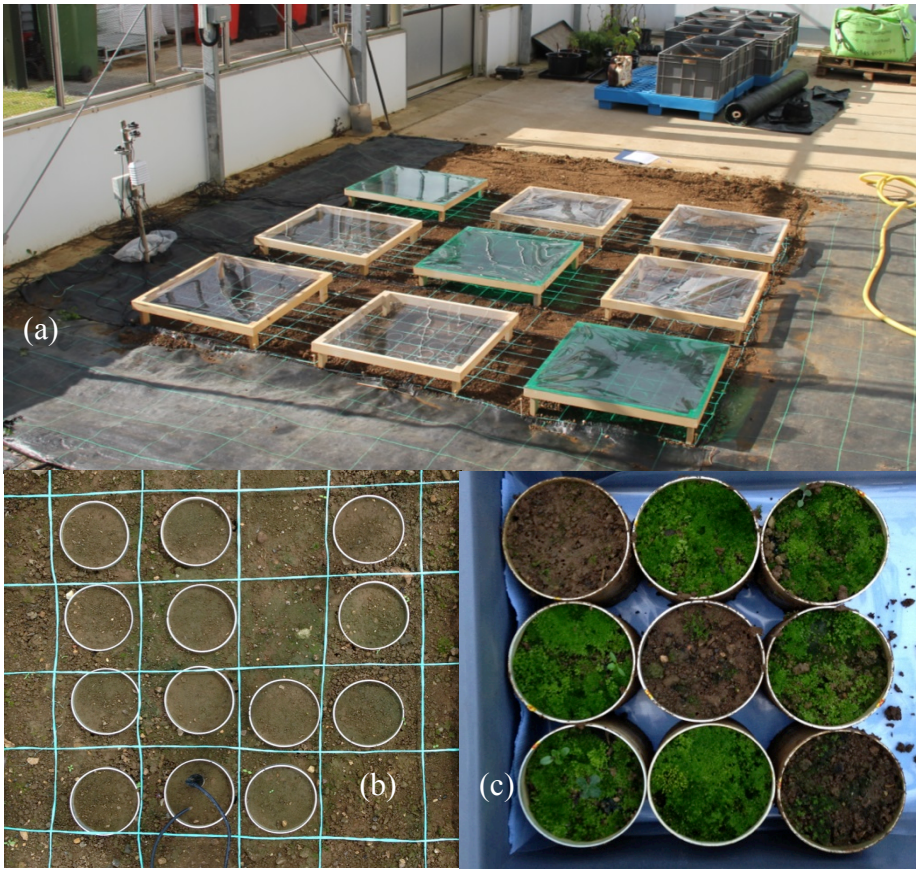

Figure II.2: (a) A photograph of the plot used in Chapters 3 & 4. (b) An example of the cores installed in the ground under a LIGHT filter at 0 DAT. (c) Cores removed from the ground pre-processing, 57 DAT.

II.2 Application rates

Field application rates were derived from the Pesticide Manual (Tomlin 2006) or internal Syngenta data.

Example: Paclobutrazol

The desired application rate of paclobutrazol was 100 g ai/ha, converted to 0.01 g ai/m^2. The radius of the soil core was 3.75 cm, giving a soil surface area of 0.0042 m^2, giving an application mass of 44.16 µg per core.

The SpecAc of paclobutrazol (4 2821 Bq/µg) was multiplied by the required mass of paclobutrazol to be applied per core (44.16 µg) to give the activity to be applied per test system (189 033 Bq)

Triplicate pre- and post-application checks were carried out, detailed in Appendix I, Section I.2, to give an average application rate of 102.2%.

II.4 Mass balance

Radioactivity in each analysed fraction was quantified by LSC as a percentage of applied radioactivity, and summed to give the mass balance of a core. The analysed fractions were composed of: surface, top bulk and lower bulk solvent extractions, washings from stones removed at the surface processing stage, and NERs. An example mass balance from a 0 DAT paclobutrazol core from under a CLEAR filter is shown in Table II.1.

Table II.1: An example of a mass balance table from the study in Chapter 3. Values shown are for a 0 DAT paclobutrazol core from under a CLEAR filter.

DAT	Solvent Extracts			Non-extractable residues			Stones	Total recovery (%)
	Surface	Top Bulk	Lower Bulk	Surface	Top Bulk	Lower Bulk		
0	57.9	41.2	0.0	0.7	0.7	0	0.1	100.6

II.5 Combination of parent values

HPLC analysis was used to quantify the amount of parent compound in solvent extracts from the surface, top bulk, and lower bulk as a percentage of applied compound (as described in Chapter 2, Section 2.2.3). These values were summed to give total parent compound remaining in the core.

II.6 Samples removed from analysis

II.6.1 Benzovindiflupyr

Table II.2 details the samples removed from benzovindiflupyr analysis due to preferential flow of radiochemical through the core.

Table II.2: Samples removed from benzovindiflupyr analysis in the Chapter 3 study.

Core	DAT	Light Filter
2	0	LIGHT (CLEAR)
10	14	LIGHT (CLEAR)
13	14	LIGHT (UV-L)
17	14	PAR-L
19	30	LIGHT (CLEAR)
22	30	LIGHT (UV-L)
24	30	LIGHT (UV-L)
30	60	LIGHT (CLEAR)
34	60	PAR-L
38	90	LIGHT (CLEAR)

II.6.2 Paclobutrazol

Table II.3 details the samples removed from paclobutrazol analysis due to preferential flow of radiochemical though the core.

Table II.3: Samples removed from paclobutrazol analysis in the Chapter 3 study.

Core	DAT	Light Filter
40	90	LIGHT (UV-L)
45	90	PAR-L

II.7 Example HPLC chromatograms

Example chromatograms from [^{14}C]-HPLC analysis of compounds investigated in Chapter III.

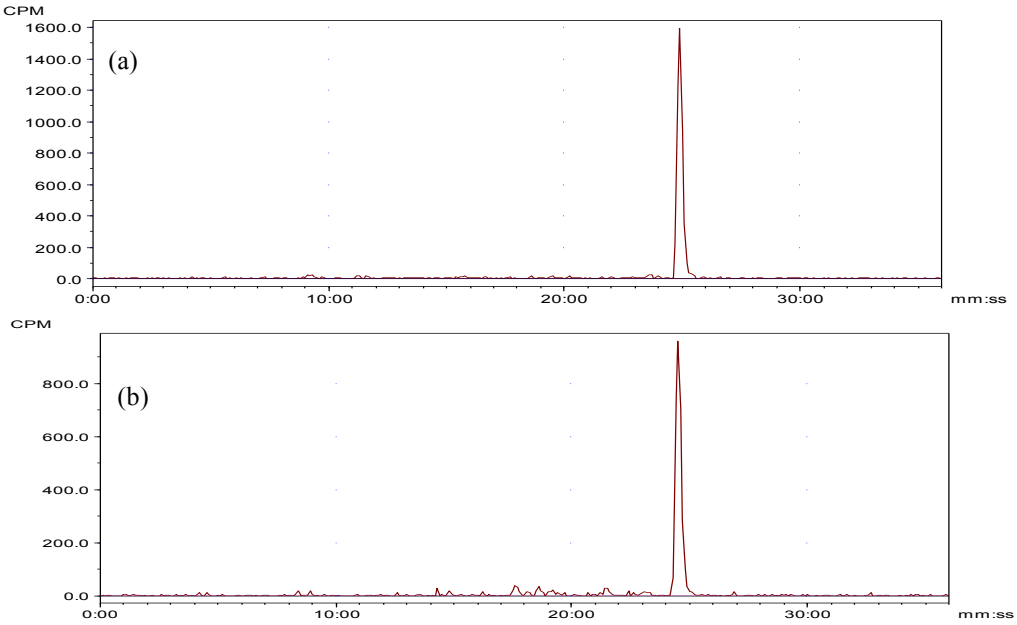

Figure II.3: Example HPLC chromatograms from analysis of ^{14}C-benzovindiflupyr at: (a) 0 DAT (b) 120 DAT Surface.

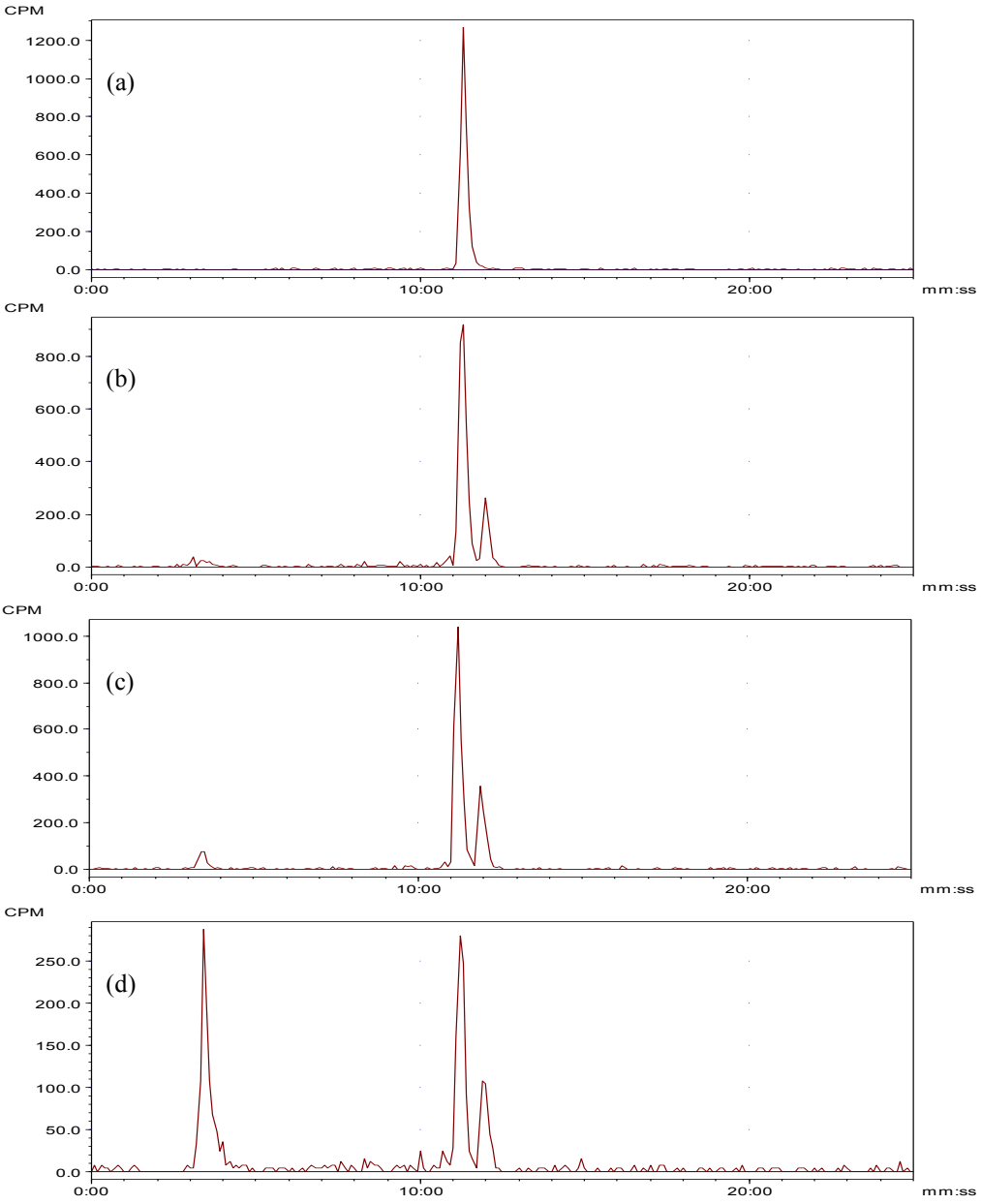

Figure II.4: Example HPLC chromatograms from analysis of ^{14}C-paclobutrazol at: (a) 0 DAT, and 106 DAT (b) Surface (c) Top Bulk (d) Lower Bulk, under a CLEAR filter.

APPENDIX III: FIELD DEGRADATION – MICROBIOLOGY FURTHER METHODS

III.1 Tree construction for unassigned OTUs – 23S rRNA

During 23S rRNA sequence processing, sequences assigned as 'No Blast Hit' were imported into ARB and aligned using parsimony criteria in a phylogenetic tree, shown in Figure III.1. Unassigned sequences are in green with the prefix 'mcjdayXX', followed by a unique ARB accession number.

Figure III.1: Phylogenetic tree of unassigned 23S rRNA sequences (green) with selected sequences from the ARB SILVA 119 LSU Ref database.

III.2 Samples lost during bioinformatic analysis

III.2.1 16S rRNA samples

Several samples were lost during the analysis of 16S rRNA sequencing samples, detailed in Table III.1. All six samples were lost at the rarefaction stage, having a sequence/sample value lower than the cut off point.

Table III.1: Details of 16S rRNA samples lost during analysis in the Chapter 4 study.

Sample ID	Compound	DAT	Treatment
228	Benzovindiflupyr	0	LIGHT (UV-L)
243	Benzovindiflupyr	30	LIGHT (CLEAR)
187	Paclobutrazol	37	LIGHT (CLEAR)
256	Benzovindiflupyr	60	PAR-L
216	Paclobutrazol	113	LIGHT (CLEAR)
275	Benzovindiflupyr	120	PAR-L

III.2.2 23S rRNA samples

Two samples were lost during the analysis of 23S rRNA sequencing samples, detailed in Table III.2. Both samples were lost at the rarefaction stage, having a sequence/sample value lower than the cut off point.

Table III.2: Details of 23S rRNA samples lost during analysis in the Chapter 4 study.

Sample ID	Compound	DAT	Treatment
229	Benzovindiflupyr	0	PAR-L
231	Benzovindiflupyr	0	PAR-L

III.3 SIMPER analysis results

SIMPER analysis was used to identify the taxa driving dissimilarity between LIGHT and PAR-L treatments and by time in bacterial and phototrophic communities. Whilst selected results were reported in the main body of the thesis, full results are included in the Table III.3 & III.4.

Table III.3: SIMPER analysis results of bacterial communities present at the soil surface in the Chapter 4 study.

Treatment (A vs. B)	Overall Average Dissimilarity (%)	Most influential species	% Contribution to difference (cumulative)	Average % abundance A	S.E A	Average % abundance B	S.E B
LIGHT vs. PAR-L	15.73	Cyanobacteria	30.73	10.51	0.79	1.77	0.52
		Actinobacteria	20.60 (51.33)	28.20	0.49	34.23	0.71
		Proteobacteria	10.16 (61.50)	22.86	0.43	21.78	0.33
		Acidobacteria	8.03 (69.53)	7.13	0.25	9.34	0.39
		Chloroflexi	6.67 (76.19)	10.36	0.21	12.16	0.26
0 vs. 120 DAT	13.82	Cyanobacteria	24.15	8.04	2.63	5.53	1.23
		Actinobacteria	14.38 (38.583)	33.85	1.42	30.04	0.49
		Proteobacteria	13.01 (51.55)	19.77	0.81	22.36	0.60
		Planctomycetes	12.78 (64.32)	5.09	0.42	8.29	0.46
		Acidobacteria	8.53 (72.86)	6.68	0.67	8.63	0.44

Table III.4: SIMPER analysis results of phototrophic communities present at the soil surface in the Chapter 4 study.

Treatment (A vs. B)	Overall Average Dissimilarity (%)	Most influential species	% Contribution to difference (cumulative)	Average % abundance A	S.E A	Average % abundance B	S.E B
LIGHT vs. PAR-L	61.19	*Microcoleus vaginatus*	18.84	23.07	2.10	15.98	3.45
		Bryophytina	17.05 (35.89)	32.62	2.23	14.32	1.60
		Kryptoperidinium	13.26 (49.15)	2.12	0.36	17.63	2.60
		Naviculales	11.55 (60.70)	2.82	0.58	15.05	1.95
		Vaucheriaceae	6.39 (67.10)	8.16	1.21	2.10	0.30
0 vs. 120 DAT	78.45	Bryophytina	25.95	2.29	0.68	34.74	6.30
		Microcoleus vaginatus	19.92 (45.87)	32.95	8.27	16.77	6.19
		Nodosilinea nodulosa	10.23 (56.10)	15.57	5.22	0.60	0.19
		Vaucheriaceae	7.57 (63.68)	1.87	0.78	9.84	3.84
		Naviculales	7.35 (71.03)	10.84	3.58	3.36	1.78

APPENDIX IV: CROP CANOPY COVER – FURTHER METHODS

IV.1 Experimental plot layout

The plot layout used for the crop canopy cover experiment detailed in Chapter 5 is shown in Figure IV.1 & IV.2. The area was comprised of nine planted plots in a Latin square design, with three dividing regions taken as bare plots.

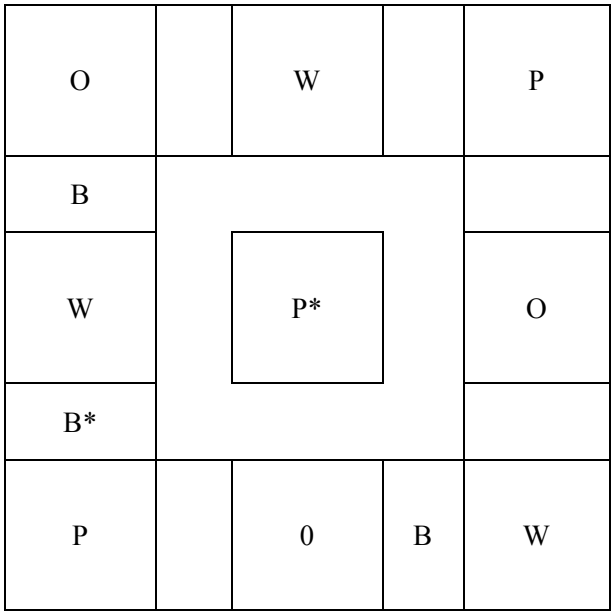

Figure IV.1: The plot layout used in the crop canopy cover study detailed in Chapter 5. Treatments were Bare (B), Onion (O), Wheat (W), and Potato (P). An asterisk denotes a plot with temperature and moisture probes.

Figure IV.2: The semi-field plot from the Chapter 5 study 14 days after planting.

IV.2 Samples lost during bioinformatic analyses

IV.2.1 16S rRNA samples

Several samples were discarded or lost during analysis of 16S rRNA sequencing samples, detailed in Table IV.1.

Table IV.1: Details of 16S rRNA samples lost during analysis in the Chapter 5 study.

Sample ID	Compound	Layer	DAP
6	Onion	Surface	0
52	Onion	Surface	30
64	Onion	Bulk	30

Samples 6 and 52 were lost at the rarefaction stage, having a sequence/sample value lower than the cut off point. When samples were analysed by NMDS, sample 64 clustered separately from the rest of the samples.

Investigation found that the phylum Fibrobacteres, typically found in rumen fluid, represented >50% relative abundance, and the sample was discarded.

IV.2.2 23S rRNA samples

Several samples were discarded or lost during analysis of 23S rRNA sequencing samples, detailed in Table IV.2.

Table IV.2: Details of 23S rRNA samples lost during processing and analysis in the Chapter 5 study.

Sample ID	Compound	Layer	DAP
12	Potato	Surface	0
42	Onion	Bulk	14
52	Onion	Surface	30
54	Onion	Surface	30
66	Onion	Bulk	30
68	Onion	Surface	60

Sample 12 was lost because joining of paired end reads was unable to take place at the start of the processing pipeline. The other five samples were lost at the rarefaction stage, having a sequence/sample value lower than the cut off point.

IV.3 SIMPER analysis results

SIMPER analysis was used to identify the taxa driving dissimilarity between treatments and by time in bacterial and phototrophic communities. Whilst selected results were reported in the main body of the thesis, full results and pairwise comparisons between treatments are included in the following tables.

Table IV.3: SIMPER analysis results of bacterial communities present in Bulk and Surface soil.

Treatment (A vs. B)	Overall Average Dissimilarity (%)	Most influential species	% Contribution to difference (cumulative)	Average % abundance A	S.E A	Average % abundance B	S.E B
Bulk vs. Surface	9.05	Actinobacteria	30.99	34.08	0.29	39.41	0.32
		Acidobacteria	17.56 (48.54)	10.68	0.18	7.75	0.15
		Proteobacteria	10.59 (59.13)	22.45	0.16	21.31	0.19
		Firmicutes	8.03 (67.16)	4.80	0.15	4.99	0.16
		Chloroflexi	8.00 (75.17)	11.01	0.14	11.24	0.15
0 vs. 150 DAP	9.05	Actinobacteria	26.41	35.48	0.40	34.75	1.22
		Acidobacteria	14.37 (40.77)	9.13	0.29	9.97	0.63
		Proteobacteria	11.91 (52.68)	22.88	0.31	21.65	0.42
		Chloroflexi	9.86 (62.54)	10.96	0.31	10.75	0.33
		Firmicutes	9.55 (72.10)	5.32	0.30	4.14	0.16

Table IV.4: SIMPER analysis results of phototrophic communities present in Bulk and Surface soil.

Treatment (A vs. B)	Overall Average Dissimilarity (%)	Most influential species	% Contribution to difference (cumulative)	Average % abundance A	S.E A	Average % abundance B	S.E B
Bulk vs. Surface	41.00	Spermatophyta	32.82	56.32	1.48	38.44	2.84
		Vaucheriaceae	10.19 (43.01)	3.24	0.33	10.29	1.10
		Chaetosphaeridiaceae	9.85 (52.86)	15.23	0.75	10.94	0.72
		Kryptoperidinium	8.33 (61.18)	2.41	0.26	7.98	0.95
		Coleochaetaceae	5.97 (67.16)	8.83	0.47	8.75	0.56
0 vs. 150 DAP	42.44	Spermatophyta	37.73	67.29	2.65	39.12	5.48
		Vaucheriaceae	9.13 (46.85)	3.14	0.38	9.95	2.30
		Chaetosphaeridiaceae	8.01 (54.86)	10.20	0.95	11.73	1.49
		Coleochaetaceae	6.09 (60.95)	7.28	0.68	8.08	1.16
		Kryptoperidinium	5.29 (66.24)	1.39	0.30	4.68	1.16

Table IV.5: SIMPER analysis results of comparisons by treatment and terminal time points of phototrophic communities present in Bulk soil.

Treatment (A vs. B)	Overall Average Dissimilarity (%)	Most influential species	% Contribution to difference (cumulative)	Average % abundance A	S.E A	Average % abundance B	S.E B
Bare vs. Onion	25.07	Spermatophyta	25.23	50.24	2.79	52.60	2.94
		Chaetosphaeridiaceae	13.90 (39.12)	14.54	1.27	16.47	1.72
		Coleochaetaceae	9.47 (48.60)	10.98	0.94	8.66	0.98
		Vaucheriaceae	6.81 (55.40)	4.41	0.96	3.65	0.76
		Kryptoperidinium	5.00 (60.40)	3.60	0.69	2.94	0.48
Bare vs. Wheat	24.09	Spermatophyta	24.14	50.24	2.79	56.30	2.38
		Chaetosphaeridiaceae	14.43 (38.57)	14.54	1.27	16.81	1.58
		Coleochaetaceae	9.32 (47.89)	10.98	0.94	7.61	0.86
		Chlorellaceae	6.48 (54.37)	3.98	0.43	4.79	0.78
		Vaucheriaceae	6.12 (60.49)	4.41	0.96	2.82	0.35
Bare vs. Potato	25.47	Spermatophyta	34.08	50.24	2.79	65.79	2.69
		Chaetosphaeridiaceae	11.72 (45.80)	14.54	1.27	13.22	1.43
		Coleochaetaceae	8.88 (54.68)	10.98	0.94	8.03	0.82
		Vaucheriaceae	6.74 (61.42)	4.41	0.96	2.14	0.35
		Kryptoperidinium	5.91 (67.34)	3.60	0.69	1.30	0.31
Onion vs. Wheat	25.16	Spermatophyta	27.87	52.60	2.94	56.30	2.38
		Chaetosphaeridiaceae	15.25 (15.25)	16.47	1.72	16.81	1.58
		Coleochaetaceae	9.51 (52.63)	8.66	0.98	7.61	0.86
		Chlorellaceae	5.62 (58.25)	3.26	0.36	4.79	0.78
		Vaucheriaceae	5.48 (63.73)	3.65	0.76	2.82	0.35
Onion vs. Potato	25.41	Spermatophyta	34.48	52.60	2.94	65.79	2.69
		Chaetosphaeridiaceae	14.44 (48.92)	16.47	1.72	13.22	1.43
		Coleochaetaceae	8.10 (57.02)	8.66	0.98	8.03	0.82
		Vaucheriaceae	5.28 (62.31)	3.65	0.76	2.14	0.35
		Kryptoperidinium	4.49 (66.79)	2.94	0.48	1.30	0.31
Wheat vs. Potato	22.6	Spermatophyta	32.51	56.30	2.38	65.79	2.69
		Chaetosphaeridiaceae	16.46 (48.97)	16.81	1.58	13.22	1.43
		Coleochaetaceae	9.01 (57.98)	7.61	0.86	8.03	0.82
		Vaucheriaceae	6.31 (64.29)	2.82	0.35	2.14	0.35
		Chlorellaceae	4.13 (68.42)	4.79	0.78	2.72	0.33
0 vs. 150 DAP	23.62	Spermatophyta	30.56	67.18	3.18	60.49	4.17
		Chaetosphaeridiaceae	13.12 (43.68)	10.43	1.34	12.47	1.93
		Coleochaetaceae	9.00 (52.68)	7.54	0.81	6.58	1.39
		Chlorellaceae	6.32 (59.00)	2.78	0.52	5.05	1.03
		Vaucheriaceae	4.92 (63.92)	2.78	0.48	2.95	0.66

Table IV.6: SIMPER analysis results of comparisons by treatment and terminal time points of phototrophic communities present in Surface soil.

Treatment (A vs. B)	Overall Average Dissimilarity (%)	Most influential species	% Contribution to difference (cumulative)	Average % abundance A	S.E A	Average % abundance B	S.E B
Bare vs. Onion	39.03	Spermatophyta	20.93	28.47	5.21	34.58	7.01
		Vaucheriaceae	10.46 (31.39)	15.13	2.76	10.28	1.99
		Kryptoperidinium	9.80 (41.19)	10.95	2.48	8.43	1.55
		Chaetosphaeridiaceae	7.65 (48.84)	9.01	1.18	9.60	1.78
		Bryophytina	6.07 (54.91)	3.69	1.46	3.74	1.94
Bare vs. Wheat	42.28	Spermatophyta	24.03	28.47	5.21	42.60	5.89
		Vaucheriaceae	11.91 (35.94)	15.13	2.76	9.91	2.10
		Kryptoperidinium	9.92 (45.86)	10.95	2.48	7.42	1.73
		Chaetosphaeridiaceae	8.24 (54.10)	9.01	1.18	11.11	1.24
		Coleochaetaceae	6.52 (60.62)	9.14	0.99	8.26	1.13
Bare vs. Potato	48.51	Spermatophyta	28.97	28.47	5.21	48.03	3.79
		Vaucheriaceae	14.03 (43.00)	15.13	2.76	5.61	1.11
		Kryptoperidinium	11.25 (54.25)	10.95	2.48	5.03	1.35
		Chaetosphaeridiaceae	8.26 (62.51)	9.01	1.18	13.98	1.44
		Coleochaetaceae	5.82 (68.33)	9.14	0.99	11.33	1.03
Onion vs. Wheat	42.21	Spermatophyta	25.89	34.58	7.01	42.60	5.89
		Chaetosphaeridiaceae	9.67 (35.56)	9.60	1.78	11.11	1.24
		Vaucheriaceae	8.16 (43.72)	10.28	1.99	9.91	2.10
		Kryptoperidinium	6.85 (50.57)	8.43	1.55	7.42	1.73
		Coleochaetaceae	5.80 (56.37)	6.01	1.09	8.26	1.13
Onion vs. Potato	49.34	Spermatophyta	31.47	34.58	7.01	48.03	3.79
		Chaetosphaeridiaceae	9.57 (41.04)	9.60	1.78	13.98	1.44
		Vaucheriaceae	8.88 (49.92)	10.28	1.99	5.61	1.11
		Kryptoperidinium	7.33 (57.25)	8.43	1.55	5.03	1.35
		Coleochaetaceae	6.59 (63.84)	6.01	1.09	11.33	1.03
Wheat vs. Potato	37.03	Spermatophyta	30.57	42.60	5.89	48.03	3.79
		Vaucheriaceae	11.22 (41.79)	9.91	2.10	5.61	1.11
		Kryptoperidinium	10.03 (51.82)	7.42	1.73	5.03	1.35
		Chaetosphaeridiaceae	8.59 (60.41)	11.11	1.24	13.98	1.44
		Coleochaetaceae	6.87 (67.28)	8.26	1.13	11.33	1.03
0 vs. 150 DAP	64.94	Spermatophyta	39.89	67.41	4.49	17.74	5.00
		Vaucheriaceae	11.71 (51.60)	3.53	0.61	16.95	3.58
		Chaetosphaeridiaceae	6.44 (58.05)	9.96	1.42	11.00	2.33
		Kryptoperidinium	5.59 (63.63)	0.99	0.31	8.33	1.76
		Coleochaetaceae	4.43 (68.06)	6.99	1.15	9.58	1.81

APPENDIX V: FIELD STUDY COMMUNITY COMPARISON

V.1 Analysis of similarities

ANOSIM was used to analyse the variation in the β diversity in bacterial and phototrophic communities between the semi-field studies in Chapters 4 and 5. Results are shown in Table V.1.

Table V.1: Analysis of similarities (ANOSIM) results evaluating the variation of bacterial and phototrophic soil surface communities between the Chapter 4 and 5 studies.

	16S rRNA	23S rRNA
STUDY – Global effect	**R = 0.468, *P* = 0.001**	**R = 0.756, *P* = 0.001**

V.2 SIMPER analysis results

SIMPER analysis was used to identify the taxa driving dissimilarity between bacterial and phototrophic communities in the studies in Chapter 4 and 5. Results are shown in Tables V.2 & V.3.

Table V.2: SIMPER analysis of bacterial communities between the Chapter 4 and Chapter 5 studies.

Experiment (A vs. B)	Overall Average Dissimilarity (%)	Most influential species	% Contribution to difference (cumulative)	Average % abundance A	S.E A	Average % abundance B	S.E B
C4 vs. C5	17.09	Actinobacteria	28.05	30.21	0.49	39.41	0.32
		Cyanobacteria	22.14 (50.19)	7.60	0.69	0.04	0.01
		Proteobacteria	8.79 (58.98)	22.50	0.31	21.31	0.19
		Firmicutes	8.49 (67.47)	2.15	0.08	4.99	0.16
		Planctomycetes	7.27 (74.14)	6.45	0.20	4.31	0.08

TableV.3: SIMPER analysis of phototrophic communities between the Chapter 4 and Chapter 5 studies.

Experiment (A vs. B)	Overall Average Dissimilarity (%)	Most influential species	% Contribution to difference (cumulative)	Average % abundance A	S.E A	Average % abundance B	S.E B
C4 vs. C5	77.25	Spermatophyta	22.44	4.35	0.47	38.44	2.84
		Bryophytina	16.43 (38.87)	26.75	1.80	2.09	0.60
		Microcoleus vaginatus	13.34 (52.22)	20.80	1.82	0.20	0.07
		Vaucheriaceae	6.44 (58.65)	6.22	0.87	10.29	1.10
		Kryptoperidinium	6.21 (64.86)	7.10	1.11	7.98	0.95